Mossbauer studies of polyvinylferrocenes.

PLIMLEY, Simon.

Available from the Sheffield Hallam University Research Archive (SHURA) at:

http://shura.shu.ac.uk/20236/

A Sheffield Hallam University thesis

44/95 16.55

ProQuest Number: 10700881

ProQuest 10700881

MÖSSBAUER STUDIES OF POLYVINYLFERROCENES

BY

SIMON PLIMLEY

A THESIS SUBMITTED TO
COUNCIL FOR NATIONAL ACADEMIC AWARDS
IN PARTIAL FULFILMENT OF THE
REQUIREMENTS FOR THE
DEGREE OF DOCTOR OF PHILOSOPHY

SPONSORING ESTABLISHMENT   : SHEFFIELD CITY POLYTECHNIC
                                  DEPARTMENT OF APPLIED PHYSICS
                                  POND STREET
                                  SHEFFIELD   S1 1WB

COLLABORATING ESTABLISHMENT : MINISTRY OF DEFENCE
                               PERME
                               WALTHAM ABBEY

MAY 1984
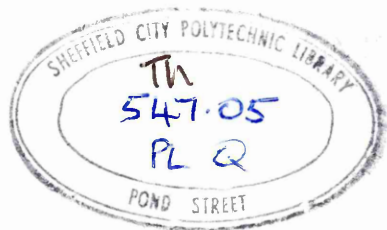
Abstract

Polymers of vinylferrocene and 1,1'divinylferrocene have been investigated using Fe^{57} Mössbauer spectroscopy and other spectroscopic techniques.

In studies of the radical polymerisation of vinylferrocene the novel FeIII species, previously proposed as the product of monomolecular termination of the reaction could not be observed. Polymerisation of vinylferrocene in chloroform occurred only in oxygen-free conditions, as previously reported, but the kinetics of the polymerisation were found to be very sensitive to impurities. ^{13}C n.m.r. studies of polyvinylferrocene have given results which contradict previously published work and correct peak assignments have now been made.

The structures of polymers from 1,1'divinylferrocene have been investigated by techniques that had not previously been used. Previous workers had concluded that the polymers produced by both radical and cationic initiation contained three carbon bridged ferrocene units. However, the Fe^{57} Mössbauer spectra revealed significant differences between the polymer structures. The quadrupole splitting (Q.S.) for polymers from cationic initiation = 2.39(2) mm s^{-1}, with Q.S. for polymers from radical initiation = 2.29(2) mm s^{-1}. This and other spectroscopic evidence supports a cyclopolymer structure for the polymers produced by radical initiation, with cationic initiation yielding polymers by an intermolecular polyaddition mechanism. The structures proposed have been confirmed by the synthesis of and spectroscopic comparisons with relevant model compounds. A polymer from anionic initiation of 1,1'divinylferrocene previously unreported, has been prepared and shown to contain a trimethylene bridge, identical to that of the radically-initiated polydivinylferrocene.

Variable temperature Fe^{57} Mössbauer studies have been carried out on ferrocene and on polymers of vinylferrocene and 1,1'divinylferrocene produced via anionic and cationic initiation. The treatment of the temperature dependence of the Mössbauer absorber recoiless fraction for crystalline solids has been extended to describe the vibrational properties of these amorphous polymers. An unusual non-linear dependence of lnA with temperature has been observed for the polymeric materials. The observed behaviour could not be explained on the basis of a modified Debye model for amorphous materials, even when intramolecular vibrations were included. However, a good fit to the experimental data was obtained with physically significant fitting parameters when it was assumed that each macromolecule vibrated within an anharmonic potential.

CONTENTS

CHAPTER SIX : VARIABLE TEMPERATURE Fe-57 MÖSSBAUER   143

STUDIES OF POLYMERS FROM VINYLFERROCENES

CHAPTER ONE - INTRODUCTION

1.1 Chemical and Physical Properties of Ferrocene and Vinylferrocene

Ferrocene was the first of the series of "sandwich" compounds to be synthesised [1], thus opening up a new area of organometallic chemistry. Its structure was proposed by Woodward [2], and firmly established by a series of X-ray studies [3] - [5], as an iron atom positioned centro-symmetrically between two cyclopentadienyl rings. The rings are eclipsed in the solid state, but the barrier to rotation is small and in solution at room temperature the separate conformations cannot be detected.

The chemical properties of ferrocene were investigated soon after its synthesis, and the most striking feature was its ability to undergo aromatic substitution reactions, whereas typical diene reactions, such as the Diels-Alder reactions, were not possible. The aromatic reactions which ferrocene can undergo include Friedel-Crafts acylation, alkylation, arylation and sulphonation. The mechanism of the electrophilic substitution is interesting as it involves the participation of the metal atom [6]. (Fig. 1.1)
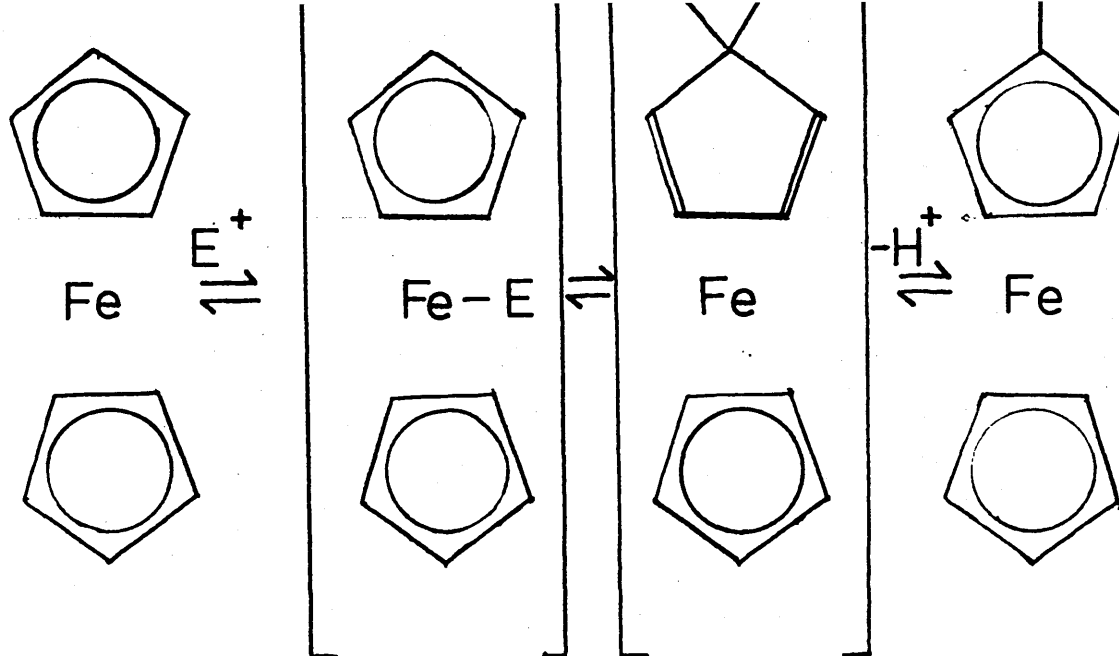
Fig. 1.1

Mechanism of electrophilic substitution reaction

One of the features of ferrocene chemistry is that reactions can occur involving the hydrocarbon rings, the metal atom, or both, as in Fig. 1.1. The metal atom in ferrocene is in the Fe(II) oxidation state, and oxidation to the more unstable Fe(III) state can be effected electrolytically, photochemically, or by using a variety of oxidising agents [7] - [10]. This oxidation involves the removal of a non-bonding iron 'd' electron [11],[12] so the bonding in the molecule is not appreciably altered. Electron-donating substituents on the cyclopentadienyl rings facilitate the removal of the electron and thus enhance the oxidation, while electron-withdrawing groups increase the oxidative stability [13] - [15]. It is because of this facile oxidation that direct nitration and halogenation of the rings is not possible and the ferricinium

ion is formed instead. Ferrocene is a weak base, but it
can be protonated by a strong acid to give the ferrocenonium
cation, I.

$$\overset{+}{Fe}-H$$
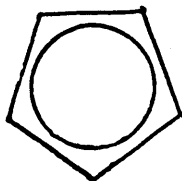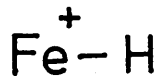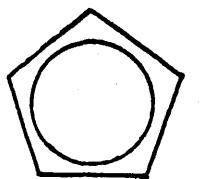
I

It has been proposed that if a hydrogen atom is bonded to
the metal, the two rings are no longer parallel and a ring
tilting effect occurs [16]. The formation of charge-
transfer complexes is another type of reaction that ferro-
cene can undergo, with reagents such as tetracyanoethylene
(TCNE) [17], benzoquinone or iodine. These compounds were
at first thought to be ferricinium salts [18], but they
have since been shown to be charge-transfer complexes, with
the electron acceptor bonded, not to the metal, but to one
of the rings [19], II.

$$NC \quad CN$$
$$NC \quad CN$$
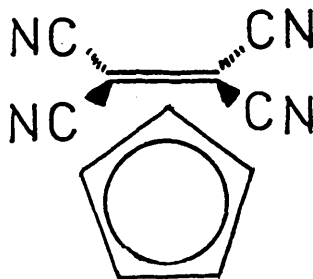
Fe
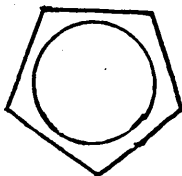
II

The chemical reactions of vinylferrocene have been investigated [20], and not surprisingly it shows properties similar to those of monosubstituted ethylenes. However, it has the ability to react with weak electrophiles such as hydrogen azide or acetic acid [21], whereas olefins will not generally react with weak acids unless catalysed [22],[23]. This unusual reactivity has been attributed to the formation of stable ferrocenyl carbo-cations involving the participation of the iron nucleus. This participation affects the reactivity of many ferrocene derivatives.

The bonding in ferrocene is best treated in the LCAO-MO approximation in which each cyclopentadienyl ring has five molecular orbitals (Fig. 1.2).
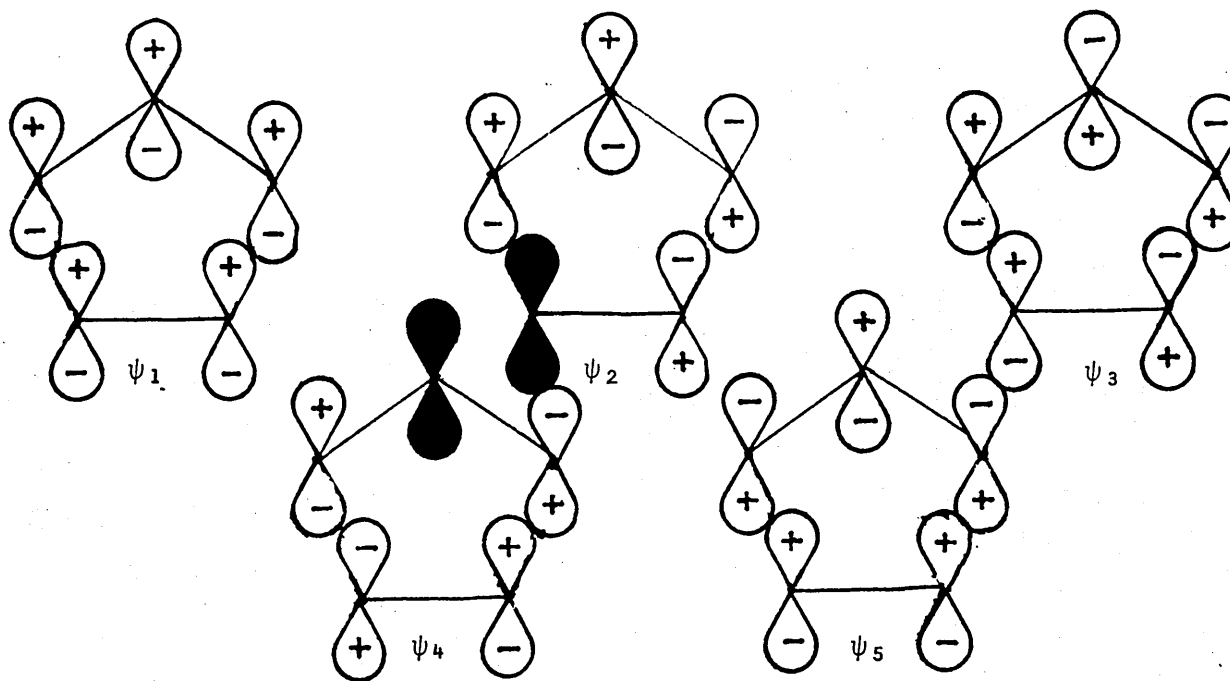
Fig. 1.2

Atomic orbitals of the cyclopentadienyl group

Interaction with metal orbitals of corresponding symmetry
leads to metal-ring σ-bonding through ψ_1, π-bonding
through ψ_2 and ψ_3 and δ-bonding through ψ_4 and ψ_5 (Fig. 1.3).
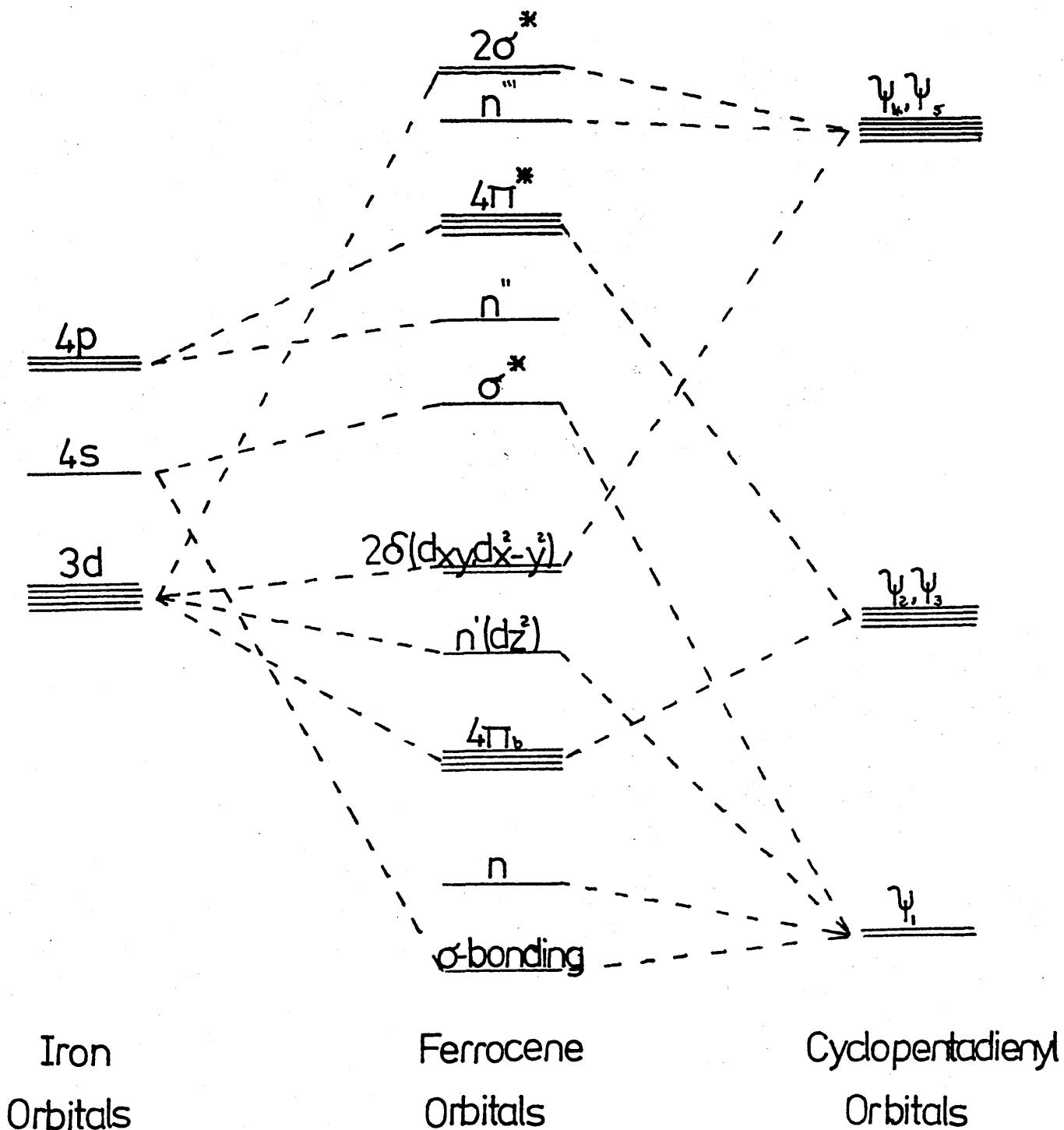
Fig. 1.3

Energy level diagram for ferrocene [24]

The $\delta(dxy, dx^2y^2)$ molecular orbitals are only partially bonding in character and retain predominantly their 3d metal orbital character, while the $n'(dz^2)$ molecular orbital is mainly the $3dz^2$ metal orbital. Therefore the three molecular orbitals of highest energy are essentially non-bonding metal orbitals, thus removal of one electron to form the ferricinium ion should not cause any appreciable difference in the bonding of the molecule. The 2δ and n' ferrocene molecular orbitals are very close in energy, but magnetic moment measurements indicate that in the formation of the ferricinium ion, the electron is lost from the 2δ orbital [24].

Information about the physical properties of ferrocenes is readily available in the literature. The infrared spectrum of vinylferrocene has been determined and assigned by Lippincott and Nelson, [25] - [27], (Table 1.1).

Table 1.1 - Infrared Spectrum of Vinylferrocene[a] [28]

Assignment	Position (cm^{-1})
Ferrocene ring C-H stretch	3090
Aliphatic C-H stretch	3004
Vinyl group C=C stretch	1631
Ferrocene ring antisymmetric C-C stretch	1411
Vinyl group CH_2, in-plane deformation	1240
Ferrocene ring antisymmetric ring breathing	1108
Ferrocene ring C-H bend, parallel to plane of ring	1002
Vinyl group =C-H wag	899
Ferrocene ring C-H bend, perpendicular to plane of ring	815

a - determined in chloroform solution

Infrared studies of a number of oxidised ferrocenes have also been carried out [29] and small changes in the spectra were observed relative to the reduced form.

The electronic spectrum of ferrocene was first reported by Wilkinson [30], though more recent work has been carried out by Scott and Becker [31], and by Soln et al [32]. An investigation of the electronic absorption spectra of aqueous $Fe(Cp)_2^+$ ions has been performed [33], with a band at 617 nm being observed, which is not present in ferrocene or vinylferrocenes. This has been assigned to the $^2E_{2y} \rightarrow {}^2E_{1u}$ transition [34], [35] and is, in part, responsible for the blue/green colouration of ferricinium ions [36].

The proton nuclear magnetic resonance of ferrocene gives a single peak at $\delta 4.14$ppm. [37], and this was found to broaden on addition of the ferricinium ion due to paramagnetism. The spectra of vinylferrocene, 1,1' divinylferrocene and other ferrocene derivatives have also been recorded [38] - [44]. The ^{13}C n.m.r. spectra of ferrocene and a number of monosubstituted ferrocenes have been studied [45] and further information is reported in Chapter 5.

Several workers have reported Mössbauer spectra of ferrocene and its derivatives, though the results obtained and published in earlier papers [46], [47] are less reliable than the more recent publications [48]. A more detailed discussion on this subject can be found in Section 2.4.

1.2 Polymerisation of Vinylferrocene

The polymerisation of vinylferrocene was first attempted by Arimoto and Haven [49] and subsequently vinylferrocene has been shown to polymerise by anionic, cationic or radical mechanisms in bulk, solution or emulsion processes [50] - [63]. The polymer obtained is a yellow powder with a melting point of approximately 285°C, soluble in most organic solvents except alcohols [49], and found to exhibit the same reversible oxidation-reduction reactions as monomeric ferrocene derivatives [11].

The infrared spectrum of polyvinylferrocene (PVF) has been studied and literature is readily available on the subject [49],[56],[57],[59],[64]. The spectrum is essentially as expected except for two bands at 850 and 920 cm^{-1} which have been attributed to unsaturation within the polymer [64]. The two bands listed above are in the region of bending modes in olefins [65] and it is postulated that vinylidene groups are introduced into the structure by transfer reactions.

The electronic spectrum of PVF differs little from ferrocene as alkyl substituents have been shown to have no marked effect on the characteristic ferrocene absorptions [66]. Oxidation of the polymer gives rise to the ferricinium cation and an absorption in the region of 635 nm.

The 'H n.m.r. spectrum gives a broad singlet in the region of δ4 ppm. due to the ring protons, while the aliphatic

protons cover the region δ2.5 - 1.0 ppm. The line
broadening and absence of any fine structure in the
spectrum has been attributed to paramagnetism within the
polymer [64]. The ^{13}C n.m.r. spectrum of PVF has also
been studied and the results interpreted in terms of
structural units [67].

The thermal properties of the polymer have been examined
using differential thermal analysis (DTA) and differential
scanning calorimetry (DSC) techniques and though a value
for the Glass Transition Temperature, Tg, of around 220°C
has been recorded by several workers [58],[61],[68],
a value as low as 184°C has also been reported [58]. The
polymers are stable up to 240°C when first weight loss
occurs due to the break-up of the aliphatic backbone and
between 400 and 500°C about 83% of the polymer is
volatalized due to the degradation of the ferrocene nucleus.

Cationic polymerisation occurs very readily at 0°C though
the product was of low molecular weight [56]. At -78°C
no polymer was formed   and this was attributed to the
competing reaction of electrophilic substitution at lower
temperatures [28]. At 0°C, the polymer formed showed only
homoannular substitution by infrared spectroscopy [70].

Anionic polymerisation has been successfully carried out
using a variety of lithium initiators [52],[71], though
the yields were much lower than in the cationic polymeri-
sation and this has been attributed to side reactions [71],
not surprisingly since ferrocene reacts readily with lithium

and its alkyls [11].

The first radical polymerisation was performed by Arimoto and Haven who used 2,2' azoisobisbutyronitrile (AIBN) as initiator and obtained polymers with number average molecular weights ($\overline{M}_n$) of around 48,000. Other radical initiators have since been used successfully though benzoyl peroxide has been found to convert the monomer to ferric benzoate by a mechanism which involves the formation of the ferricinium ion [72] - [74]. The first kinetic study was carried out by Baldwin and Johnson [54] who concluded that the free radical polymerisation kinetics of vinylferrocene were similar to those of styrene. The rate constants obtained were

$$K \text{ (vinylferrocene)} = R_p/[M][AIBN]^{0.5}$$
$$= 1.1 - 1.8 \times 10^4 \ dm^{3/2} \ mol^{-1/2} \ s^{-1}$$

$$K \text{ (styrene)} \qquad = R_p/[M][AIBN]^{0.5}$$
$$= 1.65 \times 10^4 \ dm^{3/2} \ mol^{-1/2} \ s^{-1}$$

where [M] = concentration of monomer.

These results have since been shown to be incorrect and George and Hayes have found that vinylferrocene and styrene obey totally different kinetics [75] with the rate of polymerisation, R_p, for vinylferrocene given by

$$R_p = K[M][AIBN] \qquad\qquad (1.1)$$

where K = constant.

The rate expression with the rate of polymerisation proportional to the concentration of initiator to the power 1 can be explained if the dominant termination step is

monomolecular. This is unusual since most vinyl polymeri-
sations terminate by combination or disproportionation.
both of which are bimolecular processes. A mechanism for
this unusual termination step was proposed by George and
Hayes (Figs. 1.4 and 1.5) [64],[75].
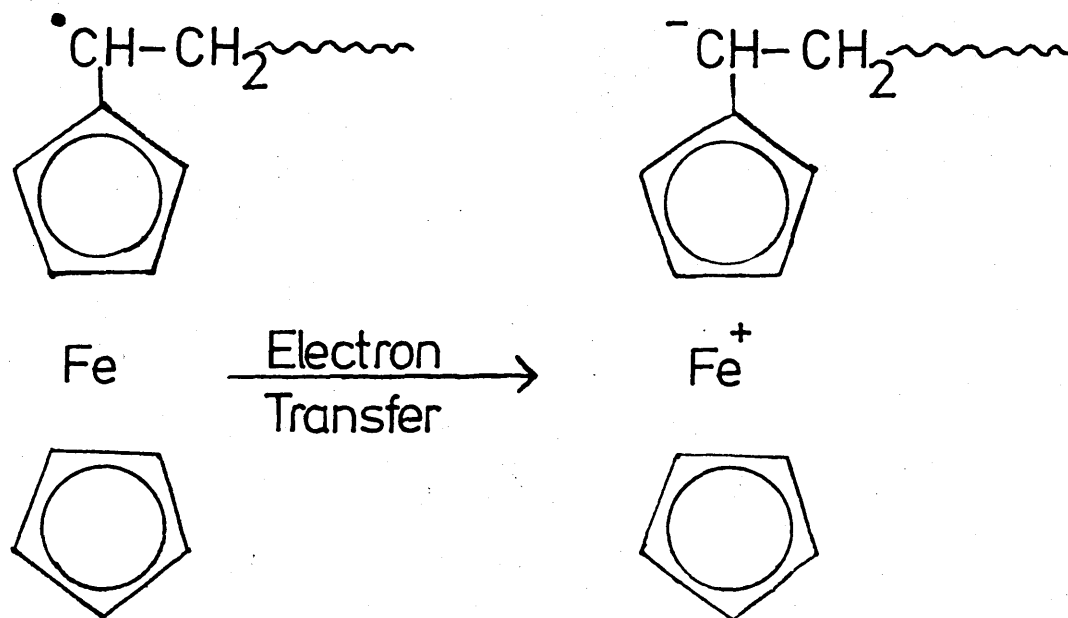
Fig. 1.4

Electron transfer termination of the polymerisation of

vinylferrocene

The ferricinium cation in Fig. 1.4 rearranges to form a
$3d^5$, high spin complex (Fig. 1.5). This mechanism implies
the production of an unpaired electron and this is
confirmed by ESR studies and by paramagnetic broadening of
the proton n.m.r. spectrum [64]. The Mössbauer spectra
of polyvinylferrocene were found to contain a third peak not
present in the monomer, which was thought to be due to an
ionically bound complex involving Fe(III) high spin [64]. If
this mechanism is correct, then there should be a correla-
tion between the degree of polymerisation ($\overline{DP}$) and the
amount of Fe(III). However, results obtained by George and
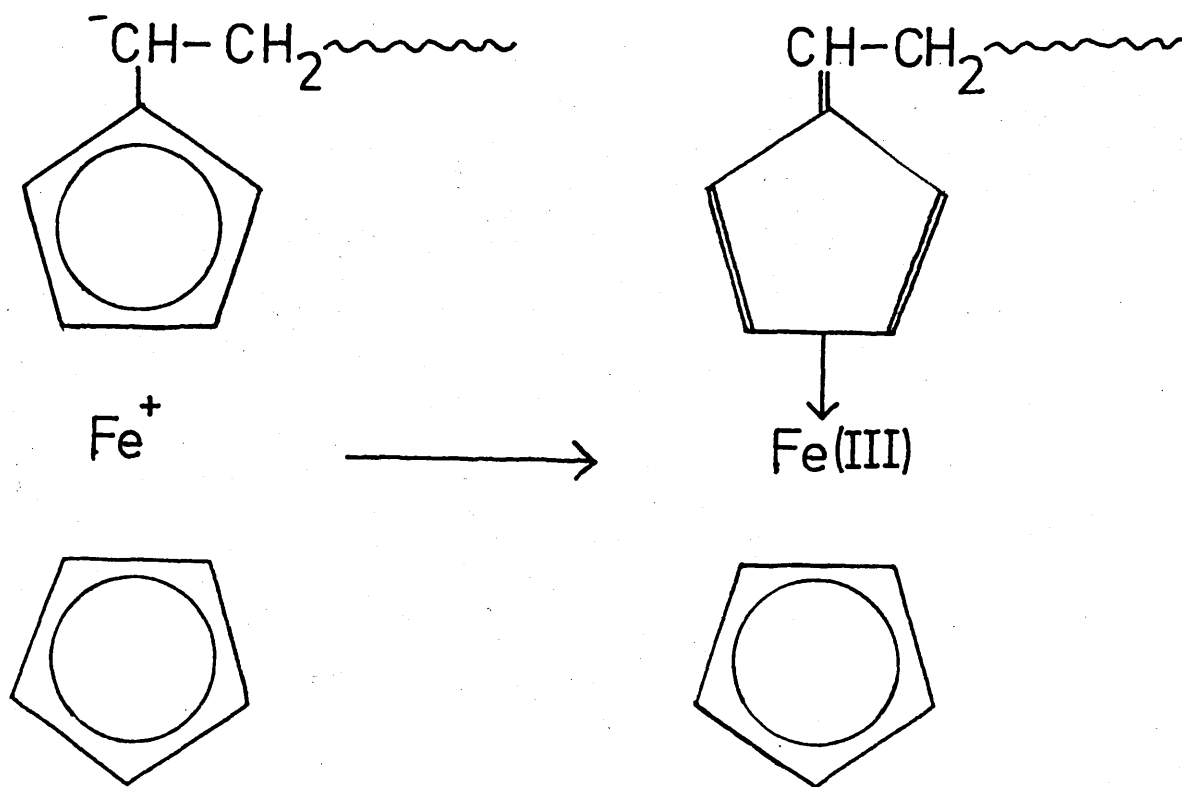
<u>Fig. 1.5</u>

<u>Formation of the Fe(III) high spin complex</u>

Hayes [64] were inconclusive, although this could be due
to transfer reactions during the polymerisation. Another
consideration is that at least 5% Fe(III) is required to
give a significant peak in the Mössbauer spectrum, and thus
at high $\overline{DP}$, the concentration of terminal unit will be low
and may not be measurable.

- 12 -

Vinylferrocene has also been found to initiate its own polymerisation in chloroform with the following mechanism proposed:

$$CH_2=CHF_C \ + \ CHCl_3 \rightarrow CH \ =CHF_C^+ \ CCl_3^- \ + \ H^\bullet \quad (F_C = \text{Ferrocenyl group})$$

$$CH_2=CHF_C \ + \ H^\bullet \rightarrow \quad \text{Polyvinylferrocene}$$
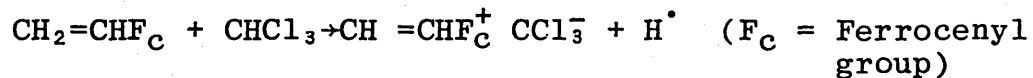
The chloroform polymers have been shown to be similar to the polymers produced with radical initiators, with almost identical IR and UV/visible spectra [28].

1.3 Polymerisation of 1,1'Divinylferrocene and related compounds

The synthesis of 1,1'divinylferrocene (DVF) was first reported by Michnick [77],[78] during the early 1960's and within a few years its ability to form polymers had been studied by Russian [79] - [81] and Japanese groups [82],[83]. The polymers produced were similar in appearance to those from monovinylferrocene. Due to the existence of a vinyl group on each cyclopentadienyl ring, the propagation

reaction can involve two competing steps, intermolecular

propagation and intramolecular cyclisation (Fig. 1.6).

Fig. 1.6

Polymerisation of 1,1'Divinylferrocene

- 14 -
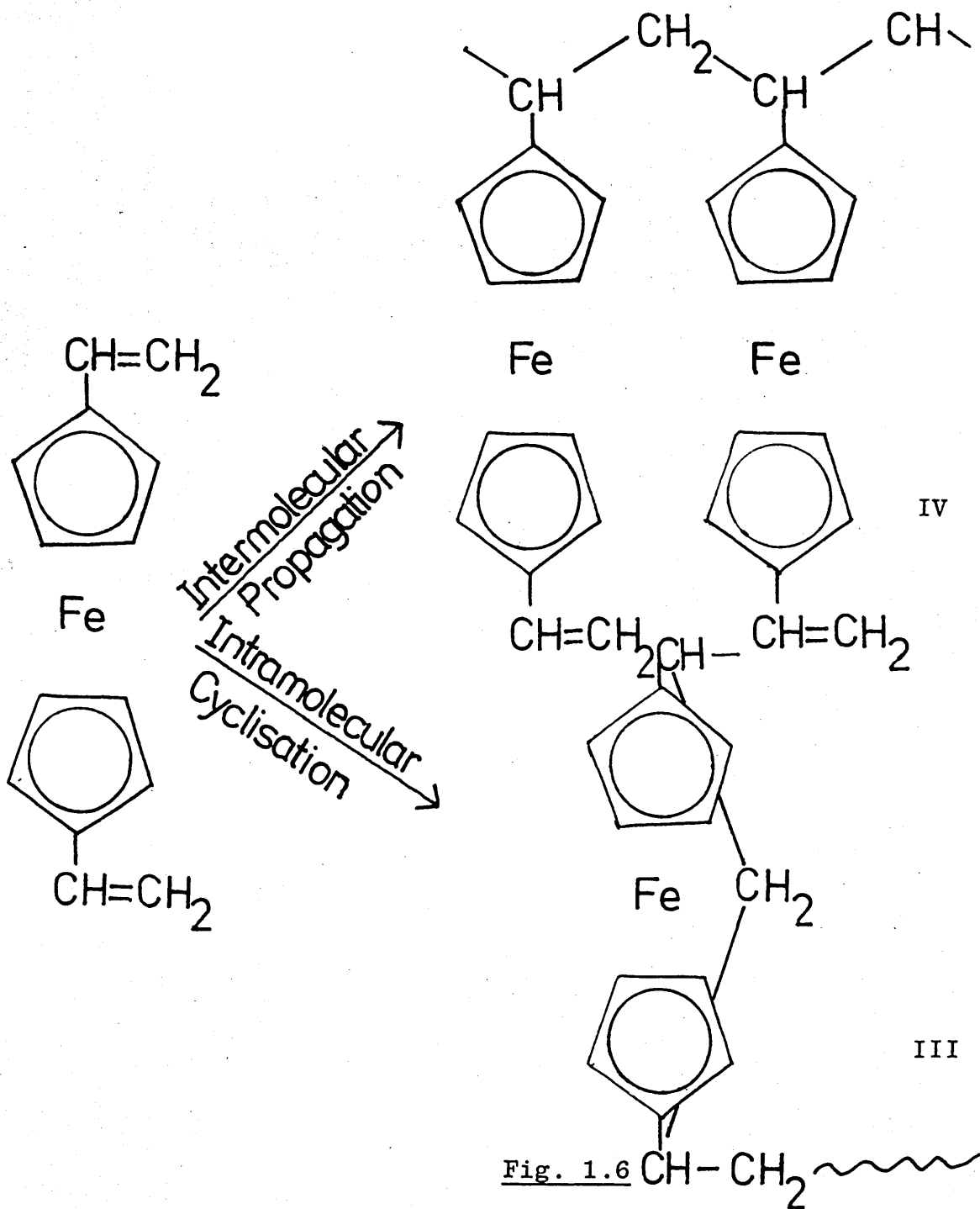
Kunitake et al [82],[83] polymerised 1,1'divinylferrocene using radical and cationic initiators and they obtained polymers which varied in solubility in organic solvents such as benzene. They concluded on the basis of 'H n.m.r. and infrared studies that their cationic polymerisations, in which they used a variety of initiators, yielded between 67-89% of the cyclic unit, III, the remainder being made up of the linear unit, IV. Using the radical initiator, AIBN, they concluded that at least 96% of the polymer consisted of cyclic units. At first they used infrared spectroscopy to quantify the extent of cyclisation, since Neuse had observed that a broad absorption at around 815 cm^{-1} exhibited by ferrocene derivatives was split into two peaks at 800 and 860 cm^{-1} in a large number of heterobridged ferrocene compounds [84]. Only partial splitting of the 820 cm^{-1} peak in the cationic polymer into two peaks at 810 and 850 cm^{-1} was attributed to the presence of non-cyclic and cyclic units in the structure. In the radical polymer the peak at 820 cm^{-1} was very small and so they concluded that the ratios D810/D820 and D850/ D820 reflected the extent of cyclisation. For the cationic polymers, a typical value of D810/D820 was 0.8 while for the radical polymer the value was greater than 3.9.

'H n.m.r. spectra were used to calculate the percentage of each unit. Their spectra showed the presence of alkene unsaturation, attributed to pendent vinyl groups, between δ5.3 ppm and δ6.1 ppm, the ferrocene ring protons between δ3.0 ppm and δ4.6 ppm and the aliphatic protons upward of

- 15 -

δ2.5 ppm.   The relative number of pendent vinyl groups and hence the linear units in the polymer chain, were calculated using equation 1.2.

$$\% \text{ Pendent Double Bond} = \frac{8x}{3y} \times 100\% \qquad (1.2)$$

where x = peak area of alkene unsaturation

and   y = peak area of ferrocene ring protons.

The effects of different catalysts and solvents on the cationic polymerisation have also been studied [83]. It was found that aluminium based catalysts exhibited a tendency to form polydivinylferrocenes with a greater percentage of the cyclic unit. A variation in the cyclisation tendency with differing catalysts has previously been observed in the cationic polymerisation of O-divinylbenzene [85],[86]. However, with divinylferrocene the percentage of cyclic units was found to increase with increasing polarity of solvents for a given initiator, which was contrary to the solvent effect observed in O-divinylbenzene and various explanations were discussed by these authors [83].

The thermal properties of polydivinylferrocenes (PDVF) have also been investigated [83]. Most of the polymers had a softening point in the range 120-200°C, though the aluminium catalysts produced polymers which did not soften, although decomposition did occur at about 230°C. In thermogravimetric studies, the polymers exhibited initial weight loss in the region 200-360°C, and in general their thermal properties were very similar to those of

polyvinylferrocene.

The polymerisation of 1,1' di-isopropylferrocene has also been studied [79] and it has been found to polymerise successfully with radical and cationic initiators. Anionic initiation did not yield any polymer. The polymers from both radical and cationic reactions were assigned linear cyclopolymer structures.

1.4   Uses of Ferrocene Compounds

Due to the rather unusual chemistry of ferrocene and its derivatives, a wide range of technological uses have been found for these compounds.

Early work showed that because of its oxidation-reduction capability, ferrocene could be employed, in low concentrations, as catalysts in processes involving fuel combustion. Its effect is to reduce 'knock' and decrease carbon deposits in the combustion of petrol [87] - [89], natural gas [90] and other fuel and propellant compositions [91],[92]. Ferrocene compounds have found use in the chemical industry; for instance, ferrocene improves the thermal stability of polysiloxane fluids, resins and greases [93] - [95], and some ferrocene derivatives, notably acyl compounds, exhibit protective effectiveness in organic coatings, such as paints, when exposed to U.V. radiation [96],[97]. Several ferrocene compounds have been shown to have biological uses, e.g. for treatment of iron deficiency in humans and animals [98] - [101] and other pharmacological properties have also been cited [102].

Macromolecular ferrocene compounds have a wide range of
uses with the added advantage that they are less volatile
than monomeric ferrocene derivatives. The variety of uses
of ferrocene compounds today is so great that the
applications are reviewed annually in the literature [103].

CHAPTER TWO : MÖSSBAUER SPECTROSCOPY

2.1 Introduction

2.1.1 The Mössbauer Effect

Mössbauer spectroscopy is concerned with the phenomena of resonant absorption and fluorescence of nuclear γ-rays in the energy range 10-100 keV. Mössbauer [104] discovered that, if the emitting nucleus is held in a lattice, then at low temperatures the recoil energy of the γ-ray is transferred, not to the single nucleus, but to the whole crystal lattice. This can only occur if the minimum energy needed to excite the vibrational energy levels of the lattice is greater than the recoil energy. If this condition is satisfied, then the γ-ray emission occurs effectively without recoil and the optimum resolution is obtained.

2.1.2 Nuclear Resonance Absorption

If the nucleus changes from a high energy or excited state to one of lower energy, then a photon of energy is emitted, corresponding to the energy difference between the two levels. This is an example of emission and the reverse transition can also occur when the photon is absorbed, resulting in a transition to a higher energy state. For nuclear cases, this is called nuclear resonance absorption and the photon must have exactly the right energy to cause the transition. Such absorbed or emitted energy can take the form of electromagnetic radiation and obeys the relationship shown in eqn. 2.1.

$$\Delta E = h\nu \qquad\qquad (2.1)$$

where h = Plancks constant

and ν = Frequency of radiation.

2.1.3 Recoil Energy and Resonance Fluorescence

The energy of the emitted photon is not equal to the exact difference in energy of the two states because, due to the law of conservation of momentum, the nucleus will experience a recoil. The energy of recoil, E_R, is given by the expression

$$E_R = \frac{P^2_{photon}}{2M} = \frac{E_\gamma^2}{2Mc^2} \qquad (2.2)$$

where P_{photon} = momentum of emitted photon,

$\qquad$ M $\qquad$ = mass of nucleus,

$\qquad$ c $\qquad$ = velocity of light,

and $\qquad$ E_γ $\qquad$ = energy of emitted γ-ray.

By the Conservation of Energy, the transition energy, E_t, is

$$E_t = E_\gamma + E_R \qquad (2.3)$$

Now E_R is small compared to E_γ so eqn. 2.2 becomes

$$E_R = \frac{E_t^2}{2Mc^2} \qquad (2.4)$$

Therefore the emission and absorption spectra for nuclear systems are not coincident due to the recoil energy, E_R.

Area of resonant fluorescence

E_γ ← E_R → E_γ' Energy
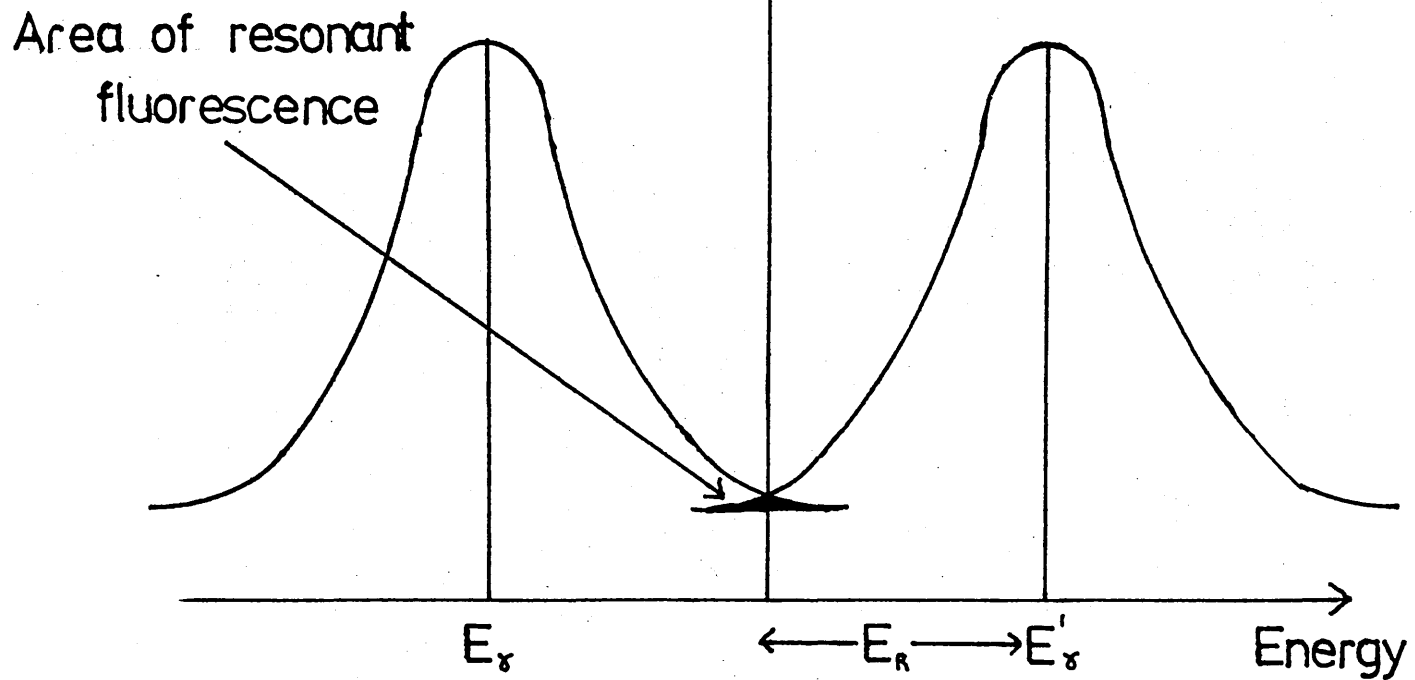
Fig. 2.1

The Effect of Recoil on the Nuclear Emission and Absorption

Spectrum

For energies in the region of 10 KeV, E_R becomes signifi-
cant and there is little overlap between the energy
profiles. Initial attempts to increase the amount of
resonant absorption included the use of high temperatures.
This gave rise to 'Doppler Broadening', E_D, which is a
result of the random thermal velocities of the source and
absorber nuclei. It can be shown that [76]

$$E_D = 2\sqrt{E_R kT} \qquad\qquad (2.5)$$

where T = temperature

and   k = Boltzmann's constant.

- 21 -

Therefore, although the overlap is increased slightly, the broadening of the lines results in a loss of precision. Removal of the recoil energy is therefore necessary in order to observe nuclear resonance absorption.

2.1.4 The Recoilless Free Fraction and Recoil Free Emission

On cooling a sample containing ^{191}Ir to 78K, Mössbauer found that instead of decreasing, the resonant absorption had increased, a fact which is contrary to eqn. 2.5. He explained this by considering the excited nucleus to be held rigidly in a solid lattice. In the Einstein model of the lattice, the nucleus has quantised energies and transitions occur through Phonon interactions. Therefore an energy of $\pm h\nu$, $\pm 2h\nu$, $\pm 3h\nu$ etc. is required to excite the lattice and $h\nu$, the minimum energy required to excite the lattice corresponding to a single phonon transition, is called the Einstein Energy, E_E. If the recoil energy, E_R, is much greater than E_E ($E_R >> E_E$), then the nucleus recoils and the energy is dissipated through the vibrational energy levels, but if $E_R < E_E$, then a zero phonon interaction occurs and the recoil is transferred to the whole crystal. As M is now large (eqn. 2.4), E_R becomes very small and the emission occurs effectively without recoil. Now the value of E_E can be raised by lowering the temperature, and so for solids at low temperatures, there is a finite probability of emission of γ-rays without recoil. Thus we define the Recoil-less Fraction, f, as the probability of emission without recoil or the fraction of zero phonon interactions.

This fraction, f, can be expressed thus:

$$f = \exp\left[\frac{-4\pi^2 \langle \chi^2 \rangle}{\lambda^2}\right] \qquad (2.6)$$

where $\langle \chi^2 \rangle$ = mean square vibrational amplitude of the
emitting (or absorbing) nucleus in the solid.

and λ = wavelength of the γ-photon.

For a finite f value, E_γ should be under 150 keV and
since $\langle \chi^2 \rangle$ has to be bounded in order that f does not
vanish, the Mössbauer effect cannot normally be observed
in a liquid.

2.1.5 Mössbauer Line Width

The energies of the emitted γ-rays are not identical and
in fact we observe a spread of energies about a mean,
with the line emitted having a certain natural breadth, Γ,
which is given in terms of an intensity distribution in the
Breit-Wigner equation [105], which describes a Lorentzian
line shape (Fig. 2.2).

$$I(E) = \frac{f_s \Gamma}{2\pi} \frac{1}{(E - E_0)^2 + (\Gamma/2)^2} \qquad (2.7)$$

where $I(E)$ = intensity of the distribution at energy, E,

f_s = probability of recoil-free emission from the
source,

E_0 = transition energy.

The approximate width of the line can be determined by
Heisenberg's Uncertainty Principle,

$$\Gamma = \frac{\hbar}{\tau} \qquad (2.8)$$

where τ = mean lifetime of the excited state.
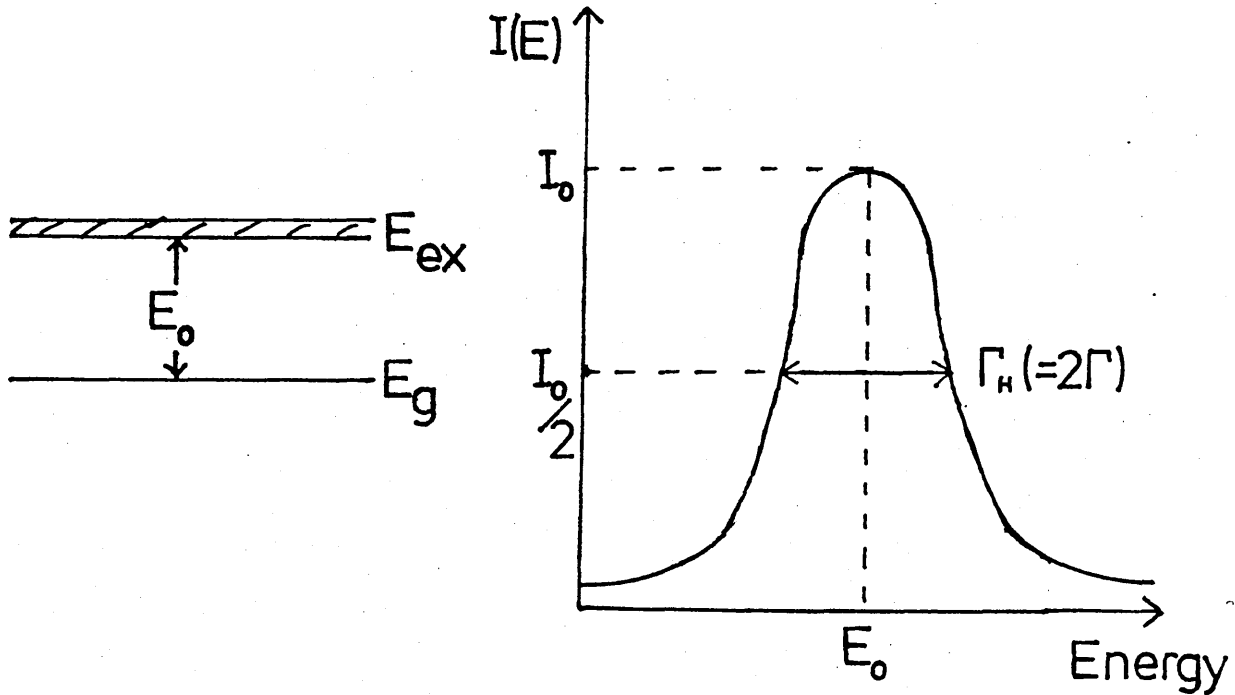
Fig. 2.2

The Line Shape of the Emitted γ-Ray

Therefore, we see that for the ground state the mean lifetime is infinite and the state is sharp, i.e. $\Delta E \rightarrow 0$. The full width at half height, Γ_H, can also be used to describe the resolution available to the technique.

For example, using ^{57}Fe, $t_{\frac{1}{2}} = 97.7$ ns and therefore $\Gamma_H = 9.34 \times 10^{-9}$ eV. The transition energy in ^{57}Fe is 14.4 KeV hence,

$$\frac{\Delta E}{E} = \frac{\Gamma_H}{E} = \frac{9.34 \times 10^{-9}}{14.4 \times 10^3} \sim 10^{-12}$$

This means that a resolution of 1 part in 10^{12} is theoretically possible.

2.1.6 The Mössbauer Spectrum

Even though the recoil energy loss and Doppler broadening effect have been minimised, resonance absorption will not be observed unless the emission and absorption profiles are exactly coincident. In general, this does not occur due to energy differences between the source and the absorber and in order to observe the resonance, the source is mounted on a vibrator, which moves backwards and forwards with a velocity V with respect to the absorber, imparting a range of energies due to the Doppler effect such that:-

$$E_\gamma = E_t + E_t \cdot \frac{V}{C} \qquad\qquad (2.9)$$

(This is in the case for the source moving towards the absorber.)

If a range of velocities is scanned, then at a particular velocity the energies will coincide, resonance will be at a maximum and the count rate at a minimum. At any higher or lower applied velocity, absorption will decrease until it is effectively zero at velocities well away from the resonant velocity. Therefore the Mössbauer spectrum comprises of a plot of absorption against a series of relative Doppler velocities between the moving source and stationary absorber. (Fig. 2.3)
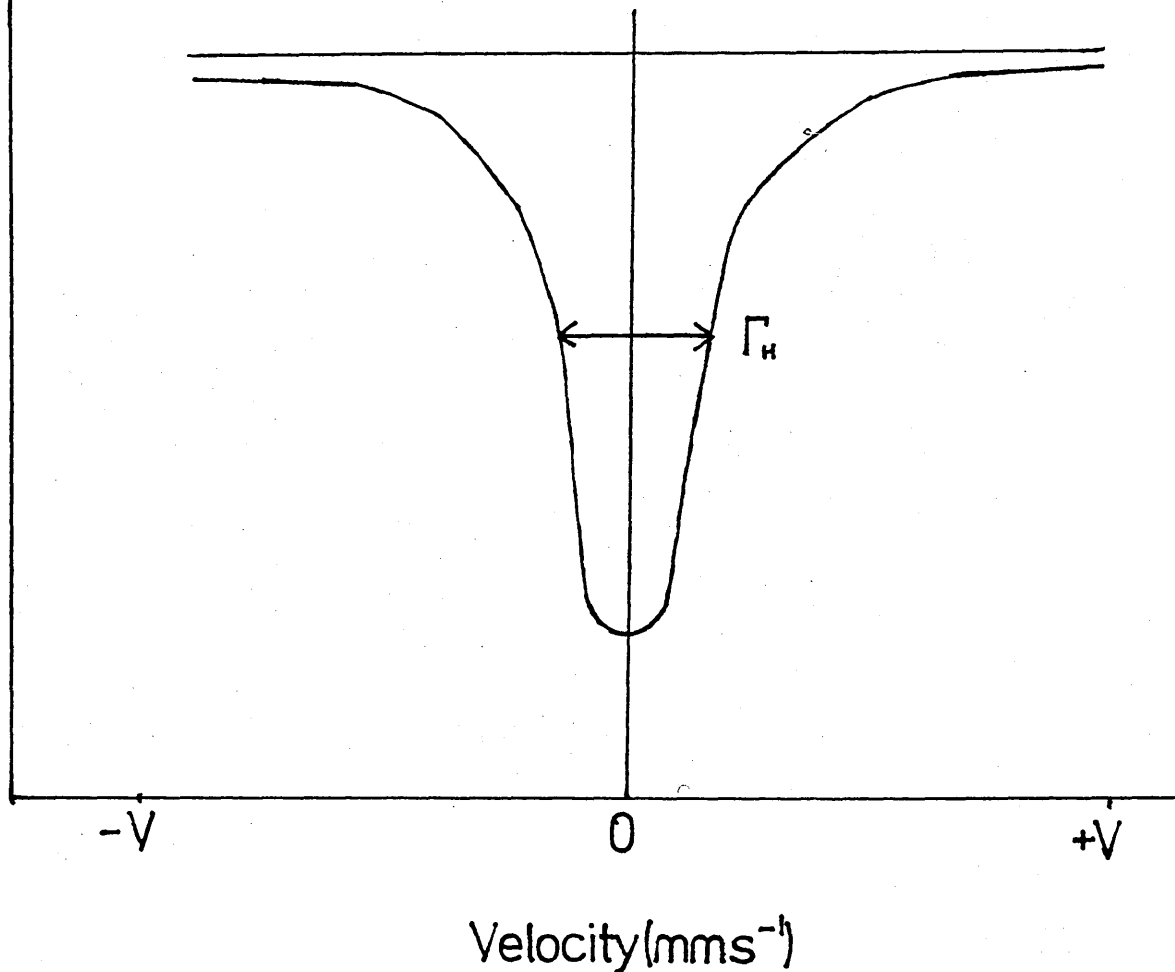
Fig. 2.3

A Mössbauer Spectrum

2.2 Hyperfine Interactions

The Mössbauer effect can be used to compare the nuclear

transition energies in two materials with high precision.

The nuclear energy levels are very sensitive to changes

in the electronic environment and therefore the Mössbauer

effect can be used to observe electronic changes resulting

from chemical bonding, magnetic interactions, impurity

effects etc. These changes arise from Hyperfine Inter-

actions between the nuclear charge distribution

and the magnetic fields and give rise to the isomer
shift (δ), quadrupole splitting (ΔE_Q) and magnetic
Zeeman splitting observed in the Mössbauer spectrum.

2.2.1 The Isomer Shift

The isomer, or chemical shift, results from the electro-
static interaction between the charge distribution of the
nucleus and those electrons which have a finite probability
of being found in the region of the nucleus, i.e. the 's'
electrons.   This interaction does not lead to a splitting
of the nuclear energy levels, but results in a slight
shift of the Mössbauer energy levels.   As the 's'-electron
density of a given absorber generally differs from that of
the source, there is an energy difference between the
source γ-ray, energy $^{s}E_{\gamma}$, and the energy required for
resonant absorption, $^{a}E_{\gamma}$.   A Doppler velocity is therefore
applied to the source, to achieve resonant absorption,
this velocity corresponding to the isomer shift (Fig. 2.4).

$^e E_0$

$^s E_\gamma$

$^a E_\gamma > ^s E_\gamma$

$^a E_\gamma$

$^g E_0$

Single line
source

Single line
absorber

bsorption

Isomer shift = $^a E_\gamma - ^s E$

-V

0

+V

Velocity (mms⁻¹)
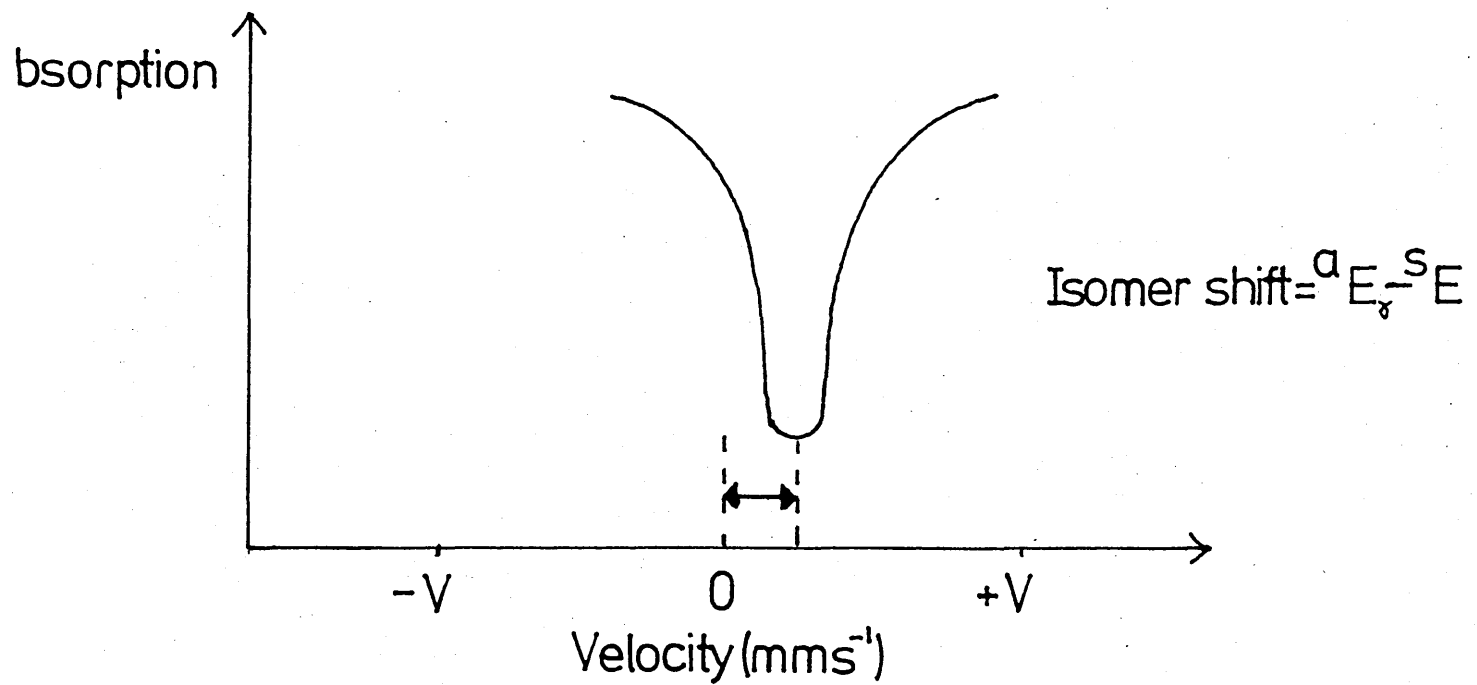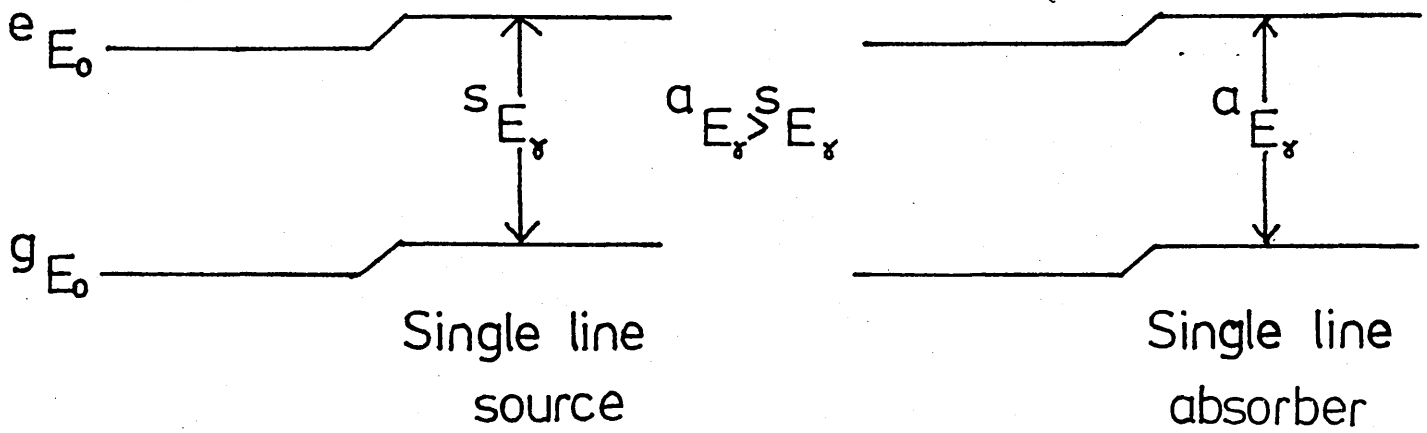
Fig. 2.4

Nuclear Energy Level and the Isomer Shift

- 28 -

The isomer shift, δ, is given by the expression:-

$$\delta = \frac{2\pi}{5}Ze^2\left\{\left[\psi(0)_s\right]^2_a - \left[\psi(0)_s\right]^2_s\right\}(R^2_{ex} - R^2_{gd}) \quad (2.10)$$

where R = radius of the nuclear volume

e = charge on the electron

Z = Atomic number

$\left[\psi(0)_s\right]^2$ = 's'-electron density

Although the 's'-electrons from the 1s,2s,3s .... levels will all contribute towards $\left[\phi(0)_s\right]^2$, the inner orbitals are not significantly affected by chemical bonding and the isomer shift will predominantly depend on the outermost occupied 's'-electron shell. The isomer shift can also be sensitive to the 'p' or 'd'-electron density due to shielding affects which cause a rearrangement of the spacial distribution of the 's'-electrons resulting in a change to the electron density at the nucleus. A decrease in the number of 'd' - electrons causes an increase in the total 's'-electron density at the iron nucleus and for iron, an increase in 's'-density leads to a decrease in the isomer shift, and the d^6-ion, Fe(II), has a larger isomer shift than a d^5-ion, Fe(III). This is because for iron the nuclear radius of the ground state, R_{gd}, is larger than that of the excited state, R_{ex}, and the term $(R^2_{ex} - R^2_{gd})$ becomes negative. For ^{119}Sn, $(R^2_{ex} - R^2_{gd})$ is positive and an increase in 's'-electron density results in a more positive isomer shift.

Therefore the isomer shift gives information about electron bonding and valency, and it is often treated as a 'measure of covalency'. If covalency occurs, then donation of electrons to the iron causes the isomer shift to become more negative, while ionic species have little or no shift.

2.2.2 Quadrupole Splitting

The theoretical models for the electrostatic interactions and isomer shift assume that the nucleus is spherical and that the charge distribution is symmetrical. If a non-spherical nucleus is considered, however, an interaction occurs between the nuclear quadrupole moment and the electric field gradient (EFG). The ground state of iron has spin, $I_g = \frac{1}{2}$ and the excited state has spin, $I_e = \frac{3}{2}$. Since only nuclei with spin 0 or $\frac{1}{2}$ are spherically symmetric and have zero quadrupole moments, the excited state of iron assumes either a prolate or an oblate shape resulting in a discrete quadrupole moment and this will interact with the EFG. The expression which describes this interaction is shown below, [76]

$$E_Q = \frac{e^2 q Q}{4I(2I-1)} \left[3M^2_I - I(I+1) \right] \left[1 + \frac{\eta^2}{3} \right]^{\frac{1}{2}} \qquad (2.11)$$

where Q = nuclear quadrupole moment

η = asymmetry parameter

M_I = magnetic quantum number

$eq = V_{zz}$ = maximum value of the electric field gradient

and $e^2 q Q$ = quadrupole coupling constant.

Now the M^2_I term in this equation results in a partial lifting of the degeneracy. Nuclear energy levels which have different values for the magnetic quantum number become split but states whose M_I differ only in sign remain degenerate. In ^{57}Fe, the excited state energy level splits into two while the ground state energy level remains degenerate, Fig. 2.5.
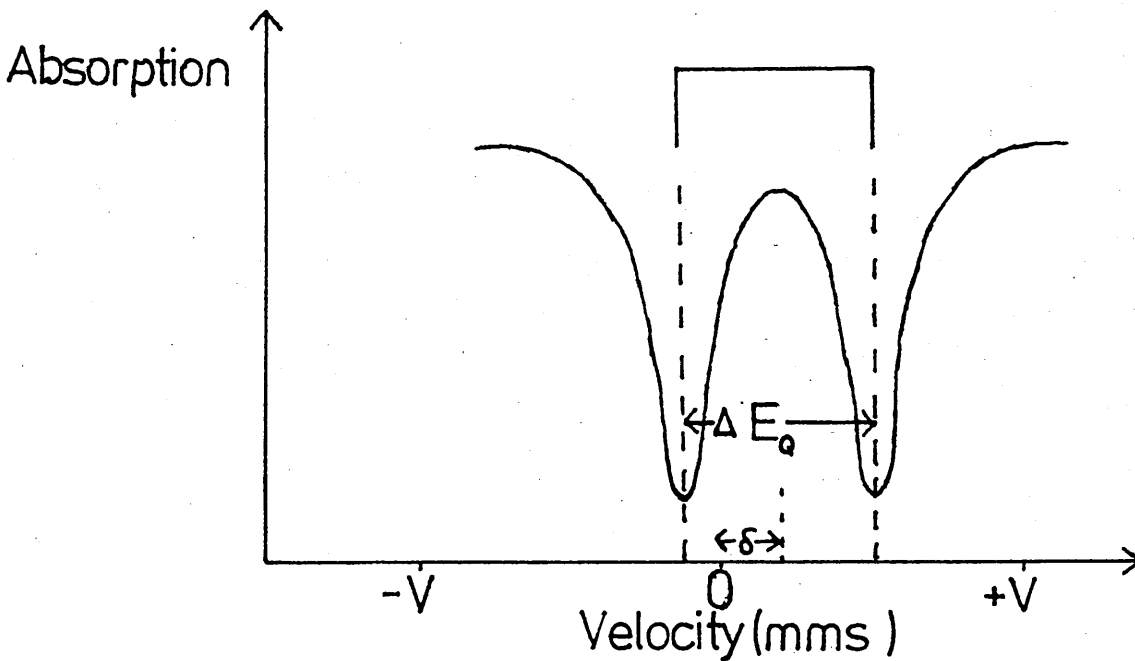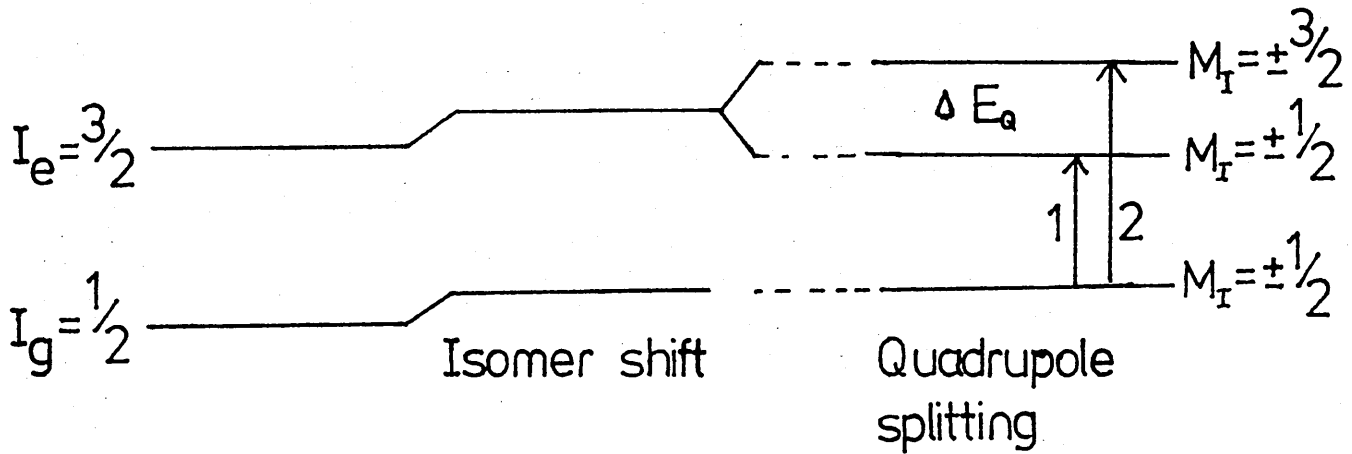
Fig. 2.5

Quadrupole Splitting in ^{57}Fe

Both the possible transitions are allowed and the characteristic two line spectrum is obtained. The separation of the two peaks is the quadrupole splitting, ΔE_Q.

The magnitude of the quadrupole splitting is proportional to the z component of the EFG tensor which interacts with the quadrupole moment of the nucleus.

The EFG tensor has nine components and the electric field at the Mössbauer nucleus is the negative gradient of the electrostatic potential, V,

$$\underline{E} = -\nabla V = -(\underline{\hat{i}}V_x + \underline{\hat{j}}V_y + \underline{\hat{k}}V_z) \qquad (2.12)$$

where $V_x = \frac{\delta V}{\delta x}$, $V_y = \frac{\delta V}{\delta y}$ and $V_z = \frac{\delta V}{\delta z}$.

Now the EFG is the gradient of the electric field, E, and can be expressed as a 3 x 3 matrix which contains the resultant combinations of the cartesian axes from the centre of the nucleus.

$$E.F.G. = \nabla E = \begin{bmatrix} V_{xx} & V_{xy} & V_{xz} \\ V_{yx} & V_{yy} & V_{yz} \\ V_{zx} & V_{zy} & V_{zz} \end{bmatrix}$$

where $V_{ij} = \frac{\delta^2 V}{\delta_i \delta_j}$

The above tensor can be reduced to diagonal form if the co-ordinate axes are properly chosen so that the EFG can be completely specified by the three components, V_{xx}, V_{yy} and V_{zz}. However, these components are not independent

- 32 -

since the Laplace equation requires that

$$V_{xx} + V_{yy} + V_{zz} = 0 \qquad\qquad (2.13)$$

There are then only two independent parameters, and these are normally chosen to be V_{zz} and an asymmetry term, η, where

$$\text{where} \quad \eta = \frac{(V_{xx} - V_{yy})}{V_{zz}} \qquad\qquad (2.14)$$

The EFG axes are then chosen such that the off diagonal components are zero and that

$$V_{zz} \geqslant V_{yy} \geqslant V_{xx}$$

which constrains η to have values between 0 and 1. From eqn. 2.14 it can be seen that, if the EFG is axially symmetric, $V_{xx} = V_{yy}$ and η becomes zero, while for spherical symmetry each of the $V_{ii} = 0$ and there is no quadrupole interaction.

The magnitude of the quadrupole splitting is therefore dependent on V_{zz} and η and any changes in symmetry will affect the value of the quadrupole splitting.

In general, the EFG has two contributions. The first contribution comes from the electrons in the atom and if the orbital population is non-spherical, then the value of V_{zz} is non-zero. Excess electron density in the xy phase (i.e. electrons in $p_x, p_y, d_{xy}, d_{x^2-y^2}$ orbitals) will make V_{zz} positive in sign while if the excess electron density is along the z axis (i.e. electrons in $p_z, d_{z^2}, d_{xz}, d_{yz}$ orbitals) then V_{zz} becomes negative. Therefore it can be

seen that the quadrupole splitting is very sensitive to changes in the electron distribution around the Mössbauer atom.

Secondly, there is also a contribution from ionic changes associated with the ligands called the Lattice contribution and this becomes important for an 's'-state ion where there is negligible valence contribution.

2.2.3 Magnetic Hyperfine Interaction

The third hyperfine interaction is the nuclear Zeeman effect which occurs if there is a magnetic field at the nucleus. The hyperfine splittings arise from the inter-action between the magnetic hyperfine field, 'B', and the Nuclear Magnetic Dipole Moment, 'μ'. The hyperfine field may be due to the atom's own electrons, to long-range exchange interactions or to an external applied magnetic field. The result is to completely remove the degeneracy associated with the nuclear levels.

The equation describing the Hamiltonian of the interaction is [76]

$$\mathcal{H} = - \underline{\mu} \cdot \underline{B} = - g_N \mu_N \, \underline{I} \cdot \underline{B} \qquad (2.15)$$

where μ_N = nuclear Bohr magneton

g_N = nuclear gyromagnetic ratio

I = nuclear spin.

The energy shifts associated with the interaction are given by

$$E_{M_I} = \frac{-\mu_N . B . M_I}{I} \qquad (M_I = I, \; I-1, \; I-2 \; .... \; -I)$$

$$= -g_N \mu_N B . M_I \qquad\qquad (2.16)$$

There is a nuclear Zeeman effect, and from equation 2.16 it can be seen that there will be 2I+1 equally spaced levels.

For ^{57}Fe there are six allowed γ-ray transitions, the symmetry being due to the selection rules, $\Delta M_I = 0, \pm 1$ for dipole radiation, (Fig. 2.6).

Because of the equal spacing between the line pair (1,2), (2,3), (4,5) and (5,6), the ^{57}Fe spectrum is used for calibration and linearity checks. Though the spacings are identical for these lines, their intensities are very different.

$$I_1 = I_6 = 3(1 + \cos^2\theta)$$
$$I_2 = I_5 = 4\sin^2\theta \qquad\qquad (2.17)$$
$$I_3 = I_4 = 1 + \cos^2\theta$$

where θ is the angle between the effective field, B, and the direction of the γ-beam.

Integrating the expressions in eqn. 2.17 gives an area ratio of the six lines as 3:2:1:1:2:3, as shown in Fig. 2.6.

$I_e = \frac{3}{2}$

No field

Magnetic field

$M_I = +\frac{3}{2}$

$M_I = +\frac{1}{2}$

$M_I = -\frac{1}{2}$

$M_I = -\frac{3}{2}$

$I_g = \frac{1}{2}$

$M_I = -\frac{1}{2}$

$M_I = +\frac{1}{2}$

Absorption

1 2 3   4 5 6

-V   0   +V

Velocity(mms^{-1})
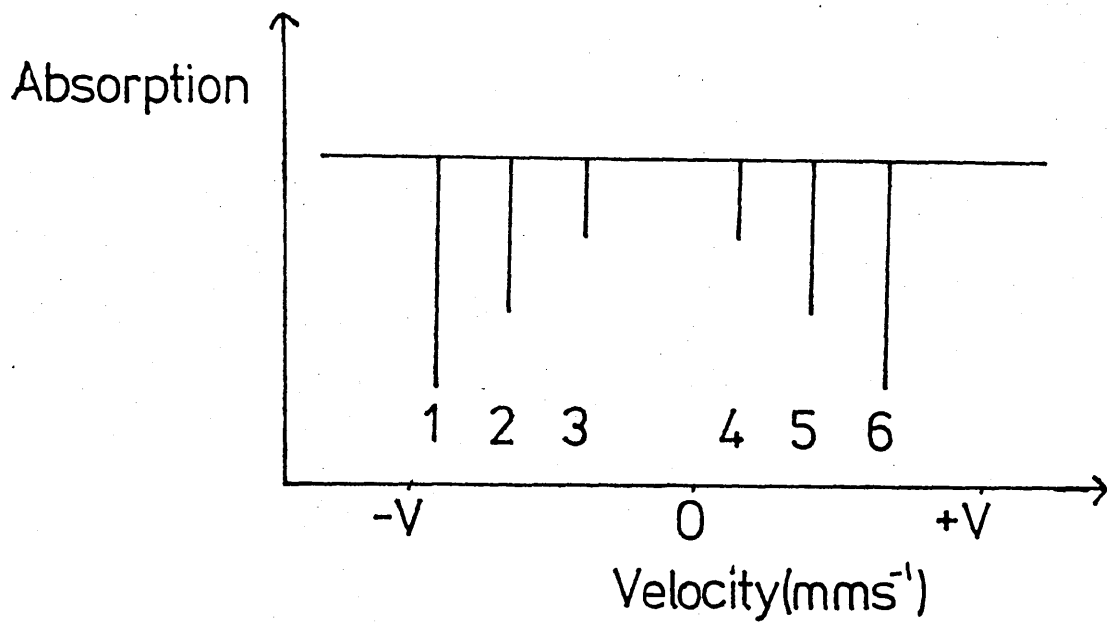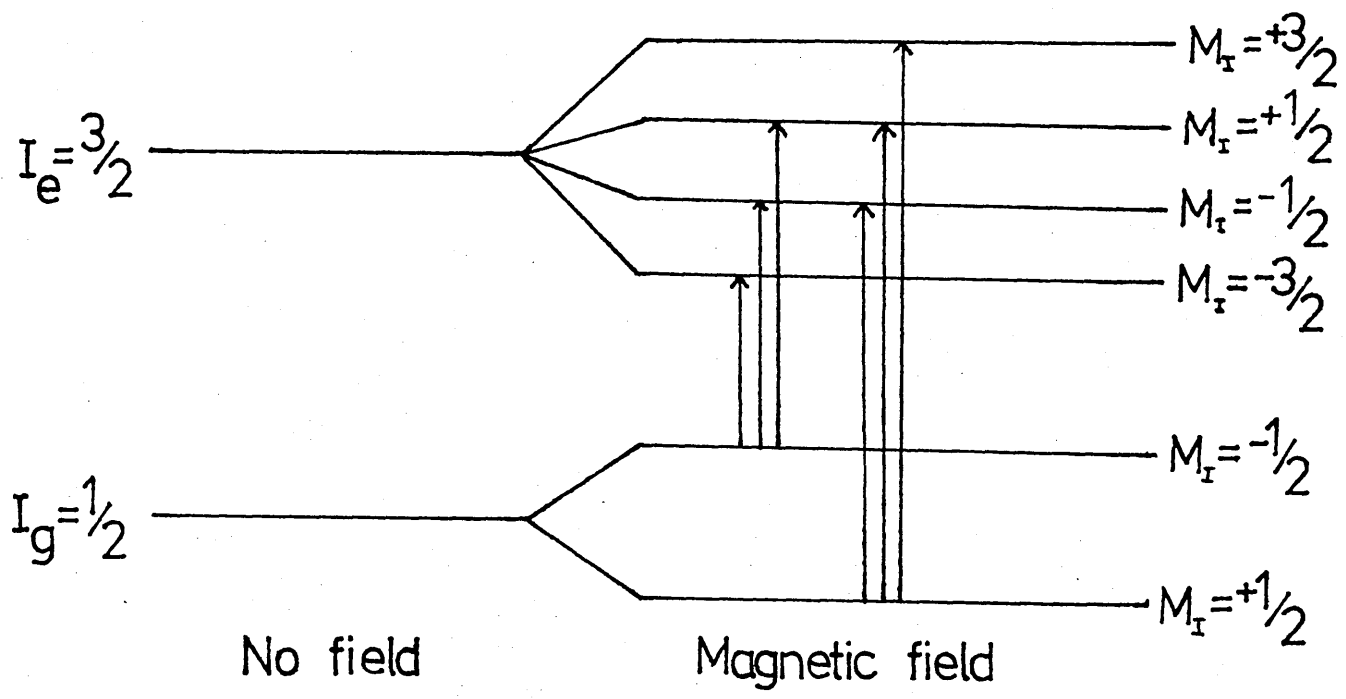
Fig. 2.6

The Magnetic Hyperfine Splitting in ^{57}Fe

2.3.1   The Mössbauer Isotope

Mössbauer Spectroscopy is not a technique open to all elements in the Periodic Table. Whether a suitable Mössbauer Spectrum is obtained or not is dependent on a number of factors:

(i)   The energy of the γ-ray should fall between 10 and 100 KeV. Lower energy γ-rays are strongly absorbed in solid matter while higher energy γ-rays give very low values of the recoil-free fraction, f, (eqn. 2.6).

(ii)   The γ-ray energy must also be well separated from other photons, otherwise background levels become inconveniently high.

(iii)   The source must emit an unsplit Mössbauer γ-ray.

(iv)   The magnitude of the Mössbauer Effect is proportional to the area of absorption lines. Now for a 'thin' Mössbauer absorption line, [107]

$$A = \tfrac{1}{2}\pi.f_a.f_s.\sigma_0.n.X \qquad (2.18)$$

where A = Area under absorption curve,

f_a, f_s = Recoil-free fraction of the absorber and source,

σ_0 = Isotope cross-section,

n = Natural abundance of isotope,

and   X = Thickness of absorber.

From eqn. 2.18 it can be seen that to obtain a good quality Mössbauer spectrum, an isotope

is required which gives high values of 'f', has a
large natural abundance and a large cross-section.

(v)   The line positions obtained must be sensitive
      to small changes in the chemical environment and
      the change in the line positions must be measurable.

(vi) The parent isotope chosen must have a reasonably
      long half-life. The parent isotope used for
      ^{57}Fe work is ^{57}Co which has a half-life of
      270 days. The decay scheme for this isotope is
      shown in Fig. 2.7
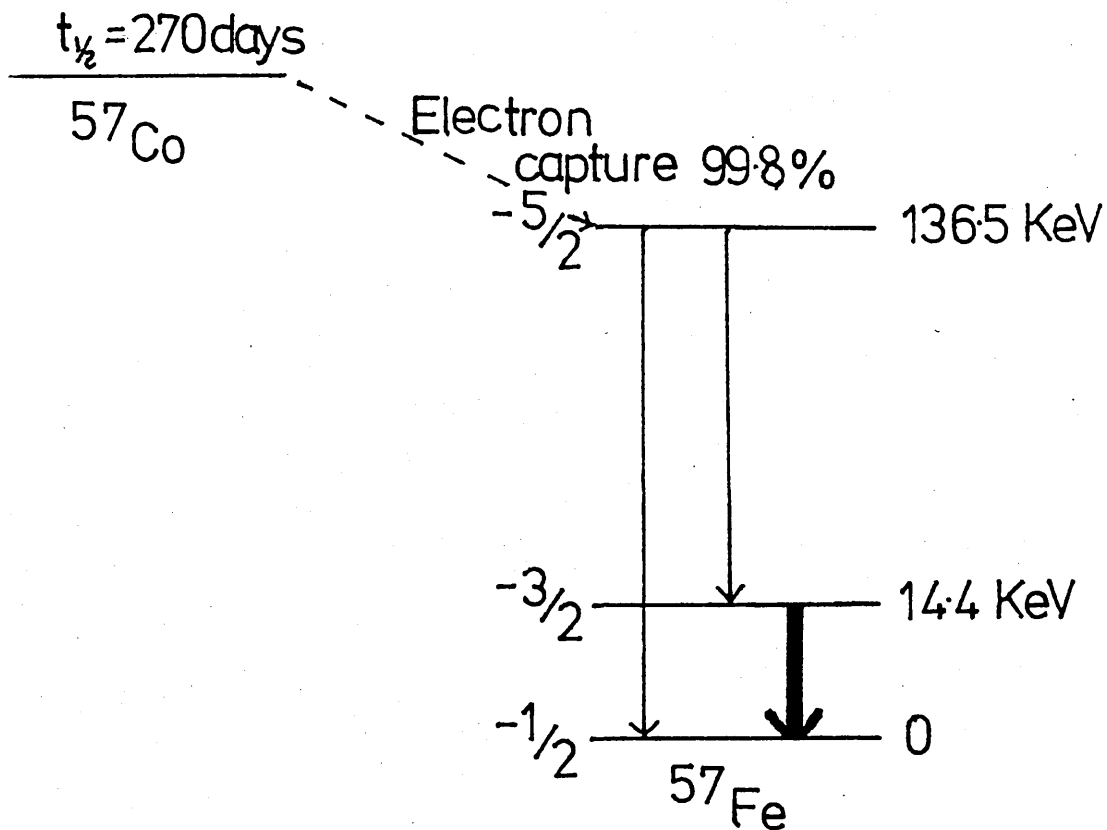
Fig. 2.7

Decay Scheme for ^{57}Co

The γ-ray used in ^{57}Fe Mössbauer Spectroscopy is the 14.4 KeV γ-ray which has a natural half width, Γ, of 0.096 mm s^{-1}, [76]. The ^{57}Co isotopes used in this work were in palladium or rhodium matrices with activities on purchase of 10-12 mCi, with typical line widths in the region of 0.11 - 0.12 mm s^{-1}. All the sources were supplied by The Radiochemical Centre, Amersham.

2.3.2 The Absorber

All the samples examined using Mössbauer Spectroscopy during the course of this work were solids. They were sealed inside a perspex cell, having a thickness of about 1 mm. The thickness of the cell is important because a very thin sample may not give any resonant absorption, while an increase in thickness results in the line shape deviating from Lorentzian shape and saturation effects are observed. An optimum thickness can be calculated by considering the area beneath the absorption wave as a function of thickness as shown by Williams and Brooks [107].

$$A(t) \; \alpha \; \tfrac{1}{2}t \; \exp(-\tfrac{1}{2}t).\left[I_0(\tfrac{1}{2}t) + I_1(\tfrac{1}{2}t)\right] \qquad (2.19)$$

where $A(t)$ = Area beneath absorption curve as a function of thickness

I_0 = Zero order Bessel function

I_1 = First order Bessel function.

For values of $t \leqslant 2$, eqn. 2.19 can be approximated to

$$A(t) \; \alpha \; f_s t(1 - 0.25t + 0.0625t^2 + ...) \qquad (2.20)$$

where f_s = Lamb-Mössbauer factor for the recoil-free fraction in the source.

The thickness of the absorber can be found using eqn. 2.21.

$$t = \beta.n.f_a.\sigma_0.X \qquad\qquad (2.21)$$

where β = relative intensity of absorption lines

(only applicable for multiple line spectra)

n = number of resonant nuclei/cm^3

f_a = absorber recoil-free fraction

σ_0 = resonant cross-section

and X = actual absorber thickness.

However, eqn. 2.21 is difficult to apply in practice because for many compounds the value of f_a is not known and only an upper and lower bound can be determined.

2.3.3 Instrumentation

The block diagram of the Mössbauer system is shown in Fig. 2.8. As mentioned in Section 2.1.6, the source is moved backwards and forwards allowing a range of energies to be scanned due to the Doppler effect. The simplest method of varying the velocity is to use a constant velocity vibrator, where the source is driven at uniform velocity, but this technique has limited use in research. The method used for this study was constant acceleration in which the velocity range $-V$ to $+V$ is repeatedly scanned at uniform acceleration (V = 4 mm/sec for most of this work, though larger scans were used for linearity checks). The amplitude of the symmetric triangular waveform determines the velocity scan and this waveform is produced by a velocity transducer (Elsint MVT-4). A driver/generator (Elsint MDF-N-5) converts this waveform into motion of the
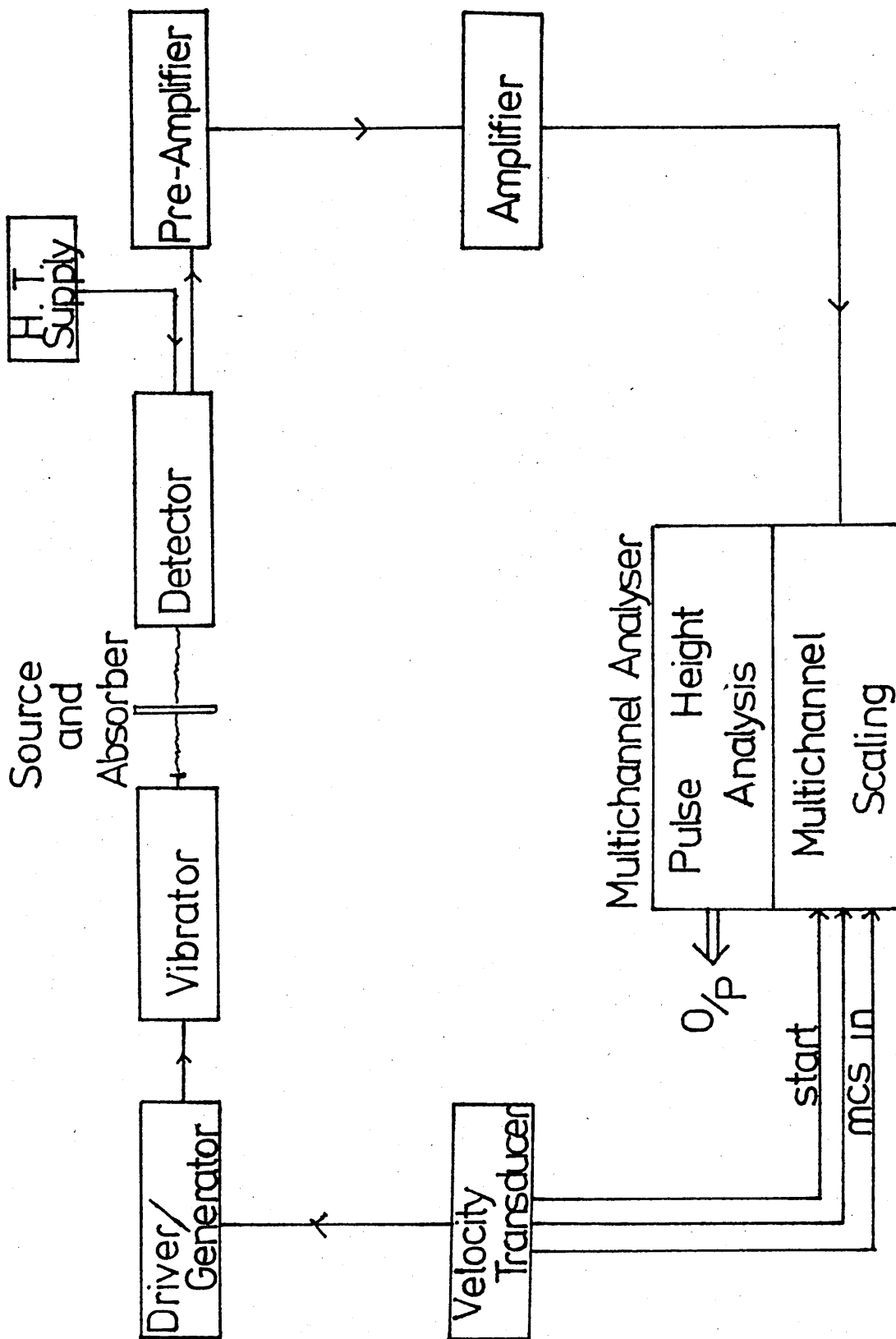
Fig. 2.8

Block diagram of the Mössbauer System

vibrator while the velocity transducer also drives the
multichannel analyser address in synchronisation with the
triangular wave.   The velocity waveform and the resulting
Mössbauer spectrum are shown in Fig. 2.9.
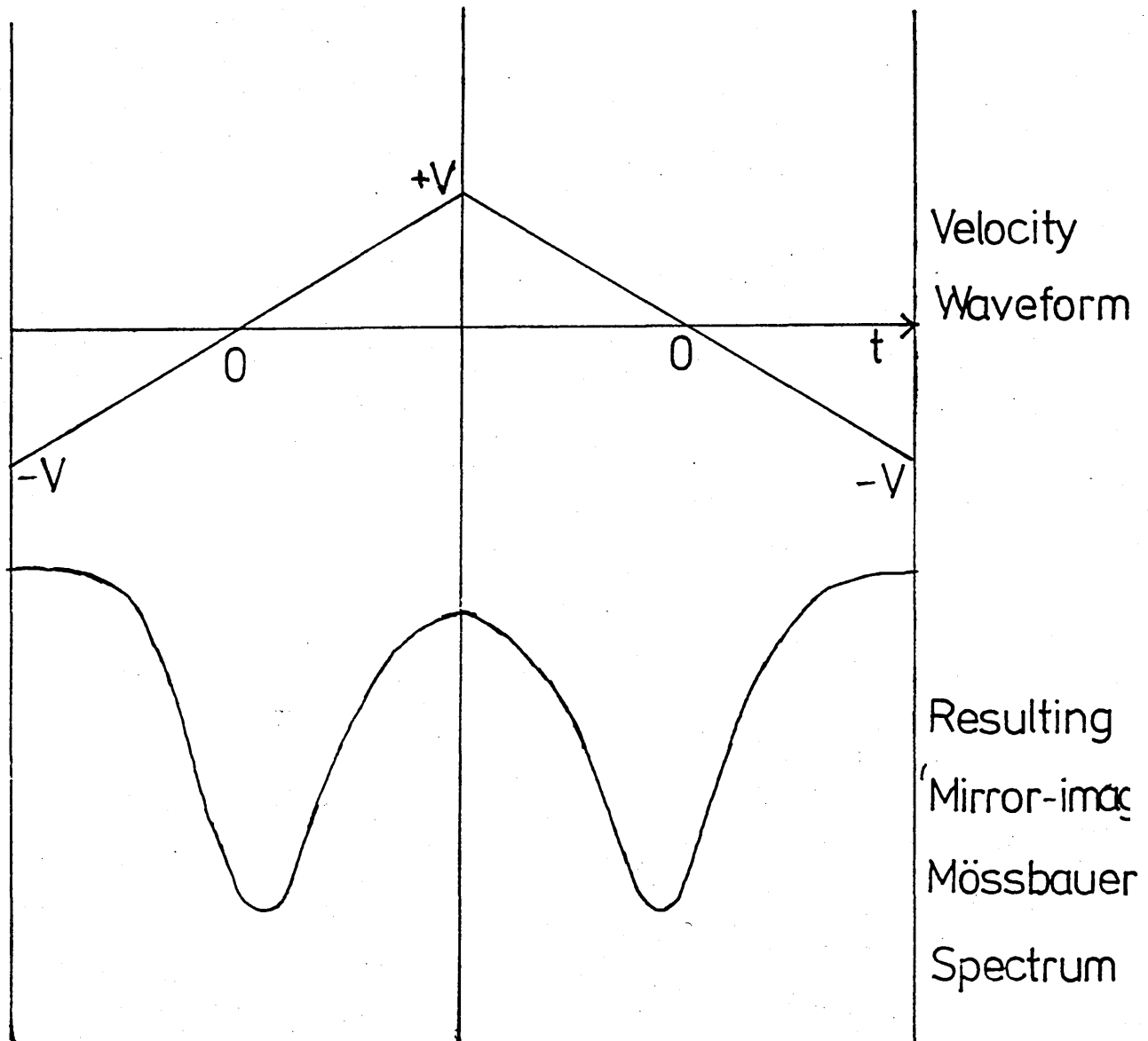
Fig. 2.9

Velocity waveform derived from constant acceleration
vibrator and resulting Mössbauer Spectrum

A 'mirror-image' is obtained and during the process of computer fitting (Section 2.3.5) the spectrum can be 'folded-over'.

The detector of the γ-rays, after they have been passed through the absorber, was a proportional counter, MPC 200. This has the special feature that the window does not contain any steel, important when studying iron compounds. It contains a mixture of 90% argon and 10% methane, giving efficiencies of the order of 65% at 14.4 KeV, whilst providing good rejection of counts from the 122 KeV γ-rays. This detector operates on a negative voltage of approximately -2.8 KV.

Once the γ-ray has been detected, the signal is passed via a pre-amplifier and an amplifier into the multichannel analyser (MCA). The MCA used in this work was a Canberra Series 30 with 1024 channels each with a capacity of 10^6 counts. It has two modes of operation available, the pulse height analysis (PHA) mode and the multi-channel scaling mode. The PHA mode sorts the random input pulses according to their peak amplitudes, and these amplitudes are proportional to the energies of the incident radiation absorbed by the detector. The resulting energy spectrum is collected over 512 channels of the MCA, and there is a facility present which can discriminate against any range of energies allowing only energies near the 14.4 KeV γ-ray to be counted. This eliminates any low energy noise in the imput signal and also the 6.4 KeV X-ray present in the pulse height spectrum.

In the multi-channel scaling mode, the MCA sweeps through the 512 channels, storing the number of counts obtained in a preset time in each channel. After all 512 channels have been used, the process is repeated. The MCA is in synchronisation with the constant acceleration drive function so that each particular channel corresponds to a particular velocity and the velocity increment per channel is constant.

2.3.4 Cryogenic System

The cryostat used to obtain temperatures down to 80K was the CF200 continuous flow cryostat, shown in Fig. 2.10.

Sample access port

Combined evacuation
and safety valve

Also- inner evacuation valve
        - 10 pin electrical connector

Helium
inlet

273 DIA
(69.3 mm)

Exchange gas space

Windows
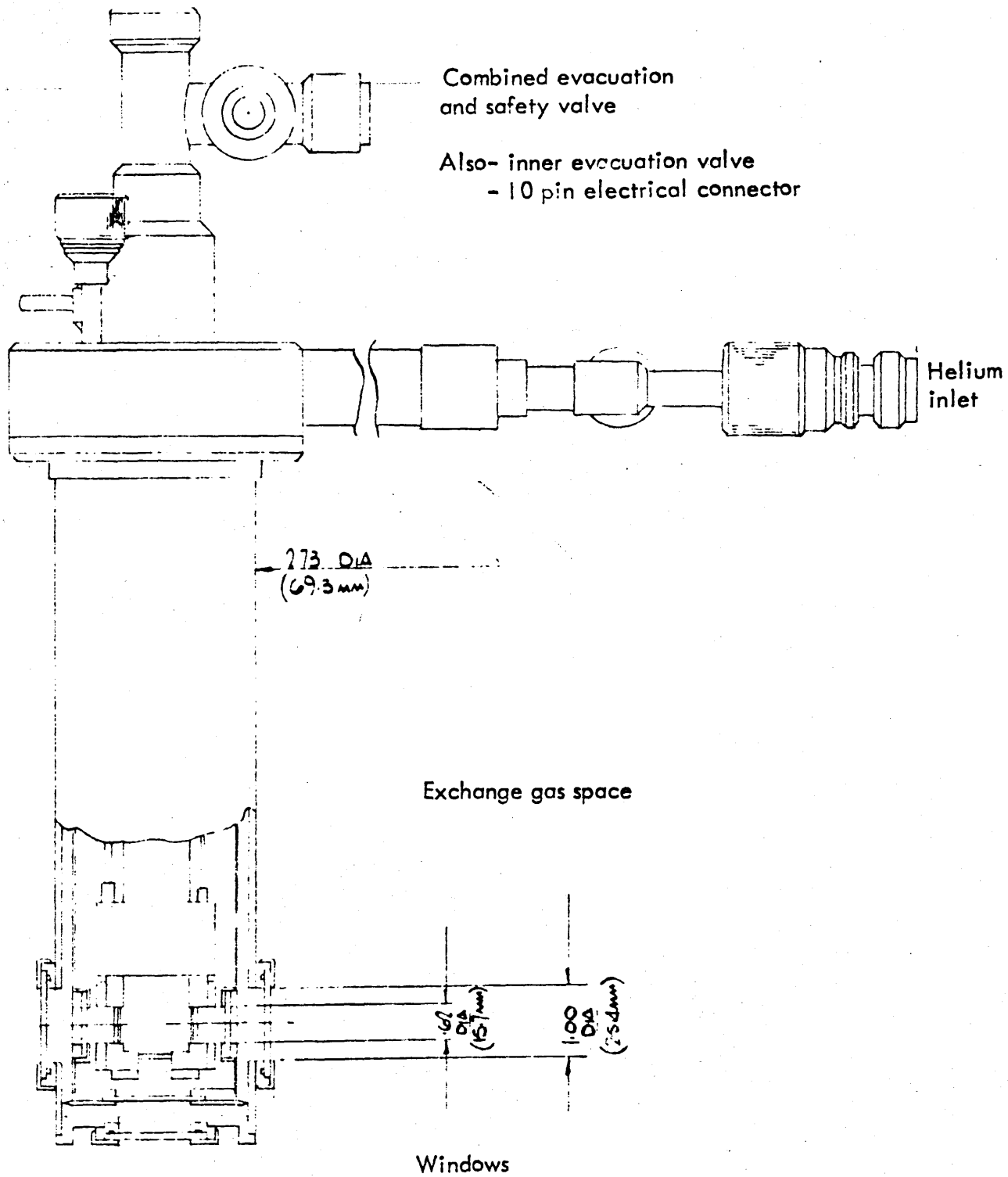
Fig. 2.10

The CF200 Continuous Flow Cryostat

The sample was put into a gold-plated sample probe (Fig. 2.11) and   inserted into the central chamber of the cryostat.
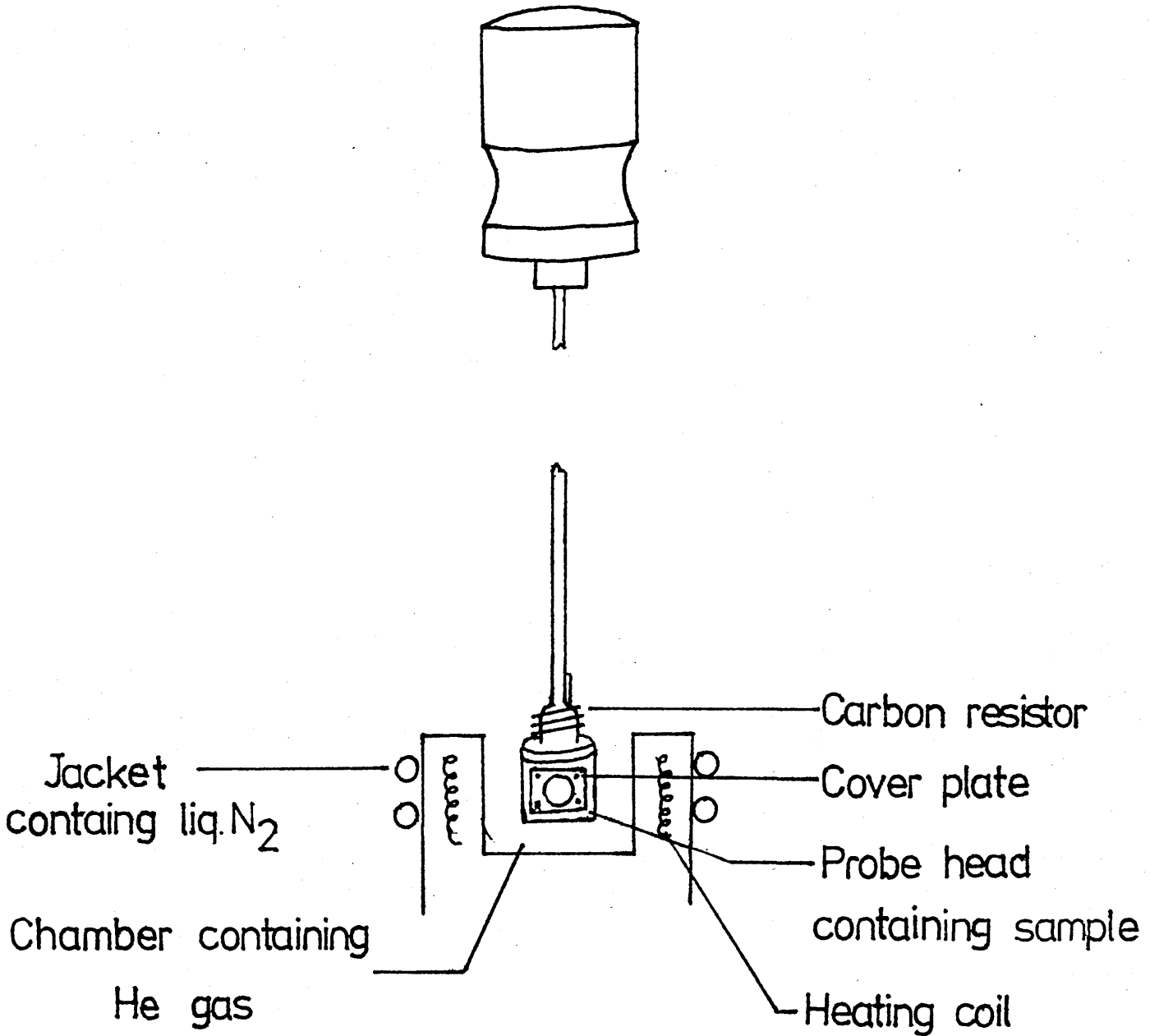
Fig. 2.11

Sample Probe used with Cryostat

The sample chamber, which was evacuated and filled with helium gas, was maintained at low temperatures by liquid nitrogen circulating around the outer jacket of the cryostat. The liquid nitrogen reached the jacket via a transfer tube which conveyed the coolant from a reservoir.

The temperature was measured using a DTC2 calibrated linear temperature sensor which showed the actual temperature inside the chamber as a four digit number. If the temperature required was higher than liquid nitrogen temperature, then a signal was generated by the DTC2 which was proportional to the increase in temperature required, and a suitable correction was made by warming the system using the heating coil.

The temperature can also be monitored using a calibrated carbon resistor and a digital multimeter. This is located at the base of the sample holder and represents, in terms of resistance, the temperature inside the sample chamber.

The solid samples were sealed inside perspex discs as mentioned previously (Section 2.3.2) and held inside the probe by means of a cover plate. The hole in the centre of this plate allows the γ-rays to pass through the sample into the detector, via the aluminised-mylor windows in the cryostat.

As ^{57}Fe studies of ferrocenes and polyvinylferrocenes give adequate Mössbauer spectra at room temperature, the cryostat was only required for the variable temperature studies (Chapter 6).

2.3.5   Computer Fitting of the Data

Once the data had been collected by the multi-channel analyser, it was fitted to a theoretical Lorentzian function (eqn. 2.7) using a program based on the work of Lang and Dale [108].

Firstly, because of the nature of the triangular waveform (Fig. 2.9), the spectrum obtained was a mirror image about channel 256. A program was used to fold the data stored in channels 0 → 256 on to the data in channels 256 → 512. By scanning 10 half-channels either side of the expected folding position, the best mirror axes for the absorption peaks was obtained so allowing for small fluctuations in the d.c. level of the drive system.

The folded data was then fitted by a non-linear least squares program to a theoretical Lorentzian line shape relative to a constant background. The program calculated the line positions, widths and relative depths and also indicated the quality of the fit by giving a value for χ^2 where

$$\chi^2 = \sum_{i=0}^{i=256} (x_i^{experimental} - x_i^{theoretical})^2 \qquad (2.23)$$

A large deviation between the theoretical and measured curves gave a large value of χ^2.

There were two types of fitting conditions used.

Option 1 : The program fits the data as individual absorption lines. The estimated position, width and depth

of each line are altered until the best fit is obtained.

Option 2 : The lines are fitted as pairs. For each set of doublets, the estimated centre, splitting/2, width and depth are altered until the best fit is obtained.

The program is also used to determine the optimum values of the background counts, baseline curvature and overall intensity of the spectrum.

The velocity range of the Mössbauer spectrum was determined by the amplitude of the triangular waveform. The positions of the lines given by the folded data were shown in channels so to obtain the results in terms of Doppler velocities, the increment per channel must be converted into mm s^{-1}. In order to calculate a calibration constant, C, the magnetic six-line spectrum of enriched iron is used (Section 2.2.3). The Doppler velocities of each line in this spectrum have been determined very accurately [109],[110] and are as follows:

Lines 1 and 6 = $\pm$ 5.312 mm s^{-1} }
Lines 2 and 5 = $\pm$ 3.076 mm s^{-1} } Error $\pm$ 0.001
Lines 3 and 4 = $\pm$ 0.8397 mm s^{-1} }

These values can be used to determine C using the following expression:

$$C = \frac{\text{Splitting of each pair}}{2 \text{ x Doppler velocity}} \quad \text{channels mm}^{-1}\text{s}^{-1} \quad (2.23)$$

The final value of C is calculated using the average value for the three pairs of lines.

As the velocity range used in this work was $\pm$ 4 mm s^{-1}, the spectrum obtained for enriched iron showed only the four inner lines and so the final value of C was calculated from the average of just two results.

A check on the linearity of the triangular wave can also be made using the magnetic six-line spectrum of iron as all the spacings between the lines should be the same (excluding lines 3 and 4 which represent the difference between the ground and excited states in the magnetic splitting).

In the calculation of the hyperfine splittings, the possible error in the results was quantified as $\pm$ 0.02 mm s^{-1}. This final value arises from errors in fitting, calibration, linearity and folding.

2.4   The Mössbauer Spectra of Ferrocene and its Derivatives

If the isomer shift is a measure of covalency, then ferrocene and its derivatives belong to the most strongly covalent compounds of iron. Ferrocene compounds, with the iron in the +2 oxidation state, give rise to larger isomer shifts than the oxidised +3 state. This is because the Fe(II), 3d^6 compounds subject the nucleus to greater shielding and therefore lower the s-electron density with respect to the Fe(III), 3d^5 species.

The Mössbauer parameters of a number of ferrocene derivatives are shown in Table 2.1.

Table 2.1 Mössbauer Parameters of Ferrocene and a Number of its Derivatives[a]

Compound $C_5H_5FeC_5H_4R$	Isomer Shift, δ[b] $(mm\ s^{-1})$	Quadrupole Splitting, Δ $(mm\ s^{-1})$	Reference
R=H	0.53	2.37	48
Cl	0.54	2.40	48
Br	0.53	2.46	48
I	0.54	2.44	48
CH_2OH	0.54	2.37	48
$COCH_3$	0.53	2.24	48
COOH	0.53	2.21	48
CN	0.53	2.30	47
CH_3	0.52	2.39	47

a   All measurements carried out at 80K

b   All isomer shifts relative to metallic iron at room temperature unless otherwise indicated.

From Table 2.1, it can be seen that ring substitution produces negligible changes in the isomer shift which is to be expected if one considers that the molecular orbitals of ferrocene are not formed with orbitals of a single ring atom but with the ring as a whole (Section 1.1).

The variation in the quadrupole splitting values within the Fe(II) high spin state is also fairly small. This is a consequence of the fact that the EFG at the nucleus arises largely from the π-bonding ligands which are not influenced by changes in the σ-bonding of various substituents on the ring as mentioned above. The small variations which are

observed are due to a small redistribution of electrons in the orbitals which can occur by ring substitution or by tilting the ring, usually achieved by forming a di- or tri-methylene bridge (Chapter 5). An attempt to quantify the redistribution has been carried out by Korecz et al [48]. The occupation of the 'd' orbitals may also be temperature dependent and so the quadrupole split may also vary with temperature.

Chapter Three : Experimental : Instrumentation, Materials and Techniques

3.1 Instrumentation

Infrared spectra of solid samples were recorded on a Pye Unicam SP200 spectrophotometer as KBr discs or in a nujol mull.

^1H Nuclear magnetic resonance (n.m.r.) spectra were recorded at room temperature in carbon disulphide using a Jeol C60 HL spectrometer and ^{13}C n.m.r. spectra were recorded in $CDCl_3$ on a Jeol PFT100 spectrometer by Dr B Taylor, University of Sheffield, or by Dr A V Cunliffe, Ministry of Defence, PERME, Waltham Abbey.

Gas-liquid chromatography was carried out using a Pye Unicam 104 chromatograph with toluene as the solvent for the samples.

Relative number average molecular masses were measured by vapour pressure osmometry [111] in toluene solution at $39^\circ C$ using a Hitachi/Perkin-Elmer Model 115 osmometer.

Molecular weight distributions were determined by gel permeation chromatography in THF at $35^\circ C$ by the Rubber and Plastics Research Association, Shawbury, Shrewsbury.

^{57}Fe Mössbauer spectra were obtained using a digital constant acceleration spectrometer having a symmetrical triangular velocity drive waveform. The data were folded to determine the zero velocity position and the folded data were fitted with Lorentzian functions by a non-linear least

squares fitting program. [108]

Mass spectra were recorded using an A.E.I./MS 30
instrument.

All melting and decomposition points were determined using
a Kofler melting point apparatus.

3.2 Materials

3.2.1 Synthesis and Purification of Vinylferrocene

Vinylferrocene (1-ferrocenylethene) was synthesised from
acetylferrocene (Aldrich Chemical Company) in two stages
via 1-hydroxyethylferrocene (1-ferrocenylethanol) as shown
in Fig. 3.1.
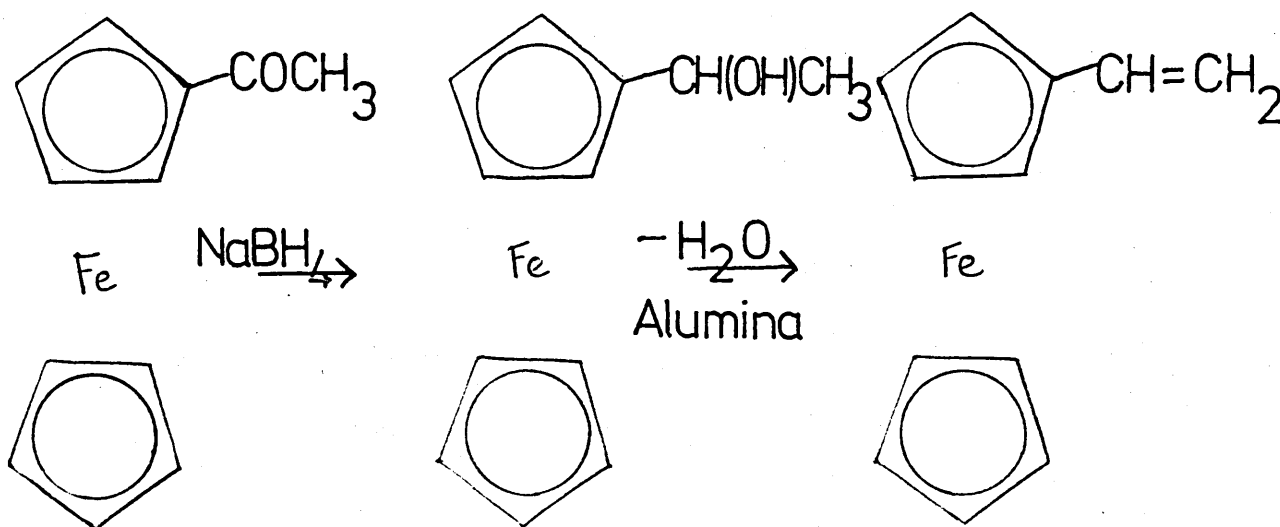
Fig 3.1 Synthetic route to vinylferrocene

1-Hydroxyethylferrocene

Acetylferrocene (25g) was dissolved in dry methanol, cooled
in ice, and treated with sodium borohydride (12.5g). The
cold solution was left until no more effervescence could be
observed and the initial red solution had changed to yellow.
Any unreacted $NaBH_4$ present was filtered off and destroyed

with dilute acetic acid. On addition of ice water to the
methanol solution, the product precipitated and was
filtered off and dried.   1-Hydroxyethylferrocene was
obtained as a yellow solid, mpt 75-77°C (lit 72-74°C [88]) in
yields of 70 to 80%.

Vinylferrocene

1-Hydroxyethylferrocene (12g) and activated alumina (25g)
were intimately ground together in a mortar, then placed
in a vacuum sublimator and heated at 140°C under reduced
pressure (~ 1 Torr) for three to four hours. The sublimed
crystals which collected on the water-cooled finger of the
sublimator yielded vinylferrocene, mpt 47-53.5°C (lit 46.5-
53.5°C). [28],[38] and[49] Yields obtained by this method were
in the range 60-75%.

Previous workers have used successive sublimations[28] or
recrystallisations [68] as a method of purification for the
monomer. Determination of the purity of vinylferrocene can
be carried out by thin layer chromatography (TLC) on silica
gel plates [68] and also by determination of the melting point.
For a more accurate determination of the purity of the
monomer, gas-liquid chromatography has been used. [28],[112]
The chromatogram has been published [28][112] but the impurity
present, which appears at a shorter retention time than
vinylferrocene, has not been identified.

Chromatograms of vinylferrocene, 1-hydroxyethylferrocene,
acetylferrocene and ferrocene were run on two different
carbowax columns (20% polyethylene glycol (PEG) 20M and 1%

PEG 20M), as used by Hayes,[23] [112] and also on diethylene glycol succinate (DEGS) and methyl silicone (SE) columns. The retention times, R_T, for each component on each column are shown in Table 3.1. R_T is dependent upon the temperature, flow rate and the column used, but it was found that under the same conditions on all four columns vinylferrocene and 1-hydroxyethyl ferrocene always gave similar R_T values and were not separable using any of the columns. Acetylferrocene gave long R_T values relative to those of vinylferrocene and the alcohol, while the retention times of ferrocene were relatively short. However, it is unlikely that ferrocene was the impurity present in published chromatograms as all traces of this compound would certainly be removed at an earlier stage in the synthesis of the monomer. However, while the impurity has not been identified, it was found to be removed after repeated recrystallisations, as confirmed by GLC.[28], [112] Therefore, it is postulated that the impurity was a result of a side reaction which took place during the final step of synthesis.

Another approach evaluated for purification of the monomer was column chromatography using an alumina or silica column. However, a small decrease in the yield of vinyl-ferrocene was observed with this approach.

3.2.2 Synthesis of 1,1'Divinylferrocene

1,1'Divinylferrocene was synthesised by the route shown in Fig. 3.2.

Table 3.1 : GLC Retention Times of Ferrocene Derivatives[a]

(a) 20% PEG 20M

Sample	Flow Rate/ cm^3 min^{-1}	Temp/ $^\circ C$	Average R_T
Vinylferrocene	40	200	18 min 35
1-hydroxyethylferrocene	40	200	18 min 37
Acetyl ferrocene	40	200	43 min 05

(b) 1% PEG 20M

Sample	Flow Rate/ cm^3 min^{-1}	Temp/ $^\circ C$	Average R_T
Vinylferrocene	40	200	4 min 10
1-hydroxyethylferrocene	40	200	4 min 12

(c) 10% DEGS

Sample	Flow Rate/ cm^3 min^{-1}	Temp/ $^\circ C$	Average R_T
Vinylferrocene	80	180	2 min 29
Vinylferrocene	40	150	6 min 02
1-hydroxyethylferrocene	80	180	2 min 32
1-hydroxyethylferrocene	40	150	6 min 07
Acetyl ferrocene	40	150	13 min 25
Ferrocene	40	150	3 min 36

(d) 10% SE30

Sample	Flow Rate/ cm^3 min^{-1}	Temp/ $^\circ C$	Average R_T
Vinylferrocene	40	200	7 min 45
1-hydroxyethylferrocene	40	200	7 min 48
Acetyl ferrocene	40	200	13 min 56
Ferrocene	40	200	4 min 33

a, All samples were dissolved in toluene as solvent and all injections were 1 µl

Fe $\xrightarrow[\text{AlCl}_3, \text{CH}_2\text{Cl}_2]{\text{CH}_3\text{COCl}}$ Fe $\xrightarrow{\text{LiAlH}_4}$ Fe $\xrightarrow[\text{Alumina}]{-\text{H}_2\text{O}}$ Fe

COCH$_3$ CH(OH)CH$_3$ CH=CH$_2$
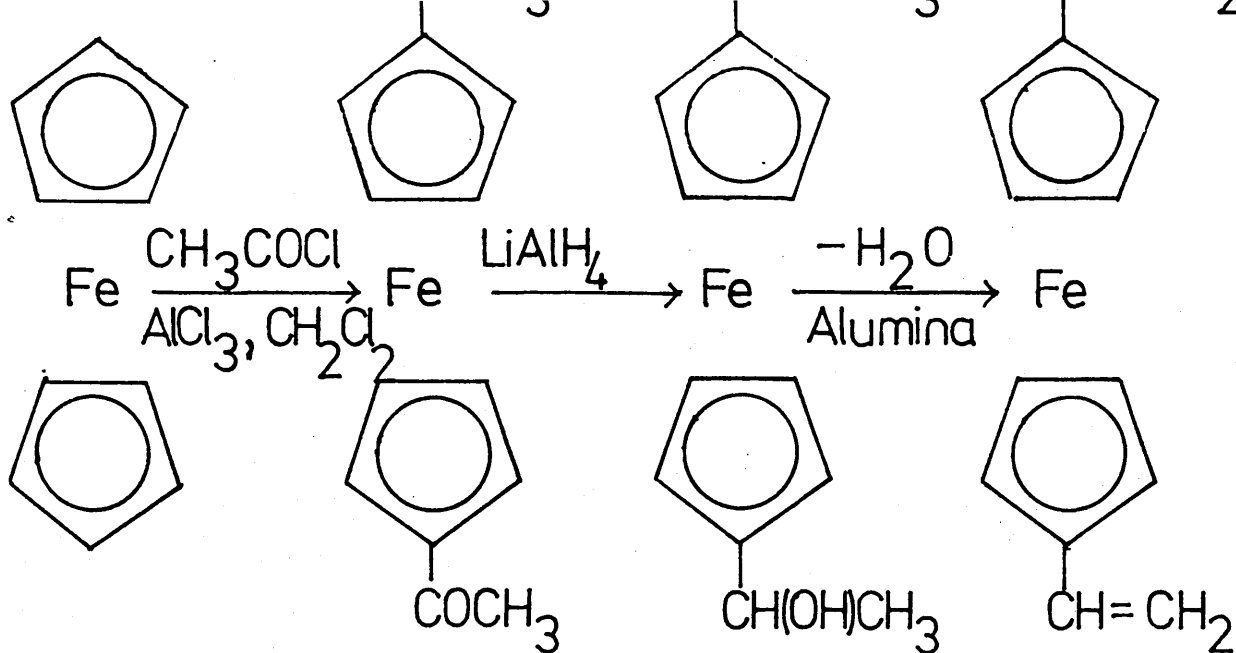
Fig 3.2   Synthetic route to 1,1'Divinylferrocene

1,1'Diacetylferrocene

Anhydrous aluminium chloride (53g), acetyl chloride (32 cm^3) and dichloromethane (100 cm^3) were stirred together at room temperature under a nitrogen atmosphere. A solution of ferrocene (30g) in dichloromethane (140 cm^3) was added to the mixture over 10 min. and the solution left stirring for a further 2h. Ice water was added to the solution to neutralise any excess acetyl chloride and the product filtered off and extracted with chloroform to give 60-70% yields of 1,1'diacetylferrocene as a ruby red solid, mpt 128.0-131.5°C (lit 127.5-128.5°C,[70] 130.0-131.0°C [113]) after recrystallisation from methanol.

1,1'Bis(1-hydroxyethyl)ferrocene

Diacetylferrocene (25g) was reduced using a suspension of lithium aluminium hydride (10g) in THF (450 cm^3). [114] The mixture was refluxed for two hours after which water was

added very slowly to destroy the excess reducing agent.
The resulting yellow solution was filtered and extracted
with diethyl ether which was dried over anhydrous sodium
sulphate. The solvent was removed under reduced pressure
and the remaining solid was recrystallised from methanol.
Yellow crystals of 1,1'bis(1-hydroxyethyl)ferrocene were
obtained in yields of 65-80%, mpt 66-69°C (lit 69-71°C [114]).

1,1'Divinylferrocene

1,1'Bis(1-hydroxyethyl)ferrocene (12g) and activated
alumina (25g) were ground together in a mortar and heated
in a vacuum sublimator at 140°C and a pressure of about
1 Torr. After 3-4 h. red crystals of 1,1'divinylferrocene
were obtained in 50-60% yields, mpt 39-41°C (lit 40-41°C [38]).
Double recrystallisation from methanol was used as a
method of purification.

Divinylferrocene is very air sensitive and appeared to
decompose very quickly at room temperature. Vinylferrocene
is slightly less sensitive, but both sets of samples were
sealed and stored under nitrogen at -20°C in the presence
of silica gel. It has been reported that no change in
the infrared spectrum or melting point of vinylferrocene
occurs under these storage conditions. [28]

3.2.3   Synthesis of 1,1'Trimethyleneferrocene

The synthesis of this compound was carried out to compare
its spectroscopic properties with those of the polymer
obtained by radical initiation of 1,1'-divinylferrocene
(Section 5.2.6).

β-Ferrocenylacrylic Acid (3-ferrocenylpropanoic acid), XII

Ferrocenealdehyde (5g), malonic acid (5g) and piperidine
(1 cm^3) were dissolved in pyridine (120 cm^3) and refluxed
under nitrogen for 3 h. The solution was cooled, diluted
with water and extracted with chloroform. The organic
layer was washed with dilute hydrochloric acid to remove
any remaining pyridine and the product extracted with dilute
sodium hydroxide solution. The aqueous solution was
acidified with dilute sulphuric acid and the resulting
red precipitate was filtered and dried at the pump.
β-Ferrocenylacrylic acid, 3.13g (53%) was obtained with
melting point 180-182°C (lit 186-187°C [115]).

β-Ferrocenylpropionic Acid (3-ferrocenylpropanoic acid), XIII

β-Ferrocenylacrylic acid (1.85g) was dissolved in absolute
ethanol (75 cm^3) and platinum oxide catalyst (0.5g) was
added. The solution was shaken under hydrogen at atmos-
pheric pressure for 1 h before the reaction was stopped and
the catalyst filtered off. The solution was then evaporated
to dryness to give 1.67g (90%) of XIII, melting point
121-122°C (lit 119-120°C [116]).

α-keto-1,1'-trimethyleneferrocene, XIV

β-Ferrocenylpropionic acid (1.50g) in dichloromethane
(35 cm^3) was added slowly, with stirring, to an ice-cooled
solution of trifluoroacetic anhydride (2.25g) in 35 cm^3 of
the same solvent. The mixture was stirred under nitrogen
for 5 h before pouring into a solution of saturated sodium
bicarbonate. The organic layer was separated, then washed

with water and dilute sodium hydroxide to remove any unreacted acid. Evaporation to dryness gave 1.22g (87%) of crude product with melting point 139-142°C. Recrystallisation from petroleum ether gave 0.87g (62%) of XIV, melting point 143-144.5°C (lit 141-142°C, 148-150°C [117], [116]).

1,1'-Trimethyleneferrocene, VII

A solution of aluminium chloride (0.45g) in dry ether (5 cm³) was added dropwise, with stirring, to a slurry of lithium aluminium hydride (0.1g) in ether (3 cm³) under a nitrogen atmosphere. The mixture was stirred for a further 15 min. at room temperature before a solution of α-keto-1,1'trimethyleneferrocene (0.5g) in ether (40 cm³) was added and the mixture was refluxed under nitrogen for 4 h. On completion of the reaction, excess lithium aluminium hydride was decomposed, firstly with wet ether and then with water, and the resulting aqueous solution was washed with ether and the organic layers combined. The organic extracts were washed with water, dried using anhydrous magnesium sulphate and then evaporated to dryness to give 0.42g (89%) of crude product, melting point 96.5-98.5°C. Recrystallisation from petroleum ether gave 0.35g (74%) of VII, melting point 102-103°C (lit 107.5 – 108.0°C [118]).

3.2.4   Synthesis of 1,3-Diferrocenylbut-1-ene, XX

1,3-Diferrocenylbut-1-ene, the model compound for the proposed structure of the polymer obtained by cationic

initiation of 1,1'-divinylferrocene was synthesised directly from 1-hydroxyethylferrocene[119] and also by a new route from acetylferrocene, as outlined in Fig. 5.15.

1,3 Diferrocenylbut-2-en-1-one, XXI [120],[121]

(a) Acetylferrocene (5g) and triethyl orthoformate (3.5g) were dissolved in benzene (100 cm^3). The solution was stirred at room temperature and hydrogen chloride gas was bubbled through the reaction mixture for 3 h. This caused the orange solution to turn dark-green and it was stirred for a further 2 h. More benzene (200 cm^3) was added before washing with water and saturated sodium bicarbonate solution, and removal of the solvent under pressure gave a red oil which was chromatographed on alumina (25g). Elution with petrol afforded three bands, the first of which was traces of 1,3-triferrocenylbenzene [120] which was not collected or studied. Further elution gave 2.10g of unreacted acetylferrocene and finally 1.13g (26%) of 1,3-diferrocenylbut-2-en-1-one. Traces of unreacted triethyl orthoformate were present and this resulted in a melting point, 116-118°C, lower than previously reported (lit 121-122°C,[120])

(b) Acetylferrocene (5g) was refluxed for 6 h in benzene (125 cm^3) with potassium t-butoxide (2.5g). The resulting solution was washed with water and dried with anhydrous magnesium sulphate before

being chromatographed on alumina as above.

1,3-diferrocenylbut-2-en-1-one (2.6g, 52%)

was isolated as a red solid (mpt 117.5-119°C).

1,3-Diferrocenylbuton-1-one, XXII

The α,β unsaturated ketone, XXI (0.2g) was dissolved

in the minimum volume of absolute ethanol and platinum

oxide catalyst (0.2g) was added. Hydrogenation for 30 min.

gave a colour change from red to yellow/orange, and

filtration and evaporation of the solvent gave an orange

oil which was purified on a silica column using 90%

petrol/10% ethyl acetate as eluent. Evaporation of the

solvent gave orange crystals (0.13g, 65%) of 1,3-diferro-

cenylbuton-1-one, melting point 143-145°C (lit 147-149°C [121]).

1,3-Diferrocenylbuton-1-ol, XXIII

(a) An attempt was made to reduce the α,β unsaturated

ketone, XXI, to the alcohol. 1,3-Diferrocenylbut-

2-en-1-one (0.1g) was dissolved in a minimum volume

of dry methanol. Sodium borohydride in 1 mol. dm^{-3}

sodium hydroxide solution (1g in 20 cm^3) was added

dropwise with stirring. The temperature of the

solution initially remained constant, so sodium

borohydride was added more rapidly until the

temperature was in the range 40-50°C. This was

maintained for 3 h before terminating the reaction.

TLC of the solution on silica, however, showed that

no reaction had taken place and only starting

material was recovered.

(b) 1,3-Diferrocenylbut-2-en-1-one (0.1g) was dissolved in THF and added to a mixture of LiAlH$_4$ (0.038g) in THF (10 cm^3). The solution was refluxed in a dry atmosphere for 1½ h before cooling and destroying excess LiAlH$_4$ with ice water. The reaction mixture was then filtered, extracted with ether, dried using anhydrous magnesium sulphate and evaporated to dryness to give a yellow oil (0.093g, 92%). This was purified on a silica column using petrol as eluent to give 0.081g (80%) of 1,3-Diferrocenylbutan-1-ol, melting point 107-108°C (lit 109-111°C [121]).

(c) The alcohol was also prepared by dissolving 1,3-Diferrocenylbut-2-en-1-one (0.4g) in methanol (250 cm^3) and adding sodium metal (10g). The mixture was refluxed for 30 min before it was cooled and the excess reducing agent destroyed with ice water. The solution was filtered and washed with dichloromethane. The organic layer was separated, dried with anhydrous magnesium sulphate, and evaporated to dryness to give a yellow oil. The product was chromatographed on a silica column; the major band was evaporated to dryness to give 1,3-Diferrocenylbutan-1-ol as a yellow solid (0.18g, 45%), melting point 107.5-109°C.

1,3 Diferrocenylbut-1-ene, XX

(a) The model compound was synthesised from the alcohol using concentrated acetic acid. 1,3-Diferrocenylbutan-1-ol (2g) was refluxed in glacial acetic acid (2g). A TLC examination of the solution showed three spots, one consistent with the starting material, one that may be due to the saturated compound 1,3-Diferrocenylbutane and a spot corresponding to the required model compound. The mixture was separated on a silica column to give 0.22g (10%) of 1,3-Diferrocenylbut-1-ene.

(b) 1,3-Diferrocenylbut-1-ene was also synthesised directly from 1-hydroxyethylferrocene [119]. The alcohol (5g) was refluxed in glacial acetic acid (5g) for 3 h before cooling and allowing the solution to form two layers. The top layer was poured off, washed with water to remove excess acid and dried using anhydrous magnesium sulphate. On evaporation of solvent, a red-brown oil was obtained which was purified by column chromatography on alumina to give the required model compound (1.4g, 61%).

The spectroscopic properties of this compound are discussed in Section 5.3.7.

3.2.5 Initiators

2,2'-Azobisisobutyronitrile (AIBN)

This radical initiator was purified by triple recrystallisation from Analar methanol, mpt 100.5-102.0°C, and stored under nitrogen at 4°C.

Boron trifluoride diethyletherate

This is a colourless liquid which darkens rapidly owing to air oxidation. The initiator (250 cm^3) was purified by distillation under vacuum (bpt 45-50°C/10 Torr) in the presence of diethyl ether (5 cm^3) and calcium hydride (1g) as recommended by Zweifel and Brown.[143] The hydride was added to remove volatile acids and reduce bumping. The initiator was stored under nitrogen at room temperature.

Diethylaluminium chloride

A 25% solution in hexane was used without further purification. It was stored at 4°C under a nitrogen atmosphere.

Butyl lithium

A 1.32 mol. dm^{-3} solution in hexane was stored under argon at 4°C.

3.2.6 Solvents

Analar benzene was dried using sodium wire.

Tetrahydrofuran was distilled from potassium.

Analar chloroform was washed thoroughly with distilled water to remove traces of ethanol stabiliser. It was redistilled from fresh phosphorus pentoxide, the middle fraction was collected and stored over calcium hydride in

the absence of light at 4°C.

Analar dichloromethane and Analar methanol were used
without further purification.

3.3 Apparatus

3.3.1 High Vacuum Line

The polymerisation of vinylferrocene in chloroform was
carriedout in an oxygen-free atmosphere using a high
vacuum line (Fig. 3.3) to de-gas the reactants. The
vacuum line used a mercury diffusion pump backed by a
rotary pump. The pumps were connected to the line via
two liquid cold-traps to prevent contamination of the line
by mercury.
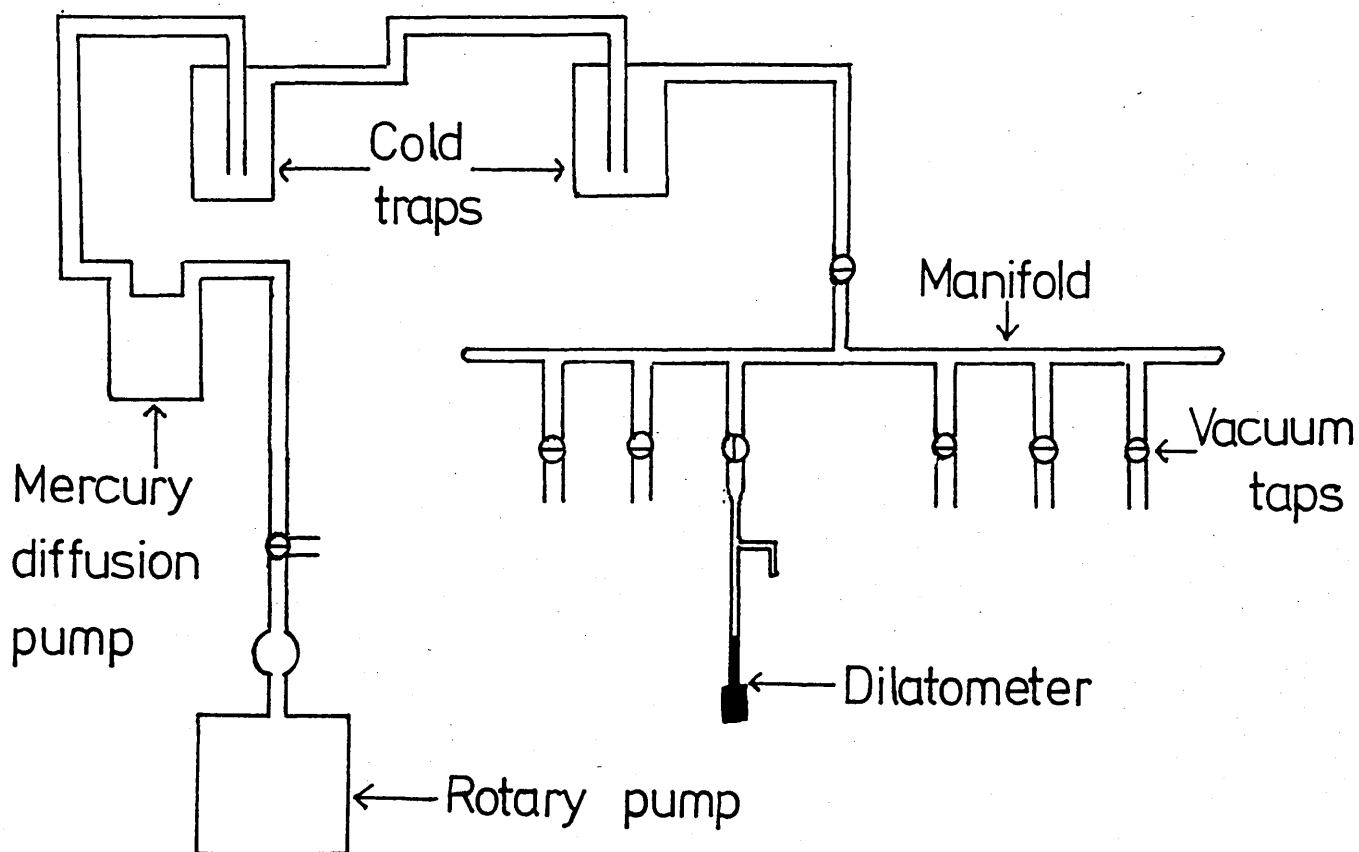
Fig. 3.3 Vacuum Line used in the Polymerisation of Vinyl-
ferrocene in Chloroform

The vacuum obtained was monitored using a high voltage discharge tester, which discharges at pressures above 10^{-4} Torr but not at higher vacuums. This method was employed to check the vacuum in the line and apparatus attached to it.

3.3.2 Dilatometers

Dilatometers (Fig. 3.4) used during kinetic experiments on the polymerisation of vinylferrocene in chloroform, consisted of a length of 2 mm precision bore tubing attached to bulbs of volumes of approximately 5.75 cm^3, which was calibrated using mercury. The dilatometer was connected to a filling tube and attached to the manifold via a ground glass socket.

Constrictions for closing and sealing

Side arm →

Ground glass joint for attachment to vacuum line

Filling bulb

Precision bore tubing
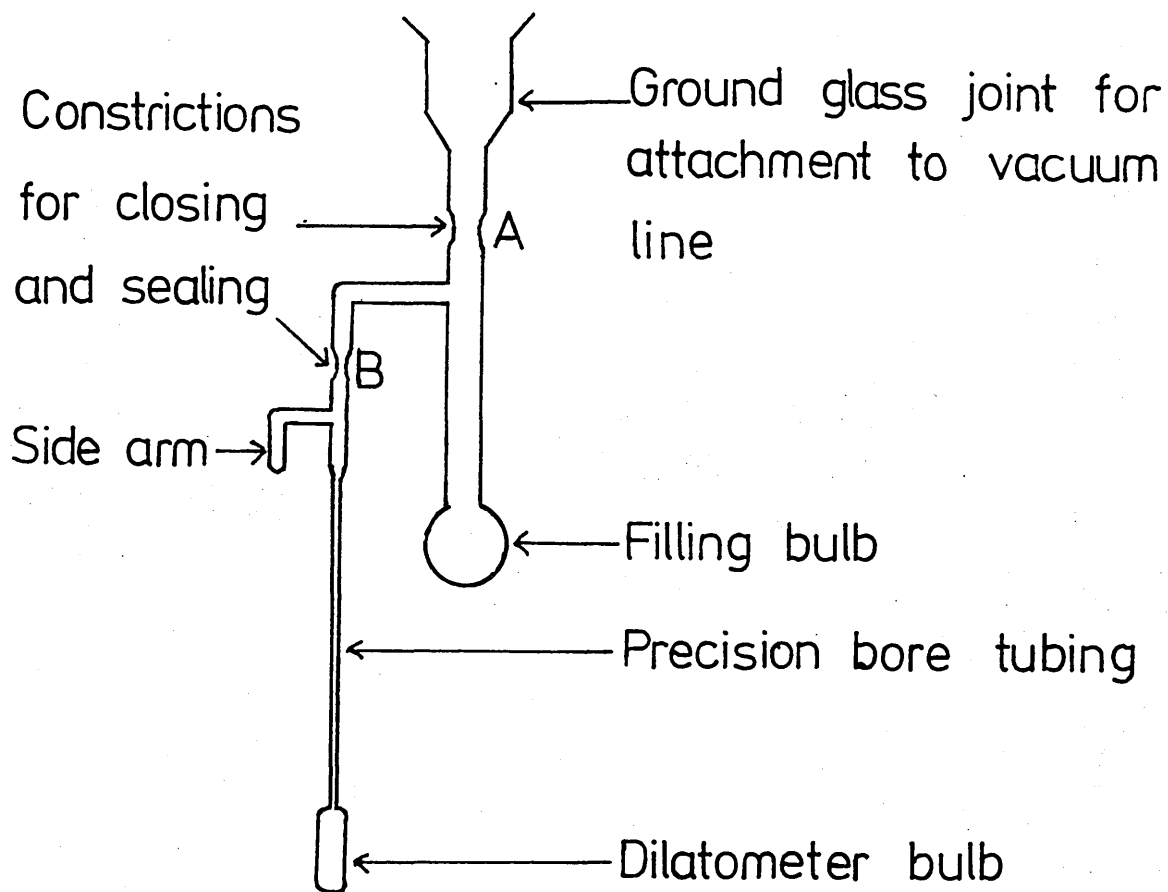
Dilatometer bulb

Fig. 3.4   Dilatometer and Filling Tube

3.4 Experimental Techniques

3.4.1 Dilatometric Procedure

Vinylferrocene was weighed into the filling bulb
(Fig. 3.4) and the apparatus attached to the manifold.
Chloroform was distilled from calcium hydride on to the
monomer which was cooled in liquid nitrogen. The reactants
were then degassed by three successive freeze-pump-thaw
cycles at around 10^{-5} Torr and finally the apparatus was
sealed at point A. The solution was then transferred to
the dilatometer bulb until sufficient sample was present
to just reach the bottom of the capilliary bore and small
excess was added to the side arm. The dilatometer was
then sealed at point B and both parts of the apparatus
totally immersed in a water bath at $60^{\circ}C$ for the required
period of time. The volume of reaction mixture in the
dilatometer was followed during the polymerisation by
monitoring the height of the meniscus at suitable time
intervals with a cathetometer (Precision Tool and
Instrument Co Ltd) accurate to 0.01 mm.

3.4.2 Other Polymerisation Methods

Radical polymerisation of the monomers was carried out
using AIBN as initiator in benzene. Three freeze-pump-thaw
cycles were carried out to ensure removal of oxygen and
the flask filled with nitrogen before sealing with a
septum. Polymerisation was carried out at $60^{\circ}C$.

Cationic polymerisation was carried out using boron
trifluoride diethyletherate or diethylaluminium chloride
in dichloromethane at $0^{\circ}C$ under nitrogen.

Anionic polymerisation was carried out using butyl lithium initiator and tetrahydrofuran as solvent. Three freeze-pump-thaw cycles were used to ensure that the system was free of oxygen. The apparatus was then refilled with nitrogen, sealed with a septum and cooled to $-78^{\circ}C$ in a solid CO_2/acetone bath. The initiator was injected directly from the storage bottle.

3.4.3 Isolation of Polymers

Polymerisation reactions were terminated by pouring the solutions into a 10 to 20 fold excess of methanol. The precipitated polymer was filtered or centrifuged, redissolved in benzene then reprecipitated in methanol. The resulting product was collected on a sintered crucible (porosity No 4) and dried.

In some cases a precipitate did not form when the reaction was initially poured into methanol. Low molecular weight oligomers in the methanol solution could be separated from unreacted monomer using a silica column.

4.1 Intramolecular Termination and the Generation of a Novel Fe(III) Species in Polyvinylferrocene

It has been suggested that the free radical polymerisation of vinylferrocene using AIBN as initiator in benzene involves termination via an intramolecular electron transfer reaction between the propagating radical and the ferrocene nucleus (Figs. 1.4 and 1.5) [28, 64, 112, 122]. ESR spectroscopy has shown that the polymer is paramagnetic, and typical paramagnetic line broadening is observed in n.m.r. spectra [64]. The product of the termination step has been proposed as an ionically bound complex of Fe(III) in a high spin $(3d^5)$ configuration from Mössbauer spectroscopic data. [64]

The Mössbauer spectrum of ferrocene and its monomeric derivatives almost always give two peaks with a quadrupole splitting in the region 2.30 - 2.40 mm s^{-1}. Ferrocene derivatives can be oxidised to give the low spin $(3d^5)$ ferricinium ion. In the absence of any Fe(II) a doublet is again observed but with a smaller splitting, of the order 0.70 - 0.80 mm s^{-1}. (Table 4.1)

Table 4.1   Mössbauer Parameters of Polyvinylferrocene and some Ferrocene Compounds

Compound	Isomer Shift mm s^{-1}	Quadrupole Splitting mm s^{-1}	Reference
Ferrocene	0.45	2.39	a
Vinylferrocene	0.45	2.34	a
Polyvinylferrocene (oxidised)	0.41	0.75	a
Polyvinylferrocene	(i) 0.44 (doublet) (ii) 0.14 (inner peak)	2.37 –	64

a   this work

The spectrum of polyvinylferrocene, reported by George and Hayes [64], contained three peaks; two outer peaks, characteristic of iron in the ferrocene nucleus, and a smaller inner peak appearing on the shoulder of the negative absorption. A typical value for the position of this peak is shown in Table 4.1. The parameters of this peak in no way correspond to those of the Fe(III) low spin ferricinium form and it has been postulated that it is due to iron in an Fe(III) high spin configuration [64], [122]. The possibility of it being due to Fe(II) low spin was ruled out on the basis of ESR data. It was considered to be ionic because the peak was obliterated at lower temperatures, due to enhancement of the other two peaks and the absence of any increase in intensity with decreasing temperature is characteristic of an ionically bound complex.

If this Fe(III) species is a result of an intramolecular termination step, then there should be a correlation between the average degree of polymerisation, $\overline{DP}$, and the amount of Fe(III) in the Mössbauer spectrum of the polymer. To investigate this possibility, George and Hayes [64] isolated a series of polymers in the range of 10 to 12% conversion of monomer; higher conversion polymers were not studied due to the increasing effect of transfer reactions in the polymerisation. It was claimed that there was a relationship between $\overline{DP}$ and the percentage of Fe(III) species, lower molecular weight polymers having Mössbauer spectra with a greater amount of this novel species. This is to be expected since each polymer

molecule terminated in this way will contain one Fe(III) unit and the mole percent of this unit will increase as the chain length decreases. On close examination of these results, the areas quoted for the Fe(III) peak are in the range 0.2 - 8.9%. Since about 5% of an absorbing species is required to obtain significant measurements from a Mössbauer spectrum, their results are really not conclusive. These authors also neglected transfer reactions to polymer, and with conversions in the range of 10-12%, this is not really justified. The molecular weights of the polymers studied were in the range 5,000 to 15,000 and it appears from this data that even lower molecular weight polymers would have to be studied to obtain measurable percentages of Fe(III). This is in agreement with the results of Pittman et al, [57] who examined the Mössbauer spectrum of a relatively high molecular weight radical polymer and found only the two Fe(II) peaks to be present.

The initial part of this work was concerned with an attempt to eliminate all possible experimental situations which could give rise to the Fe(III) species separately from the proposed termination step.

Cationic polymerisations of vinylferrocene were carried out and here the initiating species is a cation (proton) as opposed to a free-radical and since the intramolecular electron transfer step would not be possible, Fe(III) should not be observed. The presence of any Fe(III) species would indicate that the nucleus had been oxidised

by a route other than that of termination.

The conditions of these polymerisations are shown in
Table 4.2.

Table 4.2   Cationic Polymerisation of Vinylferrocene

	[Monomer] mol dm^{-3}	[BF_3 OEt_2] mol dm^{-3}	Reaction Time Hours	Conversion %
PVF 1	0.20	0.01	18	32
PVF 2	0.16	0.01	18	16
PVF 3	0.40	0.01	16	84

All three samples were examined by Mössbauer spectroscopy
and in all cases only the two Fe(II) peaks were observed,
the quadrupole splittings and isomer shifts of which were
identical to those previously recorded for the radical
polymer. [64] This established that the Fe(III) found by
previous workers was not generated during the collection
of the Mössbauer data either by direct oxidation of the
nucleus or due to any Fe(III) present in the apparatus
(e.g. sample disc or window of detector).

Polymer sample PVF 3 was separated into two, one portion
was heated in air at $120^{o}C$ for 3 hours while the other
portion was stored in air at room temperature. Fe(III)
was not observed in either sample of the polymer. The
polymer did undergo a physical change at around $118-120^{o}C$
when its form changed from a powder to 'brittle beads'.
Further heating led to decomposition at around $220^{o}C$.
This work showed that the nucleus is stable to oxidation

even on heating.

High conversion radical polymerisation was carried out to see if a polymer, which may contain a very low percentage of the novel Fe(III) species would yield a measurable amount on heating. The conditions for radical polymerisation are shown in Table 4.3.

Table 4.3   High Conversion Polymerisation of Vinylferrocene

	[Monomer] mol dm^{-3}	[AIBN] mol dm^{-3}	Time Hours	Conversion %
PVF 4	0.94	0.012	48	48
PVF 5	0.47	0.012	48	12
PVF 6	1.20	0.012	48	28

None of the three radically initiated polymers gave any Fe(III) high spin species in their Mössbauer spectra. This was to be expected since at high conversions the mole percent of the proposed novel terminal group would be very low due to transfer to solvent, which cannot be ignored at conversions over about 10%. Heating a sample of PVF 4 in air for 3 hours at 60°C did not yield any Fe(III) high spin in the Mössbauer spectrum.

The work of George and Hayes [64] was repeated in an attempt to obtain a measurable amount of the Fe(III) species. The conditions for these experiments are shown in Table 4.4.

Table 4.4   Low Conversion Polymerisation of Vinylferrocene[a]

Sample	[Monomer] mol dm^{-3}	[AIBN] mol dm$^{-3} \times 10^{-3}$	Reaction Time Hours	Conversion %
PVF 7	1.0	1.5	5	0.03
PVF 8	1.0	5.0	5	5.60

a   Polymerisations carried out in benzene in a nitrogen

atmosphere

The concentrations of initiator were slightly higher than

those used in the work of George and Hayes since their

work was carried out under high vacuum. Even with an

inert atmosphere such as nitrogen, there may be traces

of oxygen or other impurities which may reduce the quantity

of initiator effective in the polymerisation.   On isolation

of the polymers, neither sample gave evidence of the

presence of an Fe(III) species.   George and Hayes

reported Fe(III) percentages within the range 1.4% –

8.9% for comparable experiments, but as a value of above

5% is required to obtain significant measurements from

the Mössbauer spectra, it seems that very low molecular

weight products must be studied to obtain measurable

amounts of the novel terminal group species.

4.2   Polymerisation of Vinylferrocene in Chloroform

The polymerisation of vinylferrocene in chloroform has

been reported [76], [123] to give polymers which are

spectroscopically identical to the polymers produced from

AIBN in ben zene.   Nuclear activation analysis of the

chloroform polymers showed a very low chlorine content;

too low for initiation to have been via a radical species containing chlorine. [123] It was proposed that polymerisation had been initiated by a hydrogen radical and since chloroform readily decomposes to the stable CCl_3^- anion [124] the following reaction mechanism was suggested (Fig. 4.1)
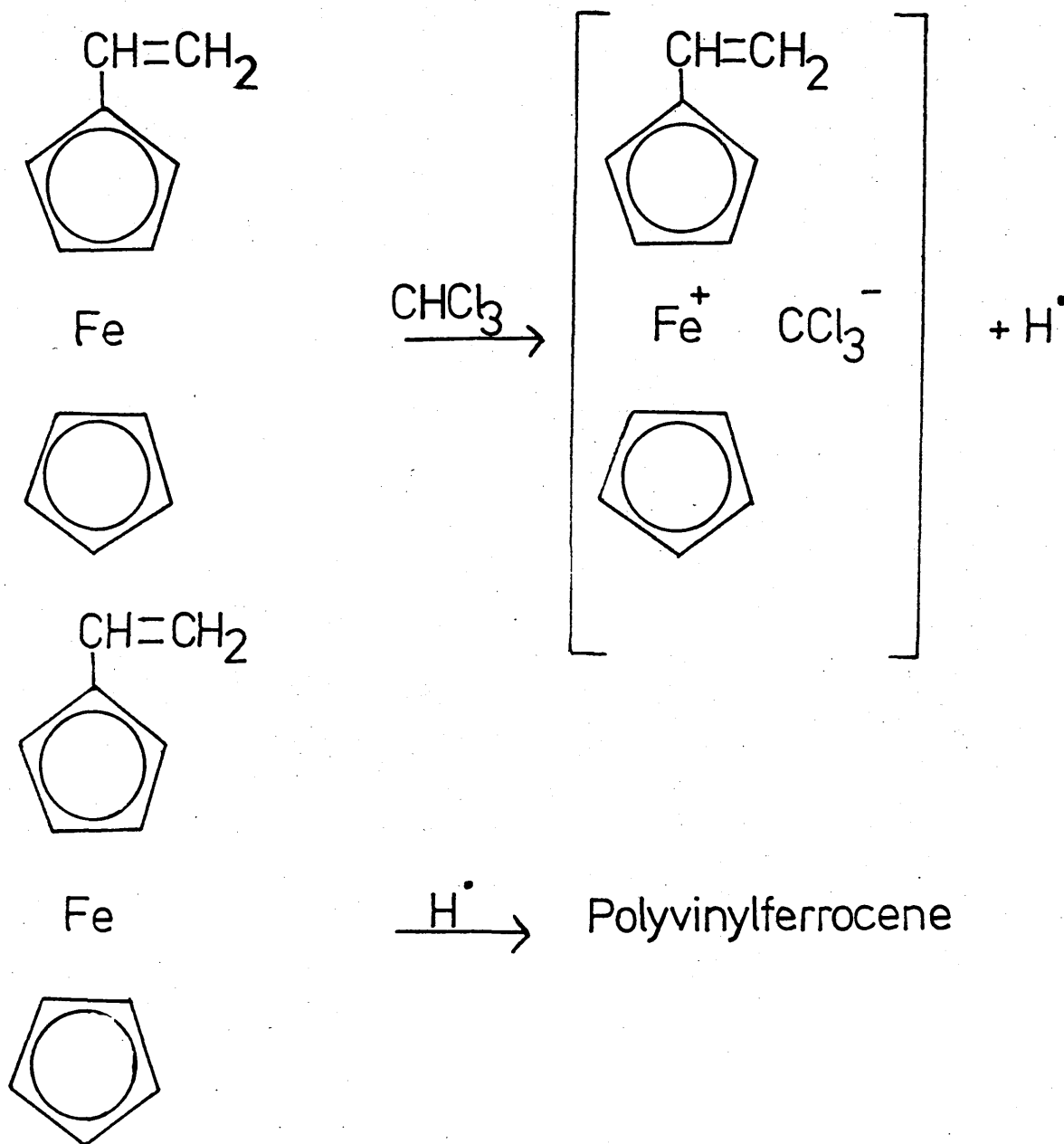

Fig. 4.1

Mechanism for the Polymerisation of Vinylferrocene in Chloroform

Further evidence for this mechanism was provided by the fact that during the polymerisations the colour of the reactants changed from orange to green, indicating the presence of a ferricinium species, as shown in Fig. 4.1.

The molecular weights of the chloroform polymers have been determined by vapour pressure osmometry and shown to be in the region of 1,000 - 1,200, with broad distributions. [123] The low molecular weights were attributed to transfer reactions, due to the high transfer activity of the monomer and chloroform [125] in radical polymerisations. The transfer to solvent was found to be negligible for the polymerisations in benzene, where higher molecular weight polymers were obtained. The ESR spectrum gave a signal which was ascribed to the presence of the Fe(III) species previously observed in polyvinyl-ferrocene prepared by radical initiation in benzene. [120]

An attempt was made to prepare polymers of this type by refluxing the monomer in chloroform. Although it has been reported that only polymerisations under high vacuum yielded polymer, [123], it was considered that the refluxing solvent may purify the system. Solutions of vinylferrocene in chloroform (1M and 2M) were refluxed for up to 24 hours, in air and under nitrogen. There was no colour change observed (i.e. orange to green) which would have indicated the production of a ferricinium species, and on completion of the reaction, no polymer was isolated.

The polymerisation of the monomer in chloroform was also carried out under high vacuum conditions as shown in Table 4.5.

Table 4.5   Polymerisation of Vinylferrocene in Chloroform

Run	[Monomer] mol dm^{-3}	Reaction Time Hours	Conversion[a] %
1a	1	1	–
1b	1	14	traces[b]
2	1	72	traces[b,c]
3a	1	2	–
3b	1	72	5
4	1	72	38
5	2	48	77
7	2	36	30
8	1.5	48	65
9	2	48	70
10	2.5	48	71

a The percentage conversion is polymer precipitated in methanol. Lower molecular weight species may be present in the filtrate.

b No precipitation was obtained on addition to methanol but on addition of water a fine precipitate was obtained.

c $\overline{M}_n$ = 535 by GPC, expressed as the polystyrene equivalent, c.f. $\overline{M}_n$ = 1,140 by VPO [123].

The high conversion polymerisations, 4-10, exhibited green solutions at the time the reactions were terminated, indicating the presence of the ferricinium species. On purification, the usual yellow colour was restored to the polymers and their spectroscopic properties were similar to those previously reported. [123] The physical appearance of the polyvinylferrocene, however, was slightly different to that of the polymer produced by AIBN initiation. Instead of being a yellow powder, on storage the chloroform polymer became a 'viscous tar'. This was accompanied by an odour of chloroform, which indicated that the polymer contained traces of the solvent which is gradually liberated from the mass.

No ferricinium or Fe(III) high spin species was evident from the Mössbauer spectra, even though the molecular weight of the polymer was found to be very low. The presence of the novel Fe(III) species has been proposed from the results of electron spin resonance spectroscopy [123], but transfer reactions are very important in this system [125] and they may have swamped the monomolecular termination mechanism in our experiments.

An attempt was also made to study the kinetics of the system. Run numbers 4, 7, 8, 9 and 10 gave contractions which were measurable using a cathetometer and the rates of reactions are shown in Table 4.6.

Table 4.6 Kinetic Studies of the Polymerisation of

Vinylferrocene in Chloroform

Run	[Monomer] mol dm^{-3}	Induction Period, Hours	Maximum Rate of Reaction,[a] mm min^{-1}
4	1	1	0.02
7	2	1	0.32
8	1.5	2	0.53
9	2	$3\frac{1}{2}$	1.00
10	2.5	> 6	--

a   The rate of reaction was monitored by the contraction
in the dilatometer.

On plotting the contraction in the dilatometer against
time, it was seen that after an initial induction period
all sets of data gave a linear contraction.   The
percentage contraction during the polymerisations was
very small, ranging from 2.4 - 3.8%, whereas values of
10 - 20% are not uncommon for some polymerisations.
However, there was no correlation between the monomer
concentration and the rate of polymerisation, measured as
shown above.   These runs were carried out using three
separate batches of vinylferrocene.   In one batch
(runs 8-10), there was an increasing induction period with
increasing monomer concentration which indicated that even
after the extensive purification of the monomer an impurity
was still present, causing inhibition of the reaction.
Because of the sensitivity of the system to impurities,
polymerisations using different batches of vinylferrocene
do not give reproducible results unless each of them is

absolutely pure. Unfortunately this does not appear to have been achieved in this case even though the monomer does not show impurities using GLC analysis.

4.3 Low Molecular Weight Products from Vinylferrocene

These polymerisations were carried out using AIBN as initiator in benzene, as shown in Table 4.7. Because of the high concentrations of initiator present, a precipitate was not produced on addition to methanol, indicating that a low molecular weight product had been produced. Removal of the solvent gave an oil which crystallized from methanol to give orange crystals.

Table 4.7 Polymerisation of Low Molecular Weight Products from Vinylferrocene

	[Monomer] mol dm^{-3}	[AIBN] mol dm^{-3}	Reaction Time Days	Conversion %	Melting Point $^{\circ}C$
PVF 9^a	0.110	0.037	7	45	166–170
PVF 10	0.092	0.100	4	39	142–146

a $\overline{M}_n$ = 530 by vapour pressure osmometry

The 'H n.m.r. spectra of these products showed no differences when compared with the spectra obtained for the higher molecular weight polyvinylferrocenes, but their infrared spectra showed a sharp peak in the region of 2,100 cm^{-1} which was previously not prominent. This is due to the CN group from the initiator which becomes attached to the ferrocene group on initiation. In the higher molecular weight polymers, the concentration of this terminal group is small and barely visible in the

infrared spectra, but in these lower molecular weight
samples the concentration of CN in the molecule is now
much larger.

Mössbauer spectra of PVF 9 and 10 exhibited a doublet,
as previously observed for the higher molecular weight
polyvinylferrocenes. The absence of an Fe(III) species
was perhaps predictable since with such a large amount
of radicals present in the solution, termination by
combination reactions is most likely to occur.

Mass spectrometry confirmed that these products were low
molecular weight compounds with little evidence of any
higher molecular weight species. The major peak in
the spectrum was 213 mass units, and there was a slightly
smaller peak at molecular mass 280, which corresponded to
the addition of an AIBN fragment to the ferrocene unit.
Two groups of small peaks in the higher molecular weight
range around 348 and 559 were attributed to structures
III and IV respectively.

$$(CH_3)_2(CN)C \diagdown \qquad CH_2C(CN)(CH_3)_2$$
$$CH$$

Fe

III

$H_3)_2$ (CN)CCH_2 _____ CH_2C(CN)(CH_3)_2

(structure with CH, cyclopentadienyl rings, Fe, labeled IV)
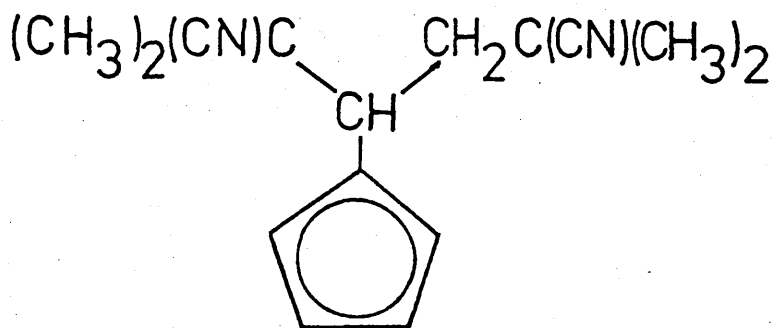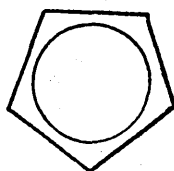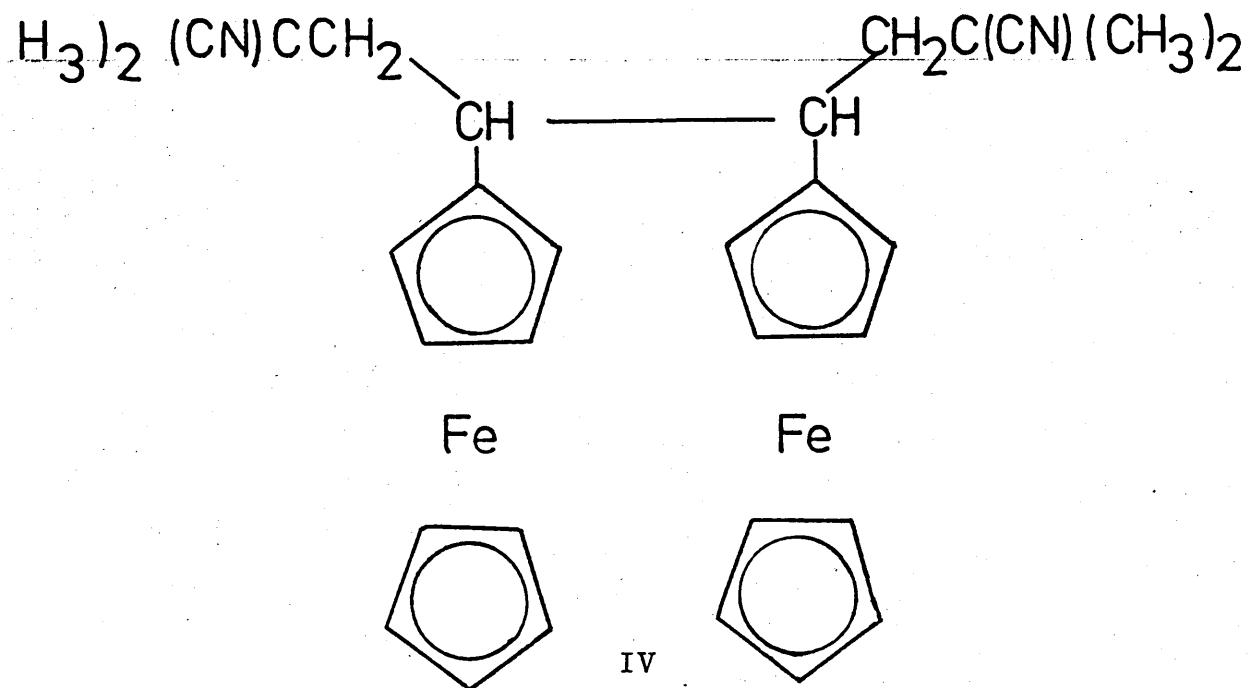
4.4 ^{13}C n.m.r. Studies of Polyvinylferrocene

The ^{13}C nuclear magnetic resonance spectrum of

polyvinylferrocene has been studied recently by Raynal et

al [67]. They prepared the polymer using an anionic

initiator as reported by Hayes and Young [71] and

attributed peaks in the 32-38 ppm range to combinations

of tetrad and hexad resonances of the methylene carbon.

They concluded that there were nine methylene resonances

present in this region and these were assigned by

comparison with a Markovian or Bernoullian statistical

model.

Details of the polymerisations carried out in this study

are shown below in Table 4.8

Table 4.8 Anionic Polymerisation of Vinylferrocene

Run	[Monomer] mol dm^{-3}	[Initiator] mol dm^{-3}	Yield[a] %
1	0.5	0.02	–
2	0.5	0.10	1 S
3	0.5	1.00	S87 I6[b]

a S and I denote percentage of benzene soluble and insoluble fractions.

b $\overline{M}_n$ = 962 by GPC expressed as the polystyrene equivalent.

Runs 1 and 2 were carried out at -78°C for 6 hours but Run 3 was allowed to warm from -78°C through to 0°C during the course of the 6 hours. The infrared, 'H n.m.r. and Mössbauer spectra of the polymers gave results identical to those previously published [64]. The ^{13}C n.m.r. spectrum recorded is shown in Fig. 4.2. The peaks corresponding to the chain carbons were observed at around 32 and 43 ppm, but the absorption pattern in the region 32-38 ppm differed from that which has been previously published [67]. Absorptions at 13.4, 22.1 and 26.6 ppm have been assigned to carbons from the butyl lithium initiator attached to the molecule. It is likely that the peak at 35.1 ppm is also due to initiator fragments, though previous workers [67] have attributed this peak to a combination of tetrad and hexad resonances of the methylene carbon.
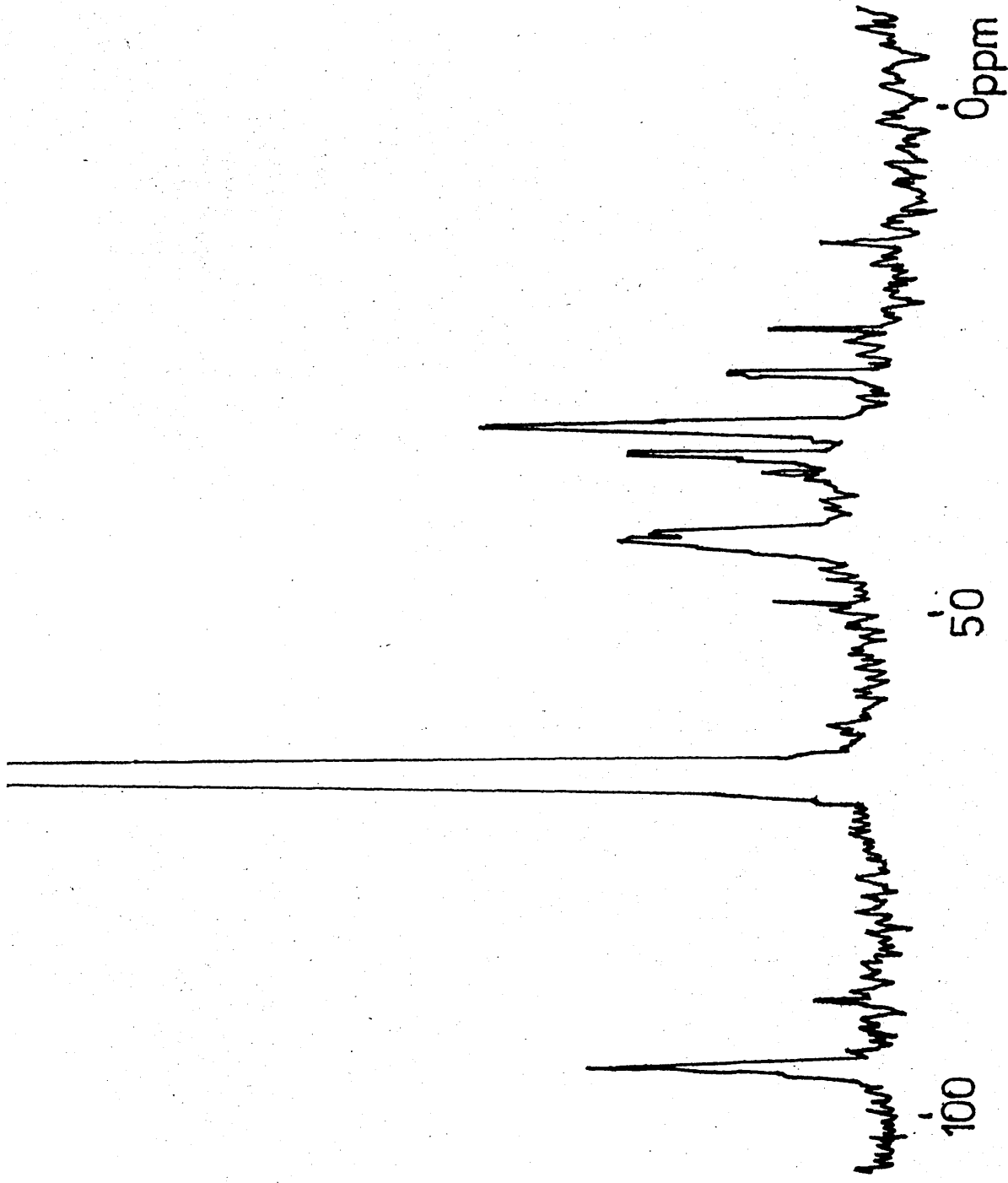
Fig. 4.2 ^{13}C n.m.r. Spectrum of PVF (anionic)

The spectrum of radical PVF gave similar results to the
anionic polymer, but because the molecular weight was
appreciably higher no initiator fragments were seen.
On proton coupling of the spectrum, the peak at 32.2 ppm
splits into a doublet as shown in Fig. 4.3

'H Decoupled

'H Coupled

50   0 ppm
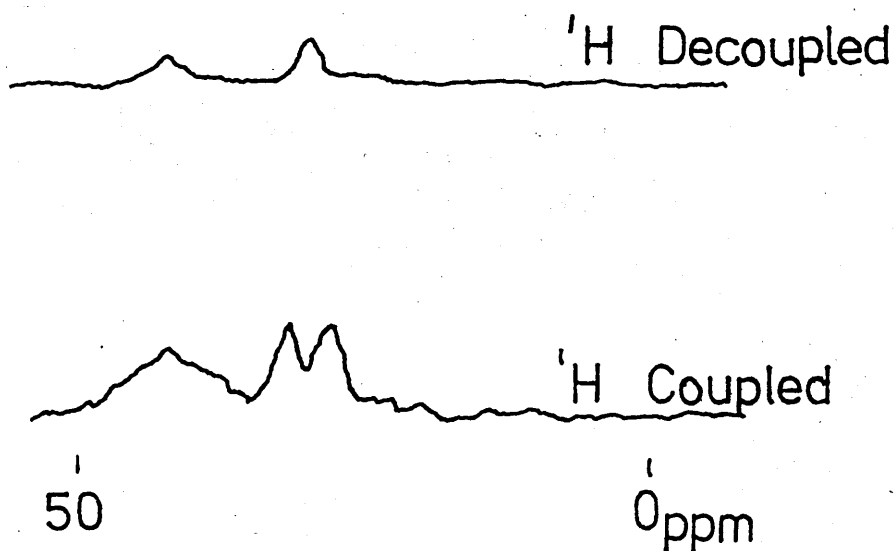
Fig. 4.3   'H Coupled and Decoupled ^{13}C n.m.r. of PVF

The fact that the peak splits to a doublet indicates that
this carbon is present as a -CH- in the molecule, not a
-CH$_2$- as previously reported [67], which would have
yielded a triplet.

Therefore it appears likely that Raynel et al [67] have
not only mistaken an initiator fragment for a carbon in
the polymeric chain, but they have also assigned the peaks

in the region of 32 ppm to $-CH_2-$ units but it has now been shown that these peaks are due to $-CH-$ units.

4.5 Conclusions

During the course of this work, the Fe(III) species reported by George and Hayes [64] has not been observed in the Mössbauer spectra of any of the polymers produced. The possibility that a measurable amount of the Fe(III) species could be generated by heating radical or cationic initiated polymers in air was investigated, but no change was observed. Radical polymerisations which were terminated at low conversions (Table 4.4) did not show any evidence of the Fe(III) species, which was contrary to the work reported by George and Hayes [64]. A possible explanation of this difference arises from the fact that the earlier reported polymerisations [64] were carried out under a high vacuum, where the level of initiator used was lower than in this work. The higher initiator levels, necessary to effect the polymerisation under nitrogen reported here, may produce a concentration of radicals that is too high to allow the intramolecular termination step to occur, and the reaction terminates by combination of radicals. Therefore, although the polymer must be of low molecular weight in order to observe the novel Fe(III) species, it must also be synthesised using a minimal amount of initiator, which demands that the polymerisation is performed under a high vacuum.

The polymerisation of vinylferrocene in chloroform
only occurred in oxygen-free systems which was in
agreement with previous studies [123]. The kinetics
of the polymerisation were found to be very sensitive
to impurities and despite rigorous purification of the
system, reproducible results could not be obtained.
The major impurity was probably oxygen which had not
been completely removed from the system. The long
induction periods recorded indicated that, despite triple
recrystallization and drying of the monomer, traces of
an inhibitor were still present. The polymers produced
were found to be low molecular weight by GPC and VPO
but, because they had been produced during kinetic
studies, they were generally high conversion products.
The majority of the polymers were in the range 30-77%
conversion and these samples predictably did not exhibit
a Fe(III) high spin peak in the Mössbauer spectrum.
Even polymers which arose from reactions taken to less
than 5% conversion did not show Fe(III) absorptions.
However, in these cases the low conversions are likely
to be a result of impurities being present in the system.
Even though a low molecular weight/low conversion polymer
is obtained, because termination has been due to
impurities, together with transfer reactions, an Fe(III)
species is not observed.

^{13}C n.m.r. studies on PVF gave results which contradicted
previously published work [67]. Absorptions previously
assigned to a combination of tetrad and hexad resonances

have been postulated to be due to initiator fragments from the butyl lithium initiator and on further examination of the spectra it was found that the $-CH_2-$ unit previously assigned to the peaks in the 32-38 ppm region was in fact a -CH- group.

5.1 Introduction

The polymerisation of 1,1' divinylferrocene was first

investigated by two independent research groups [79] – [83]

who reported that soluble polymers could readily be

obtained using free radical and cationic initiators.

These authors proposed that cyclopolymerisation had

occurred with the formation of linear polymers having

three-carbon bridged ferrocene units, V, and some

acyclic units VI, in the chain.
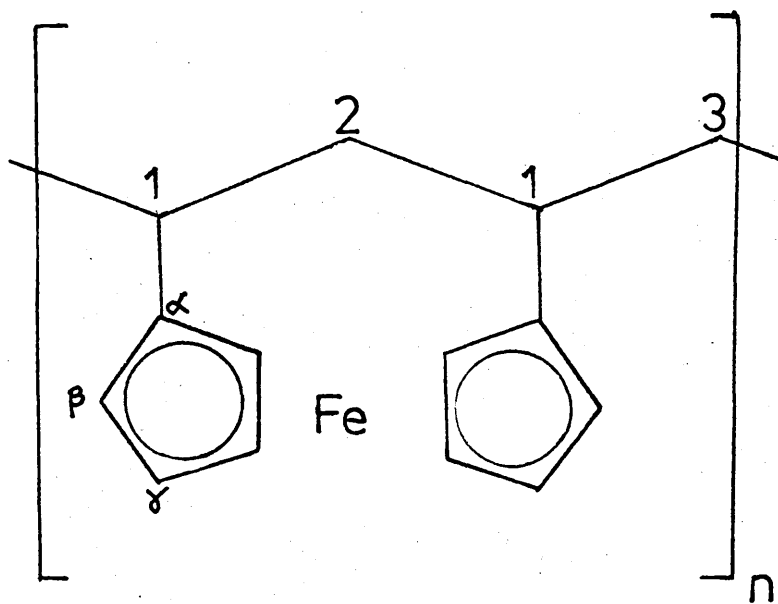
V
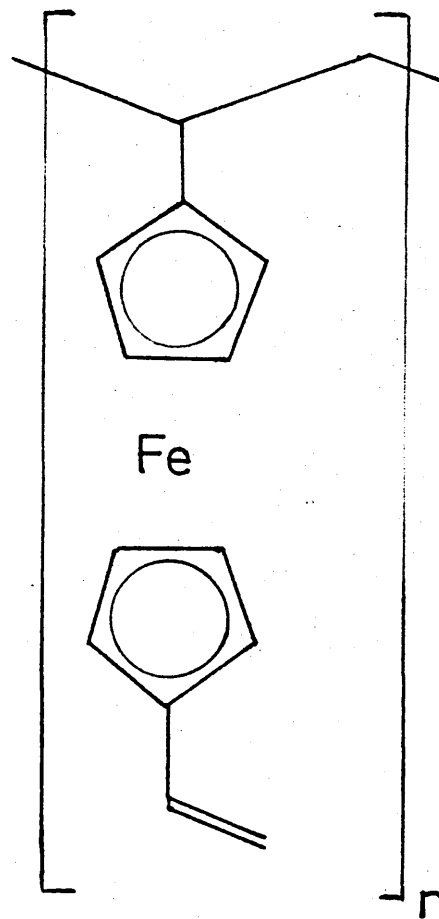
VI

Evidence for structure (V) as the predominant unit in
the polymer chain was provided by the low level of
unsaturation detectable by n.m.r. or infrared
spectroscopy, and the observation that bands
attributable to a bridged ferrocene [84] were to be
found in the infrared spectra of these polymers.

Recent Mössbauer investigations [126] of a large number
of bridged ferrocenes have demonstrated that a
trimethylene bridge across two cyclopentadienyl rings,
VII, causes changes in the iron-ring geometry. Because
the three-carbon bridge is not sufficiently long to
span, with ease, the two rings, tilting of the rings to
an angle of about 9° has been observed (Fig. 5.1).
Accommodation of the three-carbon bridge does not occur
merely by using the centroid of the cyclopentadienyl
rings as fulcrum, VIII, but in addition a decrease in
the iron-ring distance is observed, IX [127]. Thus,
there is a significant difference in the configuration
of the molecule compared to ferrocene. There is
therefore a redistribution of electrons around the iron
nucleus and this results in a signficant change in the
Mössbauer parameters relative to those of an unstrained
methylene bridged ferrocene. Bridging the cyclopenta-
dienyl rings with tetra, X, or pentamethylene groups,
XI, does not significantly alter the Mössbauer parameters
compared to ferrocene as these chains are long enough to
span the ferrocene unit without causing tilting of the
rings (Table 5.1).
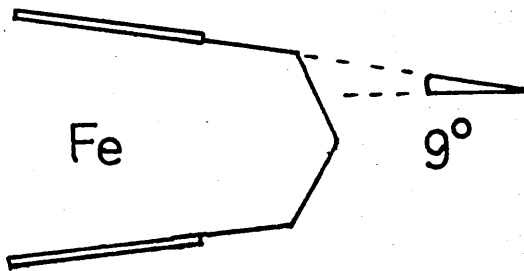
VII
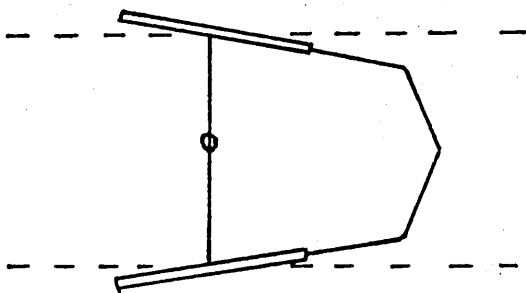
VIII
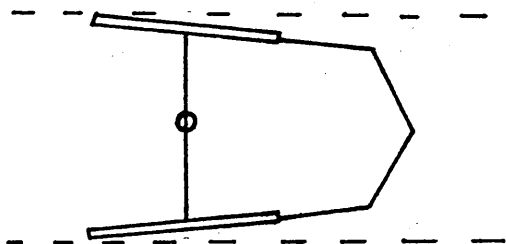
IX

Fig 5.1   Ring Tilting in Trimethylene Mono-Bridged
   Ferrocenes

X

XI
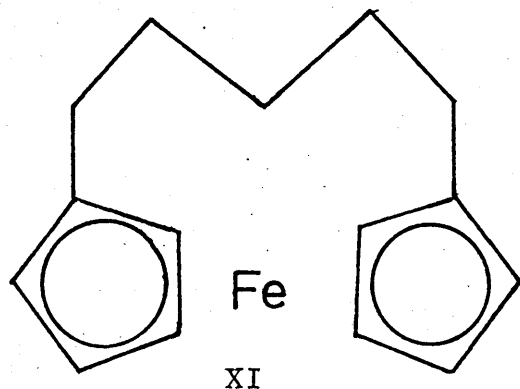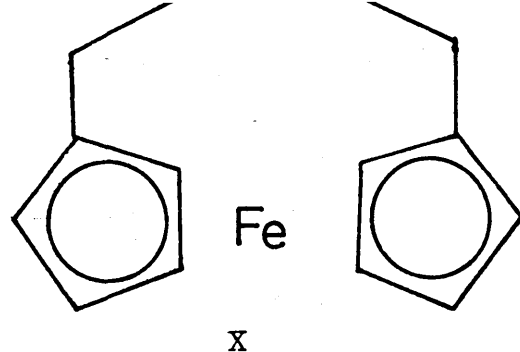
Table 5.1   Mössbauer Parameters of Bridged Ferrocenes

	Isomer Shift mm s^{-1}	Quadrupole Splitting mm s^{-1}
Ferrocene	0.43	2.37
1,1' Trimethyleneferrocene, VII	0.41	2.26
1,1' Tetramethyleneferrocene, X	0.42	2.35
1,1' Pentamethyleneferrocene, XI	0.43	2.34

The polymerisation of 1,1' divinylferrocene has been reported to yield two structurally different products, V and VI, their ratios being dependent on the initiator and solvent systems used [79] - [83].

As one of the proposed structures would involve a tilting of the rings, V, while the other is acyclic, VI, we were able to predict that Mössbauer spectroscopy would be capable of distinguishing each structure as their parameters would be significantly different.

5.2 Radical Polymerisation of 1,1'Divinylferrocene.

5.2.1 Polymer Synthesis

Radical polymerisations of 1,1' divinylferrocene with AIBN initiator in benzene at 60°C gave polymers which were predominantly soluble in benzene (Table 5.2). This was in agreement with the results reported earlier [81], [82], [128].

Table 5.2　Radical Polymerisation of 1,1' Divinylferrocene

[Monomer] mol dm^{-3}	[AIBN] mol dm^{-3} x 10^{-4}	Reaction Time, Hours	Conversion[a] %
0.080	1.25	40	S8　I2
0.098[b]	15.60	48	S50　I3

a　S and I denote percentages of benzene soluble and insoluble fractions.

b　$\overline{M}_n$ = 3,500 by GPC, relative to polystyrene

The polymers obtained were pale yellow powders which decomposed at temperatures above 220°C. The higher yield obtained on increasing the amount of initiator indicated that the reactions were subject to a significant amount of inhibition even though they were carried out under a nitrogen atmosphere.

5.2.2 Infrared Spectra

Infrared spectra of radically initiated polydivinylferrocene [PDVF (radical)], were in accordance with previously published results [82], [128] (Fig. 5.2). The double bond stretching vibration, found in the
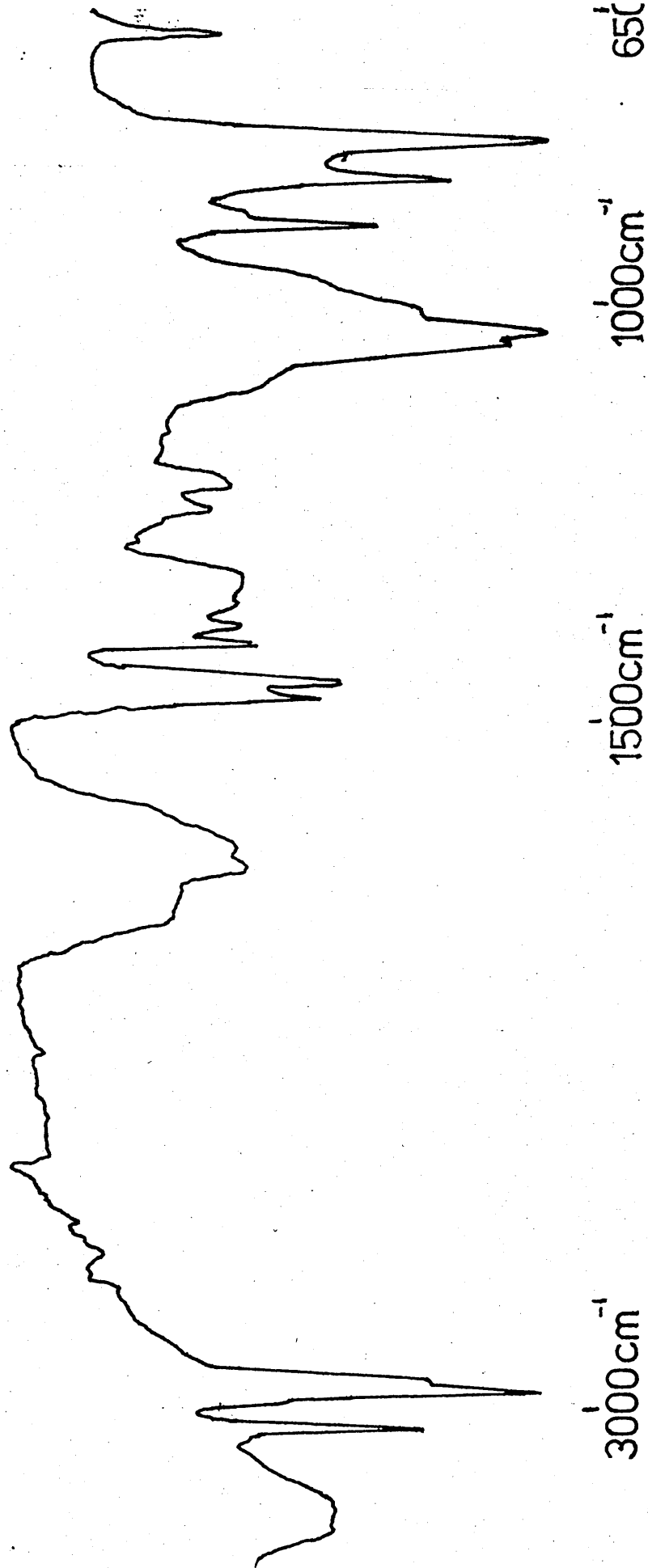
Fig. 5.2 Infrared Spectrum of Radically Initiated PDVF

monomer at 1630 cm^{-1}, would be obscured if present by the broad band at 1600 - 1750 cm^{-1}, but bands at 890 cm^{-1} and 980 cm^{-1} characteristic of vinyl groups, present in the infrared spectrum of the monomer, are completely lost. The ring breathing band at around 1100 cm^{-1}, which occurs in most ferrocene derivatives, including polyvinylferrocene, was absent, which is consistent with the cyclic structure proposed since the trimethylene bridge would fix the positions of the cyclopentadienyl rings relative to each other. The two peaks observed at 810 cm^{-1} and 850 cm^{-1} are common to a large number of heterobridged ferrocenes [84] and result from the splitting of the broad absorption at 815-820 cm^{-1} which is present in non-bridged ferrocenes, and is attributed to the ferrocene ring C-H stretch.

5.2.3 ^{1}H Nuclear Magnetic Resonance Spectra

Proton n.m.r. spectra obtained for these polymers were as previously reported [82] (Fig. 5.3). The cyclopentadienyl ring protons appeared as a broad peak centred around δ3.8 ppm while the aliphatic protons fall between δ2.3 ppm and δ1.0 ppm. No peaks were observed downfield of the ring protons, indicating an absence of unsaturation in the polymer structure, which was in agreement with the previously proposed structure.
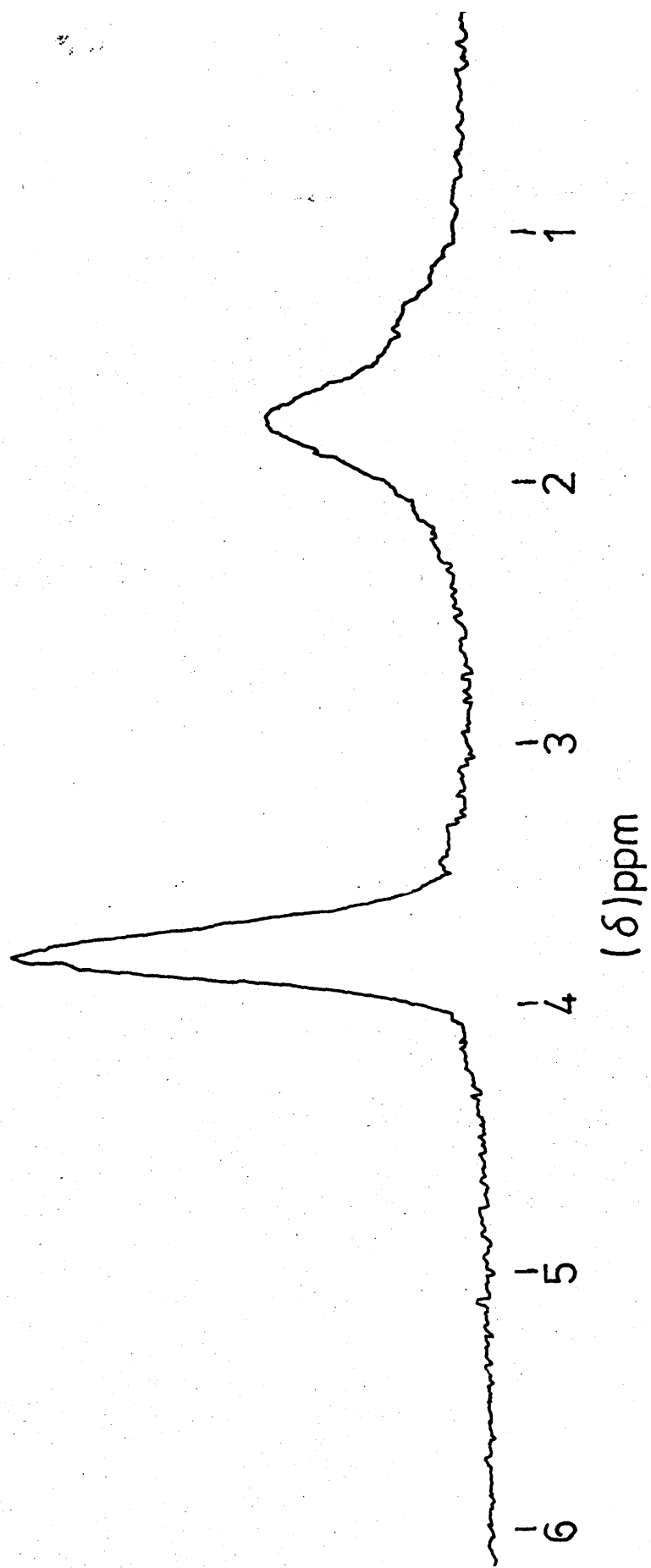
Fig. 5.3   'H n.m.r. Spectra of Radically Initiated PDVF

5.2.4 ^{13}C Nuclear Magnetic Resonance Spectra

^{13}C n.m.r. spectra of these polymers (Fig. 5.4)
(Table 5.8) support the cyclopolymer structure. The
β and γ ring carbons, V, appear in a similar position to
those in PVF, although with considerably more resolution
which is indicative of non-equivalence. The α-carbon
signal was shifted upfield relative to other ferrocene
derivatives from around 96 ppm to 90 ppm. This shift
is attributed to the distortion in the ferrocene ring
system and a similar shift for this carbon can be
observed by comparing other strained and unstrained
carbon-bridged ferrocenes [129], [130]. The polymer
is not totally comprised of cyclic units since a small
peak at about 96 ppm indicates the presence of unstrained
α-carbons. Aliphatic carbon 1 was assigned by comparison
with the spectrum of PVF (Section 4.4) and the three-
carbon bridged model compound (Section 5.2.6). Two
methylene carbons, 2 and 3, were observed at 43.9 ppm
and 52.4 ppm, the latter falling at lower field since it
is situated outside the ring system. Small peaks
observed in the region 19 ppm – 28 ppm were assigned to
initiator fragments at the ends of the polymer chain.
AIBN fragments contain methyl groups and the peaks are in
the region expected for methyl carbons.
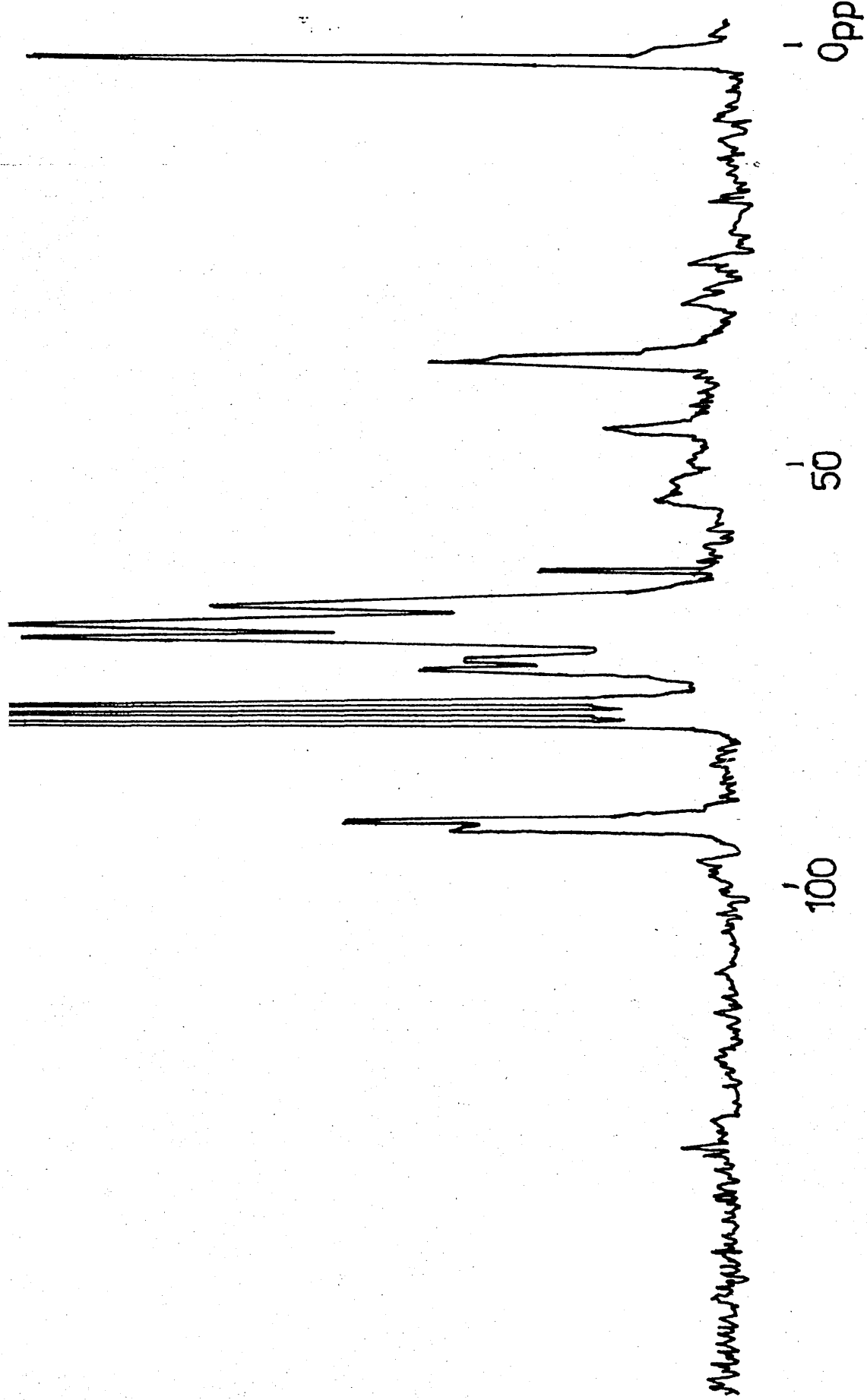
Fig. 5.4   13C n.m.r. Spectrum of PIVE (radical)

5.2.5 Mössbauer Studies of Radical Polymers from 1,1' Divinylferrocene

The strongest evidence that the structure of the radical polymer is almost entirely comprised of a three-carbon bridged cyclic unit was provided by Mössbauer spectroscopy (Table 5.3). The decrease in the quadrupole splitting and isomer shift for PDVF (radical) compared to acyclic ferrocene compounds corresponded to those predicted and observed for the model compound, 1,1' trimethyleneferrocene, VII (Table 5.3). Alkyl groups have been shown to have little or no effect on the Mössbauer parameters of ferrocenes [47], and the results for PVF were similar to ferrocene and independent of the type of initiator used. Therefore the evidence strongly supports the cyclic structure as the repeating unit in PDVF (radical).

5.2.6 Synthesis of 1,1'-Trimethyleneferrocene

An important part of the evidence for the cyclopolymer structure as repeating unit in the radically initiated polymer required the synthesis of 1,1'-trimethylene-ferrocene, VII, and its spectroscopic examination. Attempts to prepare the model by the route published by Rinehart et al [118] proved unsuccessful until certain modifications were made to their method. The route used in this study is shown in Fig. 5.5.

The Mössbauer parameters of the intermediates in this synthetic route have been determined and compared to previously reported values (Table 5.4)

Table 5.3   Mössbauer Parameters of Polyvinylferrocenes

and Model Compounds

|	Isomer Shift mm s^{-1}	Quadrupole Splitting mm s^{-1}
Measured Parameters		
Ferrocene	0.45(2)	2.39(2)
α-keto-1,1'-trimethyleneferrocene	0.41(2)	2.26(2)
1,1'-Trimethyleneferrocene	0.42(2)	2.30(2)
PVF (radical)	0.45(2)	2.40(2)
PVF (cationic)	0.45(2)	2.40(2)
PVF (anionic)	0.45(2)	2.39(2)
PDVF (radical)	0.42(2)	2.29(2)
PDVF (cationic)	0.45(2)	2.39(2)
PDVF (anionic)	0.41(2)	2.30(2)
Theoretical Parameters[a]		
Ferrocene	--	2.397
α-keto-1,1'-trimethyleneferrocene	--	2.285

a   Ref 124
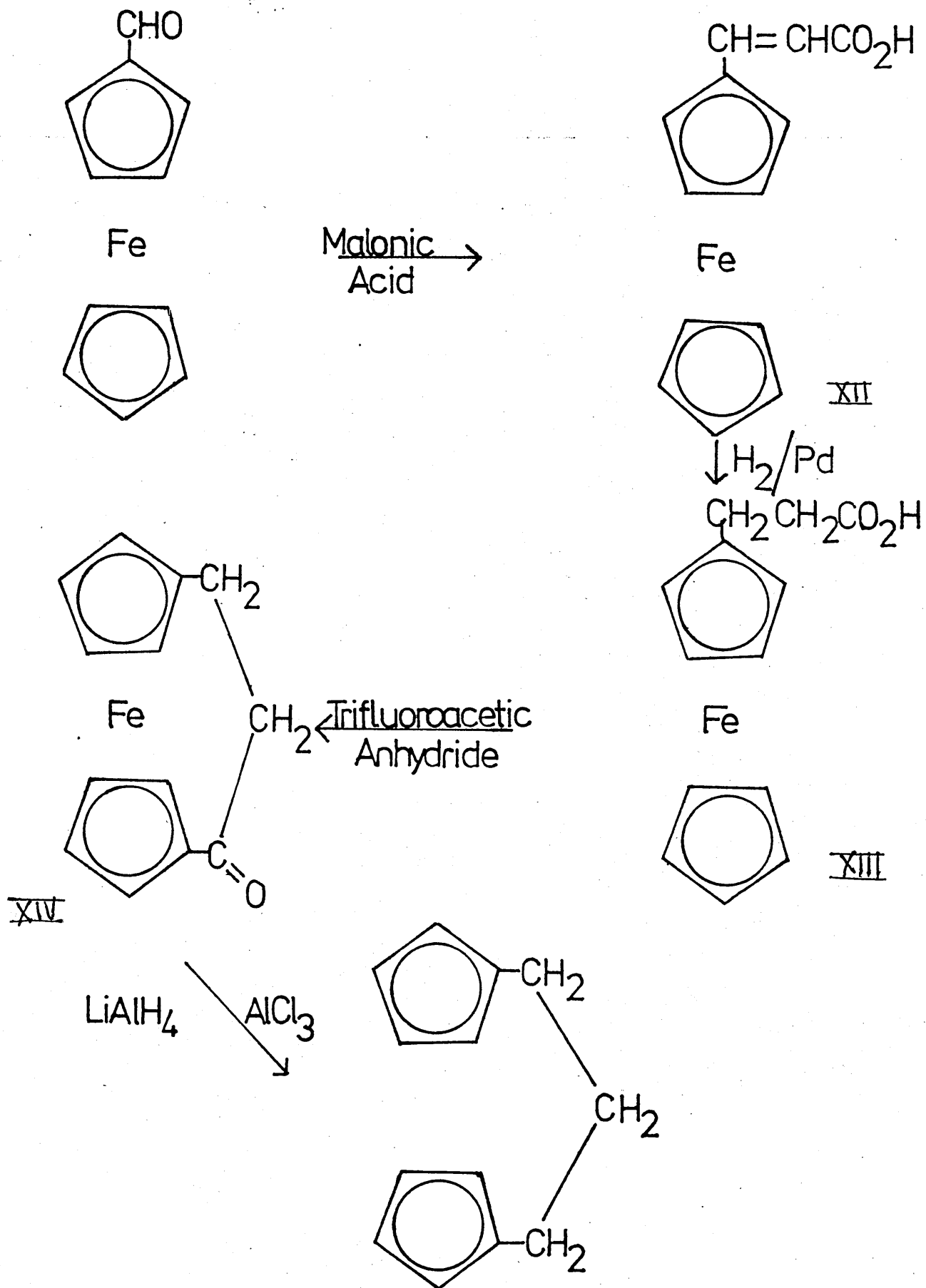
Fig. 5.5   Synthetic Route to 1,1'-Trimethyleneferrocene
[115], [116], [118]

Table 5.4   Mössbauer Parameters of the Precursors to

Model Compound (VII)

	Isomer Shift mm s^{-1}	Quadrupole Splitting mm s^{-1}	Reference
β-Ferrocenylacrylic Acid, XII	0.45(2)	2.29(2)	a
Ferrocenylpropionic Acid, XIII	0.44(2)	2.40(2)	a
	0.53(1)	2.22(3)	47
α-keto-1,1'-trimethylene-ferrocene, XIV	0.41(2)	2.26(2)	a
	0.52(2)	2.05(5)	47
1,1'-Trimethylene-ferrocene	0.42(2)	2.30(2)	a
	0.51	2.30	46
	0.408(2)	2.256(3)	126

a   This work

The values of the quadrupole splitting obtained for

ferrocenylpropionic acid and α-keto-1,1'trimethylene-

ferrocene do not agree with those previously published

by Lesikar [47]. The quadrupole splitting previously

reported for ferrocenylpropionic acid is very low

relative to ferrocene (Table 5.3) and, although a similar

difference can be observed where there is a π-electron

donating system attached to one or both of the cyclo-

pentadienyl rings (e.g. β-ferrocenylacrylic acid or

acetylferrocene [47]), or where there is a three-carbon

bridged unit, in the case of ferrocenylpropionic acid

this does not exist. Ferrocenylcarboxylic acid has been

reported to have a quadrupole splitting of 2.16 [46],

but in the propionic acid derivative there are two carbons between the acid group and the cyclopentadienyl ring which should significantly reduce its electron donating power. Therefore, Mössbauer parameters similar to ferrocene are much more likely such as those we have determined. To give reasons for the differences in the Mössbauer parameters between this work and earlier studies for the bridged ketone, XIV, is much more difficult, because not only is there a carbonyl group adjacent to the ring (cf. acetyl ferrocene, Q.S. = 2.26 mm s^{-1}), but there is also the effect of the bridging across the rings, and this distortion would be expected to alter the parameters. There are no similar compounds to refer to in this case, but the Q.S. value recorded in this work does appear high considering the combination of these two structural features. Additivity is unlikely to be applicable but a value of around 2.15 mm s^{-1} would be expected if this were the case, as each feature has been shown to reduce the quadrupole splitting by approximately 0.12 mm s^{-1}. This value does not correspond to either of the observed results and, at present, no explanation can be offered for these differences.

The infrared spectrum of 1,1'-trimethyleneferrocene showed very similar bands to that of the radical polymer (Fig. 5.6). In both cases there was little evidence for the ring breathing band at around 1100 cm^{-1} and the broad absorption at 815-820 cm^{-1} was split into two peaks at 810 cm^{-1} and 850 cm^{-1}.
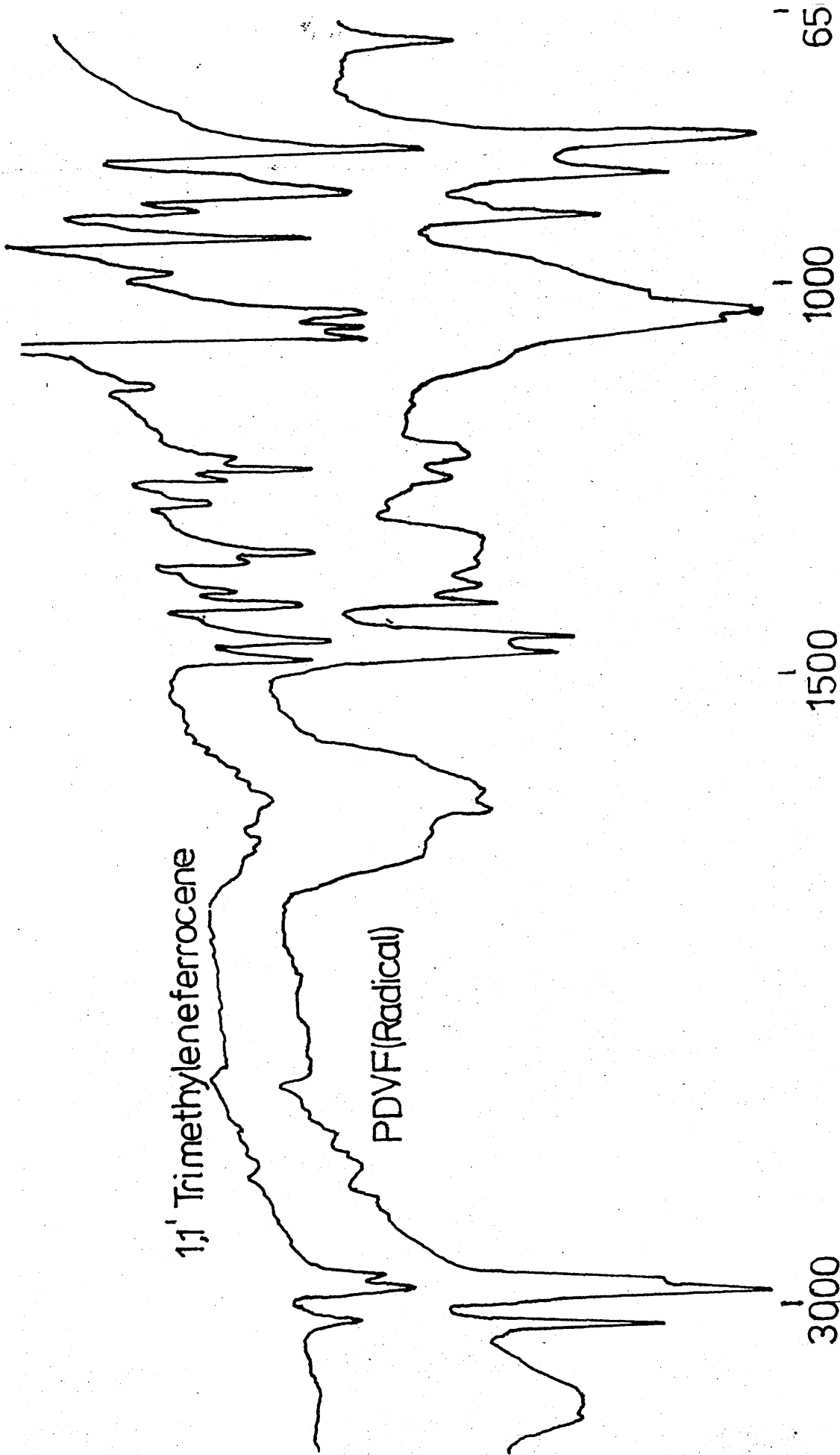
Fig. 5.6   Comparison of the Infrared Spectra of 1,1'-Trimethyleneferrocene and PDVF (radical)

The 'H n.m.r. spectrum of the model compound showed just two peaks at about $\delta 3.70$ ppm and $\delta 1.85$ ppm. (Fig,5.7) The former peak was due to the ring protons and its sharpness indicates that the degree of tilting is insufficient to introduce any detectable magnetic inequivalence. The equivalence of the methylene protons has been reported previously [116], [131], and attributed to a rapid inversion of the chain which effectively averages the spacial orientations of the protons and their distances from the metal atom. Low temperature n.m.r. studies have been used [131] to 'freeze out' this motion, and two complex multiplets were obtained in the ratio 2:1, corresponding to the two types of methylene protons. The spectrum of the model compound was similar to that of the polymer, although the methylene peak in the polymer was much broader and fell at a slightly higher field. This broadness is typical of polymers due, in part, to the different possible conformations of the methylene groups within a polymer chain.

The ^{13}C n.m.r. of 1,1'-trimethyleneferrocene did not exhibit the same equivalence within the types of carbons as was seen with the proton spectrum. The α, β and γ ring carbons appear as three separate peaks at 85.4, 68.1 and 69.3 ppm respectively while the two types of methylene carbons are at 35.1 and 24.5 ppm respectively. The bridge carbons in the model compound fell at slightly higher fields than those in
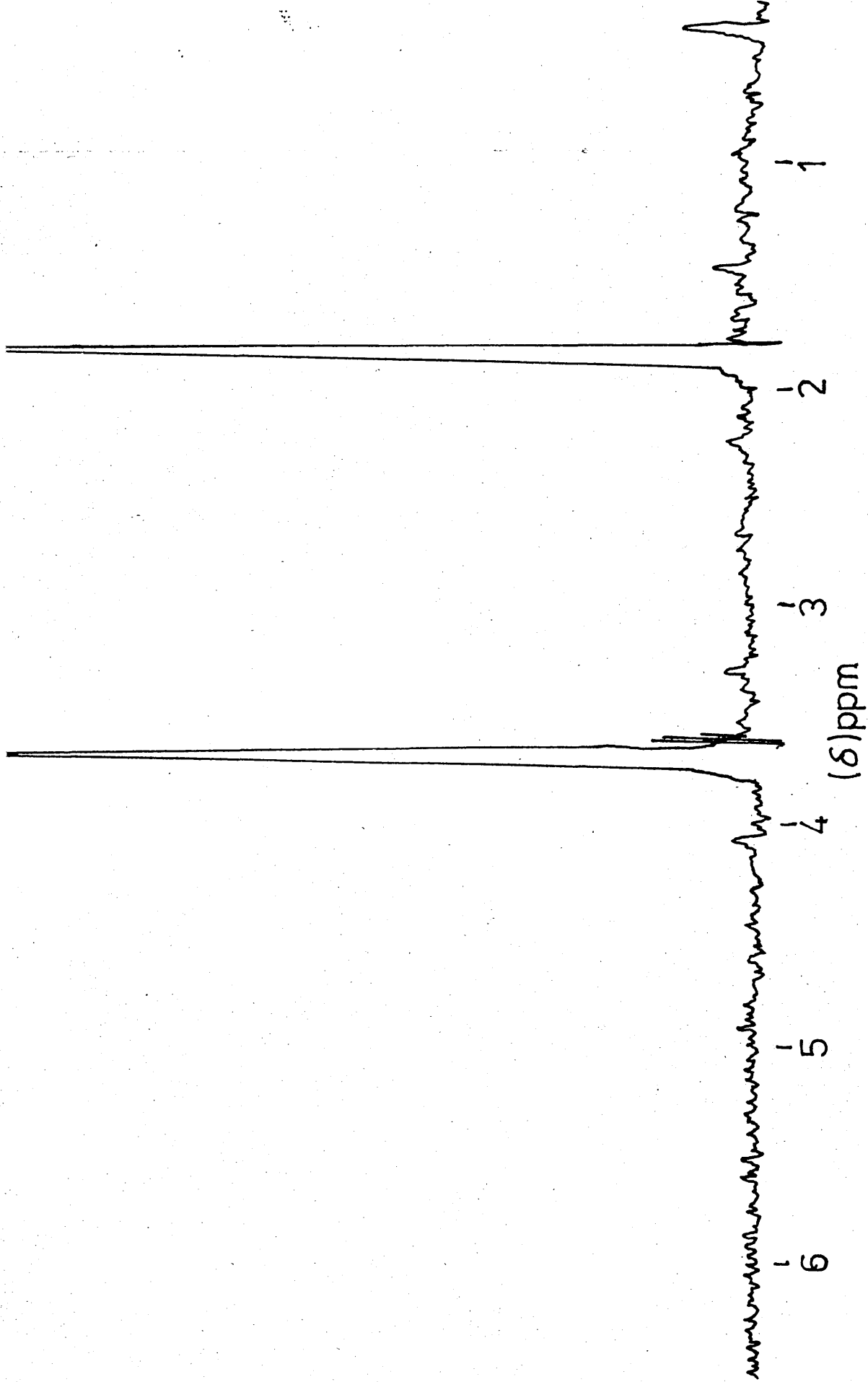
Fig. 5.7 ^{1}H   n.m.r. Spectrum of 1,1'-Trimethyleneferrocene

the polymer but absolute comparisons are difficult because of the additional groups present in the polymer structure.

The details of the Mössbauer spectrum of this compound are given in Table 5.4 and the parameters recorded were in good agreement with those of the radical polymer.

5.2.7 Low Molecular Weight Radical Polymers From 1,1' Divinylferrocene

An attempt was made to synthesise low molecular weight oligomers from DVF using AIBN initiator, since it was considered that lower molecular weight material would provide greater resolution in the n.m.r. spectra. The conditions used were similar to those outlined in Section 5.2.1 but a greater proportion of initiator was used and the reaction time was extended. The larger amount of initiator results in a greater number of propagating radicals present in solution and the monomer is quickly used up before the propagating species can attain a high molecular weight. The details of these polymerisations are shown in Table 5.5.

Table 5.5   Low Molecular Weight Radical Polymerisations of 1,1'-Divinylferrocene

[Monomer] mol dm^{-3}	[AIBN] mol dm^{-3}	Reaction Time Days
0.12	0.044	7
0.12	0.050	6

Because of the low molecular weight of the products,
they were not isolated by precipitation into methanol
but were recovered by evaporation of the solvent
yielding crystalline solids (mpt 93-97°C). The products
had almost identical infrared spectra to those of the
higher molecular weight polymers except that these
lower molecular weight materials showed better
resolution of the peaks. The proton n.m.r. spectra
exhibited three peaks, one due to the ring protons at
about δ4.0 ppm and two sharp peaks, close together in
the region δ1.3-δ1.5 ppm, due to methylene protons.
As in the infrared spectrum, the lower molecular weight
material provided much better resolution of the peaks.

Mass spectra were recorded and the significant peaks
are shown below, in Table 5.6.

Table 5.6   Mass Spectrum of Low Molecular Weight
            Radical PDVF

m/e	I	Assigned Ion
56	8.6	Fe^{+}
121	15.3	$C_5H_5Fe^{+}$
134	13.3	$C_6H_6Fe^{+}$
163	45.8	$FeC_5H_4CH_2CH_2CH_3^{+}$
213	17.4	$(C_5H_5FeC_5H_4CH_2CH_3-H)^{+}$
214	18.3	$C_5H_5FeC_5H_4CH_2CH_3^{+}$
241	50.8	$C_5H_4FeC_5H_4CH_2CH_2CH_2CH_3^{+}$
259	100	---
260	18.5	---

The mass spectrum showed the product to be mainly monomeric th ough there were some small peaks in the higher molecular weight range. An attempt has been made to assign the peaks in Table 5.6 with reference to work carried out on other alkyl ferrocenes [132]. However, there was difficulty in proposing an assignment for the major peak at e/m = 259, which may be the molecular ion.

5.3 Cationically Initiated Polymers from 1,1'Divinyl-Ferrocene

5.3.1 Polymer Synthesis with Boron Trifluoride-Diethyl Etherate Initiator

Cationic polymerisation of 1,1'-divinylferrocene was carried out in dichloroethane solution at $8^{\circ}C$ as shown in Table 5.7.

Table 5.7   Cationic Polymerisation of 1,1'-Divinylferrocene

[Monomer] mol dm^{-3}	[BF_3OEt_2] mol dm^{-3}	Reaction Time Hours	Conversion[a] %	
0.200	0.010	16	S51	I16
0.200	0.010	40	S48	I16
0.080	0.010	16	S46	I13
0.058[b]	0.007	120	S44	I6
0.050	0.007	72	S70	I3

a   S and I denote percentage of benzene soluble and benzene insoluble fractions

b $\overline{M}_n$ = 4,000 by vapour pressure osmometry

$\overline{M}_n$ = 1,600 by GPC relative to polystyrene

The insoluble fraction was most probably due to the
presence of the ionic ferricinium species which was
detected in the Mössbauer spectra of the crude polymers.
As the more dilute polymerisations gave a smaller insoluble
fraction, some crosslinking of the polymer may have
occurred at higher concentrations, though with molecular
weights of only 4,000 this is unlikely to be the major
cause of insolubility.

The benzene-soluble polymer produced was a pale yellow
powder which decomposed at temperatures above 220°C.

5.3.2 Infrared Spectra

The infrared spectrum of the polymer was identical to
those previously recorded [82], [83] and is shown in
Fig. 5.8. Partial splitting of the peak at about
820 cm^{-1} was previously attributed to the presence of
cyclised and uncyclised units, V and VI. The spectrum
of the cationic polymer is very different to that of the
radical polymer, but despite this previous workers
explained the differences as being due to differences
in the proportions of the two structures, V and VI in
the polymeric material.

5.3.3 'H n.m.r. Spectra

The 'H n.m.r. spectrum showed three broad bands centred
around about δ1.2 ppm, δ3.9 ppm and δ5.9 ppm (Fig 5.9)
and was similar to the spectra reported previously [82],
[83]. In these earlier studies, the peak at δ1.2 ppm was
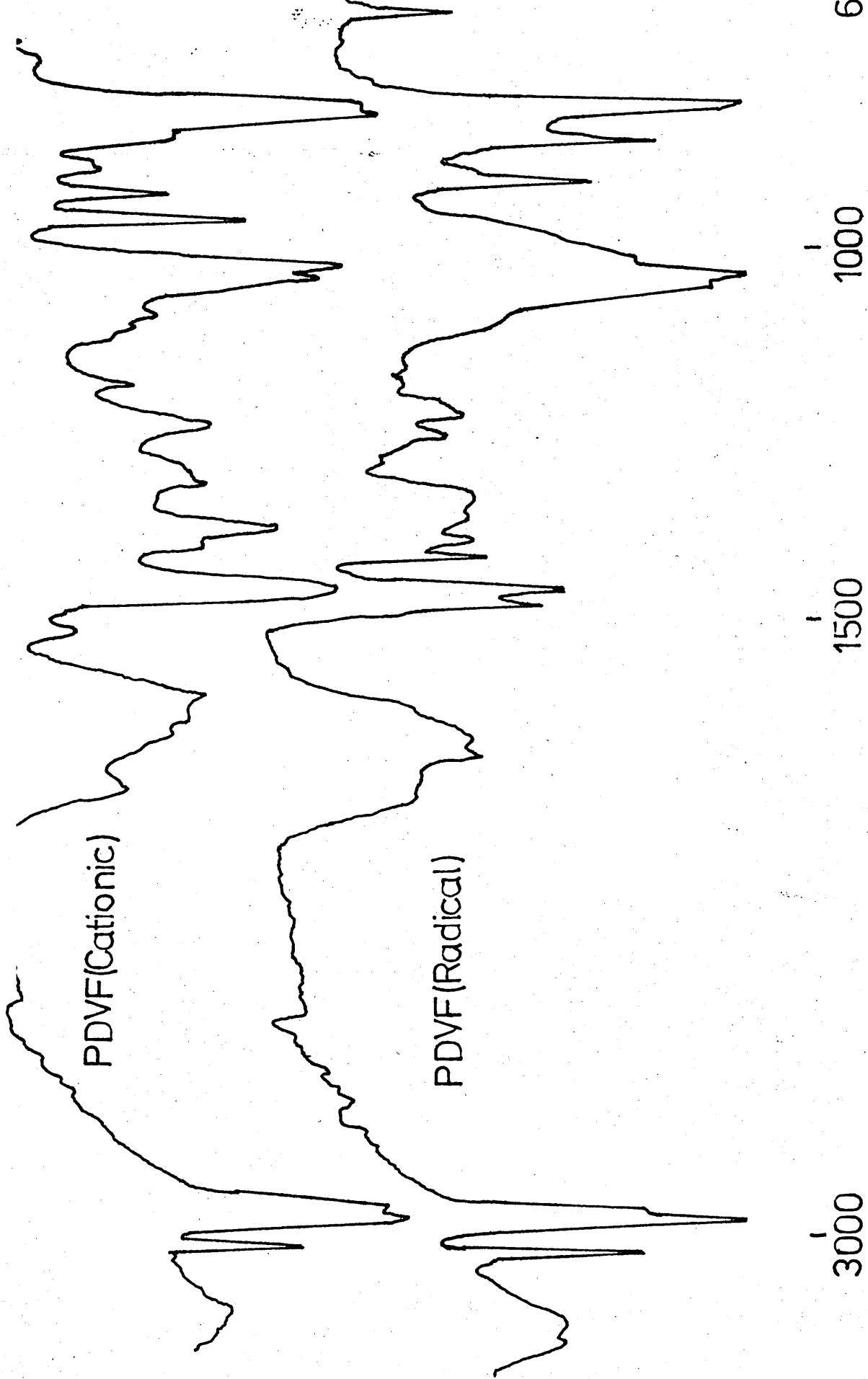
Fig. 5.8 Infrared Spectra of PDVF (cationic) and PDVF (radical)

Fig. 5.9 'H n.m.r. Spectra of PDVF (cationic) and PDVF (radical)

PDVF (Cationic)

PDVF (Radical)

(δ)ppm
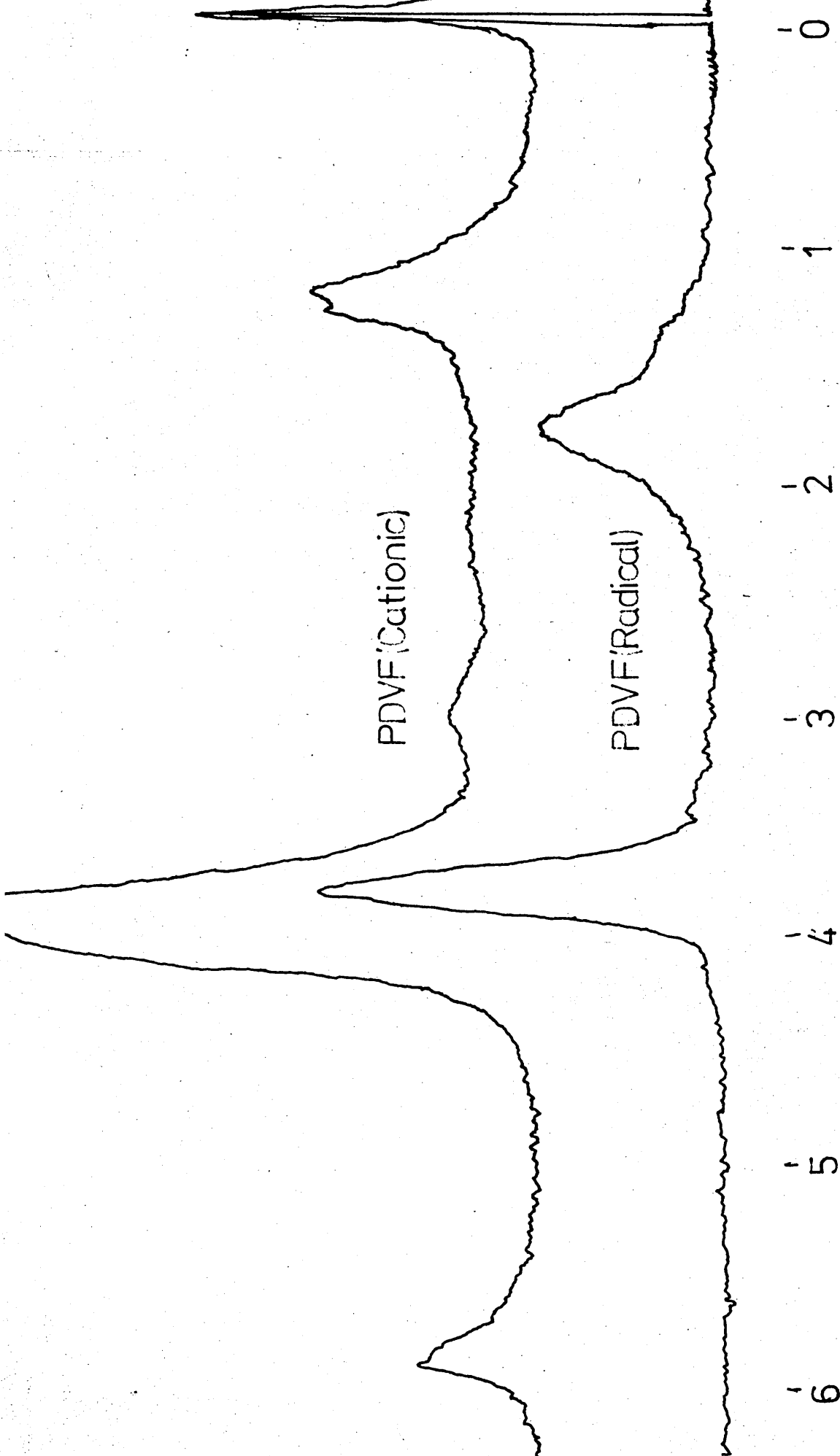
assigned to the methylene protons, that at $\delta 3.9$ ppm to
the rings protons, with the peak at $\delta 5.9$ ppm attributed
to vinyl unsaturation resulting from polymerisation
occurring through one ring only, structure VI. The
amount of vinyl unsaturation was calculated by earlier
authors using eqn. 1.2 and was found to be 25-34%, which
is considerably less than that expected if one vinyl
group remained unreacted in each unit of a linear polymer
(this being taken as 100%). This calculation was used
as supporting evidence that both structures V and VI
were present in the polymer chain [82], [83]. No
consideration was given to the fact that the methylene
protons in the cationic and radical polymers did not
coincide; they are centred at $\delta 1.2$ ppm and $\delta 1.6$ ppm
respectively. The proton n.m.r. of vinylferrocene shows
two peaks due to unsaturation, at approximately $\delta 4.9$
and $\delta 6.5$ ppm, in agreement with previously published
data [38], and considerably different to the unsaturation
observed in the cationic polymer. Clearly, an alternative
explanation of the infrared and proton n.m.r. results
is that the polymers obtained by radical and cationic
initiation are structurally quite different.

5.3.4 <u>Mössbauer Studies of PDVF (Cationic)</u>
Mössbauer studies have been carried out on the cationic
polymer and have provided the evidence to substantiate
the proposal that structural differences exist between
the polymers obtained using radical and cationic
initiators.

The two structural units which were assumed to be present in PDVF (cationic), V and VI, would result in two different Mössbauer doublets with different parameters. However, the parameters that are actually obtained for PDVF (cationic), shown in Table 5.3, differ significantly from those observed for the radical polymer (Fig. 5.10). The co-existence of strained (ΔE_Q = 2.29 mm s^{-1}) and unstrained (ΔE_Q = 2.40 mm s^{-1}) units, as proposed, would result in a Mössbauer spectrum having two overlapping quadrupole doublets. Clear evidence for this would be given by corresponding changes in line widths and asymmetry in line intensities but no significant line broadening or intensity asymmetry was observed for the polymers studied. Therefore Mössbauer spectroscopy showed that there is not a three-carbon bridge present in the structure of the cationic polymer. But, the level of unsaturation is apparently well below that expected for a polymer consisting totally of the non-cyclic structural unit, VI. An explanation was sought that accounted for the apparent loss of unsaturation in a linear polymer without production of a strained cyclic unit. Infrared spectroscopy indicates that the structure is experiencing some constraint across the two rings as the 'ring breathing' peak, which appears at around 1110 cm^{-1} in polyvinylferrocene, is not observed.

One explanation for the low level of unsaturation would be the formation, not of a three-carbon bridge, but of a four-carbon bridge, XV, where the tetramethylene chain
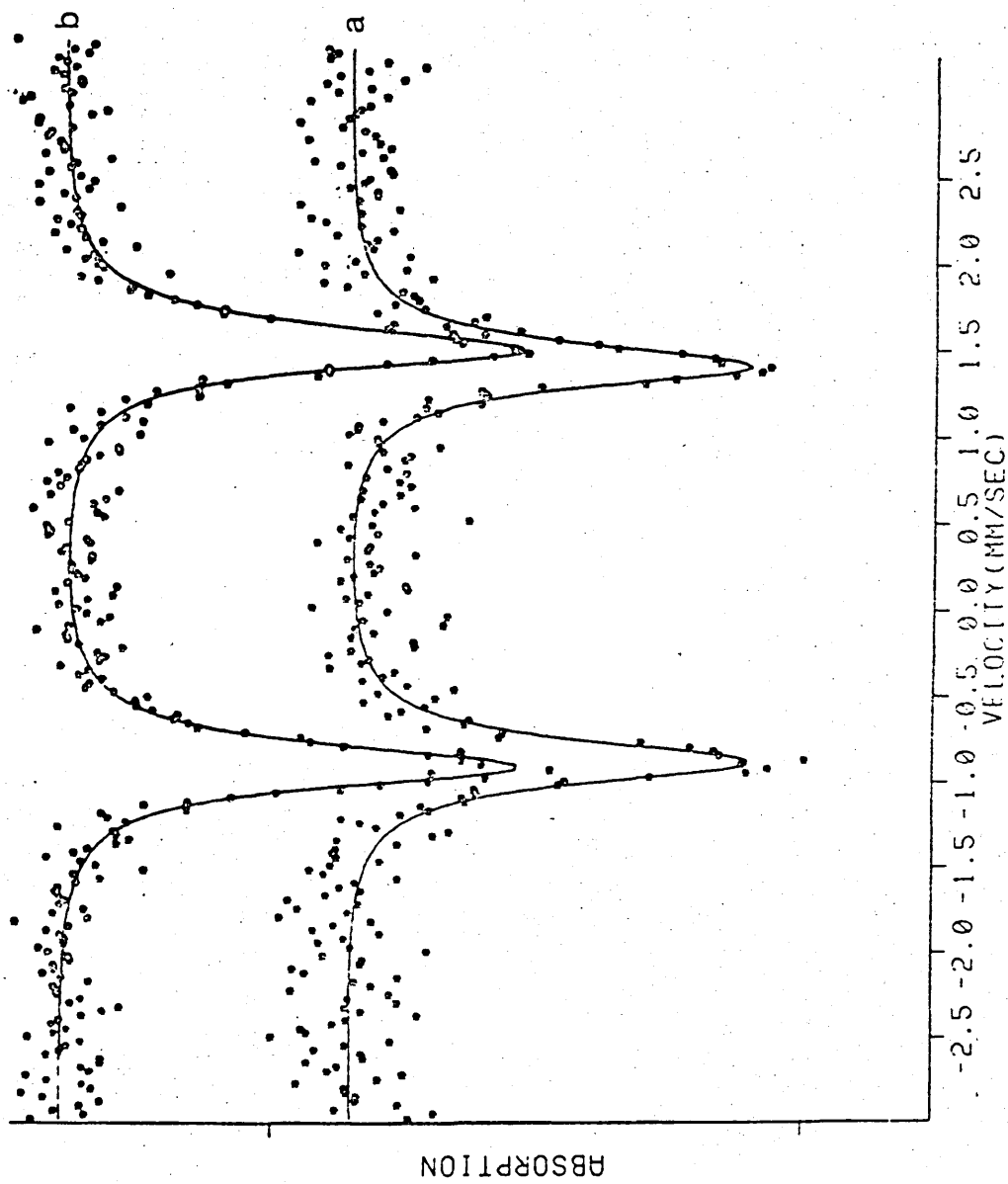
Fig. 5.10   Mössbauer Spectra of PDVF (cationic),and PDVF (radical),b.

is sufficiently long to span the cyclopentadienyl rings
without causing strain which would lead to a decrease in
the quadrupole splitting in the Mössbauer spectra [126].
Formation of this structure would involve an unusual
tail-tail intramolecular step, rather than the more
common head-tail mechanism leading to the three-carbon
bridge.

XV
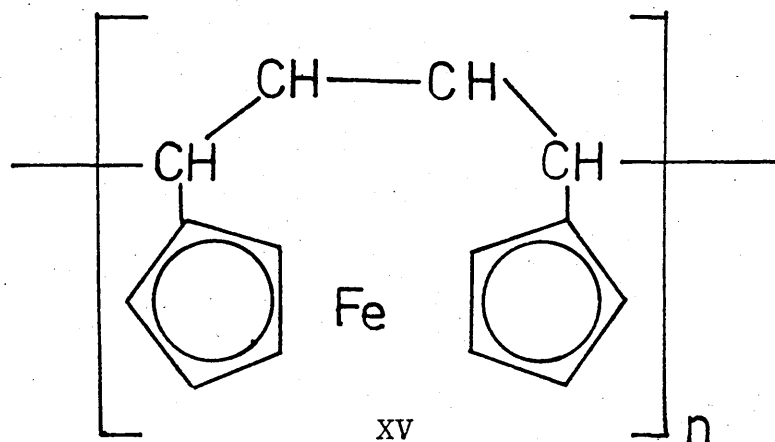
The proton n.m.r. of tetramethyleneferrocene, X, has
been recorded [116] and the peaks at δ 2.42 ppm and
δ 1.83 ppm attributed to the α and β bridge resonances
do not coincide with the broad peak centred at δ 1.2 ppm
observed in the spectrum of the cationic polymer.
Thus the four-carbon bridge is unlikely to be present.

Another possibility considered was the formation of
a 'ladder' structure, XVI.

XVI
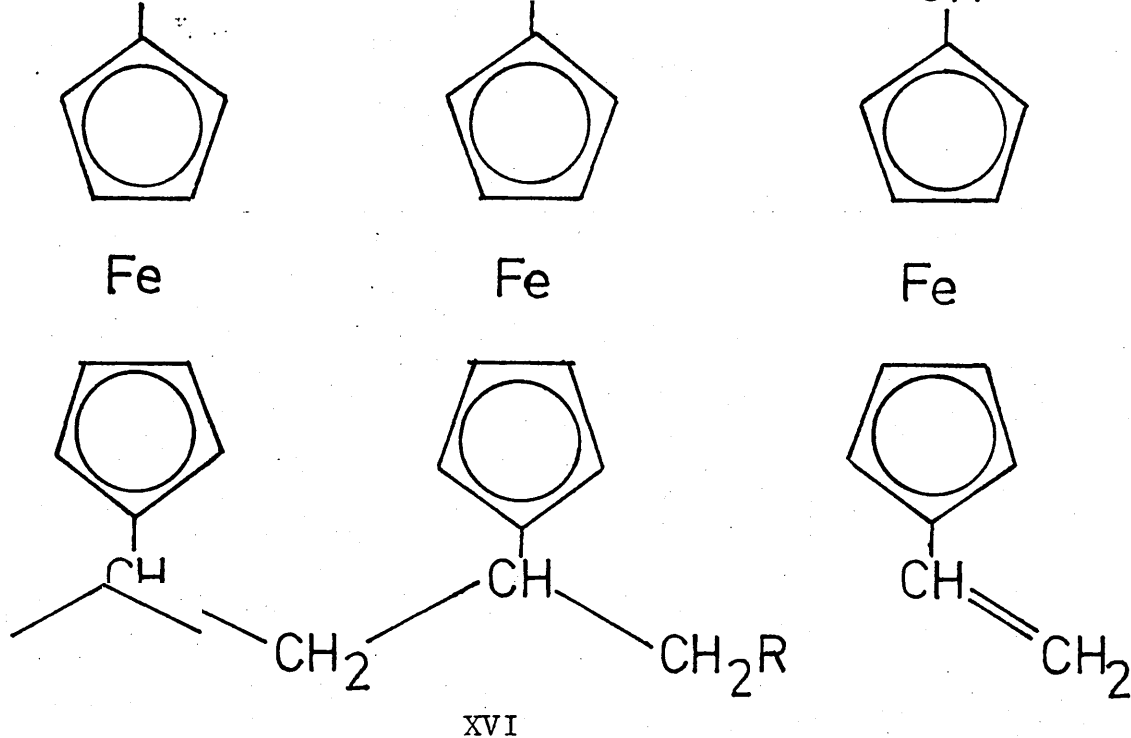
The formation of this structure would probably occur

via the linear uncyclised polymer with 100% pendant

double bond present. One of these residual vinyl

groups could then become initiated and the polymerisation

could occur along the bottom rings as well. Incomplete

reaction and termination could explain the presence of

residual unsaturation. This type of structure is very

similar to that of polyvinylferrocene but the infrared

spectra of the cationically-initiated polymer of DVF

and that of polyvinylferrocene are different, hence this is

unlikely to be the correct structure.

Both of the structures proposed above would give

unstrained Mössbauer parameters and neither would be

expected to show the characteristic ring breathing peak

at about 1110 cm^{-1} in their infrared spectra. However,

the evidence suggests that neither is the correct

structure. Further spectroscopic studies were therefore

necessary to establish the most likely structure for these polymers.

5.3.5 ^{13}C Nuclear Magnetic Resonance Spectra

The ^{13}C n.m.r. spectrum of PDVF (cationic) is shown in Fig. 5.11. It was generally less well resolved than the spectrum of the radical polymer which suggests that a mixture of structures exist. The β and γ carbons, are comparable with those of PVF, with little evidence of non-equivalence in these carbons, as observed in the PDVF (radical) spectrum. Important structural information is provided by the presence of the peak at about 21 ppm which is attributed to a methyl group, a fact that cannot be explained by any of the previously proposed structures. This methyl group probably accounts for the peak observed at δ1.2 ppm in the 'H n.m.r. spectrum. Also, the unsaturated carbons at 124.8 ppm and 133.3 ppm are not due to a vinyl group but have been shown by proton coupling of the spectra to be HC= signals. The α-carbon is observed at about 96.7 ppm which confirms the evidence provided by Mössbauer spectroscopy that predominantly a 'non-strained' structure is present; however a small absorption at 89.4 ppm suggests that a trace of the bridged structure may be present. The results are reviewed below in Table 5.8.
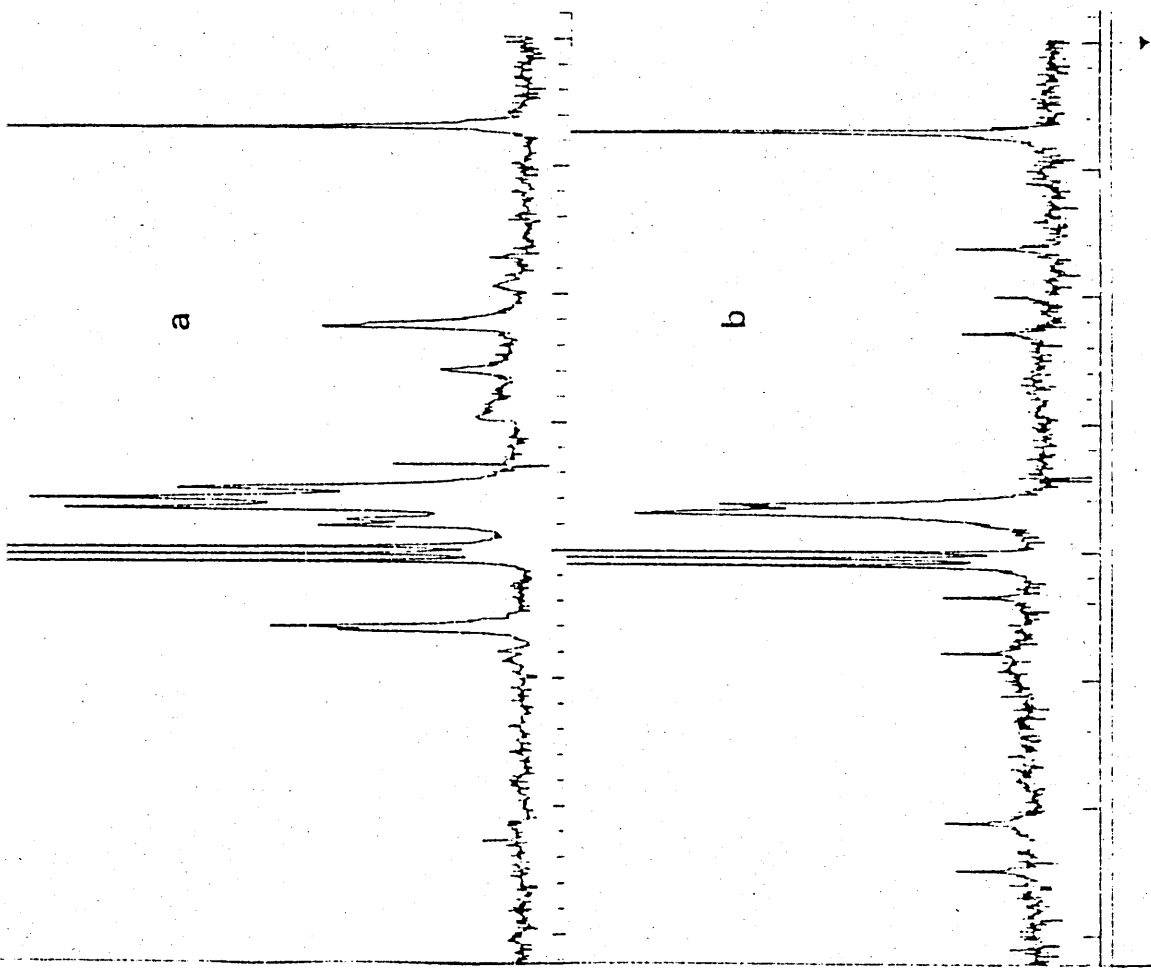
Fig. 5.11. ^{13}C n.m.r. Spectra of PDVF (cationic) and PDVF (radical)

Table 5.8   Carbon Chemical Shifts of Polymers

| Carbon	PVF	PDVF (radical)	PDVF (cationic)
		Chemical Shift/ppm from TMS in CDCl$_3$	
α	96.1	89.8, 90.6	96.7;
β,γ	67.1-68.5	65.1-70.9	66.9-68.8
1	32.2	36.0	36.2
2	44.0	43.9, 52.4	
CH$_3$			21.1
-CH=CH-			124.8, 133.3

PDVF (radical)

PVF
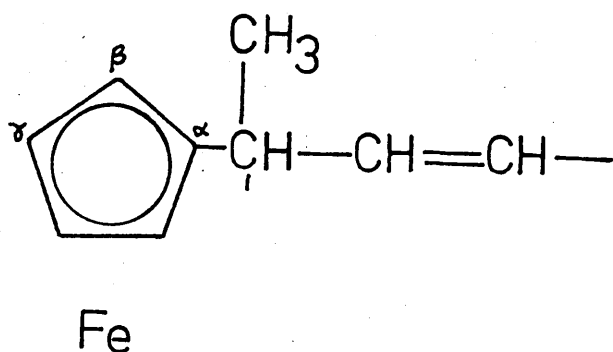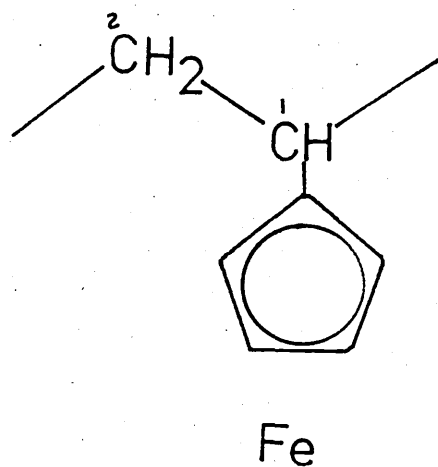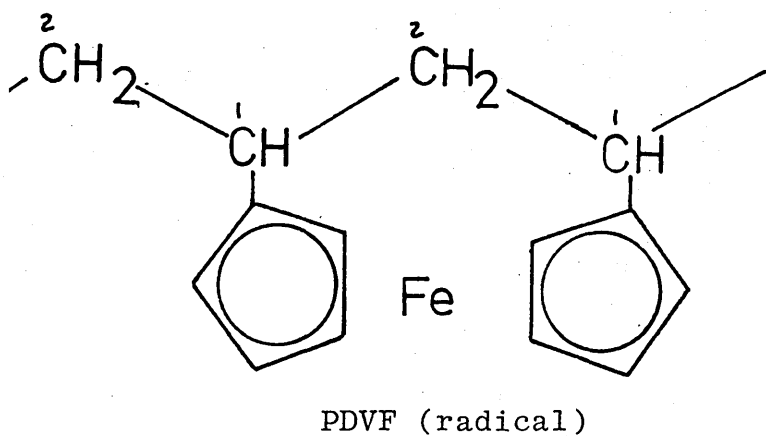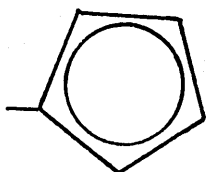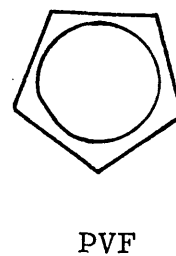
PDVF (cationic)

5.3.6 Proposed Structure for PDVF (cationic)

On the basis of the spectroscopic results obtained,

a structure for the cationic polymer is proposed, XVII.
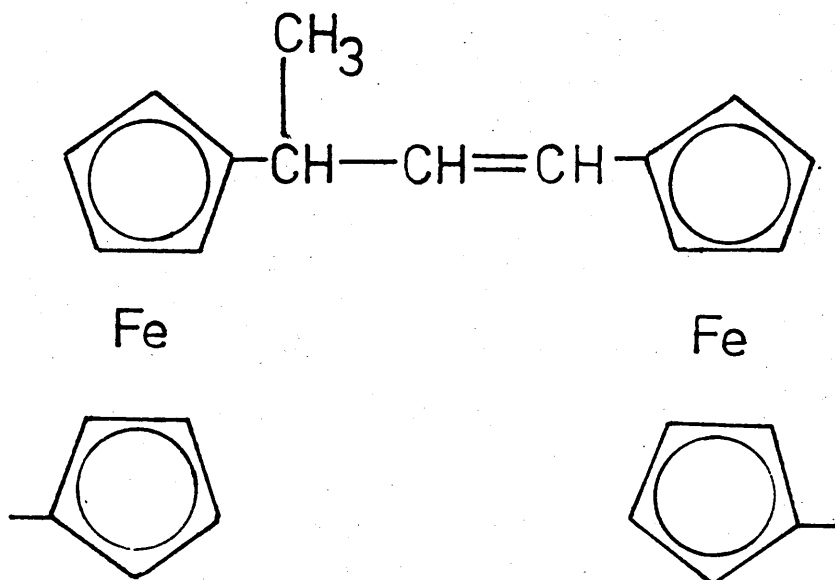
XVII

This type of structure has been observed with polymers

from α,ω-bis(4-vinylphenyl)alkanes, XVIII. [133]-[136]

XVIII
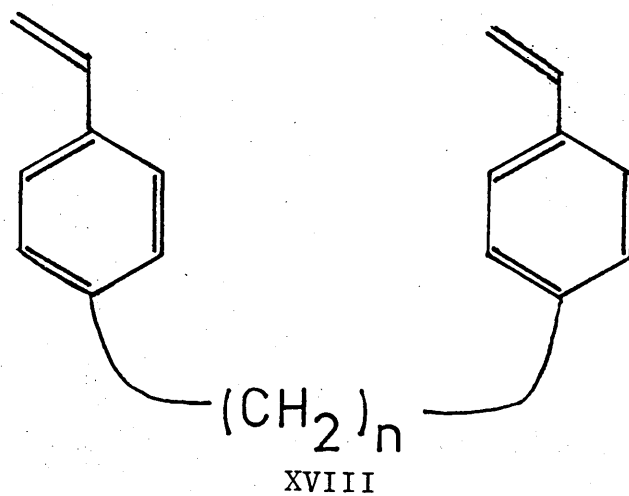
When n = 3, the alkane chain is sufficiently long to allow cationic cyclopolymerisation resulting in the formation of [3,3]-paracyclophane units (Fig. 5.12). However, if n = 1 or 2, the formation of the cyclopolymer becomes unfavourable and a linear polymer, XIX, (Fig. 5.12) is formed. These polymers exhibited an infrared absorption at 966 cm^{-1} characteristic of a CH out-of-plane vibration of a trans-double bond and closer examination of the infrared spectrum of the cationic polymer from DVF showed a corresponding peak at about 965 cm^{-1}. Their 'H n.m.r. results showed the olefinic protons gave a broad singlet at around δ6.3 ppm which was in the same region as the unsaturation in PDVF (cationic) observed at δ5.9 ppm.

The proposed mechanism for the cationic polymerisation of 1,1'-divinylferrocene using $BF_3.OEt_2$ initiator is outlined in Fig. 5.13. The proton initiates the reaction but after one addition to another monomer molecule, a proton is eliminated to produce an alkene unit within the polymer chain. Repetition of this process with the vinyl group on the other cyclopentadienyl ring introduces a third monomer unit into the structure. It is by this intermolecular polyaddition mechanism that the polymer can be produced. There may be a small amount of cyclopolymerisation as there was an absorption in the ^{13}C n.m.r. spectrum corresponding to a strained α-carbon.

Fig. 5.12   Cationic Polymerisation of α,ω-bis(4-vinylphenyl) alkane

$$BF_3.OEt_2 \rightleftharpoons OEt_2 + BF_3 \overset{H_2O}{\rightleftharpoons} H_2O.BF_3 \rightleftharpoons [HO.BF_3]^- + H^+$$
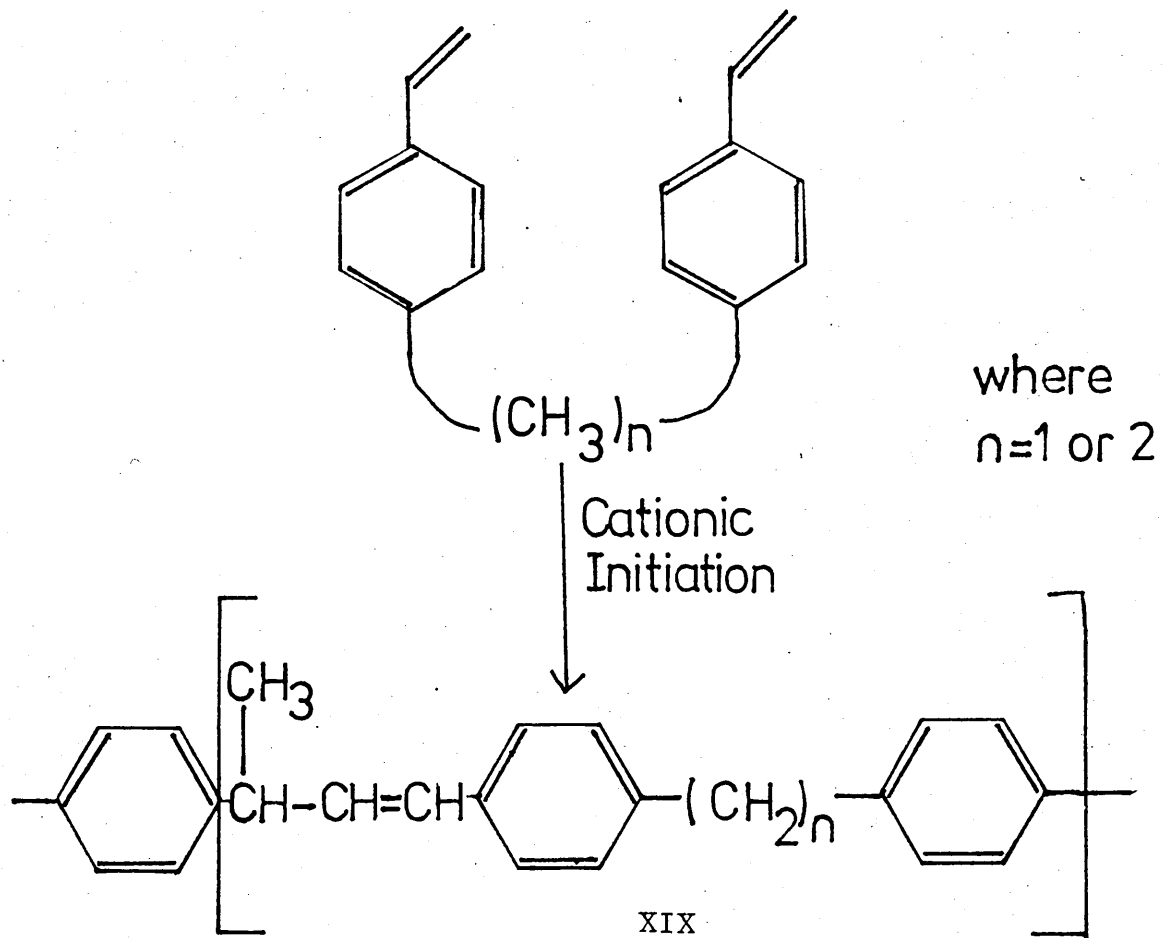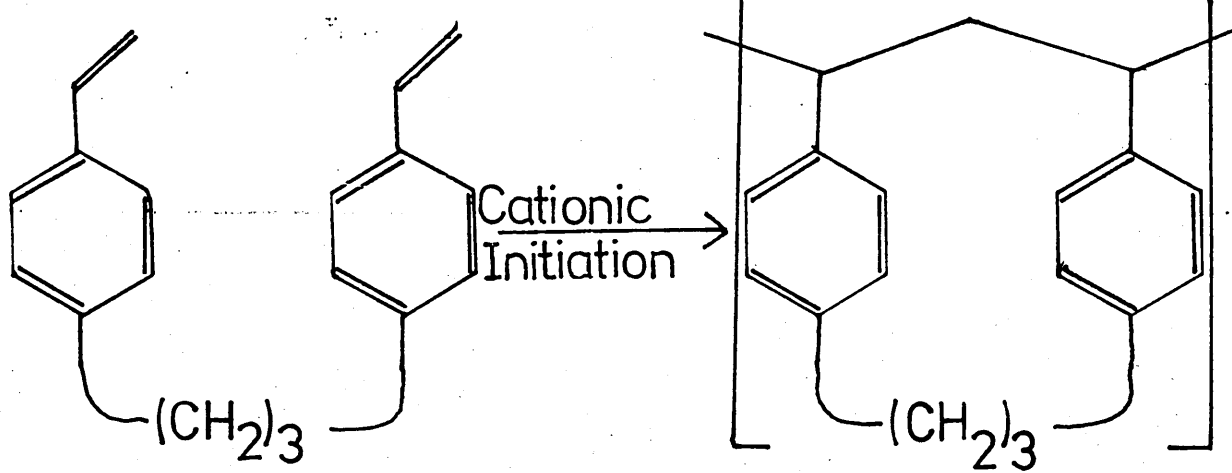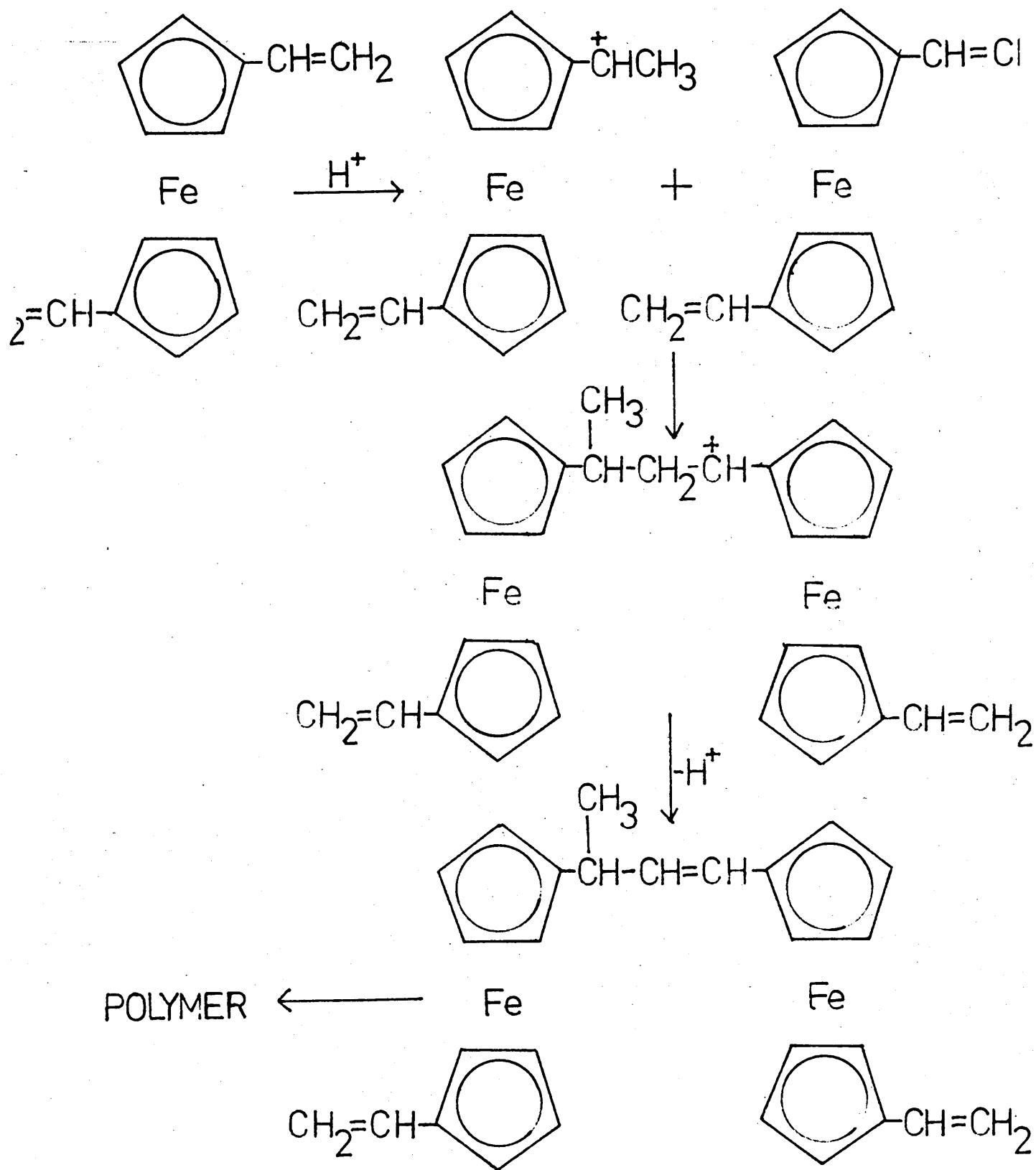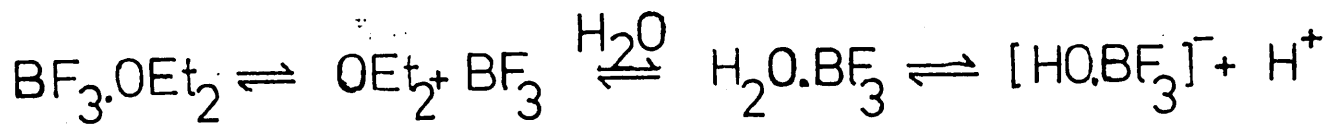
Fig. 5.13   Proposed Mechanism for $BF_3.OEt_2$ Initiated
Polymerisation of 1,1'-Divinylferrocene

- 126 -

To substantiate this proposal for the structure of the cationic polymer, the synthesis of the model compound, XX, was carried out and its spectroscopic properties compared with those of the cationic polymer.
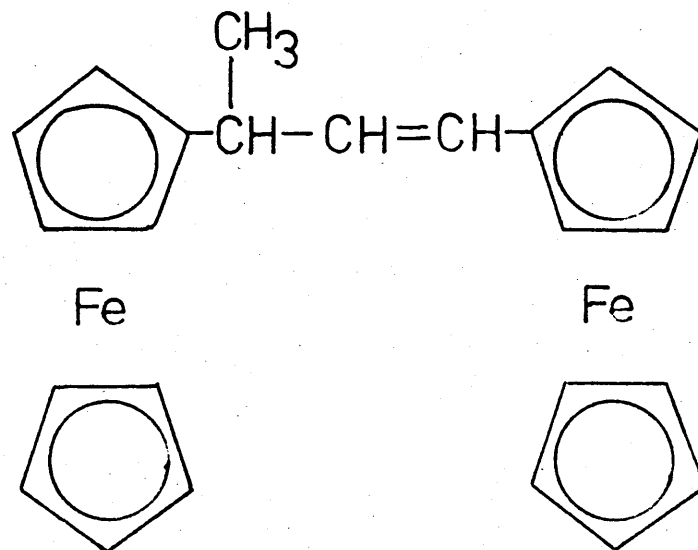
XX

5.3.7   Synthesis of 1,3-Diferrocenylbut-1-ene, XX

The synthesis of the model compound was successfully effected from 1-hydroxyethylferrocene [119] as shown in Fig. 5.14.   The synthesis is described in detail in Section 3.2.4.
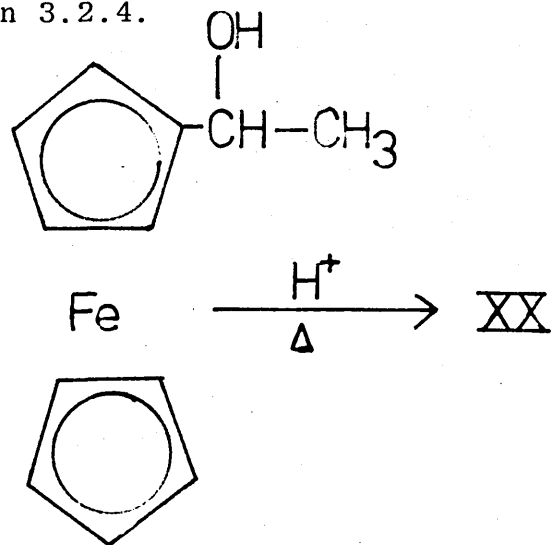
Fig. 5.14   Synthesis of 1,3-Diferrocenylbut-1-ene

The same compound has also been synthesised by the novel route outlined in Fig. 5.15. The Mössbauer parameters of the products of each step of this route are given in Table 5.9.

Table 5.9   Mössbauer Parameters of the Precursors
            to the Model Compound (XX)

	Isomer Shift mm s^{-1}	Quadrupole Splitting mm s^{-1}
Acetyl ferrocene	0.44	2.26
1,3-Diferrocenylbut-1-one-2-ene, XXI	0.44	2.25
1,3-Diferrocenylbutan-1-one, XXII	0.44	2.34
1,3-Diferrocenylbutan-1-ol, XXIII	0.45	2.37
1,3-Diferrocenylbut-1-ene, XX	0.45	2.37

From Table 5.9, it appears that the carbonyl containing derivatives show the lowest quadrupole splitting, as predicted by comparison with the results for acetyl-ferrocene. None of the structures, however, gave more than one quadrupole doublet as might have been expected for structures with two iron atoms in different electronic environments. Whereas, it is easy to envisage in XXI that the different electronic effects are averaged via electron delocalisation, the latter three structures (XXII, XXIII and XX) do not provide any obvious means of electron delocalisation. In XX and XXII, steric factors may prevent ring-olefin or ring-carbonyl π-overlap, while in structure XXIII, the parameters for hydroxy and alkyl substituted ferrocenes are similar and the two quadrupole doublets must overlap.
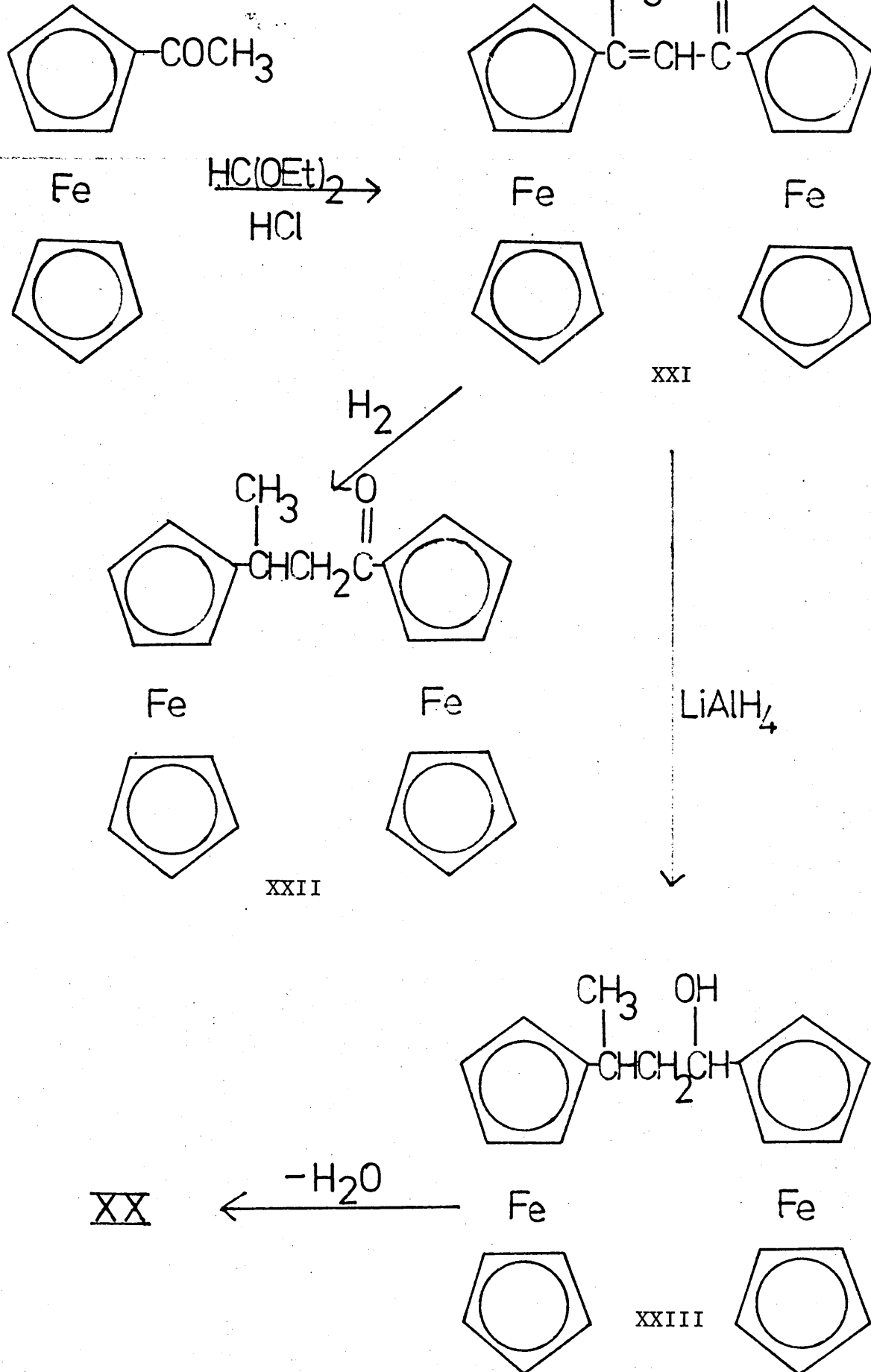
Fig. 5.15 Synthetic Route to Cationic Model Compound

The infrared spectrum of the model compound was almost identical to that of the cationic polymer (Fig. 5.16). One of the major differences observed was the presence of the 1,110 cm^{-1} 'ring breathing' peak in the model, which is to be expected as there is no restraint present across the rings. In the polymer, this peak will be considerably reduced as both cyclopentadienyl rings are incorporated into the polymer chain and ring 'breathing' is inhibited.

The proton n.m.r. spectrum of the model compound showed greater resolution than that of the polymer, but the positions of the absorptions relative to TMS were comparable (Fig. 5.17). The CH=CH protons in the model compound were centred at approximately δ5.85 ppm and the ring protons, showing some inequivalence, were observed at around δ3.7 ppm - δ4.4 ppm. The positions of these absorptions agree very well with those exhibited by the polymer. The aliphatic protons of the model compound also fall at a comparable position to those of the cationic polymer, but instead of there being one broad peak, the model showed two peaks centred at approximately δ1.3 ppm and δ0.9 ppm which are assigned to the methyl group and the aliphatic -CH-, respectively.

The ^{13}C n.m.r. of 1,3-diferrocenylbut-1-ene (Fig. 5.18) also provided confirmation that the structure proposed for PDVF (cationic) is correct. The assignment of the peaks is shown in Table 5.10.
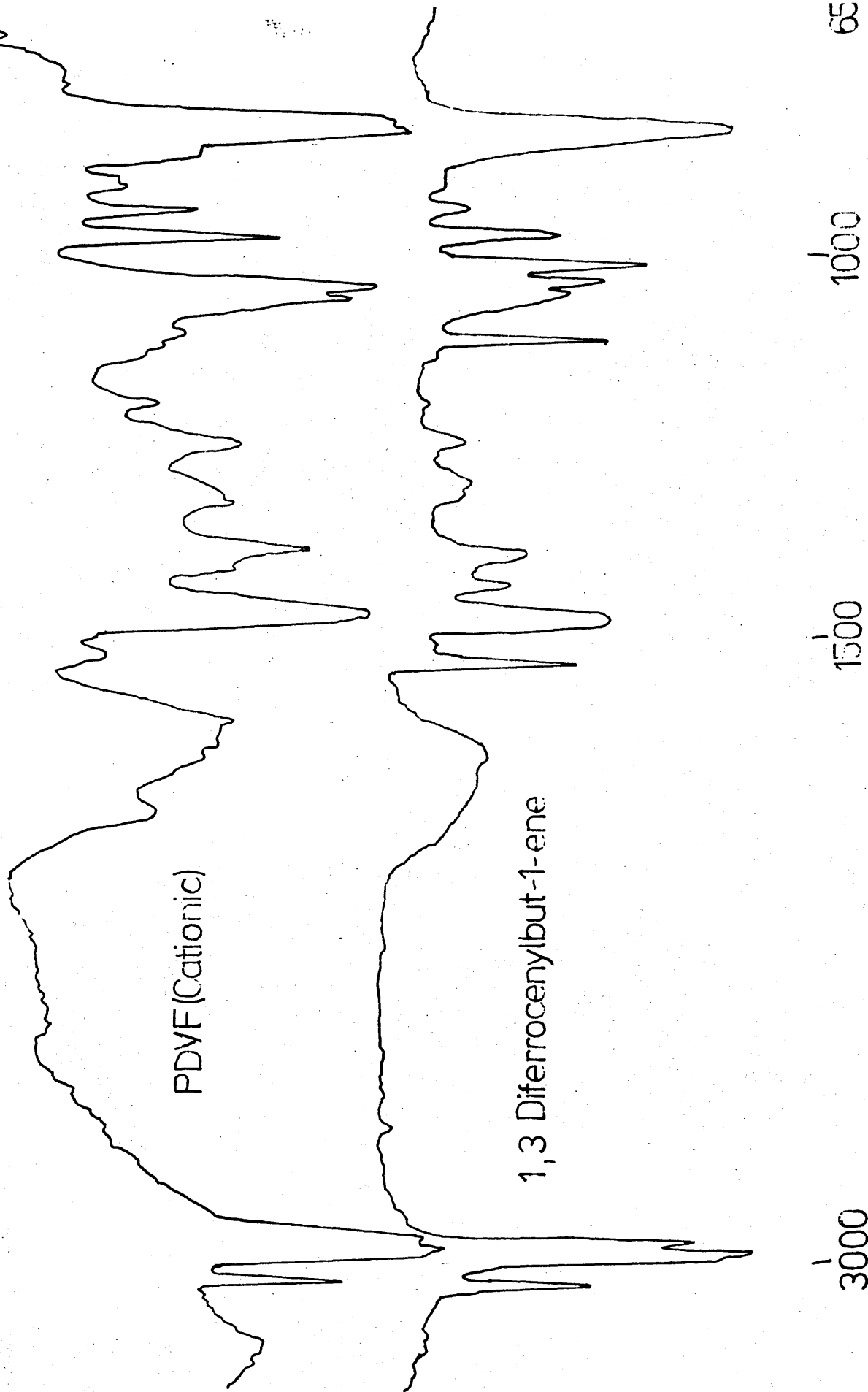
Fig. 5.16 Infrared Spectra of PDVF (cationic) and Model Compound

PDVF (Cationic)

1,3 Diferrocenylbut-1-ene

3000

1500

1000

65
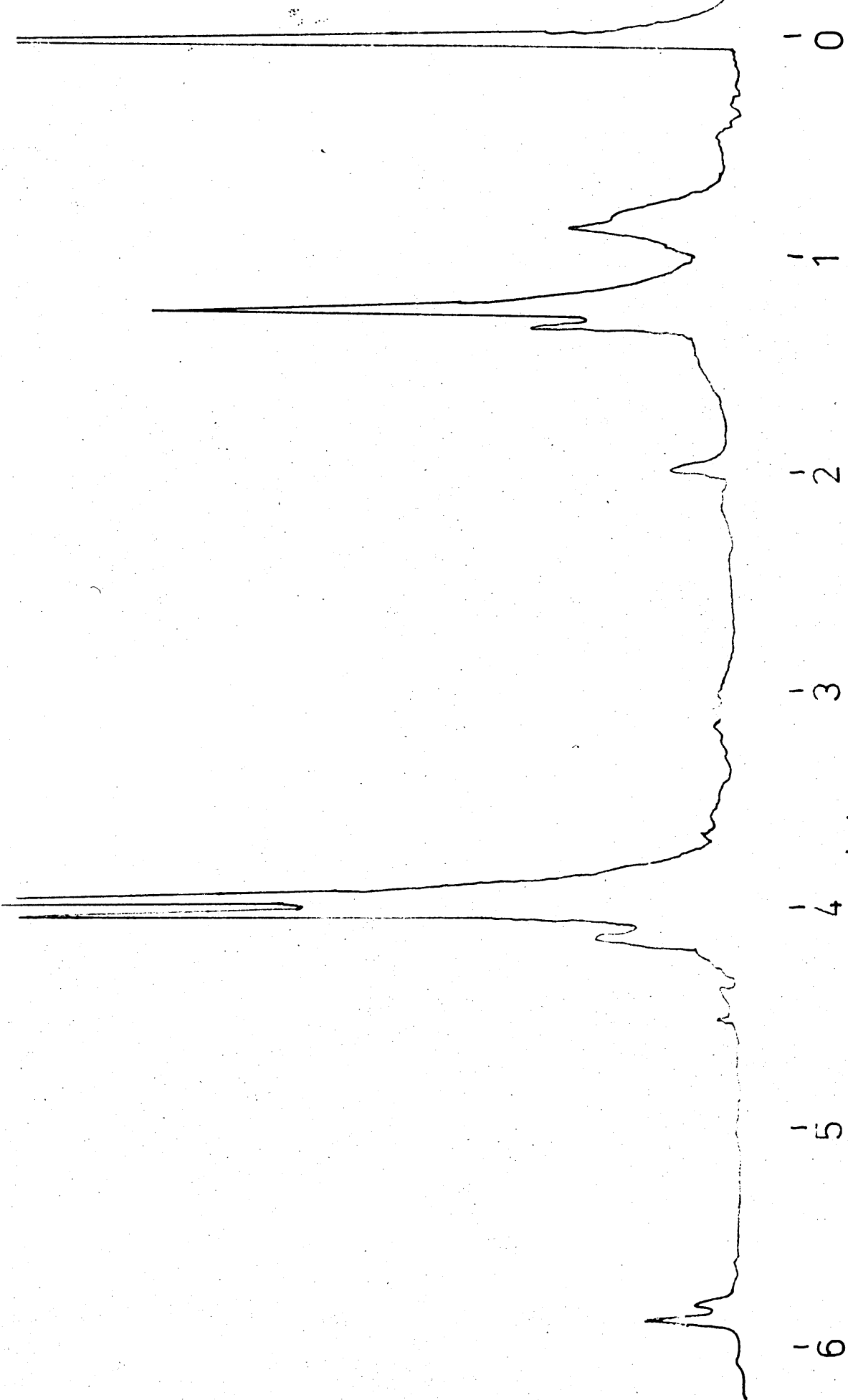
Fig. 5.17 'H n.m.r. of Model Compound
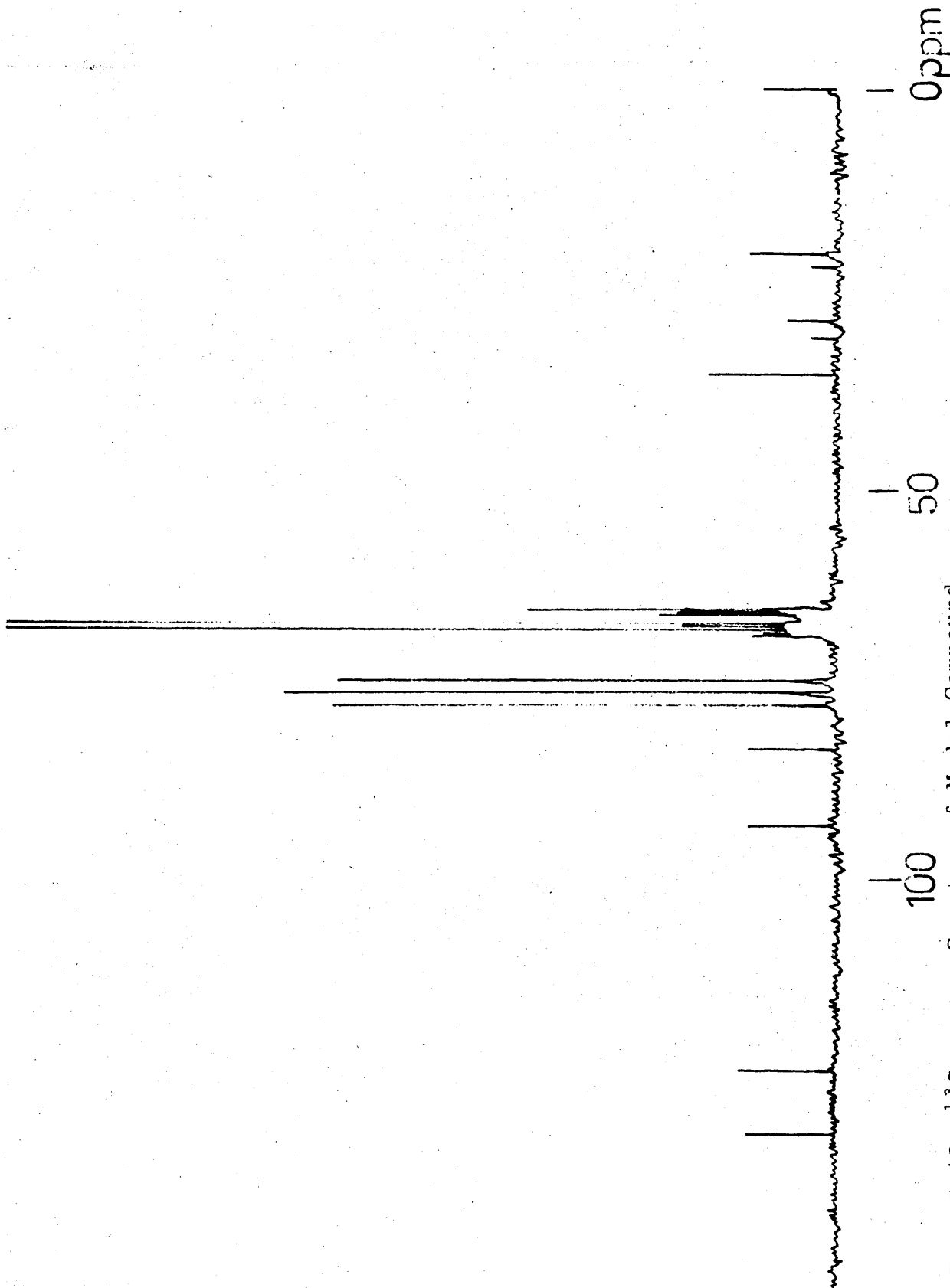
Fig. 5.18 ^{13}C n.m.r. Spectra of Model Compound

Table 5.10 ^{13}C n.m.r. Chemical Shifts for

1,3-Diferrocenylbut-1-ene and PDVF (cationic)

Position of Peak/ppm relative
to TMS

1,3-Diferrocenyl-but-1-ene	PDVF (cationic)[a]	Assignment
133.01	133.36	Olefinic CH adjacent to ring system
124.95	124.74	Other olefinic carbon
93.93	94.16	Quarternary carbon adjacent to non-olefinic CH
84.02	84.03	Quarternary carbon adjacent to olefinic CH
69.83–66.29	68.80–66.92	β and γ ring carbons
36.44	36.22	-CH-
21.13	21.17	-CH$_3$-

a Polymer examined from Run 2, Table 5.7.

The absorption at 84.03 ppm, which was previously
assigned to the quarternary carbon of a bridged
structure, has been reassigned to the α-carbon adjacent
to the olefinic CH in structure XX. This assignment
was made after ^{13}C n.m.r. studies were carried out on the
monomer, 1,1'-divinylferrocene and also on the mono-
substituted derivative, vinylferrocene (Table 5.11).

Table 5.11 ^{13}C n.m.r. Chemical Shifts of Vinylferrocene and 1,1' Divinylferrocene

Position of Peak/ppm relative to TMS

Vinylferrocene	1,1'Divinylferrocene	Assignment
134.57	134.03	Olefin carbon adjacent to α-carbon
110.95	111.17	CH_2 = olefinic carbon
83.43	84.13	α-carbon on substituted ring
69.13–66.53	69.83–67.88	Remaining ring carbons

Therefore the peak at 84.03 ppm in the spectrum of the cationic polymer was due to the quarternary carbon directly attached to the olefin group. The olefin carbons in the vinylferrocene studied were assigned by proton coupling of the spectra. The spectra were in good agreement with those recorded by previous workers [44], [45].

Therefore the major structure present in the cationic polymer has been shown to be XX, but the amount of unsaturation present in the proton n.m.r. spectra was still lower than one double bond per ferrocene unit. Previous calculations assumed the unsaturation to be due to a pendant vinyl group and a suitable equation was derived (eqn. 1.2). Now this equation needs to be modified to comply with the new structure.

If the polymer is assumed to consist of the following structures:
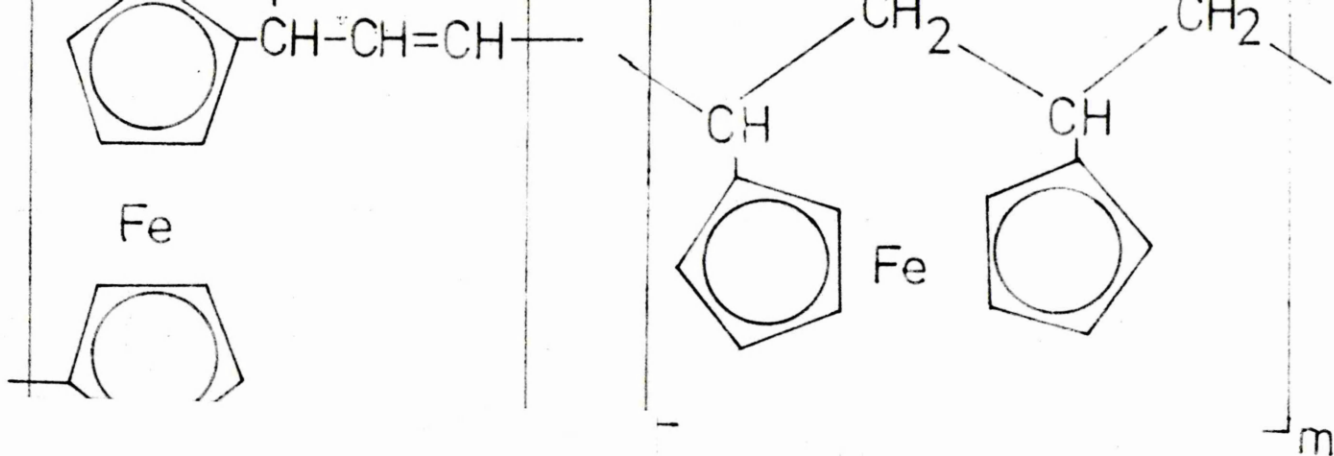
Y moles $n \gg m$

unsaturation

ene ring protons

tic protons

Therefore in terms of B:

$$\%X = \frac{\frac{A}{2}}{\frac{A}{2} + \frac{B - 4A}{8}} \times 100 = \frac{\frac{A}{2}}{\frac{B}{8}} \times 100 = \frac{4A}{B} \times 100 \qquad (5.1)$$

- 136 -

or in terms of C:

$$\%X = \frac{\dfrac{A}{2}}{\dfrac{A}{2} + \dfrac{C - 2A}{6}} \times 100 = \frac{\dfrac{A}{2}}{\dfrac{A + C}{6}} \times 100 = \frac{3A}{A + C} \times 100$$

(5.2)

Using eqns. 5.1 and 5.2, the percentage of non-cyclised structure present calculated from the 'H n.m.r. spectrum for the BF_3 OEt_2 initiated polymers was in the range 70-85% which was in agreement with other spectroscopic evidence.

Therefore it has been shown that the polymers from BF_3 OEt_2 consist predominantly of the proposed structure XVII, and that previous proposals [79] - [83] were in error.

5.3.8   Cationic Polymerisation with Et_2AlCl

Further cationic polymerisation studies were carried out using an aluminium based initiator. Minor differences had previously been noted in the infrared and 'H n.m.r. spectra of PDVF initiated by a number of different cationic initiators [83]. It was anticipated that with the further knowledge available on the structure of the cationic polymer that these differences could be explained.

Polymerisations were carried out in dichloromethane as shown in Table 5.12.

Table 5.12   Cationic Polymerisations of 1,1'-Divinylferrocene
using Et_2AlCl Initiator

[Monomer] moles dm^{-3}	[Et_2AlCl] moles dm^{-3}	Reaction Temp ^0C	Reaction Time Hours	Conversion %
0.40	0.022	0	16	10S 4I
0.40	0.022	0	16	3S 7I
0.48	0.088	-78	168	26S 13I

The infrared spectrum of the polymer is very similar to the spectrum observed for the BF_3OEt_2 initiated polymer except for the additional peak at about 1,000 cm^{-1} which is also present in the spectrum of the model compound (XX) but has not been assigned. On the whole, the infrared spectrum indicated that the structure was similar to that proposed in Section 5.3.6.

The 'H n.m.r. spectrum of the polymer showed similar aliphatic and ring proton absorption patterns as in the BF_3OEt_2 initiated polymer. The olefinic region of the spectrum, however, showed three very broad bands centred around δ4.8, 5.1 and 5.6 ppm, though absorption was still present up to a value of δ6.3 ppm. Part of the unsaturation pattern exhibited was similar to that of vinylferrocene (Section 5.3.3) and this indicated that the polymer may contain the linear polymer unit, VI, together with structure, XVII.

5.4 Anionically Initiated Polymers from 1,1'Divinyl-Ferrocene

5.4.1 Polymer Synthesis

Though vinylferrocene has been successfully polymerised using anionic initiators [71], there have not been any previous reports of polymers produced from 1,1'-divinylferrocene by the same method. Anionic polymerisation was carried out in tetrahydrofuran under the conditions shown in Table 5.13.

Table 5.13 Anionic Polymerisation of 1,1'-Divinylferrocene

[Monomer] mol dm^{-3}	[BuLi] mol dm^{-3}	Reaction Temp ^{o}C	Reaction Time Hours	Conversion %	
0.53[a]	0.20	-78	16	S0	I4
0.53[a]	0.30	-78	24	S0	I11
0.53[b]	2.00	0	6	S33[c]	I2

a   Reaction carried out under nitrogen atmosphere

b   Reaction carried out under vacuum

c $\overline{M}_n$ = 1,154 by GPC, expressed as the polystyrene equivalent.

5.4.2 Spectroscopic Studies of PDVF (anionic)

The infrared spectrum of the benzene soluble fraction of the product gave a similar result to comparable products obtained by radical initiation. The 'H n.m.r. spectrum was also consistent with the cyclopolymer structure, and the Mössbauer parameters for the product were characteristic of a bridged structure. (I.S. = 0.41 mm s^{-1}, Q.S. = 2.30 mm s^{-1}). Examination of the

benzene insoluble fractions indicated that the iron in the polymer had been oxidised to the Fe(III) low spin ferricinium state (I.S. = 0.38 mm s^{-1}, Q.S. = 0.79 mm s^{-1}).

The ^{13}C n.m.r. spectrum of the polymer was very similar to that obtained for the radical polymer and is shown in Fig. 5.19. The major peaks have been assigned previously (Section 5.2.4), but the smaller absorptions in the region 14-31 ppm present in the spectrum of the anionic polymer were assigned to fragments of the butyl lithium initiator.

5.5 Conclusions

The structures of polymers from 1,1'-divinylferrocene have been thoroughly investigated using more extensive spectroscopic techniques than had previously been used. Earlier workers, Kunitake et al [82] - [83] and Sosin et al [79] - [81] had proposed structures for these polymers on the basis of infrared and 'H n.m.r. spectroscopic data, and their conclusions were that the polymers, produced by both radical and cationic initiation of DVF, were cyclopolymers containing a three-carbon bridged ferrocene unit. The Mössbauer parameters obtained for cationic initiated polymers of DVF (I.S. = 0.45 mm s^{-1}, Q.S. = 2.39 mm s^{-1}) did not provide evidence for the trimethylene bridge and by use of ^{13}C n.m.r., and with further consideration of 'H n.m.r. and infrared spectra of these polymers, an alternative structure has been proposed for these polymers. The
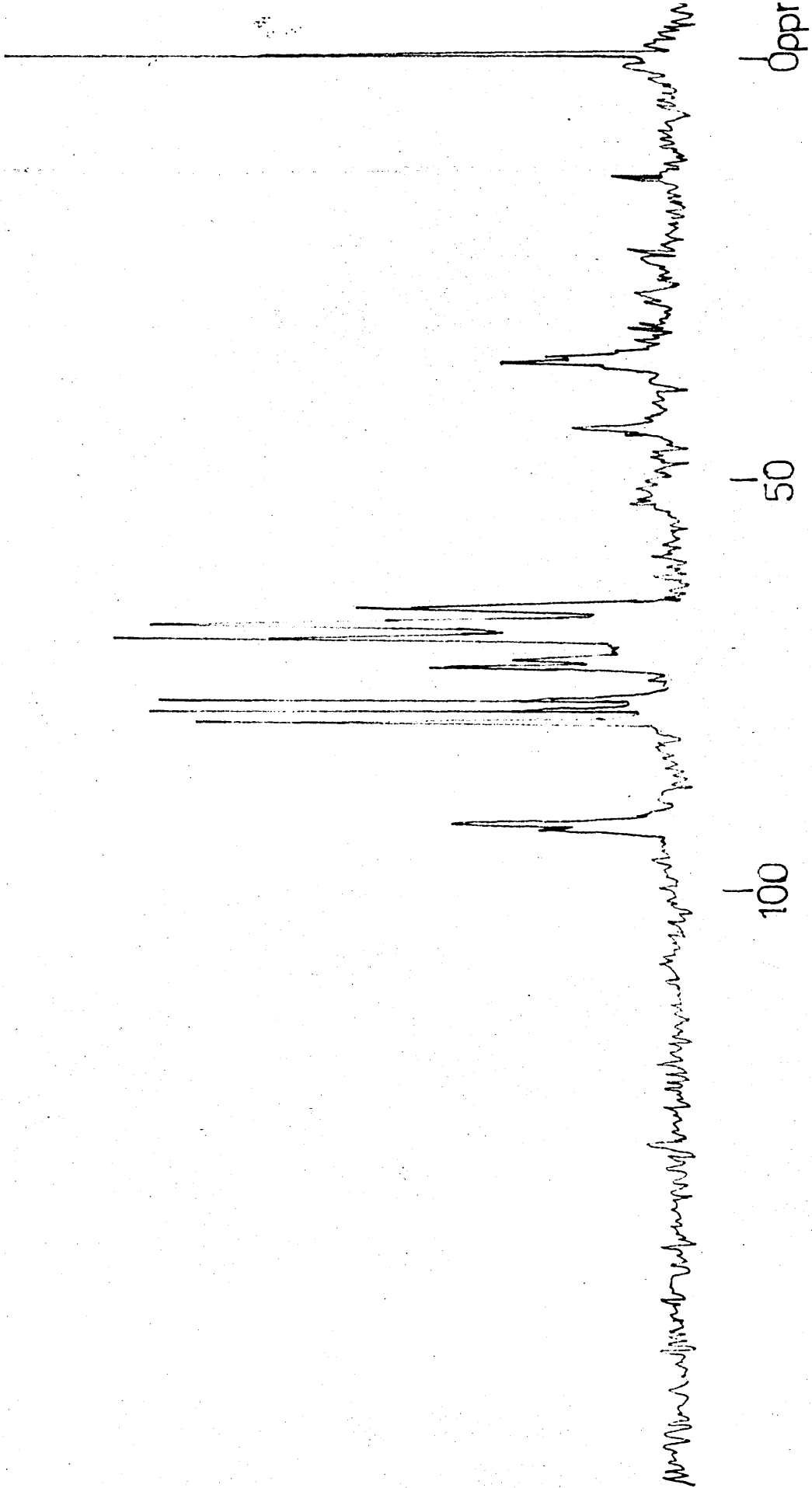
Fig. 5.19 ^{13}C n.m.r. Spectrum of PDVF (anionic)

proposed structures of both the radical and cationic polymers have been confirmed by the synthesis of relevant model compounds and by comparison of their spectroscopic properties with those of the polymers.

The anionic polymer from DVF, previously unreported, has been prepared and its structure shown to contain a three-carbon bridged ferrocene, as with the radical polymer.

CHAPTER SIX : VARIABLE TEMPERATURE FE-57 MÖSSBAUER STUDIES OF POLYMERS FROM VINYLFERROCENES

6.1 Introduction

Variable temperature Mössbauer studies were undertaken to obtain additional structural information about the polymers from monovinyl and divinylferrocene. In the previous two chapters, the application of Mössbauer spectroscopy has been used to give information about the electronic state of the iron atom and the structure of surrounding atoms. By studying the temperature dependence of the recoilless fraction, f_a, it was hoped to yield additional dynamic vibrational properties. Investigations of this nature have previously been made on crystalline solids [138] and it was hoped to extend this treatment to describe the vibrational properties of amorphous polymers. Comparisons between the differing PDVF structures were also of interest during the studies.

6.2 Variable Temperature Mössbauer Studies

Six sets of variable temperature experiments were performed under identical experimental conditions within the temperature range of approximately 80 to 300 K. A sample of crystalline ferrocene was studied together with two samples of cationically initiated PDVF (linear) and a sample of the cyclopolymer, anionic PDVF (cyclic). These polymer samples were chosen because they were shown to be structurally different in Chapter 5.

The Mössbauer absorption line area is related to the absorber thickness t by the expression:

$$A(t) \; \alpha \; \frac{t}{2} \exp \left(-\frac{t}{2}\right) \left[I_0 \left(\frac{t}{2}\right) + I_1 \left(\frac{t}{2}\right) \right] \qquad (6.1)$$

where I_0 and I_1 are the zero and first order Bessel functions [107].

The Mössbauer absorber thickness t is given by

$$t = nf_a\sigma_0 \qquad (6.2)$$

for a single line. Small t expansion of Eq. 6.1 gives

$$A(t) \; \alpha \; t \; (1 - 0.25t + 0.0625 \; t^2 + \ldots) \qquad (6.3)$$

Thus for small t, the absorption area is proportional to the absorber recoilless fraction, f_a.

The normalised absorber line areas were determined in the usual way using the fitted line width and depths of the quadrupole doublet. The units of line width chosen were channels to give easy handling of results.

The absorption line areas were corrected for thickness effects using the recoiless fraction determined for PVF by Litterst et al [142]. No attempt was made to determine absolute values of f_a for any of the polymers.

A typical value of f for the macromolecules was calculated as follows:

Molecular weight of a ferrocene unit in PVF = 212

Sample disc diameter = 1.7 cm, therefore area = 2.27 cm^2

Each sample disc contains approximately 30 mgs of polymer.

Therefore, there are $\dfrac{30 \times 55.85}{2.27 \times 212}$ mgs of Fe^{57}/cm^2

and $2.14 \times 10^{-2} \times \dfrac{30 \times 55.85}{2.27 \times 212}$ mgs of Fe^{57}/cm^2 = 0.075 mgs Fe^{57}/cm^2.

$\therefore$ Number of atoms of Fe^{57}/cm^2 = $\dfrac{0.075}{55.85} \times 6.022 \times 10^{23} \times 10^{-3}$

$n = 8.09 \times 10^{17}$ atoms/cm^2

Now $t = nf\sigma_0\beta_i$, and for a quadrupole doublet $\beta_i = \frac{1}{2}$.

$\therefore$ $t = 8.09 \times 10^{17} \times 2.56 \times 10^{-18} \times 0.5 \times f$

$\therefore$ $\underline{t = 1.04\ f}$

Approximate values for the recoiless fraction of amorphous PVF were obtained from the work of Litterst et al [142].

From the published graph, $- \ln f = 1.2$ at 80K, $\therefore t \approx 0.301$.

$\qquad\qquad\qquad\qquad\quad - \ln f = 3.3$ at 300K, $\therefore t \approx 0.037$.

Hence t has values of 0.301 - 0.037 for PVF over the temperature range 80 - 300K.

From equation 6.3:

If $A^1 = t$ and $A = t - 0.25t^2 + 0.0625t^3$, then for $t = 0.301$

$\qquad A^1 = 0.313$

and $\quad A = 0.290$

Giving a % error at 80K of $\approx$ 8%.

For $t = 0.037$

$\qquad A^1 = 0.038$

$\qquad A = 0.0376$

Giving a % error at 300K of $\approx$ 1%.

Therefore it has been shown that the deviation due to the thickness effect was at most 8% over the temperature range studied, compared to the observed deviation of about 60%.

To correct the data for the thickness effect, it was assumed in the first instance that f(T) follows a Debye model.

Then $A(t) = Kt(1 - 0.25t + 0.0625t^2)$ $\qquad\qquad$ (6.3)

and $\quad A_0 = Kt$

$\qquad A(t) = A_0(1 - 0.25t + 0.0625t^2)$

$\qquad K = 1 - 0.25t + 0.0625t^2$

$\therefore \quad A_0 = \dfrac{A(t)}{K} \qquad\qquad K < 1$

Using the values of f determined by Litterst [142] the correction factors for the data, K, are shown in Table 6.1

- 146 -

Table 6.1 Correction Factors for the Polymeric Samples

T	ln f	f	t	K
80	−1.30	0.27	0.28	0.93
100	−1.50	0.22	0.23	0.94
120	−1.69	0.18	0.19	0.95
140	−1.89	0.15	0.16	0.96
160	−2.09	0.12	0.12	0.97
180	−2.30	0.10	0.10	0.97
200	−2.50	0.082	0.085	0.98
220	−2.70	0.067	0.069	0.98
240	−2.90	0.055	0.058	0.985
260	−3.10	0.045	0.046	0.987
280	−3.30	0.037	0.038	0.989
300	−3.50	0.030	0.031	0.990

The corrected line area Mössbauer data is shown in Appendix 1.

The results are shown in Figs. 6.1, 6.2 and 6.3 and the temperature dependence of lnA for ferrocene over the range studied gave the expected linear relationship. [138] However, as can be seen in Fig. 6.1, the amorphous polymers show a deviation away from linearity, PVF being fitted as two straight lines with a change in gradient at approximately 200 K. Studies on the Mössbauer parameters are shown in Figs. 6.4, 6.5 and 6.6 and they show a linear
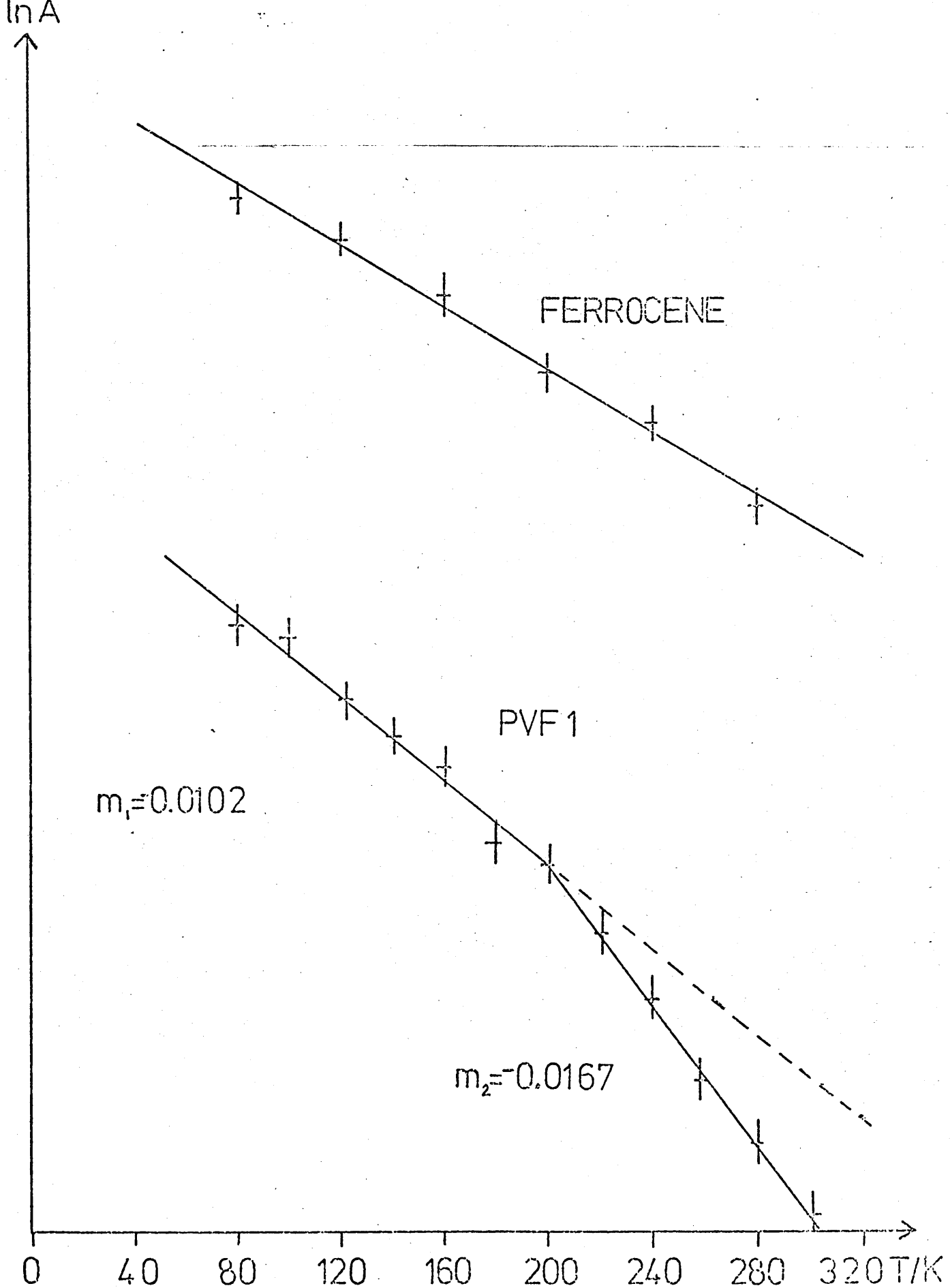
Figure 6.1   Temperature Dependence of lnA for Ferrocene
and PVF

- 148 -
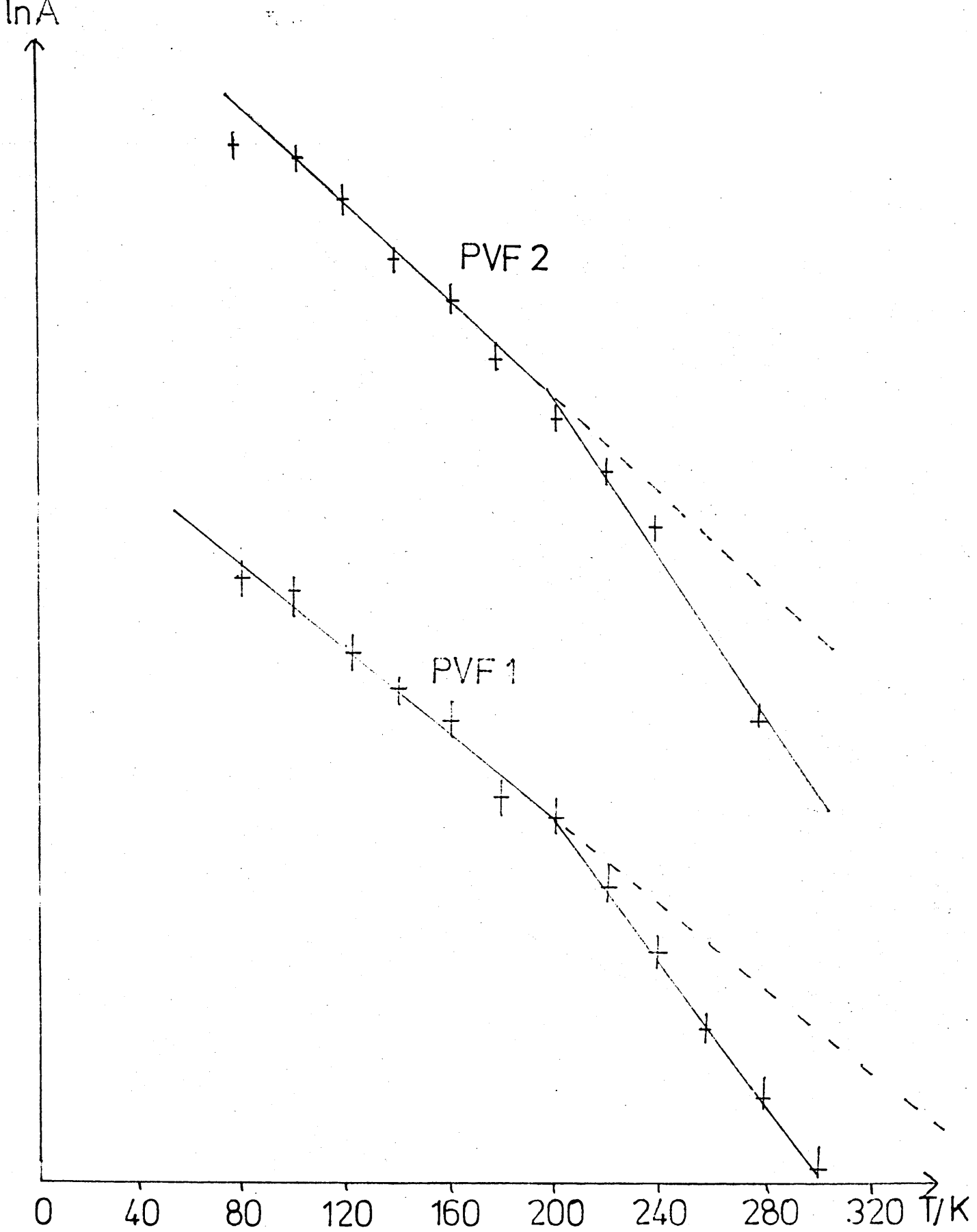
Fig. 6.2   Temperature Dependence of lnA for PVF
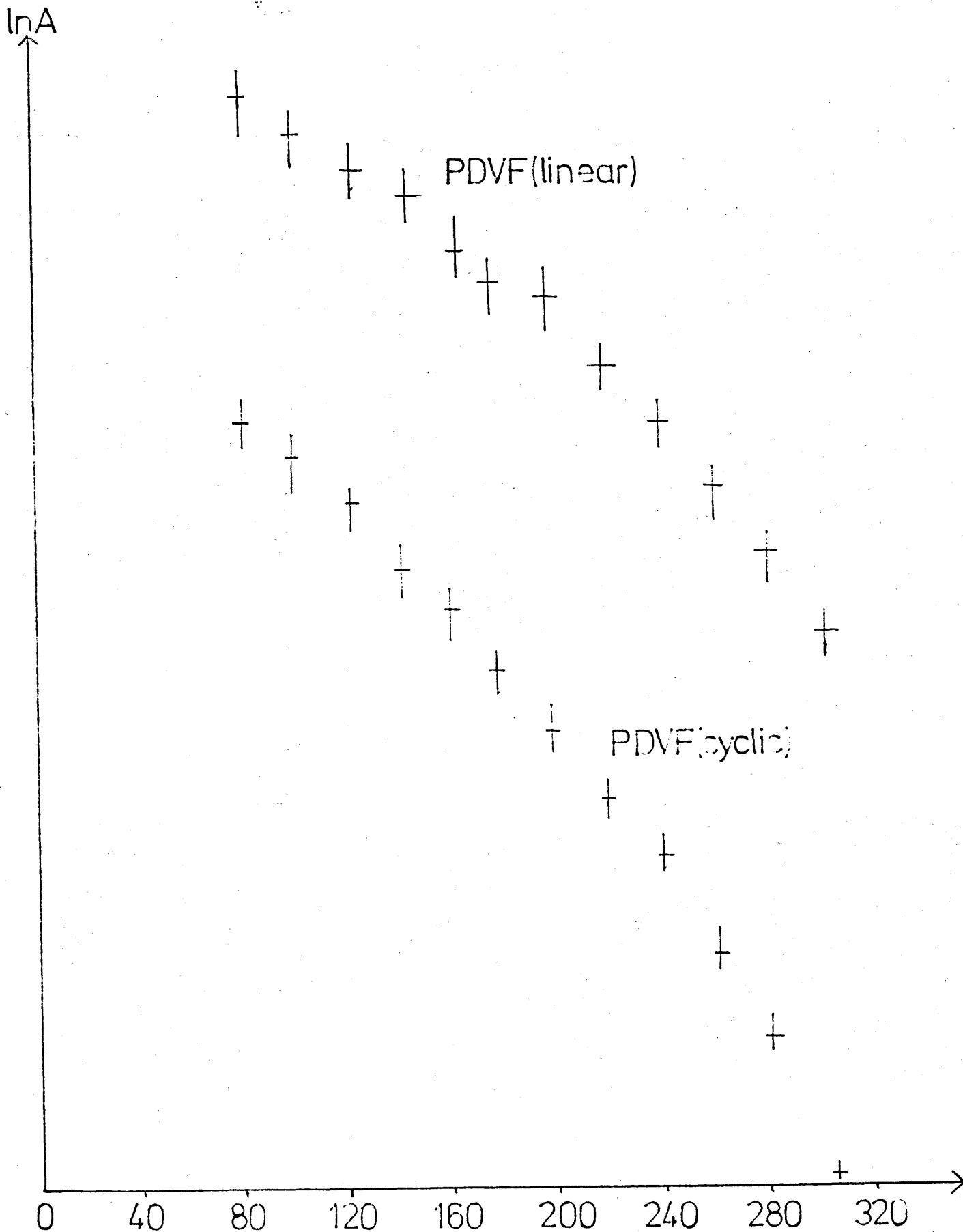
Fig. 6.3 Temperature Dependence of lnA for PDVF (linear) and PDVF (cyclic)
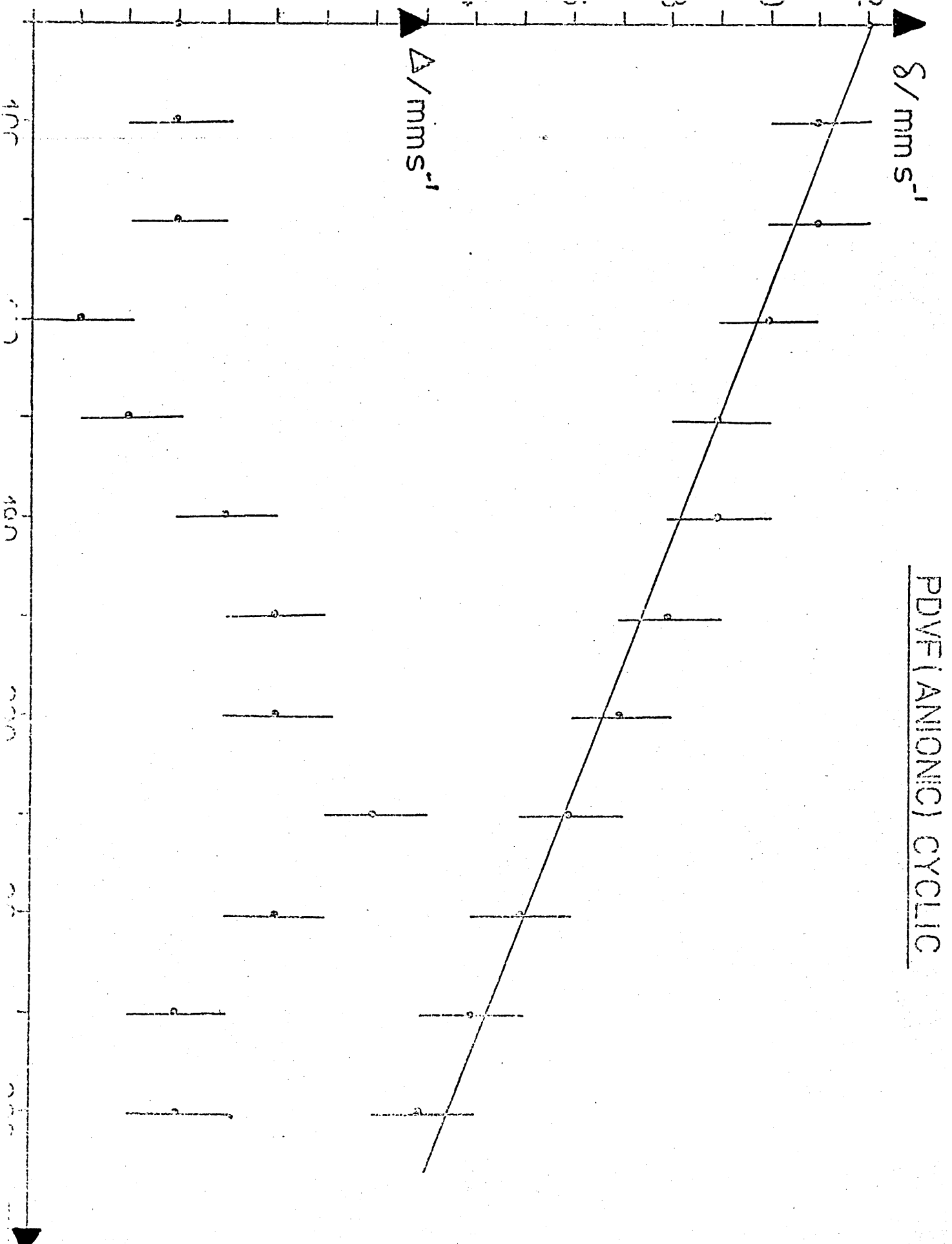
Fig. 6.4   Temperature Dependence of the Isomer Shift and
Quadrupole Splitting for PDVF (Cyclic)
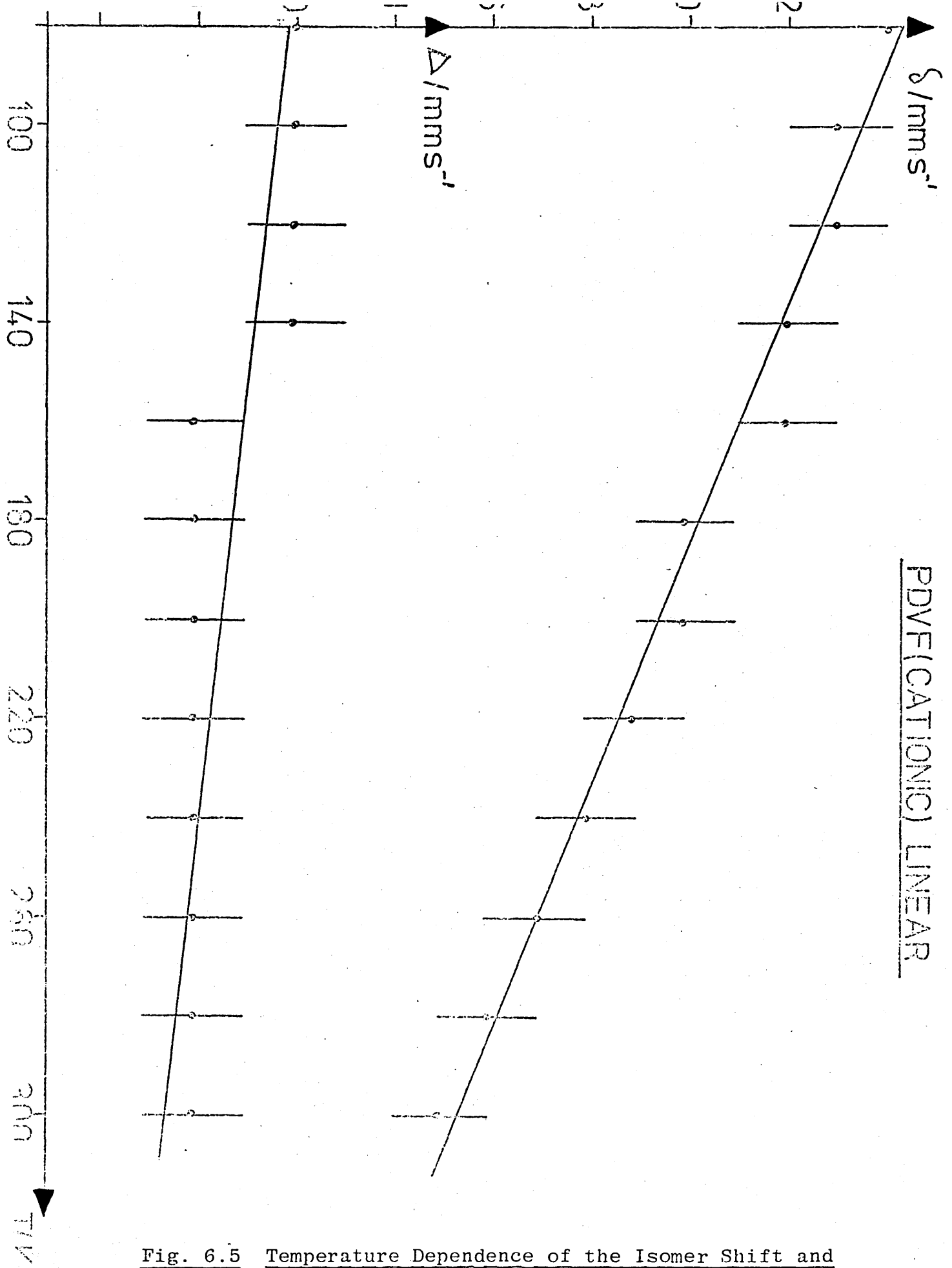
Fig. 6.5   Temperature Dependence of the Isomer Shift and
Quadrupole Splitting for PDVF (Linear)
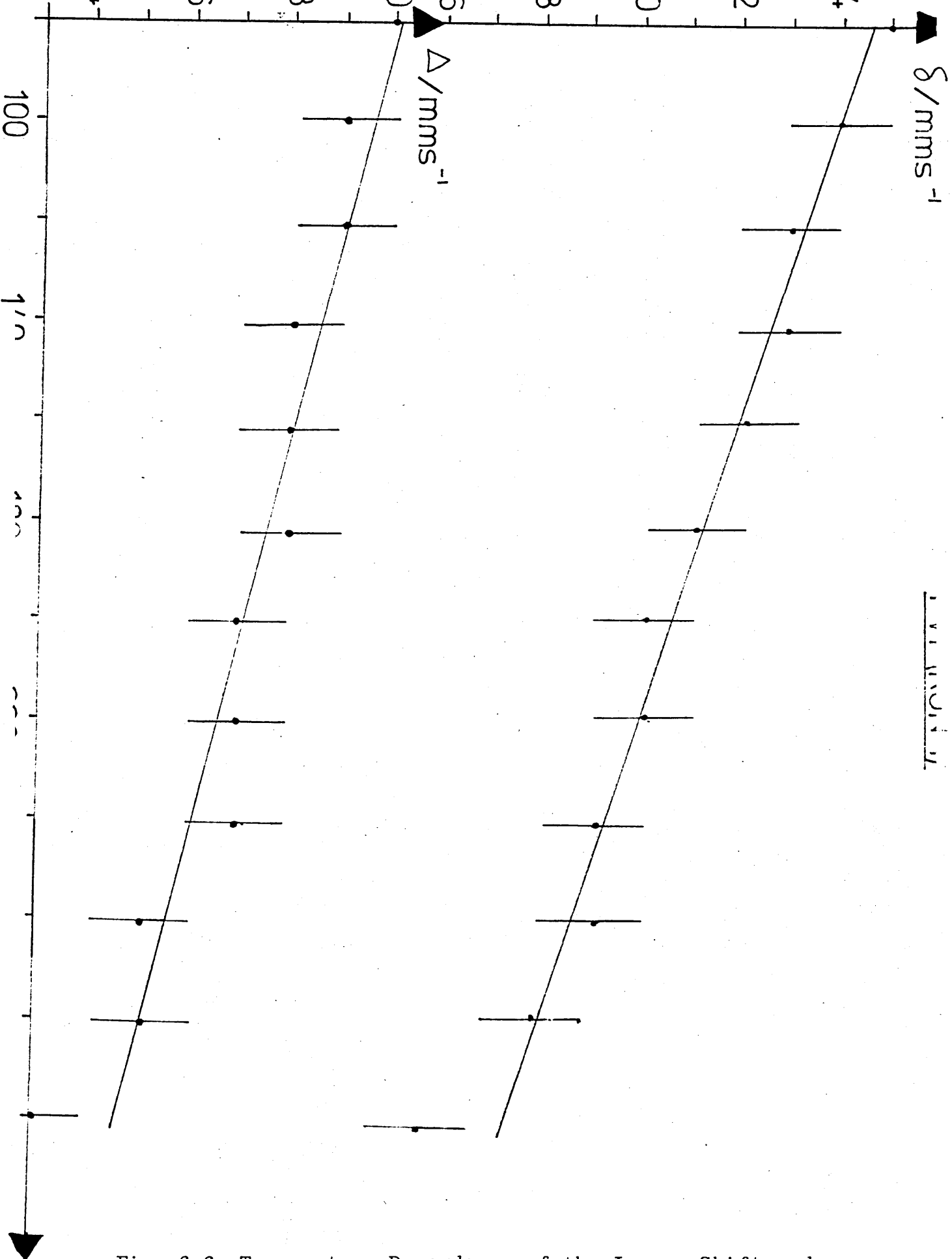
Fig. 6.6   Temperature Dependence of the Isomer Shift and
Quadrupole Splitting for PVF

decrease in the quadrupole splitting in each case. The isomer shift values are largely unchanged, though an unexplainable variation is observed in the PDVF (cyclic) studies, Fig. 6.4 The above results as a whole indicated that no structural change occurred in the region of 200 K.

6.3 Theory

6.3.1 Debye Model of Crystalline Solids

The area under the resonance curve A(T) is used in examining the temperature dependence of the recoil-free fraction, f.

A is given by

$$A = \frac{\pi}{2} \ f_\Gamma L(t) \tag{6.4}$$

where L(t) is a saturation function of absorber thickness, t_a, and for small values of t_a, L(t) tends to 1. [139]

Assuming the Debye model of solids, f is given by

$$f(T) = \exp\left\{-\frac{3}{2} \frac{E_R}{K\Theta} \left[1 + 4\left(\frac{T}{\Theta}\right)^2 \int_0^{\frac{\Theta}{2}} \frac{x}{e^x - 1} \ dx \right]\right\} \tag{6.5}$$

At high temperatures, the integral in Equation 6.5 simplifies to $\frac{\Theta}{T}$, giving

$$f(T) = \exp\left\{-\frac{3}{2} \frac{E_R}{K\Theta} + \exp\frac{-6E_R T}{K\Theta^2}\right\} \tag{6.6}$$

or

$$\ln f(T) = -\frac{3}{2} \frac{E_R}{K\Theta} - \frac{6E_R T}{K\Theta^2} \tag{6.7}$$

Differentiating with respect to T:

$$\frac{d\ln f}{dT} = \frac{-6E_R}{K\Theta^2} \tag{6.8}$$

where Θ_m is a characteristic temperature and from the Debye model is equivalent to the Debye temperature, Θ_D.

Now

$$E_R = \frac{E_\gamma^2}{2M_c^2}$$

so Equation 6.5 becomes

$$\frac{d\ln f}{dT} = \frac{-3E_\gamma^2}{M_c^2 k\Theta_m^2} \qquad (6.9)$$

From Equation 6.9 it can be seen that the gradient of lnA against T is dependent upon the effective recoiling mass. It was, therefore, expected that the amorphous polymers would give a different gradient to that of ferrocene, but the apparent change in gradient cannot be explained using this model.

6.3.2 <u>The Debye Model for Amorphous Materials</u>

The application of the Debye model to amorphous materials has been performed by Dr C M Care, Department of Applied Physics, Sheffield City Polytechnic, and is presented in the Appendix 2.

It is initially assumed that the amorphous polymer is a disordered array of N macromolecules, where each macro-molecule can be treated as a rigid mass. This is because the intermolecular bonding is assumed weak relative to intramolecular bonding and the entanglements between molecules are ignored. The model, as in the crystalline case, predicts that lnf depends linearly on temperatures, as shown by the Debye-Waller factor at the high temperature

limit $(T \geqslant \frac{1}{2}\Theta_D)$

$$2W = \frac{3E_0{}^2 T}{M_c{}^2 K_B \Theta_D{}^2} \qquad (6.10)$$

where M = mass of each macromolecular unit.

Therefore, any deviation from linearity was thought to arise from the excitation of intramolecular modes or from anharmonic effects in the intermolecular potential.

6.3.3 Excitation of Intramolecular Modes

In the previous model, intramolecular vibrations were ignored but at higher temperature these vibrations will become excited. Therefore the model was extended to include vibrations between ferrocene units within each macromolecule, which were treated as Einstein oscillators. Vibrations within the repeating units were ignored, an approximation which was considered acceptable since these modes will be excited only at high frequencies.

An expression was derived for the mean square displacement of the repeating unit

$$<x^2>_{\omega_E} = \frac{h}{6m_R n_R \omega_E} \coth \left(\frac{h\omega_E}{2K_B T} \right) \qquad (6.11)$$

where m_R = mass of each repeating unit

n_R = number of repeating units

and ω_E = angular frequency associated with the intra-
molecular modes.

The intramolecular and intermolecular modes were combined
to give the expression

$$<x^2>_{TOT} = \frac{h}{6MN} \int_0^\infty \frac{g(\omega)}{\omega} \coth \left[\frac{h\omega}{2k_BT}\right] d\omega + \frac{3(n_R - 1)h}{6M\omega_E} \coth \left[\frac{h\omega_E}{2k_BT}\right]$$

$$(6.12)$$

where $M = m_R n_R$

By choosing a suitable Einstein frequency, the above
expression was found to give a reasonable fit to the
experimental results. At low temperatures, the amorphous
polymer only shows vibration between polymeric chains but
on raising the temperature, a stage is reached where the
intramolecular vibrations become excited and a deviation
from linearity is predicted.

However, this model does not adequately explain the large
change in slope. It is shown that if the transition
temperature is approximately 180 K, then the number of
repeating units in the polymer must exceed 375.
Measurements have been made showing the number of repeating
units to be of the order of around 5-15 (Table 6.2) and
though modifications were made to allow a range of values
of ω_E, no reasonable value of n_R was obtained. It was
therefore impossible to associate any physical significance
to the fit obtained to the experimental data.

Table 6.2 Molecular Weights of Variable Temperature

Samples Studied

Sample

Ferrocene	186
PVF 1	961[a]
PVF 2	1090[a]
PDVF (linear)	1659[a]
PDVF (cyclic)	1164[a]

a $\overline{M}_n$ - expressed as the polystyrene equivalent by GPC

Comparison of the GPC results against Vapour Pressure
Osmometry showed the GPC values obtained are approximately
half the absolute values.

6.3.4 Anharmonic Potential

The non-linear temperature dependence observed during the
course of this work has previously been known to occur
in metallic tin in the temperature range 142 - 568 K
[140], and Boyle et al explained the non-linearity by
considering each tin atom to oscillate anharmonically.

Zener and Bilinsky [141] considered the effect of thermal
expansion and showed that

$$2\omega \simeq \frac{3E_0^2 T}{M_c^2 k_B \Theta_D^2} \left[1 + \frac{2V_\beta^2}{3RK} \left(T - \frac{3}{8} \Theta_D \right) \right] \qquad (6.13)$$

where R = gas constant

K = isothermal compressibility

V = molar volume

and   β = high temperature volume expansion coefficient.

The experimental results were fitted by a least squares
method to the equation

$$\ln A = B - CT - DT^2 \qquad\qquad (6.14)$$

in the temperature range 80-300K.   The results for each
sample are shown in Table 6.3 and it can be seen in
Fig. 6.7 that a good fit to the data was obtained.

Table 6.3   Parameters Derived from Fitting $\ln f = A-BT-CT^2$

to the Experimental Data for Polyvinylferrocene

	B $Kx10^{-3}$	ΔB $Kx10^{-3}$	C $Kx10^{-3}$	ΔC $Kx10^{-3}$	Θ [a] K	$\Delta\Theta$ K
PVF - Run 1	3.5	1.4	2.6	0.4	43	9
PVF - Run 2	2.6	1.4	2.4	0.4	49	14
PVF - Run 3	2.7	0.4	2.4	0.1	48	4
PDVF (cyclic)	3.1	1.0	2.6	0.3	46	8
PDVF (linear)	2.5	0.8	1.8	0.2	50	9

a   M = 1,100

The parameter $\dfrac{2V\beta^2}{3RK}$ for polyvinylferrocenes was estimated
by comparison with values for polystyrene which have
previously been determined.   Polystyrene was used as it was
considered a chemically close analogue to the polyvinyl-
ferrocene

i.e. $\beta = 2 \times 10^{-4} K^{-1}$

$K = 3 \times 10^{-10} Pa^{-1}$

ANHARMONIC POTENTIAL MODEL

ln A

PDVF(linear)

PDVF(cyclic)

PVF(RUN2)

0   80   160   240   300 T/K
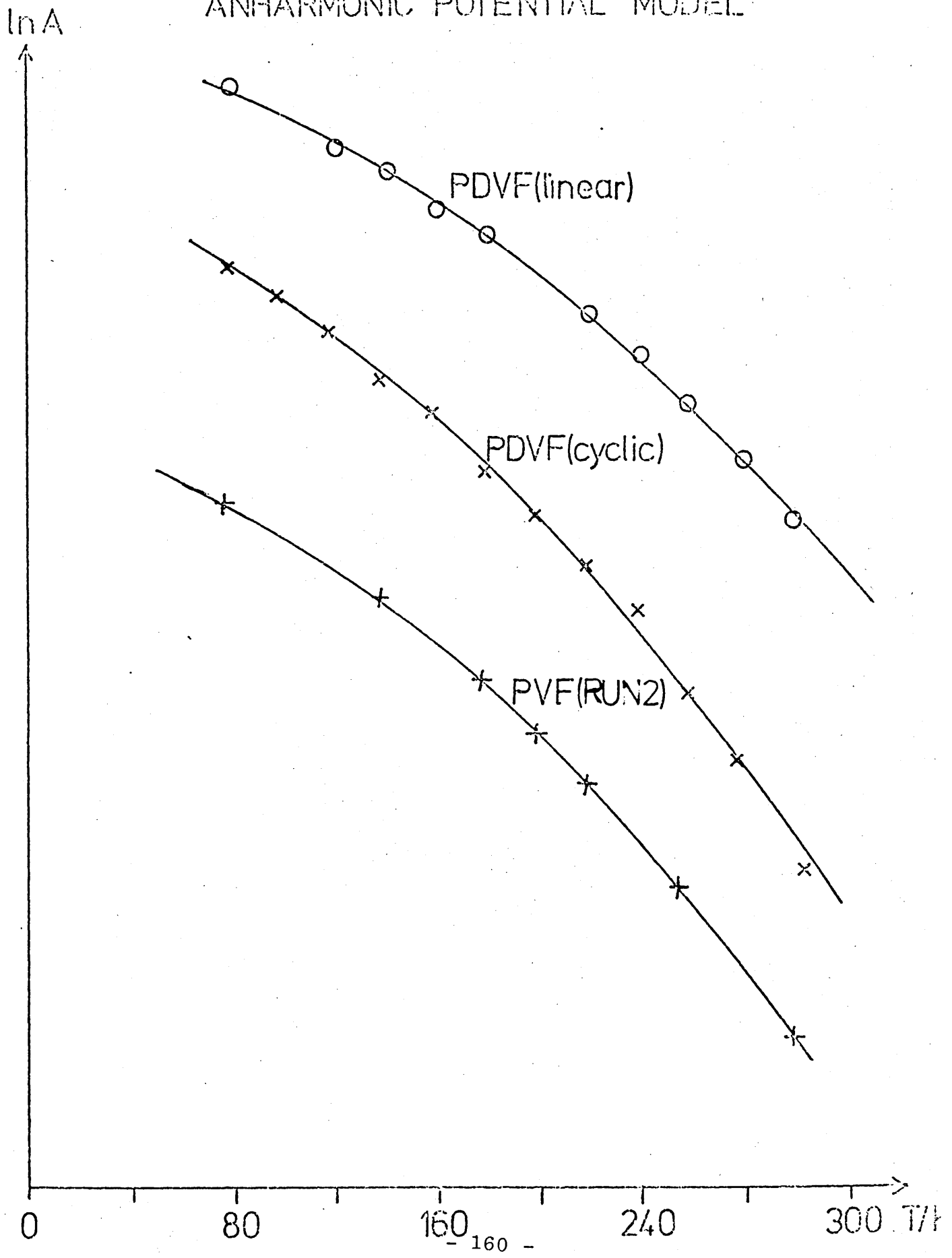
Fig. 6.7   Fitting of the Data to the Anharmonic Potential Model

If the density is assumed to be 2×10^3 Kg/m^3 and the molecular weight is taken as 1000, the molar volume V is 5×10^{-4} m^3/mole.

Hence $\dfrac{2V\beta^2}{3RK} \approx 5 \times 10^{-3}$ K^{-1}

This is a factor of 2 to 3 times less than the experimentally observed parameter and a similar discrepancy was observed for tin by Boyle et al. [140]

The results suggested that the non-linear temperature dependence of lnA arises from the anharmonic potential well in which each macromolecule is situated. Therefore as the temperature increases the mean point of vibration changes as shown in Fig. 6.8.
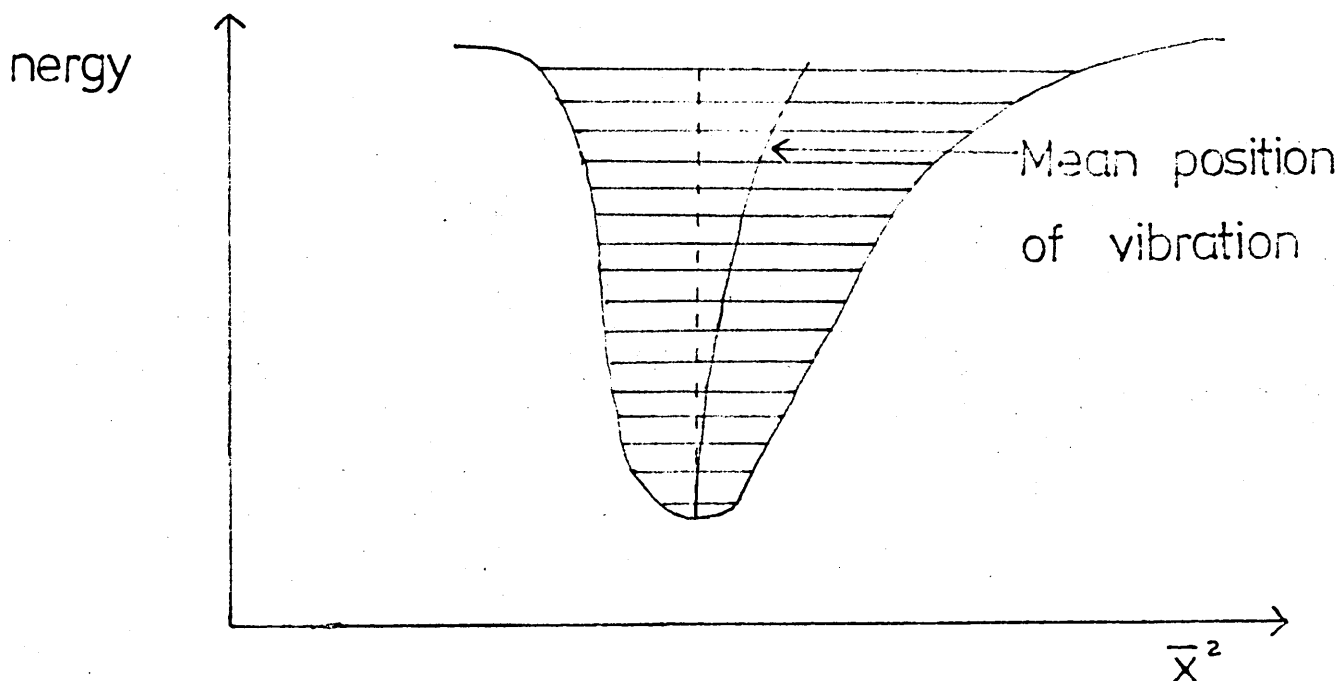
Fig. 6.8 Anharmonic Potential

Further evidence supporting this model was provided by the fact that the non-linearity was independent of the internal structure of the molecules.

6.4 Discussion and Conclusions

Treatment of the amorphous polymer by the Debye model ignoring any intramolecular vibrations, gave essentially the same result as for a crystalline solid, e.g. ferrocene, and no deviation from linearity was predicted. When this model was extended to include intramolecular vibrations, treated as Einstein oscillators, a fit to the data was obtained, but the parameters were not physically realistic.

Using the anharmonic potential model, however, there was good agreement between the experimental and fitted data for all the polymers studied. Using this proposed model, the fact that the deviation is independent of internal molecular structure can be explained, something which cannot be accounted for by the previous models.

Litterst et al [142] have recently reported studies on the dynamic properties of polymers and copolymers of vinylferrocene. They have also observed anomalous behaviour in the temperature dependence of the recoil-free fractions of the polymers similar to our results but line broadening effects which are reported were not observed in this study. Fig. 6.9 shows the variation of line width with temperature for PVF, but as the error quoted for the line width is $\pm$ 0.02 mm s^{-1}, all values fall within
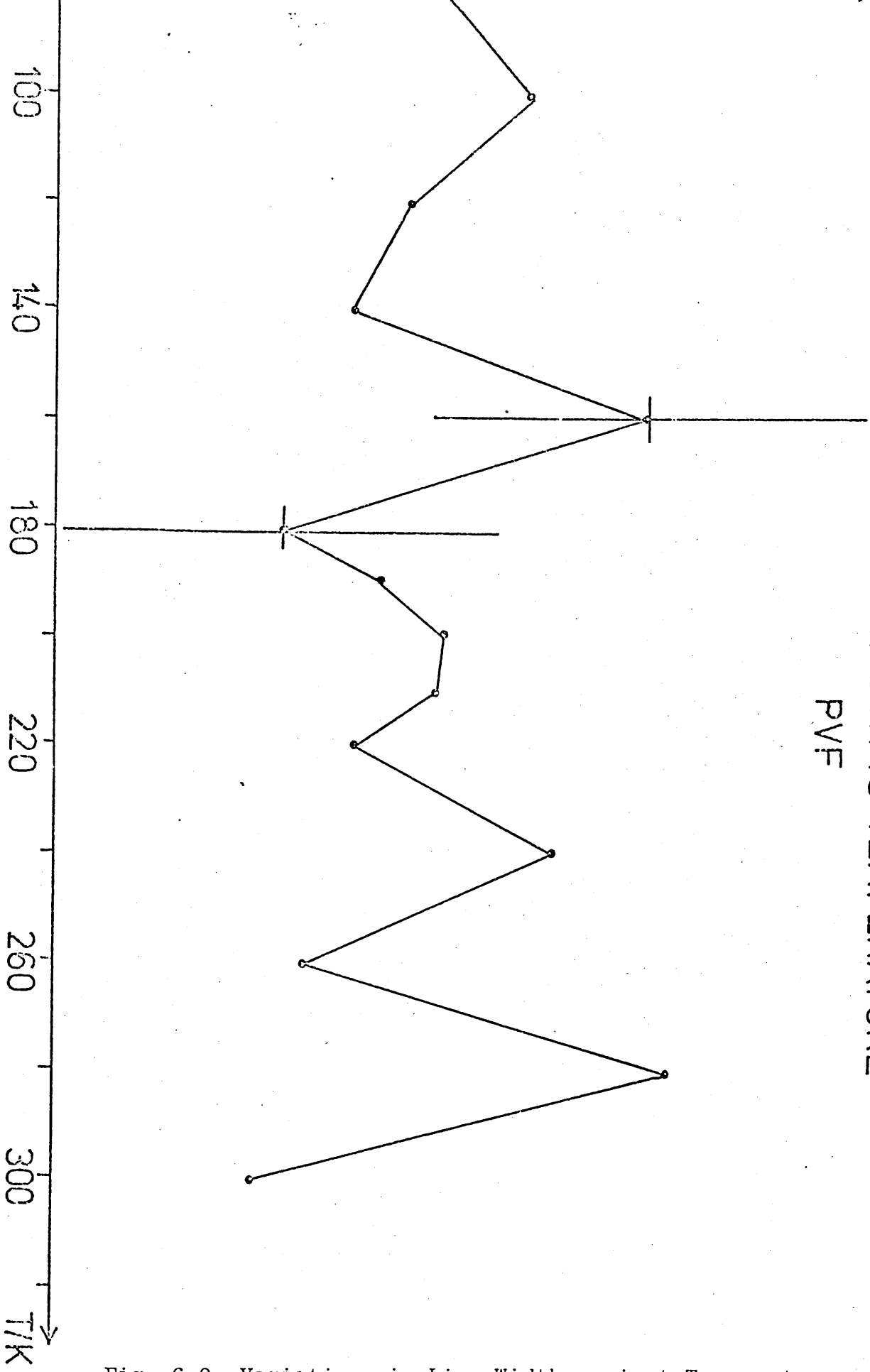
Fig. 6.9   Variations in Line Width against Temperature for PVF

experimental error and a significant increase in line width at around 130K was not observed.

The temperature dependence of the recoil-free fraction, f, observed [142] was in agreement with the results published in this work. They attributed their deviation from linearity as being due to an anharmonic hindered motion of the ferrocene sidegroup as a whole, and they noted that polymers containing ferrocene as a crosslink between the backbone chains show comparatively less change of f with temperature since the ferrocene motion is 'locked'. It is proposed in this work that the anharmonic motions are vibrations between ferrocene units within the macro-molecule. As PDVF (cyclic) and PDVF (linear) both gave a similar temperature dependence of lnA, it is unlikely that the anharmonic motions are structurally dependent. Therefore, although there is agreement about the presence of anharmonic potentials, this work has shown that it is unlikely to be caused by motion of the ferrocene sidegroup, as the ferrocene unit in PDVF (cyclic) is fixed rigidly by a three-carbon bridge.

CHAPTER SEVEN : SUMMARY AND CONCLUSIONS

In this study, the technique of Fe^{57} Mössbauer spectroscopy complemented by chemical and other spectroscopic investigations, has been used to provide new information concerning the polymerisation of vinylferrocene and 1,1'divinylferrocene, and the structures and properties of the resulting polymers.

The polymerisation of vinylferrocene using cationic, anionic and radical initiators (to low conversions) has been investigated, but using Mössbauer spectroscopy the previously reported [64] novel Fe(III) species could not be observed in any system. With cationic or anionic initiators, the absence of the Fe(III) high spin absorption from the Mössbauer spectra would be expected, since a mechanism for the formation of this species is not available in these cases. However, even though radical-initiated polymerisation reactions were terminated at conversions of 5% or less, the Fe(III) species was not observed, in contrast to the previous studies [64]. In this work, the corresponding polymerisation reactions were carried out under a nitrogen atmosphere and it was found necessary to use a higher level of initiator (1.5 - 5.0 mol. dm^{-3}) to effect the polymerisation than that used by the earlier workers (0.4 - 2.5 x 10^{-2} mol. dm^{-3}). It is likely that the larger concentration of radicals thus present in the system would lead to termination reactions by combination of radicals, rather than by an intra-

intramolecular termination mechanism which would lead to the novel Fe(III) species. Clearly, further studies would demand the use of high vacuum conditions, such that small concentrations of propagating radicals could be introduced into the system.

Polymerisation of vinylferrocene in chloroform could only be effected in an oxygen-free environment which was in agreement with previous reports. [123]. Kinetic studies of the polymerisation showed that the system was very sensitive to impurities and despite rigorous purification methods, reproducible results could not be obtained. The major impurity present was thought to be traces of oxygen which remained even after several freeze-pump-thaw cycles had been carried out. However, the longer induction periods observed with solutions of higher monomer concentration indicated that another impurity in the monomer may have been present, despite the rigorous purification methods used. The polymers produced by this method were of low molecular weight, but because the polymerisations had been taken to high conversions, it was not unexpected that these samples did not exhibit an Fe(III) high spin absorption in their Mössbauer spectrum.

[13]C n.m.r. studies on the polymers from vinylferrocene produced results which did not agree with previously published work [67]. Absorptions in the region 32-38 ppm did not correspond to the published data. Proton coupling of the spectra showed that the absorption at approximately

32 ppm can be assigned to —CH— and not —CH$_2$— as previously proposed [67]. Comparison of the ^{13}C n.m.r. spectra of radically and anionically initiated polymers revealed some small differences. As the molecular weight of the anionic polymer was lower, initiator fragments were observed and a peak at 35.1 ppm, previously attributed to a combination of tetrad and hexad resonances of the methylene carbon [67] was assigned as a fragment of the butyl lithium initiator.

Polymers from 1,1'divinylferrocene have been synthesised and their structures studied using more extensive spectroscopic techniques than had previously been used. Previous workers [79-83] had concluded that the polymers produced by both radical and cationic initiation were predominantly cyclopolymers containing a three-carbon bridged ferrocene unit. However, using Fe^{57} Mössbauer spectroscopy, significant differences were observed between the polymers. The linear, saturated polymers obtained by radical initiation exhibited the Mössbauer parameters (δ = 0.23(2) mm s^{-1}, ΔE_Q = 2.29(2) mm s^{-1}) expected for cyclopolymers with three-carbon bridged ferrocene units in the main chain. However, cationic initiation yielded polymers with significantly different Mössbauer parameters (δ = 0.27(2) mm s^{-1}, ΔE_Q = 2.40(2) mm s^{-1}). Using ^{13}C n.m.r. spectroscopy, and with further consideration of 'H n.m.r. and infrared spectra, structure XVII has been proposed for the cationically initiated polymer.
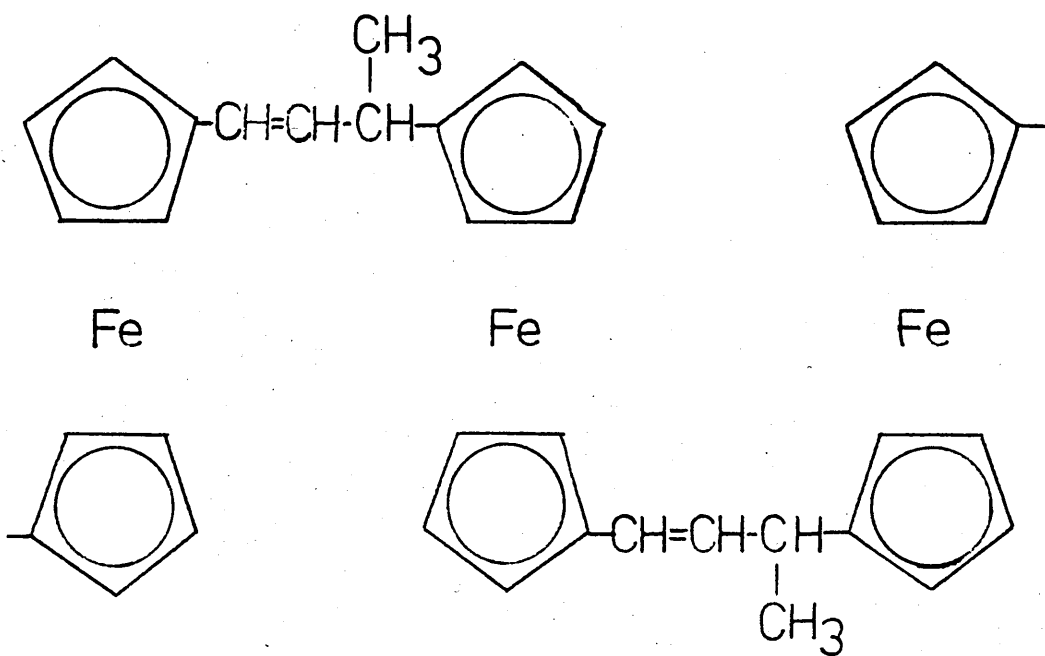
XVII

Confirmation was provided by the synthesis and subsequent
spectroscopic analysis of the model compound II.
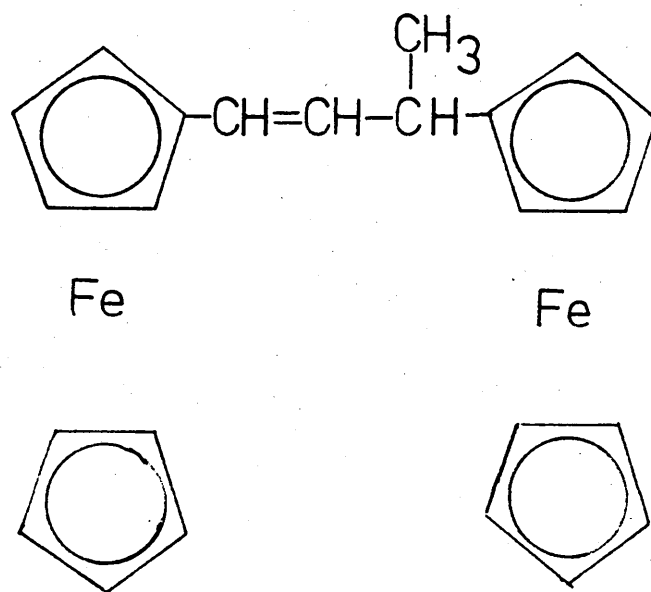
XX

Polymers containing this structure can arise from 1,1'divinylferrocene by an intermolecular polyaddition mechanism.

Studies on polymers produced using other cationic initiators gave similar results, although in some cases there was evidence for the presence of small amounts of a linear unit, VI.
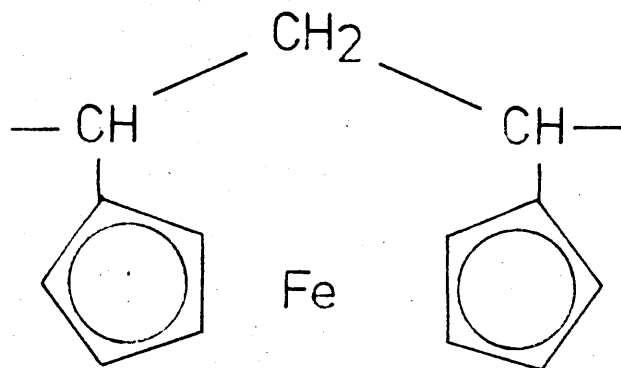
VI

Further spectroscopic studies on the radical polymer from 1,1'divinylferrocene and comparisons with the model compound 1,1'trimethyleneferrocene, confirmed the presence of a three-carbon bridged ferrocene unit in the polymer, as previously proposed [79-83]. Polymers produced by anionic initiation of 1,1'divinylferrocene, previously unreported, have been shown also to contain a trimethylene bridge in the structure.

The temperature dependence of the Mössbauer absorption areas (A) has been studied for polymers of vinylferrocene and 1,1'divinylferrocene. For small values of the Mössbauer absorption thickness (t), the absorption line area is proportional to the absorber recoiless fraction (f_a) and thus variations in f_a with temperature could be studied indirectly. Whereas crystalline ferrocene gave a linear relationship of lnA with temperature, the amorphous polymers of vinylferrocene and 1,1'dinvinylferrocene, studied over the range 80-300 K, gave non-linear temperature dependencies despite the differences in their structure. These non-linear relationships could not be explained by a development of the Debye model for amorphous materials, which considers each macromolecule as a rigid mass and ignores any intramolecular vibrations or entanglements between macromolecules. Nor could these results be explained by extending the model to include intramolecular vibrations. However, a good fit to the experimental data was achieved when an anharmonic potential was assumed for each macromolecule, this vibration becoming increasingly important at higher temperatures (> 200 K).

REFERENCES

1. Kealy, T. J. and Pauson, P. L., Nature, London, 168, 1039 (1951).

2. Wilkinson, G., Rosenblum, M., Whiting, M. C. and Woodward, R. B., J. Amer. Chem. Soc., 74, 2125 (1953).

3. Eiland, P. F. and Pepinski, R., J. Amer. Chem. Soc., 74, 4971 (1952).

4. Dunitz, J. D. and Orgel, L. E., Nature, London, 171, 121 (1953).

5. Dunitz, J. D., Orgel, L. E., and Rich A., Acta Cryst., 9, 373 (1956).

6. Richards, J. H., 135th National Meeting of Amer. Chem. Soc., Boston, Mass., Abstr., p.86 (1959).

7. Page, J. A. and Wilkinson, G., J. Amer. Chem. Soc., 74, 6149 (1952).

8. Brand, J. C. D. and Snedden, W., Trans. Faraday Soc., 53, 894 (1957).

9. Epton, R., Hobson, M. E. and Marr, G., J. Organomet. Chem., 149, 231 (1978).

10. Smith, T. W., Kuder, J. E. and Wychick, D., J. Poly. Chem. Ed., 14, 2433 (1976).

11. Rosenblum, M., Chemistry of the iron-group metallocenes, Part 1, Interscience, New York (1965).

12. Shustorovich, E. M. and Dyatkina, M. E., Zh. Strukt. Khim, 7, 139 (1966).

13. Kuwana, T., Bublitz, D. E. and Hoh, G., J. Amer. Chem. Soc., 82, 5811 (1960).

14. Mason, J. G. and Rosenblum, M., J. Amer. Chem. Soc., 82, 4206, (1960).

15. Nesmeyanov, A. N. Perevalova, E. G., Gubin, S. P., Nikitina, T. V., Ponomarenko, A. A., and Shilovtseva, L. S., Dokl. Akad. Nauk SSSR, 139, 888 (1961).

16. Ballhausen, C. J. and Dahl, J. P., Acta. Chem. Scand., 15, 1333 (1961).

17. Rosenblum, J. Fish R. W. and Bennett C., J. Amer. Chem. Soc., 86, 5166 (1964).

18. Webster, O. W., Mahler, W. and Benson, R. E., J. Amer. Chem. Soc., 84, 3678 (1962).

19. Adman, E., Rosenblum, M., Sullivan, S. and Margulis, T. N., J. Amer. Chem. Soc., 89, 4540 (1967).

20. Dub M. - Ed., Organometallic Compounds, Vol. 1., Compounds of Transition Metals, Springer-Velag, Berlin (1966).

21. Buel, G. R., McEwan, E. and Kleinberg, J., Tet. Letters, 5, 16 (1959); J. Amer. Chem. Soc., 84, 40, (1962).

22. Chablay, A., Comp. Rend., 250, 2722 (1960).

23. De La Mare, P. and Bolton, R., Electrophilic additions to unsaturated systems, Elsevier (1966).

24. Organometallic Chemistry, Open Univ. Press, Unit 23, p.83 (1977).

25. Lippincott, E. R. and Nelson, R. D., J. Chem. Phys., 21, 1307 (1953).

26. Lippincott, E. R. and Nelson, R. D., J. Amer. Chem. Soc., 77, 4990 (1955).

27. Lippincott, E. R. and Nelson, R. D., Spectrochim. Acta, 10, 307 (1958).

28. Hayes, G. F., PhD Thesis, Imperial College London (1973).

29. Spilners, I. J., J. Organomet. Chem., 11, 381 (1968).

30. Wilkinson, G., Rosenblum, M., Whiting, M. C., and Woodward, R. B., J. Amer. Chem. Soc., 74, 2125 (1952).

31. Scott, D. R. and Becker, R. S., J. Chem. Phys., 35, 516 and 2246 (1962).

32. Sohn, Y. S., Hendrickson, D. N. and Gray, H. B., J. Amer. Chem. Soc., 93, 3603, (1971).

33. Barr, T. H., and Watts, W. E., J. Organomet. Chem., 15, 177 (1968).

34. Brins, R. and Reinders, F. J., J. Amer. Chem. Soc., 91, 4929 (1969).

35. Sohn, Y. S., Hendrickson, D. N. and Gray, H. B., J. Amer. Chem. Soc., 92, 3233 (1970).

36. Duggan, D. M. and Hendrickson, D. N., Inorg. Chem., 14, 955 (1975).

37. Rausch, M. D. and Mark V., J. Org. Chem., 28, 3225 (1963).

38. Rausch, M. D. and Siegel, A., J. Organomet. Chem., 11, 317 (1968).

39. Fraenkel, G., Carter, R., McLachlan, A. and Richards, J. H., J. Amer. Chem. Soc., 82, 5846 (1960).

40. Lets, J. R., Cotton, F. A. and Waugh, J. S., Nature, 180, 978 (1957).

41. Braun, S., Abram, T. S. and Watts, W. E., J. Organomet. Chem., 97, 429 (1975).

42. Koridze, A. A., Petrovskii P. V., Gubin, S. P. and Fedin, E. I., J. Organomet. Chem., 93, 2, C26 (1973).

43. Lauterbur, P. C., J. Amer. Chem. Soc., 83, 1838 (1961).

44. Koridze, A. A., Petrovskii, P. V., Mahkov, A. I. and Lutesenko, A. I., J. Organomet. Chem, 136, 57 (1977).

45. Nesmeyanov, A. N., Petrovskii, P. V., Fedorov, L. A., Robas, B. I. and Fedin, E. I., Zh. Strukt. Chim., 14, 49 (1973).

46. Wertheim, G. K., and Herber, R. H., J. Chem. Phys., 38, 2106 (1963).

47. Lesikar, A. V., J. Chem. Phys., 40, 2746 (1964).

48. Korecz, L., Abou, H., Ortaggi, G., Graziani, M., Belluco, U., and Burger, K., Inorg. Chim. Acta, 9, 209 (1974).

49. Arimoto, F. S. and Haven, A. C. Jr., J. Amer. Chem. Soc., 77, 6295 (1955).

50. Haven, A. C. Jr., US Patent 2, 821, 512 Jan (1958).

51. Chen, Y., Fernandez-Refojo, M. and Cassidy, H. G., J. Poly. Sci., 40, 433 (1959).

52. Fitzgerald, W. P. Jr., PhD Thesis, Perdue Univ., West Lafayette (1963).

53. Ma, T. T., Yeh, P. C., Lu, C. C. and Wu, L. F., Ko Fen Tzu Tung Hsun, 6, 148 (1964).

54. Baldwin, M. G. and Johnson, K. E., J. Poly. Sci., Part A-1, 5, 2091 (1967).

55. Baldwin, M. G., Rohm and Hass Tech. Report, No. 5-124, (1965).

56. Aso, C., Kunitake, T. and Nakashima, T., Makromol. Chemie, 124, 232 (1969).

57. Pittman, C. U. Jr., Lai, J. C., Vanderpool, D. P., Good, M. and Prado, R., Macromolecules, 3, 105, 746 (1970).

58. Lai, J. C., Rounsfell, T. and Pittman, C. U. Jr., J. Poly. Sci., Part A, 9, 651 (1971).

59. Simionescu, C., Lixandru, T., Negulescu, I., Marzilu, I. and Tartaru, L., Makromol. Chemie., 163, 59, (1973).

60. Sasaki, Y., Walker, L. L., Hurst, E. L., and Pittman, C. U. Jr., J. Poly. Sci., Polym. Chem. Ed., 11, 1213 (1973).

61. Aso, C., Kunitake, T. and Nakoshima, T., Kogyo Kagaku Zosski, 72, 1411 (1969).

62. Pittman, C. U. Jr., J. Poly. Sci., Part B, 6, 19 (1968).

63. Pittman, C. U. Jr., Voges, R. L. and Elder, J., J. Poly. Sci., Part B, 9, 191 (1971).

64. George, M. H. and Hayes G. F., J. Poly. Sci., Poly. Chem. Ed., 14, 475 (1976).

65. Bellamy, L. J., Advances in Infrared Group Frequencies, Methuen, London (1968).

66. Hauser, C. R. and Cain, C. E., J. Org. Chem., 23, 1142 (1958).

67. Raynal, S. Gautier J.-C., Sledz, J., Schue, F. and Supamo, S., Polymer, 22, 257 (1981).

68. Tinker, A. J., George, M. H. and Barrie, J. A., J. Poly. Sci., Poly. Chem. Ed., 13, 2621 (1975).

69. Dietrich, M. W. and Wahl, A. C., J. Chem. Phys., 38, 1591 (1963).

70. Rosenblum, M. and Woodward, R. B., J. Amer. Chem. Soc., 80, 5443, (1958).

71. Hayes, G. F. and Young, R. N., Polymer, 18, 1286 (1977).

72. Pausacker, K. H., Aust. J. Chem., 11, 509 (1958).

73. Broadhead, G. D. and Pauson, P. L., J. Chem. Soc., 367, (1955).

74. Beckwith, A. L. J. and Leydon, R. J., Tet. Letters, 6, 385 (1963).

75. George, M. H. and Hayes, G. F., J. Poly. Sci., Part B, 11, 471 (1973).

76. Greenwood, N. N. and Gibb, T. C., Mossbauer Spectroscopy, Chapman and Hall, London (1971).

77. Michnick, M. J., PhD Thesis, Univ. of Kansas (1964).

78. Michnick, J. J., Diss. Abstr., <u>25</u>, 5565 (1965).

79. Sosin, S. L., Korshak, V. V. and Frunze, T. M.,
    Dokl. Akad. Nauk SSSR, <u>179</u>, 1124 (1968).

80. Sosin, S. L. and Dzhashi, L. V., Kinet. Mech.
    Polyreactions Int. Symp. Macromol. Chem. Prepr.,
    <u>1</u>, 327 (1969).

81. Sosin, S. L., Dzhashi, L. V., Antipova, B. A., and
    Korshak, V. V., Vysokomol. Soedin, Ser. B., <u>12(9)</u>,
    699 (1970).

82. Kunitake T., Nakoshima T. and Aso C., J. Poly. Sci.,
    A-1, <u>8</u>, 2853 (1970).

83. Kunitake, T., Nakashima T. and Aso C., Makromol. Chem.,
    <u>146</u>, 79 (1971).

84. Neuse, E., Crossland, R. K., and Koda, K., J. Org.
    Chem., <u>31</u>, 2409 (1966).

85. Aso, C., Kunitake, T., and Kita, R., Makromol. Chem.,
    <u>97</u>, 31 (1966).

86. Aso, C., Kunitake, T., Matsuguma, Y., and Imaizumi,
    Y.-J., J. Poly. Sci, A-1, <u>6</u>, 3049 (1968).

87. Pederson, C. J., German Patent 935,467 (1955).

88. Moldavskii, B. L. and Blimova, M. B., Russian Patent
    104,937 (1957).

89. Beynon, J. H. and Jackson, R. G., German Patent
    1,052,743 (1959).

90. Pederson, C. J., US Patent, 2,867,516 (1959).

91. Bozak, R. E., US Patent, 3,322,793 (1967).

92. Pruett, R. L., US Patent, 3,322,804 (1967).

93. Wilkus, E. V. and Berger, A., French Patents 1,396,273 and 1,398,255 (1965).

94. Wilkus, E. V. and Berger, A., US Patent 3,313,835 (1967).

95. Tubyanskaya, G. S., Koblzova, R. I., Oparina, E. M., Zaitsov, V. A. and Egorova, A. A., Plast. Mossy. 437 (1967).

96. Mattice, J. J., Off. Dig. Fedn. Soc. Paint Technol., 34, 603 (1962).

97. Schmitt, R. G. and Hirt, R. C., J. Appl. Poly. Sci., 7, 1565 (1963).

98. Jones, W., Leigh, T. and Madinoveitia, J. L., British Patent 841,710 (1960).

99. Leigh, T., US Patent 3,036,106 (1962).

100. Leigh, T., US Patent 3.099,669 (1963).

101. Lattrell, R., Lief, H. and Baehr, H., (Hoechat), German Patent 2,742,201, Chem. Abs., 91, 57182 (1979).

102. Cusic, J. W., and Yonan, P., US Patent 3,265,621, British Patent 1,040,038 (1966).

103. Rockett, B. W., and Marr, G., J. Organomet. Chem., 277, 373 (1982).

104. Mössbauer, R. L., Z. Physik, 151, 124 (1958).

105. Breit G., and Wigner, E., Phys. Rev., 49, 519 (1936).

106. Wertheim, G. K., Mössbauer Effect : Principles and Applications, Acad. Press, New York and London (1968).

107. Williams, J. M. and Brooks, J. S., Nucl. Instrum. Methods, 128, 363 (1975).

108. Lang, G. and Dale, B. W.; Nucl. Instrum. Methods, 116, 567 (1974).

109. Schwenk, A., Phys. Lett., 31A, 513 (1970).

110. Stevens, J. G. and Stevens, V. E., ed, 1975, Mössbauer Effect Data Index, Plenum Data Corp., New York (1976).

111. Billingham, N. C., Molar Mass Measurements in Polymer Science, Kagan Page (1977).

112. George, M. H. and Hayes, G. F., J. Poly. Sci., Poly. Chem. Ed., 13, 1049 (1975).

113. Woodward, R. B., Rosenblum, M., and Whiting M. C., J. Amer. Chem. Soc., 74, 3458 (1952).

114. Yamakawa, K., Ochi, H., and Arakawa, K., Chem. Pham. Bull. (Japan), 11, 905 (1963).

115. Broadhead, G. D., Osgerby, J. M. and Pauson, P. L.,
J. Chem. Soc., 650, (1958).

116. Rosenblum, M., Banerjee, A. K., Danidi, N.,
Fish, R. W., and Schlatter, V., J. Amer. Chem. Soc.,
85, 316 (1963).

117. Rinehart, K. L. Jr. and Curby, R. J. Jr., J. Amer.
Chem. Soc., 79, 3290 (1957).

118. Rinehart, K. L. Jr., Curby, R. J. Jr., Gustafson, D. H.,
Harrison, K. G., Bozak, R. E. and Bublitz, D. E.,
J. Amer. Chem. Soc., 84, 3263 (1962).

119. Ashmore, C. I., US Patent 3,577,449 (1971), Chem.
Abs., 75, 36354 (1971).

120. Sasaki, Y. and Pittman, C.U. Jr., J. Org. Chem., 38,
3723 (1973).

121. Pauson, P. L. and Watts, W. E., J. Chem. Soc.,
3880 (1962).

122. Hayes, G. F. and George, M. H., Organomet. Polymers,
Acad. Press, p.13 (1978).

123. George, M. H. and Hayes, G. F., Polymer, 15, 397
(1974).

124. Walling, C., Free Radicals in Solution, Wiley,
New York, p. 158 (1957).

125. Gregg, R. A. and Mayo, F. R., J. Amer. Chem. Soc.,
75, 3530 (1953).

126. Hillman, M. and Nagy, A. G., J. Organomet. Chem., 184, 433 (1980).

127. Trautwein, A., Reschke, R., Dezsi, I. and Harris, F. E., J. de Physique, 37, C6 (1976).

128. Korshak, V. V. and Sosin, S. L., Organomet. Polymers, p.26 (1978).

129. Nesmeyanov, A. N., Shulpin, G. B. and Rubinskya, M. I., Dokl. Akad. Nauk SSSR, 218, 1107 (1974).

130. Senda, Y., Kamiyama, S., Kosahara, A., Izumi, T., and Murakomi, S., Bull. Chem. Soc. Jpn., 53, 3381 (1980).

131. Abel, E. W., Booth, M., Brown, C. A., Orrell, K. G., and Woodford, R. L., J. Organomet. Chem., 214, 93 (1981).

132. Mysov, E. I., Lyalicov, I. R. , Materikova, R. B., and Korchetkova, N. S., J. Organomet. Chem., 169, 301 (1979).

133. Furukawa, J. and Nishimura, J., J. Poly. Sci., Poly. Lett. Ed., 14, 55 (1976).

134. Furukawa, J., and Nishimura, J., J. Poly. Sci., Symposium No. 56, 437 (1976).

135. Nishimura, J., Ishida, Y., Mimura, M., Nakazawa, N. and Yamashita S., J. Poly. Sci., Poly. Chem. Ed., 18, 2061 (1980).

136. Nishimura J., Mimura, M., Nakazawa, N., and
Yamashita, S., J. Poly. Sci., Poly. Chem. Ed.,
18, 2071 (1980).

137. Williams, J. M. and Brooks, J. S., Nucl. Inst.
Meth., 128, 363 (1975).

138. Boyle, A. J. F. and Hall, H. E., The Mossbauer
Effect, Rep. Prog. Phys., 20, 441 (1962).

139. Hafemeister, D. W., and Shera, E. B., Nucl. Instr.
Methods, 41, 133 (1966).

140. Boyle, A. J. F., Bunbury, D. St. P., Edwards, C.
and Hall, H. E., Proc. Phys. Soc., 77, 129, (1960).

141. Zener C., and Bilinsky, S., Phys. Rev., 50, 101 (1936).

142. Litterst, F. J., Lerf, A., Nuyken, O., and Alcala, H.,
Hyperfine Int., 12, 317 (1982).

143. Zweifel, G. and Brown, H. C., Org. Reactions, 13,
28 (1963).

ACKNOWLEDGEMENTS

APPENDIX 1

PVF 1

T	ln A	Corrected ln A
80	0.3738	0.4464
100	0.3288	0.3907
120	0.0482	0.0995
140	−0.1319	−0.0911
160	−0.2840	−0.2535
180	−0.6605	−0.6300
200	−0.7610	−0.7408
220	−1.0823	−1.0623
240	−1.3947	−1.3796
260	−1.7790	−1.7660
280	−2.0859	−2.0748
300	−2.4245	−2.4145

PVF 2

T	ln A	Corrected ln A
80	0.7575	0.8301
100	0.6970	0.7589
120	0.5567	0.6080
140	0.3032	0.3440
160	0.1500	0.1805
180	−0.0968	−0.0663
190	−0.2188	−0.1936
200	−0.3190	−0.2988
210	−0.3821	−0.3620
220	−0.5080	−0.4880
240	−0.7404	−0.7253
280	−1.4584	−1.4473

PVF 3

T	ln A	Corrected ln A
80	0.8049	0.8775
140	0.3397	0.3805
180	−0.0514	−0.0209
200	−0.2968	−0.2766
220	−0.5459	−0.5259
260	−1.1233	−1.1103

PDVF (LINEAR)

T	ln A	Corrected ln A
80	0.8425	0.9151
100	0.7053	0.7672
120	0.5565	0.6078
140	0.4378	0.4786
160	0.2562	0.2867
180	0.1398	0.1703
200	0.0978	0.1180
220	-0.2365	-0.2165
240	-0.4362	-0.4211
260	-0.6771	-0.6641
280	-0.9367	-0.9256
300	-1.2379	-1.2279

PDVF (CYCLIC)

T	ln A	Corrected ln A
80	0.9529	1.0255
100	0.8118	0.8737
120	0.6305	0.6818
140	0.3940	0.4348
160	0.2287	0.2592
180	-0.0467	-0.0162
200	-0.2497	-0.2295
220	-0.5090	-0.4890
240	-0.7338	-0.7187
260	-1.1234	-1.1104
280	-1.4675	-1.4564
306.8	-1.9966	-1.9866

APPENDIX 2

(a) Theory

The temperature dependence of the recoilless fraction is described by Debye-Waller factor which may be written to a good approximation

$$f = \exp\{-k^2 <x^2>\} = \exp(-2W)$$

where $<x^2>$ is the mean square displacement of the Fe atom from its equilibrium position in the direction of $\underline{k}$. The evaluation of f is particularly complicated in this problem because we are considering an amorphous, macro-molecular solid. The principal experimental observation we must explain is the non-linear temperature dependence of ln f. It is first shown that the Debye model should give a reasonable first approximation for the Debye-Waller factor and this predicts that ln f depends linearly upon temperature. Two possible explanations for the departure from linearity are then considered.

(b) The Debye Model for Amorphous Materials

The solid is assumed to be a topologically disordered array of N molecules, each of mass M. The intramolecular bonding is assumed to be much stronger than the inter-molecular bonding and consequently each macromolecule is treated as a rigid mass. Thus intramolecular vibrations are ignored initially. The problem of entanglements between macromolecules is also ignored. The solid is treated as an isotropic, dispersionless, elastic continuum

and the frequency distribution of allowed modes is the usual Debye distribution function

$$g(\omega) = \begin{cases} \dfrac{3V\omega^2}{2\pi^2 c^3} & \omega \lesssim \omega_m \\ \\ 0 & \omega > \omega_m \end{cases} \qquad (1)$$

where the maximum frequency ω_m is chosen such that the total number of modes is 3N. Thus

$$\int_0^\infty g(\omega)\,d\omega = 3N \qquad\qquad N = \text{no. of macromolecules}$$

and hence

$$\omega_m^3 = 6\,\frac{N}{V}\,\pi^2 c^3 \qquad\qquad V = \text{volume of solid}$$

The Debye temperature is given by the relation $\hbar\omega_m = k_B\Theta_D$. The velocity, c, in equation (1) is an average velocity defined by

$$\frac{3}{c^3} = \frac{1}{c_L^3} + \frac{2}{c_T^3}$$

where c_L is the velocity of the longitudinal modes and c_T is the velocity of the transverse modes. These modes are assumed to be degenerate. Each mode is treated as a quantised harmonic oscillator which has energy $(n + \tfrac{1}{2})\hbar\omega$ with probability $p(n)$ given by

$$p(n) = (1 - e^{-\hbar\omega/kT})e^{-n\hbar\omega/kT}$$

The mean energy in the mode will be

$$\bar{E}_\omega = \sum_{n=0}^\infty p(n)(n + \tfrac{1}{2})\hbar\omega$$

But

$$\sum_{n=0}^{\infty} p(n)n = \frac{1}{e^{\hbar\omega/kT} - 1}$$

which is the usual Bose-Einstein distribution, and

$$\sum_{n=0}^{\infty} p(n) = 1$$

Hence the mean energy for a mode ω is

$$\overline{E}_{\omega} = \frac{\hbar\omega}{2} \coth\left[\frac{\hbar\omega}{2kT}\right]$$

In order to estimate $<x^2>$ for an amorphous material, it is assumed that on average each macromolecule will have energy $(\overline{E}_{\omega}/N)$ associated with this mode. If the ith molecule is considered to be a classical harmonic oscillator, its mean square displacement in one direction is

$$<x_i^2> = \frac{1}{3}\left[\frac{\overline{E}_{\omega}/N}{M\omega^2}\right]$$

The three degenerate modes at frequency ω will each give a contribution to the mean square displacement of

$$<x_i^2>_{\omega} = \frac{\hbar}{6MN\omega} \coth\left[\frac{\hbar\omega}{2kT}\right] \qquad (2)$$

This is the standard result for an Einstein oscillator of frequency ω. This arises essentially because of the assumption that the energy is shared equally between the N molecules. This will be a reasonable assumption since the Mössbauer technique effectively measures a site averaged mean square displacement.

The total mean square displacement is found by integrating over the distribution function $g(\omega)$. Hence

$$<x^2> = \frac{\hbar}{6MN} \int_0^\infty \frac{g(\omega)}{\omega} \coth \left(\frac{\hbar\omega}{2kT}\right) d\omega$$

The Debye Waller factor is thus

$$2W = \frac{E_0{}^2}{6Mc^2\hbar N} \int_0^\infty \frac{g(\omega)}{\omega} \coth \left(\frac{\hbar\omega}{2kT}\right) d\omega$$

where E_0 is the energy of the incident γ ray photon.

This is the standard result from the Debye model (Boyle and Hall) and in the high temperature limit ($T \gtrsim \frac{1}{2}\Theta_D$)

$$2W = \frac{3E_0{}^2 T}{Mc^2 k_B \Theta_D{}^2}$$

where Θ_D is the characteristic Debye temperature for the lattice. Thus the Debye model predicts that $\ln f$ will depend linearly upon temperature.

The departure from linearity observed in experiment was thought to arise either from the excitation of intra-molecular modes or from anharmonic effects in the inter-molecular potential. It is found that the latter gives a good fit to the data.

(c) Intramolecular Modes

As the temperature of the solid rises, intramolecular modes will become excited. It was first thought that such modes with a characteristic temperature of approximately 180K were responsible for the change in gradient in the experimental plot of $\ln f$ against T. The intra-

molecular modes are treated as Einstein oscillators since they are equivalent to the optic modes in a crystalline material. In principle there will be $3(n-1)$ modes where n is the number of atoms in the macromolecule. However, some of these modes will only be excited at high temperature and consequently n is taken to be n_R, the number of repeating units in the molecule. This is equivalent to ignoring any vibrations which occur within the repeating unit, which is a good approximation since these will be very high frequency modes.

In the absence of a detailed model of the molecular structure and force constants, it is not possible to determine the motion of each repeating unit for the intramolecular modes. As before, it is assumed that the energy of each mode is shared equally between the repeating units. This is a reasonble assumption since the Mössbauer technique effectively averages over the repeating units in the molecule. The $3(n_R - 1)$ intramolecular modes are all assumed to have the same angular frequency ω_E and the mean square displacement of a repeating unit associated with one such mode will be

$$\langle x^2 \rangle_{\omega_E} = \frac{\hbar}{6 m_R n_R \omega_E} \coth \left(\frac{\hbar \omega_E}{2 k_B T} \right)$$

where m_R is the mass of a repeating unit. Noting that $m_R n_R = M$, the intramolecular and intermolecular modes may be combined to give

$$\langle x^2 \rangle_{TOT} = \frac{\hbar}{6MN} \int \frac{g(\omega)}{\omega} \coth\left[\frac{\hbar\omega}{2k_BT}\right] d\omega + \frac{3(n_R - 1)h}{6M\omega_E} \coth\left[\frac{\hbar\omega_e}{2k_BT}\right] \qquad (3)$$

This expression was found to give an adequate fit to the experimental results with a suitable choice of Einstein frequency. However, the parameter premultiplying the second term in the expression was found to be unacceptably high.

The cause of the failure may be seen by the following simplified argument. In the temperature region above Θ_D, but below the Einstein temperature $\Theta_E = \hbar\omega_E/k_B$, the Debye Waller factor derived from equation (3) may be written

$$2W \simeq \frac{3E_0^2}{Mc^2k_B} \left[\underbrace{\frac{T}{\Theta_D^2}}_{s_0} + \frac{(n_R - 1)}{6}\Theta_E \right] \qquad (\Theta_D < T < \Theta_E)$$

For temperatures above the Einstein temperature

$$2W \simeq \frac{3E_0^2}{Mc^2k_B} \underbrace{\left[\frac{T}{\Theta_D^2} + \frac{T(n_R - 1)}{3\Theta_E^2} \right]}_{s_1} \qquad (\Theta_E < T)$$

Thus the maximum fractional change in slope, s, of the ln f against T graph will be

$$\frac{s_1 - s_0}{s_0} = \frac{(n_R - 1)}{3} \frac{\Theta_D^2}{\Theta_E^2}$$

From experiment, it is found that the fractional change in slope in the temperature range 80K to 300K is typically 0.5. This suggests that

$$\frac{(n_R - 1)}{3} \frac{\Theta_D^2}{\Theta_E^2} > 0.5 \qquad (4)$$

It was first thought that the results showed a transition at approximately $T_0 = 180K$ and this can be identified with the temperature at which the function $\coth\left[\frac{\hbar\omega_E}{2k_B T}\right]$ shows the greatest change in slope. This occurs when

$$\frac{\hbar\omega_E}{2k_B T_0} \simeq 2.2$$

i.e. $\Theta_E \simeq 4.4\ T_0 = 790K$

The Debye temperature is typically $\sim 50K$ and hence the inequality (4) becomes

$$n_R > 375$$

This is in clear disagreement with the experimental value for n_R of approximately 10. The expression (3) was modified to allow a range of values of ω_E but this still failed to give a reasonable value for n_R.

Hence it was concluded that the intramolecular modes cannot explain the large change in slope observed experimentally.

(d) Anharmonic Potential

Boyle et al (1960) observed a non-linear temperature dependence for the recoilless fraction in metallic tin in the temperature range Θ_D to $4\Theta_D$ where Θ_D for tin is 142K. They demonstrate that this non-linearity arises because

of the anharmonic nature of the potential in which each tin atom is situated.

Zener and Bilinsky (1936) considered the effect of thermal expansion and showed that

$$2W \simeq \frac{3E_0{}^2T}{Mc^2k_B\Theta_D{}^2} \left[1 + \frac{2V\beta^2}{3RK} \left(T - \frac{3}{8}\Theta_D\right)\right] \qquad (5)$$

where R is the gas constant, K is the isothermal compressibility, β is the high temperature volume expansion coefficient and V the molar volume.

The experimental results were fitted to the equation

$$\ln(A) = B - CT - DT^2 \qquad (6)$$

using a least squares method. The parameters C, D and Θ_D are given in Table 6.3 for each sample, and the corresponding fits are shown in Figure 6.7.

References

Boyle A J F, Bunbury D St P, Edwards C and Hall H E, Proc. Phys. Soc., 77 (1960) 129-35.

Zener C and Bilinsky S, Phys. Rev. 50 (1936), 101.

APPENDIX 3

COURSES ATTENDED

1. The Polymer Molecule : 6 x 1 hour lectures, November 1979

2. Mössbauer Spectroscopy (Chemistry Department) :
   6 x 1 hour lectures, November 1979

3. Polymerisation Mechanisms : 6 x 1 hour lectures,
   January 1980

4. An Introduction to BASIC Computing : 8 x 2 hour lectures,
   February 1980

5. Mössbauer Spectroscopy (Applied Physics Department) :
   15 x 1 hour lectures, January 1981.

CONFERENCES ATTENDED

1. 21st Mössbauer Spectroscopy Discussion Group Meeting,
   Heriot Watt University, Edinburgh, July 1980.

2. 22nd Mössbauer Spectroscopy Discussion Group Meeting,
   Sheffield City Polytechnic, September 1981 (paper
   presented).

3. 23rd Mössbauer Spectroscopy Discussion Group Meeting,
   University of Essex, Colchester, July 1982.

Mössbauer Studies of Polymers from 1,1'-Divinylferrocene

G. C. CORFIELD, J. S. BROOKS, and S. PLIMLEY

Sheffield City Polytechnic, Sheffield S1 1WB, England

*Linear, saturated, polymers obtained by radical init-
iation of 1,1'-divinylferrocene have the Mossbauer
parameters (δ, 0.23 mm s^{-1}; ΔE_Q, 2.29 mm s^{-1}) expec-
ted for cyclopolymers with three-carbon bridged
ferrocene units in the main chain. However, cat-
ionic initiation yields polymers which exhibit
differences from the radical polymers in Mossbauer
(δ, 0.27 mm s^{-1}; ΔE_Q, 2.40 mm s^{-1}) and other spec-
troscopic studies. The cationic polymers may con-
tain a bicyclic unit or a ladder structure in the
chain.*

The use of modern spectroscopic methods can reveal infor-
mation on the microstructures of cyclopolymers which previously
went undetected (1). Here we report the application of Mossbauer
spectroscopy to a study of the polymers of 1,1'-divinylferrocene
(DVF).

The polymerisation of DVF was first investigated by two
independent research groups (2-7) who reported that soluble
polymers could readily be obtained using free radical and cat-
ionic initiators. These authors proposed that cyclopolymerisa-
tion had occurred with the formation of linear polymers having
three-carbon bridged ferrocene units (I), and some acyclic units
(II), in the chain. Evidence for structure (I) as the predomi-
nant unit in the polymer chain was provided by the low level of
vinyl unsaturation detectable by NMR or infrared spectroscopy
and the observation that bands attributable to a bridged ferro-
cene (8) were to be found in the infrared spectra of these
polymers.

Recent investigations (9, 10) of bridged ferrocenes by
Mossbauer spectroscopy have demonstrated that a short three-
carbon bridge causes changes in the iron-ring geometry which
leads to differences in Mossbauer parameters between three-
carbon bridged ferrocenes and compounds with four- or five-
carbon bridges. We have re-investigated the polymerisation of

AIBN
or
$BF_3 \cdot OEt_2$

Fe

I

II

n

m
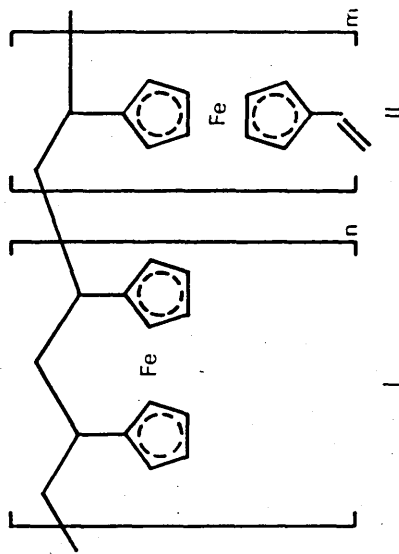
SCHEME I
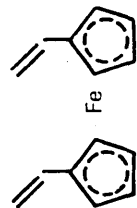
DVF and studied the polymers by Mossbauer spectroscopy, using the isotope Fe-57, to seek supporting evidence for the three-carbon bridged unit (I) as the predominant unit in the chain.

Experimental

DVF was prepared from ferrocene by established procedures (2, 3, 4, 11, 12, 13), recrystallised from methanol (m.p. 39.5-41.0 °C), and shown to be pure by thin layer chromatography (silica gel with toluene as eluent).

Polymerisations using free radical and cationic initiators were carried out essentially as described by Kunitake et al (2, 3, 4).

^{57}Fe Mossbauer spectra were obtained using a digital constant acceleration spectrometer having a symmetrical triangular velocity drive waveform. A 10 m Ci ^{57}Fe in Pd source was used and all experiments were carried out at room temperature. The spectrometer was calibrated between runs using the magnetic splitting of enriched ^{57}Fe absorber foil. The data were folded to determine the zero velocity position and the folded data were fitted with Lorentzian functions by a non-linear least squares fitting program (14).

Results and Discussion

Polymerisation. DVF has been polymerised using radical and cationic initiators, and typical results are given in Table I. Radical initiation in dilute solutions gave products which were predominantly soluble in benzene. Cationic initiation resulted in higher conversions, again mainly to soluble polymers. These results, which are similar to those obtained by Kunitake et al (2, 3, 4), indicate that linear polymers, possibly cyclopolymers, have been obtained.

TABLE I POLYMERISATION OF 1,1'-DIVINYLFERROCENE

Initiator/ mol.dm^{-3}	Monomer mol.dm^{-3}	Solvent	Temp °C	Conversion[a] % Soluble, % Insoluble[b]	
AIBN/ 1.56x10^{-3}	0.10	C_6H_6	64	50	3
BF$_3$.OEt$_2$/ 0.01	0.20	CH_2Cl_2	0	48	16

[a]Precipitated into methanol

[b]Solubility in benzene

Infrared Spectroscopy. The infrared spectra of the poly-

mers (Figure 1) were in accord with previous work (2, 3, 4). Of particular interest in the spectrum of the polymers obtained by radical initiation [PDVF(radical)] are the distinct bands at 810 cm^{-1} and 850 cm^{-1}, which have been observed in a large number of heterobridged ferrocene compounds (8). This pair of characteristic bands is not clearly seen in the polymers obtained by cationic initiation [PDVF(cationic)] where a broad absorption, centred at approximately 830 cm^{-1}, is observed. Other differences between the spectra can be seen, particularly in the *fingerprint* region of the spectrum. These differences have been interpreted (2, 3, 4) as due to differences in the extent of cyclisation in the polymers. However, an alternative explanation is that this indicates that the polymers have significantly different structures.

NMR Spectroscopy. The ^{1}H NMR spectra of the polymers (Figure 2) were also similar to those previously published. The spectrum of PDVF (radical) contained no detectable vinyl unsaturation, whereas that of PDVF (cationic) showed a significant amount of unsaturation, but considerably less than that expected if one vinyl group remained unreacted on each ferrocene unit. However, it is of interest that the signal ascribed by Kunitake *et al* (2, 3, 4) to vinyl unsaturation is a single broad peak at δ5.90 ppm rather than the pair of signals expected at approximately δ4.9 and 6.1 ppm for a vinyl substituent on a ferrocene ring. Also, the aliphatic protons patterns are different for PDVF (radical) and PDVF (cationic). Kunitake *et al* observed this and attributed it to a difference in polymer conformations, influenced by the degree of cyclisation. Again, an alternative explanation is that the polymers are structurally different.

^{13}C NMR spectra of these polymers (Figure 3) also exhibit clear differences, which support our suggestion that the polymers are structurally different. A detailed analysis and discussion of the ^{13}C NMR spectra will appear in a subsequent publication.

Mössbauer Spectroscopy. Mössbauer spectroscopic studies of the polymers are reported here, and these provide the evidence to substantiate the structural differences between the polymers.

The Mossbauer effect can be used to compare nuclear transition energies in two materials with high precision. This is useful in obtaining chemical information as the nucleus is sensitive to changes in its electronic environment. Two hyperfine interactions which give rise to information about the electronic environment are isomer shift (IS) and quadrupole splitting (QS). Figure 4 shows a Mossbauer spectrum, typical of that obtained from ferrocene compounds, with these two parameters distinguished. IS results from the electrostatic interaction between the charge distribution of the nucleus and those electrons which
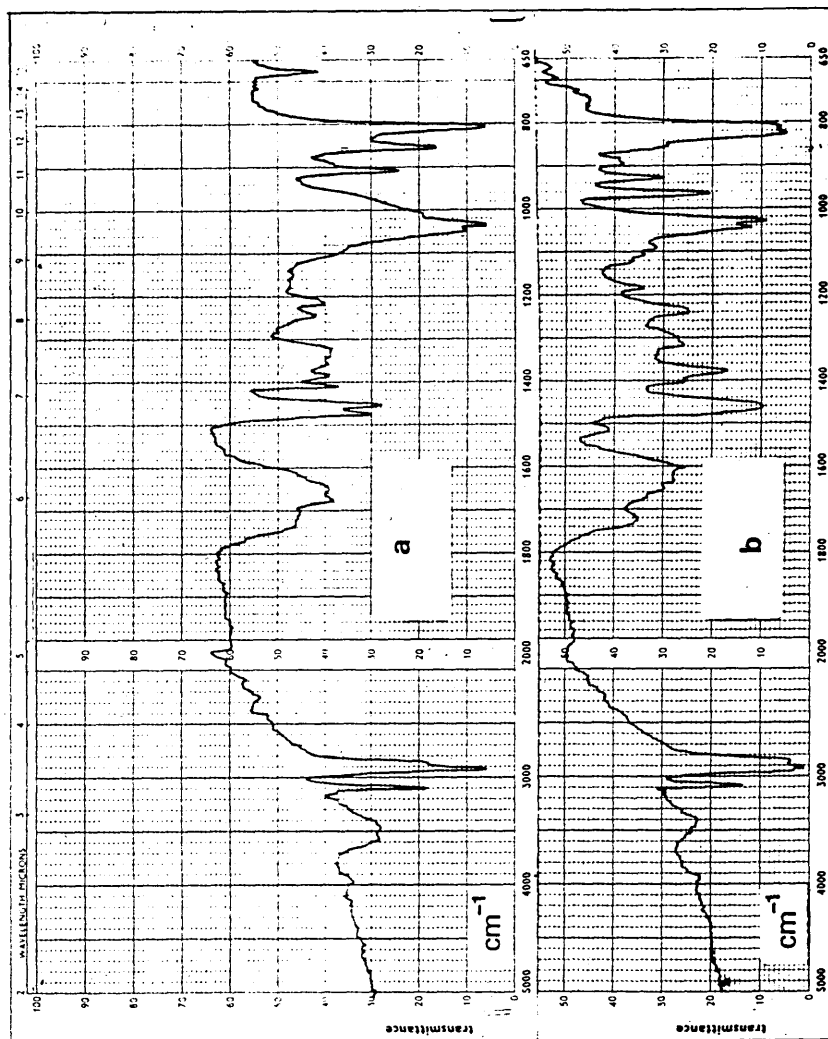
*Figure 1.   IR spectra of PDVF(radical) (a) and PDVF(cationic) (b).*
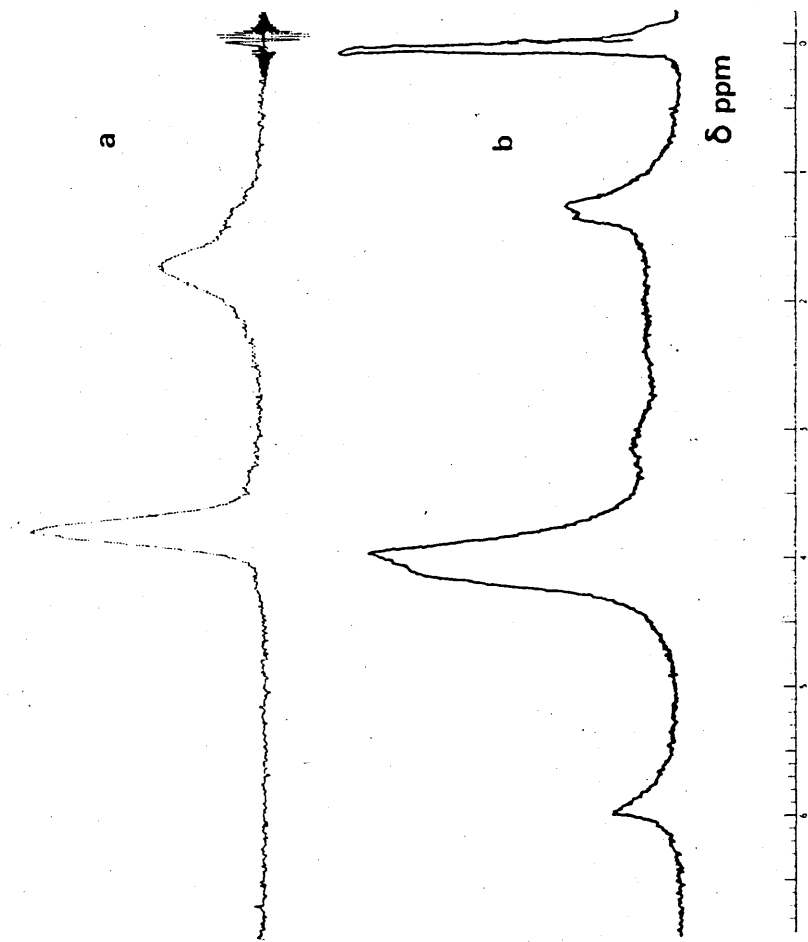
Figure 2. *¹H NMR spectra of PDVF(radical) (a) and PDVF(cationic) (b).*

δ ppm

a

b
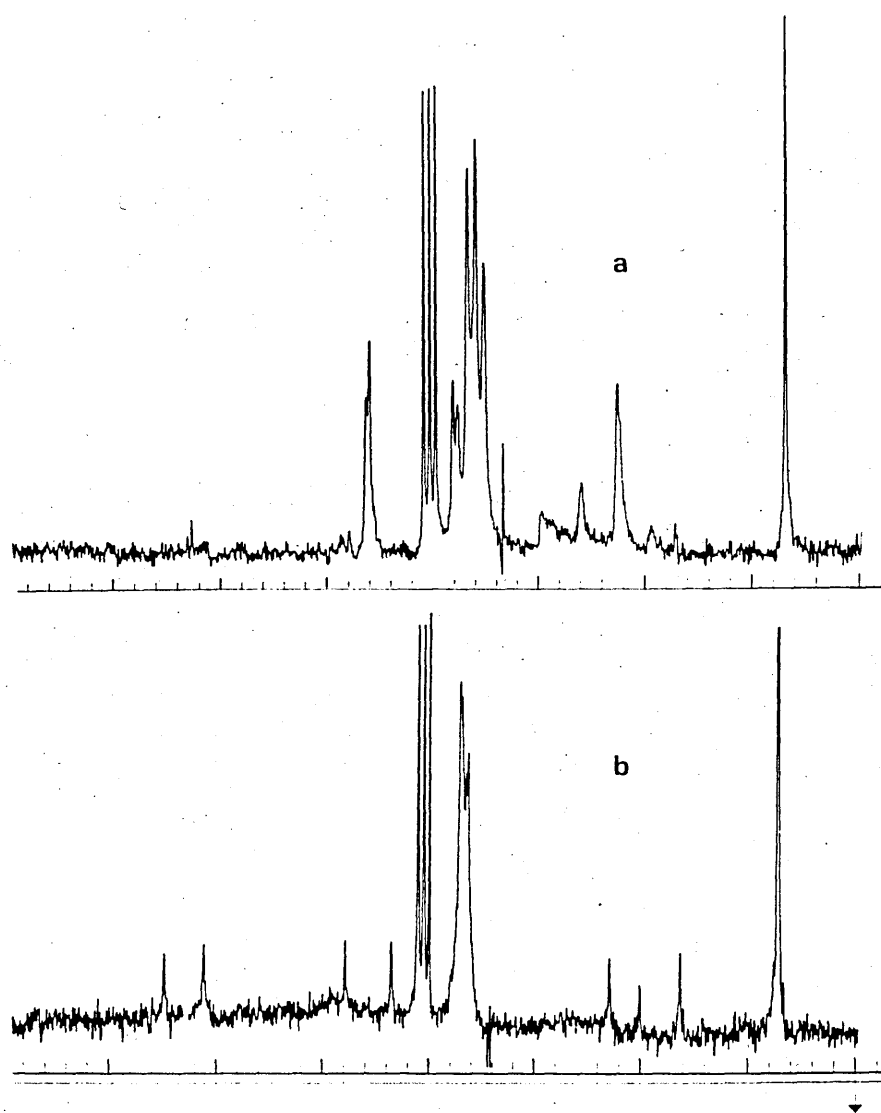
Figure 3. ^{13}C *NMR spectra of PDVF(radical) (a) and PDVF(cationic) (b).*
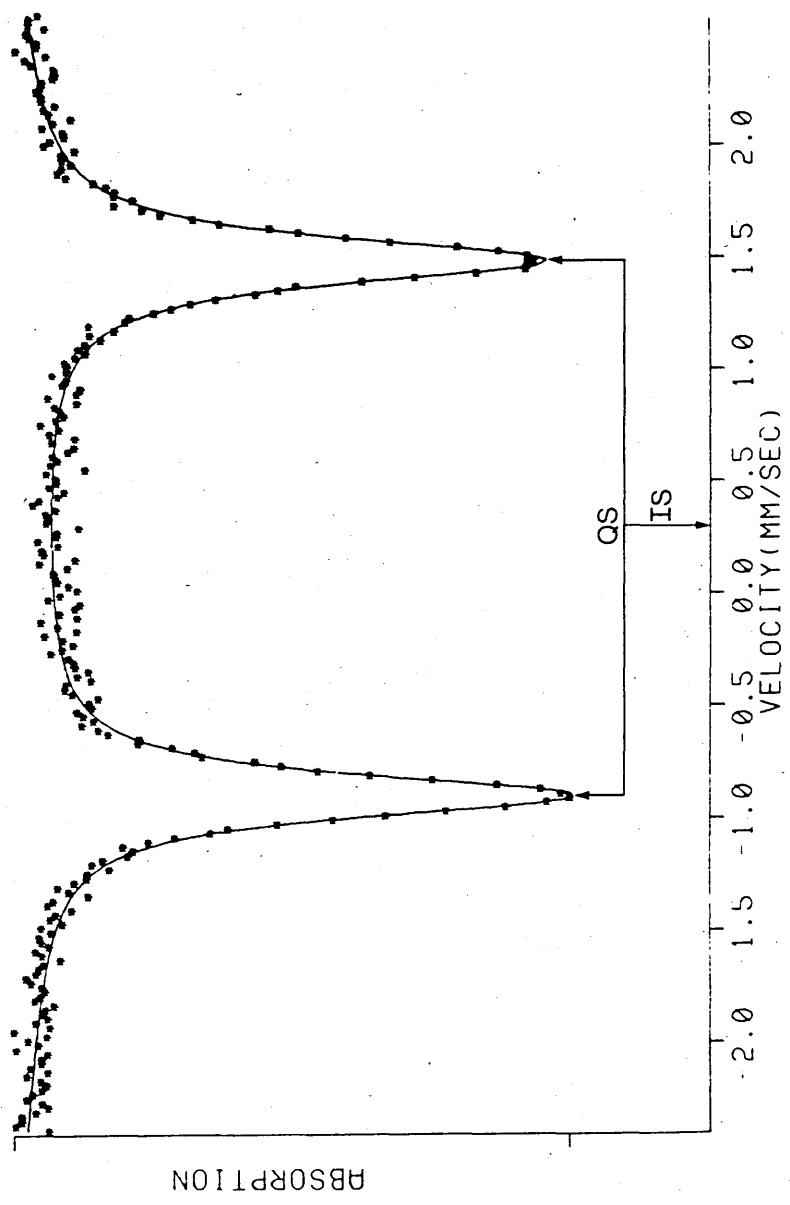
Figure 4. Mössbauer spectrum typically found for ferrocene compounds. Key: IS, isomer shift; and QS, quadrupole splitting.

have a finite probability of being found in the region of the nucleus. Thus, IS is influenced by the s-electron density at the nucleus; these being the only orbitals which have a finite probability of interacting with the nuclear charge density. The s-electron density, and hence IS, of the iron atom is related therefore to its bonding and valency, since other orbitals can affect the s-electron nuclear density by shielding effects. QS results from the interaction between the nuclear quadrupole moment and the electric field gradient of the nucleus. Variations in the distribution of electrons within the d-orbitals of the iron atom, due to variations in the substituents attached to the atom, cause changes in the electric field gradient tensor and hence give rise to differences in QS.

IS leads to a shift of the centre of gravity of the Mossbauer spectrum away from zero Doppler velocity. QS results in partial removal of the degeneracy of the nuclear excited state resulting, for Fe-57, in a doublet in the Mossbauer spectrum. The Mossbauer spectra are computer fitted using IS (δ/mm s^{-1}) and QS (ΔE_Q/mm s^{-1}) as position parameters for each pair of Lorentzian lines, with the *full width at half height* (Γ/mm s^{-1}) and the relative depth as line shape parameters. The computer program varies the fitting parameters to minimise χ^2, and the solid line drawn through the data points represents the *best fit* to the data.

Table II gives Mossbauer parameters for the compounds which comprise the synthetic route from ferrocene to DVF. It can be seen that for these compounds, which are all in the same oxidation state, IS remains fairly constant. Ring substitution produces negligible changes in IS since the molecular orbitals of ferrocene are not formed with orbitals of a single ring atom but with the ring as a whole. The variations in QS are more significant. The electric field gradient at the nucleus arises largely from the π-bonded ligands and little change is observed when a σ-bonded substituent is introduced to the ferrocene ring, as in 1,1'-bis(1-hydroxyethyl)ferrocene. However, where π orbital overlap can occur, there is some redistribution of the electrons and variations are observed, as with 1,1'-diacetyl-ferrocene and DVF.

Investigation of PDVF by Mossbauer spectroscopy shows that PDVF (radical) and PDVF (cationic) have significantly different parameters (Table III and Figure 5). Thus the repeating units in these polymers must have different structures, which influence the ferrocene ring system in different ways. Mossbauer measurements on a variety of bridged ferrocene compounds (9, 10) have demonstrated that for compounds with only three carbons in a heteroannular bridge (for example, III) the strain causes a significant decrease in the values of IS and QS (Table III) due to a decrease in the iron-ring distances, caused by the tilting of the ring system (Figure 6). With less-strained bridges comprising four (IV) or five (V) carbons the IS and QS values are

Table II

Mössbauer Parameters of Monomer and Intermediates

Compound	Isomer Shift,[a] δ/mm s^{-1}	Quadrupole Splitting, ΔE_Q/mm s^{-1}	Line Width Γ/mm s^{-1}
Ferrocene	0.27(2)	2.39(2), 2.397[b]	0.12(1)
1,1'-Diacetylferrocene	0.26(2)	2.19(2)	0.13(1)
1,1'-Bis(1-hydroxyethyl)ferrocene	0.27(2)	2.39(2)	0.12(1)
1,1'-Divinylferrocene	0.27(2)	2.27(2)	0.12(1)

[a]Relative to Fe in Pd

[b]Theoretical QS, Trautwein et al (15)

Table III

Mössbauer Parameters of Polymers and Model Compounds

Compound	Isomer Shift,[a] $\delta/mm\ s^{-1}$	Quadrupole Splitting, $\Delta E_Q/mm\ s^{-1}$	Line Width $\Gamma/mm\ s^{-1}$
PDVF (radical)	0.23(2)	2.29(2)	0.13(1)
PDVF (cationic)	0.27(2)	2.40(2)	0.12(1)
PVF (radical)	0.28(2)	2.40(2)	0.12(1)
PVF (cationic)	0.27(2)	2.39(2)	0.13(1)
Methylferrocene[b]		2.39(5)	
3-carbon ring model (III)[c]	0.231(2)	2.256(3), 2.30[b], 2.285[d]	
4-carbon ring model (IV)[c]	0.244(2)	2.351(5)	
5-carbon ring model (V)[c]	0.253(4)	2.344(5)	

[a]Relative to Fe in Pd
[b]Lesikar (18)
[c]Nagy et al (9, 10)
[d]Theoretical Q.S., Trautwein et al (15)
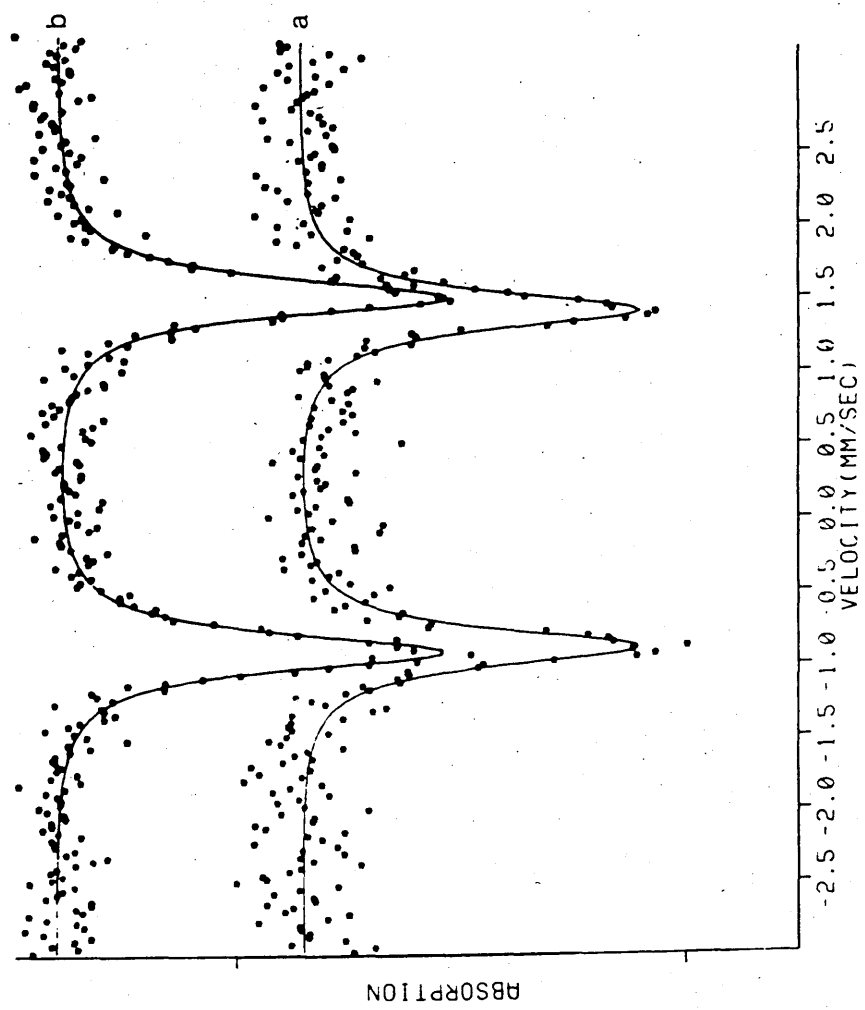
*Figure 5.   Mössbauer spectra of PDVF(radical) (a) and PDVF(cationic) (b).*
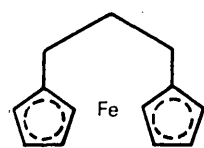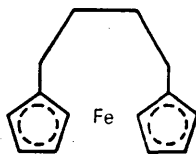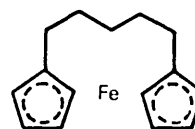
III IV V
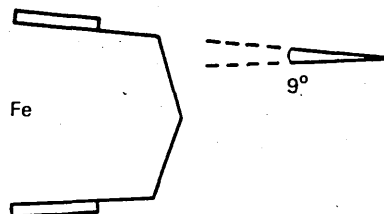
Figure 6.   *Three-carbon bridged ferrocene compound having a tilted ring system with a dihedral angle of 9°.*
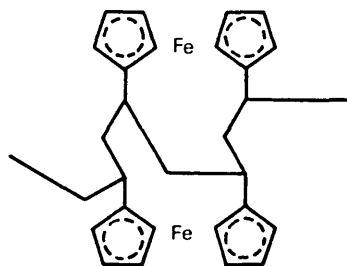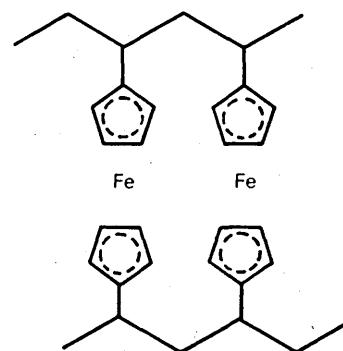
VI VII

not as greatly affected. PDVF(radical) exhibits IS and QS values which are similar to those observed and predicted for the model compound having three carbon atoms bridging the ferrocene rings. This provides strong evidence that this is a cyclopolymer with a three-carbon bridge (I) as the repeating unit. However, PDVF(cationic) has IS and QS values similar to those that have been obtained for the unstrained ferrocene units in polyvinylferrocene [PVF(radical) and PVF(cationic), Table III]. It has been observed (16, 17) that the bonding of the iron atom to the rings is not affected by alkyl substituents in the cyclopentadiene rings, and methylferrocene exhibits a similar QS (18). The experimental data was computer fitted as a single quadrupole doublet. The co-existence of strained ($\Delta E_Q = 2.29$ mm s^{-1}) and unstrained ($\Delta E_Q = 2.40$ mm s^{-1}) units would result in a Mossbauer spectrum having two overlapping quadrupole doublets. Clear evidence for this would be given by corresponding changes in line widths and asymmetry in line intensities. No significant line broadening (Tables II and III) or intensity asymmetry (Figure 5) was observed for the polymers studied.

Conclusions

These results therefore indicate that the soluble, saturated polymers produced by radical initiation of DVF are cyclopolymers containing a three-carbon bridged ferrocene unit (I). However, the Mossbauer spectra obtained for polymers produced by cationic initiation do not show evidence for the three-membered bridge. Certainly PDVF(cationic) contains some acyclic unsaturated units, not necessarily pendant vinyl groups (II), but the low level of unsaturation suggests that cyclic units exist. Thus, for example, a five-carbon bridged bicyclic unit (VI) or a ladder structure (VII) may be found in these polymers, and would be consistent with the Mossbauer parameters obtained. Further polymerisation studies and Mossbauer and other spectroscopic studies of these polymers are in progress.

Acknowledgements

Literature Cited

1. Corfield, G.C.; Butler, G.B. "Cyclopolymerisation and Cyclocopolymerisation"; Chapter 1 in "Developments in Polymerisation Vol. 3"; Haward, R.N., Ed.; Applied Science Publishers: London, 1982.

2. Kunitake, T.; Nakashima, T.; Aso, C. J. Polym. Sci., Part A-1 1970, 8, 2853.
3. Kunitake, T.; Nakashima, T.; Aso, C. Makromol. Chem. 1971, 146, 79.
4. Aso, C.; Kunitake, T.; Tagami, S. "Progress in Polymer Science, Japan Vol. 1"; Imoto, M.; Onogi, S., Eds.; Halsted Press: Tokyo, 1971; p 170.
5. Sosin, S.L.; Jashi, L.V.; Antipova, B.A.; Korshak, V.V. Vysokomol. Soedin. Ser. B 1970, 12, 699.
6. Sosin, S.L.; Jashi, L.V.; Antipova, B.A.; Korshak, V.V. Vysokomol. Soedin. Ser. B 1974, 16, 347.
7. Korshak, V.V.; Sosin, S.L. "Organometallic Polymers"; Carreher, C.E.; Sheats, J.E.; Pittman, C.U., Eds; Academic Press: New York, 1977; p 26.
8. Neuse, E.; Crossland, R.K.; Koda, K. J. Org. Chem. 1966, 31, 2409.
9. Nagy, A.G.; Dezsi, I.; Hillman, M. J. Organometal. Chem. 1976, 117, 55.
10. Hillman, M.; Nagy, A.G. J. Organometal. Chem. 1980, 184, 433.
11. Rosenblum, M.; Woodward, R.B. J. Amer. Chem. Soc. 1958, 80, 5443.
12. Yamakawa, K.; Ochi, H.; Arakawa, K. Chem. Pharm. Bull. (Japan) 1963, 11, 905.
13. Rausch, M.D.; Siegel, A. J. Organometal. Chem. 1968, 11, 317.
14. Lang, G.; Dale, B. Nucl. Inst. Meths. 1974, 116, 567.
15. Trautwein, A.; Reschke, R.; Dezsi, I.; Harris, F.E. Journal de Physique 1976, 12, C6-463.
16. Good, M.L.; Buttone, J.; Foyt, D. Ann. N.Y. Acad. Sci. 1974, 239, 193.
17. Korecz, L.; Abou, H.; Ortaggi, G.; Graziani, M.; Belucco, U.; Burger, K. Inorg. Chim. Acta 1974, 9, 209.
18. Lesikar, A.V. J. Chem. Phys. 1964, 40, 2746.

13C NMR STUDIES OF POLYMERS FROM 1,1'-DIVINYLFERROCENE

by

G C Corfield, J S Brooks and S Plimley
Sheffield City Polytechnic, Sheffield S1 1WB,
England,

and

A V Cunliffe, Ministry of Defence, PERME, Waltham
Abbey, England.

The polymerisation of 1,1'-divinylferrocene (DVF)
was first investigated by two independent research
groups[1,2] who reported that soluble polymers could
readily be obtained using free radical and
cationic initiators. These authors proposed that,
in both cases, cyclopolymerisation had occurred
leading to the formation of linear polymers con-
taining three-carbon bridged ferrocene units (I),
with residual unsaturation in the cationic polymer
being due to acyclic units (II).

We reported recently[3] our investigation of these
polymers by Mössbauer spectroscopy. This showed
that the samples of poly(1,1'-divinylferrocene)
(PDVF) produced by radical and cationic initiation
had significantly different Mössbauer parameters.
Our interpretation of these differences is that
the repeating units of these polymers are
different structures. In PDVF (radical) the IS
and QS values (δ, 0.23 mm s^{-1}; ΔE_Q, 2.29 mm s^{-1})
are similar to those predicted and observed for
the model compound with three-carbon atoms
bridging a ferrocene ring, which supports the
cyclopolymerisation mechanism. However, PDVF
(cationic) has IS and QS values (δ, 0.27 mm s^{-1};
ΔE_Q, 2.40 mm s^{-1}) similar to those observed for
the non-cyclic polyvinylferrocene (PVF). We now
report our 13C NMR studies of these polymers which
provide further information on their microstructure.

Results and Discussion

13C NMR spectra of PDVF (radical) and PDVF
(cationic) exhibit clear differences (Figure 1),
which supports our evidence from Mössbauer spect-
roscopy that these polymers are structurally
different. To assist with our analysis of these
spectra, the carbon chemical shifts of PVF
(radical) (III) are given in the Table.

PDVF (radical) - The spectrum is shown in
Figure 1(a) and assigned carbon chemical shifts
are given in the Table. The β and γ ring carbons
appear in a similar region to those in PVF,
although with considerably more resolution which
is indicative of non-equivalence. Of particular
interest is the upfield shift compared to PVF, of
the α carbon signal, which is attributed to
distortion of the ferrocene ring system, which will
be tilted to approximately 9° in the cyclopolymer
unit (I). A similar shift for this carbon can be
observed by comparing strained and unstrained
carbon-bridged ferrocenes.[4] Aliphatic carbon 1
was assigned by comparison with the spectra of
PVF and the model compound with a three-carbon
bridge. Two methylene carbons are observed, as
expected for structure (I). Thus, the 13C NMR
spectrum supports our evidence from Mössbauer
spectroscopy that the soluble, saturated polymers
produced by radical initiation of DVF are cyclo-
polymers containing a three-carbon bridged
ferrocene unit (I).

PDVF (cationic) - The spectrum is shown in
Figure 1(b) and assigned carbon chemical shifts
are given in the Table. This is generally a less
well resolved spectrum and has broad peaks, which
suggests that a mixture of structures exists. The
α, β, and γ carbons are comparable with those of
PVF, with little evidence of non-equivalence in
the β and γ carbons. Important structural
information is provided by the presence of a signal
attributable to a methyl group, and the fact that
the unsaturated (olefinic) carbon signals are not
due to vinyl groups, but are HC= signals. A small
amount of absorption due to the α carbon of a
bridged unit (I) is observable. However, as
indicated by Mössbauer spectroscopy, the cyclo-
polymer unit (I) is not the major repeating unit
in PDVF (cationic). Previous authors[1,2] proposed
that residual unsaturation was due to the presence
of acyclic units (II), but 13C and 1H NMR[3] studies
do not support this structure. The evidence
strongly suggests that (IV), which could arise by
an intermolecular cationic polyaddition mechanism
is the major structural unit in PDVF (cationic).

REFERENCES

1. T Kunitake, T Nakashima and C Aso, J Polym Sci
   A-1, 8, 2853 (1970); T Kunitake, T Nakashima
   and C Aso, Makromol Chem, 146, 79 (1971);
   C Aso, T Kunitake and S Tagami, Progress in
   Polymer Sci. Japan, 1, 170 (1971).

2. S L Sosin, L V Jashi, B A Antipova and
   V V Korshak, Vysokomol Soedin, 12, 699 (1970);
   S L Sosin, L V Jashi, B A Antipova and
   V V Korshak, Vysokomol Soedin, 14, 347 (1974);
   V V Korshak and S L Sosin, Organometallic
   Polymers, Academic Press, p26 (1978).

3. G C Corfield, J S Brooks and S Plimley,
   Polymer Preprints, 22 (1), 3 (1981); ACS
   Symposium Series, in press.

4. Y Senda, S Kamiyama, A Kasahara, T Izumi and
   S Murakami, Bull. Chem. Soc. Jpn, 53, 3381
   (1980).

5. J Nishimura, Y Ishida, M Mimura, N Nakazawa
   and S Yamashita, J Polym Sci Polym Chem Ed,
   18, 2061 (1980).
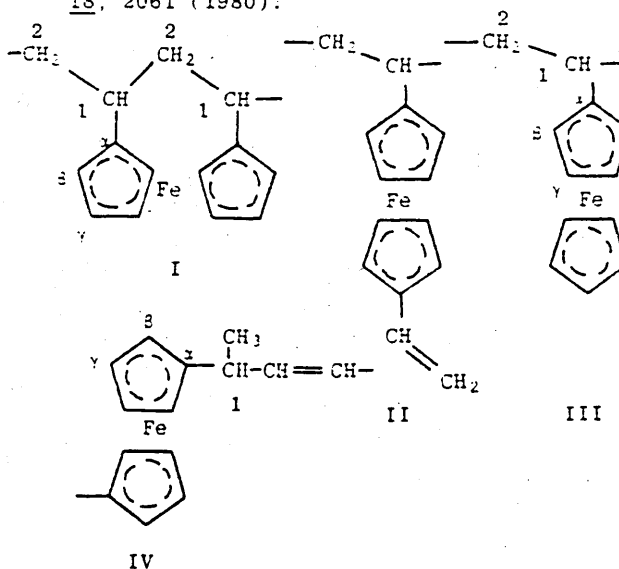
TABLE : Carbon Chemical Shifts of Polymers

|	Chemical shift/ppm from TMS in CDCl$_3$		
Carbons	PVF (radical) (III)	PDVF (radical) (I)	PDVF (cationic) (IV)
α	96.1	89.8, 90.6	96.7
β,γ	67.1-68.5	65.1-70.9	66.9-68.8
1	32.2	36.0	36.2
2	44.0	43.9, 52.4	
CH$_3$			21.1
-CH=CH-			124.8, 133.3

Figure 1 ^{13}C NMR spectra of:

(a) PDVF (radical);

(b) PDVF (cationic).

VARIABLE TEMPERATURE ^{57}Fe MÖSSBAUER STUDIES ON POLYMERS OF VINYLFERROCENE AND 1, 1'-DIVINYL-FERROCENE

J.S. BROOKS, C.M. CARE and S. PLIMLEY

Department of Applied Physics, Sheffield City Polytechnic, Sheffield S1 1WB, UK

and

G.C. CORFIELD*

Department of Chemistry, Sheffield City Polytechnic, Sheffield S1 1WB, UK

(L)
(lower case ℓ)

Variable temperature ^{57}Fe Mössbauer spectra have been recorded in the range 80–300 K for a number of low molecular weight amorphous polymers containing ferrocene units. These include samples of polyvinylferrocene, polydivinylferrocene by anionic initiation and polydivinylferrocene by cationic initiation. A similar non-linear temperature dependence of ℓnA was observed for all the polymers, although they contain ferrocene units in different structural arrangements. A Debye model was extended to include intramolecular vibrations, and a fit to the experimental data was obtained. However, the model did not yield satisfactory fitting parameters. The observed behaviour of the experimental data could be accounted for by assuming that each macromolecule vibrates within an anharmonic potential.

*Present address: School of Science, Humberside College of Higher Education, Hull HU6 7RT, UK.

1.   Introduction

The polymerisation of vinylferrocene has been investigated previously and various spectroscopic and other physical properties of the polymer have been reported [1]. The Mössbauer parameters are typical of ferrocene and support other evidence for the expected unstrained structure (I) for the polymer.
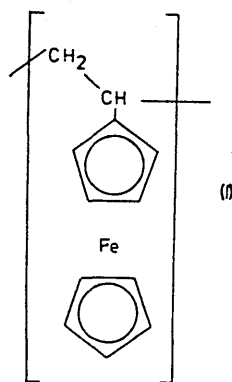
(I)

The polymerisation of 1, 1'-divinylferrocene (DVF) was first investigated by two independent groups [2,3]. These authors proposed that cyclopolymerisation had occurred with the formation of linear polymers having three-carbon bridged ferrocene units (II), with any residual unsaturation being due to acyclic units (III).

Free radical or cationic initiators

(II)   (III)
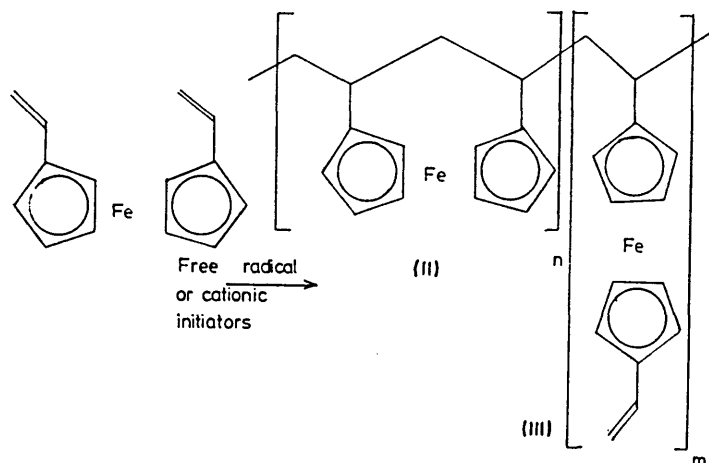
Recent investigations of bridged ferrocenes using Mössbauer spectroscopy [4,5] have shown that a three-carbon bridge causes significant changes in the iron-ring geometry, resulting in a reduction in the quadrupole splitting parameter. We have recently re-investigated the polymerisation of DVF and have studied the polymers using ^{57}Fe Mössbauer and ^{13}C NMR spectroscopy [6,7]. Our results showed that the soluble, completely saturated polymers produced by radical initiation of DVF are cyclopolymers containing the three-carbon bridge unit (II). However, the Mössbauer spectra obtained for polymers produced by cationic initiation did not exhibit ring strain and therefore did not appear to contain the three-carbon bridged unit. ^{13}C NMR spectra also supported the evidence that the cyclopolymer unit (II) was not the predominant unit. Our results [6] strongly suggest that the major structure in the polymers from cationic initiation of DVF is (IV), which can result from an intermolecular polyaddition mechanism.
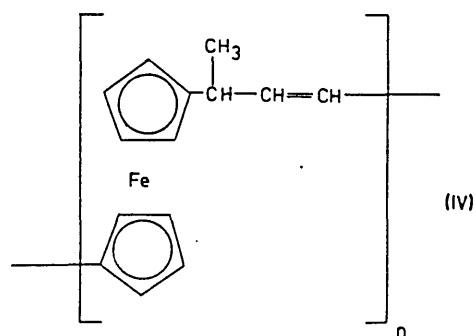

In this study, we have carried out a series of variable temperature Mössbauer experiments on crystalline ferrocene and the amorphous polymers from vinylferrocene and 1, 1'-divinylferrocene. The application of Mössbauer spectroscopy to the study of amorphous polymers has normally been limited to a study of their hyperfine interactions to yield information on the electronic state of the iron atom [1]. However, it was anticipated that additional dynamic vibrational properties could be obtained from a study of the temperature dependence of the absorber recoilless fraction f_a. The recoilless fraction relates directly to the mean square displacement of the iron atom from its equilibrium lattice position. The temperature dependence of f_a for crystalline solids is well established [8]. In this work we have developed this treatment to describe the vibrational properties of these amorphous polymers. While this work was in progress, Litterst et al. [9] reported a variable temperature Mössbauer study of polyvinylferrocene and copolymers of acrylonitrile and vinylferrocene. They observed an anomalous decrease of f_a between 80 and 130 K accompanied by line broadening, and were able to interpret this behaviour in terms of an anharmonic, hindered motion of the ferrocene sidegroup.

2. Experimental

2.1. MATERIALS

Vinylferrocene was synthesised from acetylferrocene (Aldrich Chemical Company) in two steps via 1-hydroxyethylferrocene (i). 1, 1'-divinylferrocene was synthesised from ferrocene in three steps via 1, 1'-diacetylferrocene and 1, 1'-bis(β-hydroxyethyl)ferrocene (ii). After purification by repeated recrystallisations, monomers were stored at $-20\,°C$ under a nitrogen atmosphere.

2, 2'-azobisisobutyronitrile (AIBN) was purified by triple recrystallisation from methanol and stored under nitrogen. Boron trifluoride diethyletherate ($BF_3 \cdot OEt_2$) was purified by distillation under vacuum in the presence of diethyl ether and calcium hydride, then stored under nitrogen. Butyl lithium (BuLi, 25% solution in hexane) was stored under argon at $4\,°C$.

2.2. POLYMERISATION

Radical polymerisation of vinylferrocene was carried out using AIBN as initiator in benzene. Three freeze-pump-thaw cycles were carried out to ensure removal of oxygen and the flask filled with nitrogen before sealing. Polymerisation was carried out at $60\,°C$.

Anionic polymerisation of the monomers involved butyl lithium as initiator and tetrahydrofuran as solvent. Three freeze-pump-thaw cycles were used to ensure removal of oxygen. The apparatus was filled with nitrogen before sealing. Polymerisation was carried out at $-78\,°C$ in a solid CO_2/acetone bath with initiator injected directly from the storage bottle via a septum.

Cationic polymerisation of 1, 1'-divinylferrocene was carried out using boron trifluoride diethyletherate in dichloromethane at $0\,°C$ under nitrogen (see table 1).

Table 1

	Monomer (mol dm^{-3})	Initiator (mol dm^{-3})	T (°C)	Reaction time (h)	Conversion[d] (%)
PVF (radical)	1.00	5×10^{-3}[a]	60	5	S5
PVF (anionic)	0.5	1.0[b]	−78	6	S87 I6
PDVF (cationic:linear)	0.058	0.007[c]	0	120	S44 I6
PDVF (anionic:cyclic)	0.53	2.00[a]	−78	6	S33 I2

[a]AIBN.
[b]BuLi.
[c]$BF_3 \cdot OEt_2$.
[d]S and I denote benzene soluble and benzene insoluble fractions.

The polymers were precipitated by pouring solutions into an excess of methanol. The precipitated polymer was filtered, reprecipitated from benzene into methanol, then filtered again and dried.

2.3. MOLECULAR WEIGHT DETERMINATIONS

Relative number average molecular masses were measured by vapour pressure osmometry (VPO) in toluene solution at 30 °C using a Hitachi/Perkin-Elmer Model 115 osmometer or by gel permeation chromatography (GPC) in tetrahydrofuran at 35 °C by the Rubber and Plastics Research Association, Shawbury, Shrewsbury.
The values obtained were:

Sample	$\bar{M}_n$ GPC	$\dfrac{\bar{M}_w}{\bar{M}_n}$ (GPC)	$\bar{M}_n$ VPO
PVF (radical)	961	1.1	
PVF (anionic)	1090		
PDVF (cationic:linear)	659	1.9	4000
PDVF (anionic:cyclic)	1164	1.3	

1659

GPC results which are expressed as polystyrene equivalents, yield lower values for $\bar{M}_n$ than determinations by VPO.

2.4. MÖSSBAUER EXPERIMENTS

-3 mg Fe cm⁻²
?
pts)
L

Thin Mössbauer samples ($\mathcal{I}$-3 mg ^{57}Fe cm^{-2}) were packed into perspex discs and cooled using a continuous flow of liquid nitrogen cryostat with helium exchange gas. Spectra were recorded using a constant acceleration spectrometer, with a 10 mCi ^{57}Co in rhodium matrix source at room temperature (source recoilless fraction 0.75, linewidth 0.097 mm s^{-1}). The Mössbauer parameters were obtained from computer least-squares fits to the spectra using Lorentzian line shapes.

3. Results

4

Six sets of variable temperature experiments were performed under identical experimental conditions, within the temperature range 80 to 300 K. The samples studied comprised: two samples of polyvinylferrocene from radical initiation (PVF radical); one sample of polyvinylferrocene from anionic initiation (PVF anionic); one

sample of polydivinylferrocene from anionic initiation (PDVF cyclic); one sample of polydivinylferrocene from cationic initiation (PDVF linear); and a sample of crystalline ferrocene. A typical Mössbauer spectrum for PDVF cyclic at 200 K is shown in fig. 1. Table 2 gives the Mössbauer hyperfine parameters recorded at 300 K for the samples under investigation, together with some model compound data.

The PVF (radical) and PVF (anionic) samples had identical parameters which support the expected structure (I). For PDVF (anionic) the parameters are identical to the polymer produced by radical initiation [6,7], and are similar to those predicted and observed for the model compound with three carbon atoms bridging a ferrocene ring (V), which supports the cyclopolymerisation mechanism leading to structure (I). However, PDVF (cationic) has parameters similar to those observed for ferrocene, ethylferrocene or the non-cyclic polyvinylferrocene (PVF).

The Mössbauer absorption line area is related to the Mössbauer absorber thickness t by the expression

$$A(t) \propto \tfrac{1}{2}t \exp\left(-\tfrac{1}{2}t\right)\left[I_0\left(\tfrac{1}{2}t\right) + I_1\left(\tfrac{1}{2}t\right)\right],\tag{1}$$

where I_0 and I_1 are the zeroth and first-order Bessel functions [11]. The Mössbauer absorber thickness t is given by

$$t = nf_a\sigma_0\tag{2}$$

for a single line. Small t expansion of eq. (1) gives

$$A(t) \propto t(1 - 0.25\,t + 0.0625\,t^2 + \ldots).\tag{3}$$

Thus for small t the absorption line area is proportional to the absorber recoilless fraction f_a.

The normalised absorber line areas were determined in the usual way using the fitted linewidths and depths of the quadrupole doublet. The absorption line areas were corrected for thickness effects using the recoilless fraction determined for PVF by Litterst et al. [9]. No attempt was made to determine absolute values of f_a for any of the polymers. In figs. 2, 5 and 6 the logarithm of the corrected area is plotted in arbitrary units on the vertical scale, and the behaviour for different materials has been superimposed to illustrate the relative curvature. All of the amorphous polymers gave substantially similar results. Fig. 2 compares the variation of $\ln A$ with T for crystalline ferrocene and amorphous PVF. The temperature dependence of $\ln A$ for ferrocene over the high temperature range studied is linear, as expected [8]. However, all the amorphous polymers exhibited a deviation from linearity towards higher temperatures.

PDVF(CYCLIC) AT 200K
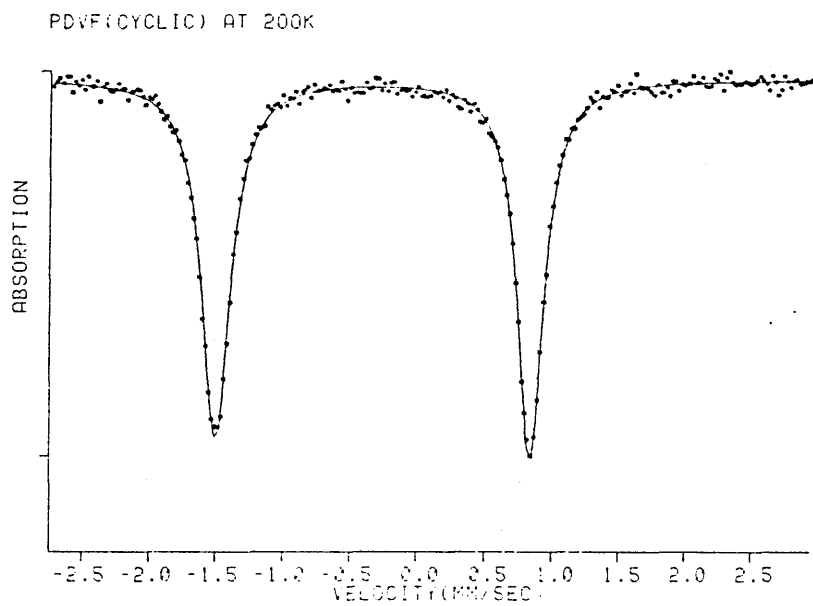
Fig. 1. Mössbauer spectra of anionic polydivinylferrocene (cyclic) recorded at 200 K.
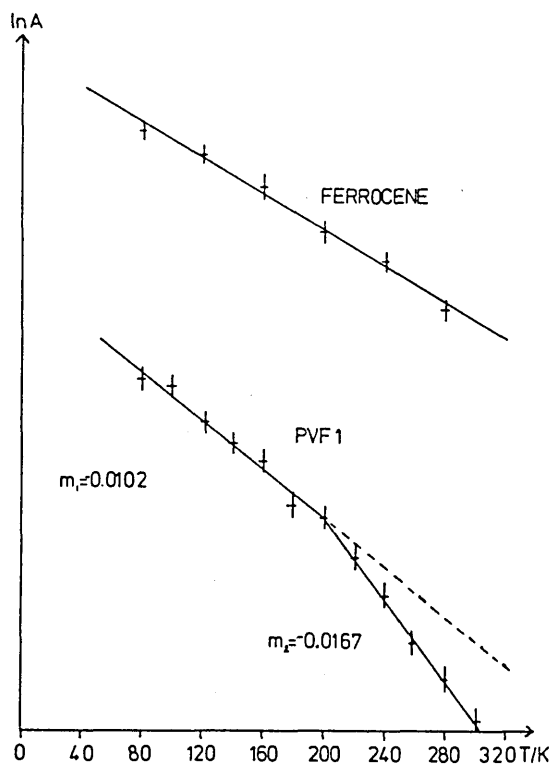
Fig. 2. Variation of Mössbauer absorption line area with temperature for ferrocene and polyvinylferrocene.

Table 2

Mössbauer parameters

Sample	Isomer shift[a] δ (mm s^{-1})	Quadrupole splitting Δ (mm s^{-1})	linewidth Γ (mm s^{-1})
PVF (radical)	0.28(2)	2.40(2)	0.12(1)
PVF (anionic)	0.27(2)	2.39(2)	0.13(1)
PDVF (anionic:cyclic)	0.23(2)	2.29(2)	0.13(1)
PDVF (cationic:linear)	0.27(2)	2.40(2)	0.12(1)
ferrocene	0.27(2)	2.39(2)	0.12(1)
3-carbon ring model (V)	0.24(2)	2.30(2) 2.285[b]	0.12(1)
linear model (VI)	0.27(2)	2.37(2)	0.12(1)

[a]Relative to Fe in Pd at room temperature.
[b]Theoretical Q.S., Trautwein et al. [10].

CH$_3$

Fe   Fe   Fe

(V)   (VI)
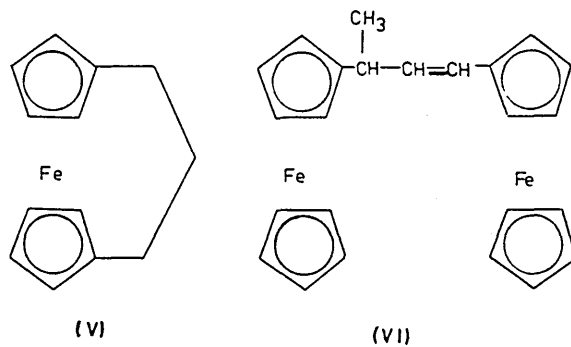
The variation of isomeric shift and quadrupole splitting with temperature was smooth for all polymers, as illustrated in fig. 3 for polyvinylferrocene (anionic). Also, the line-widths showed no systematic variation with temperature as illustrated in fig. 4. This evidence indicates that the observed deviation of $\ln A$ from linearity is unlikely to be associated with a structural change in the polymer. To explain these results, a number of models of the vibrational properties of the amorphous polymers have been considered and their predictions compared with the experimental data.

4. Theory

The temperature dependence of the recoilless fraction can be described by the Debye–Waller factor, which may be written to a good approximation:

$$f_a = \exp\left\{-k^2 \langle x^2 \rangle\right\} = \exp(-2W),$$

where $\langle x^2 \rangle$ is the mean square displacement of the Fe atom from its equilibrium position. The evaluation of f_a is particularly complicated in this case since an amorphous, macromolecular solid is being considered. The principal experimental observation which must be explained is the non-linear temperature dependence of $\ln f_a$. It is first shown that a Debye model should give a reasonable first approximation for the Debye–Waller factor and that this predicts a linear variation of $\ln f_a$ with temperature. Two possible explanations for the observed departure from linearity have then been considered.

4.1. THE DEBYE MODEL FOR AMORPHOUS MATERIALS

The solid is assumed to be a topologically disordered array of N macro-molecules each of mass M. Intramolecular bonding is assumed to be much stronger than intermolecular bonding, and consequently each macromolecule is treated as a rigid mass with intramolecular vibrations being ignored initially. The solid is treated as an isotropic, dispersionless, elastic continuum where the frequency distribution of allowed modes is the usual Debye distribution function. Each mode is treated as a quantised harmonic oscillator which has energy $(n + \frac{1}{2})\hbar\omega$ with probability $p(n)$ given by

$$p(n) = (1 - e^{-\hbar\omega/kT}) e^{-n\hbar\omega/kT}.$$

This gives the mean energy for a mode ω as

$$\bar{E}_\omega = \frac{\hbar\omega}{2} \coth\left(\frac{\hbar\omega}{2kT}\right). \tag{4}$$
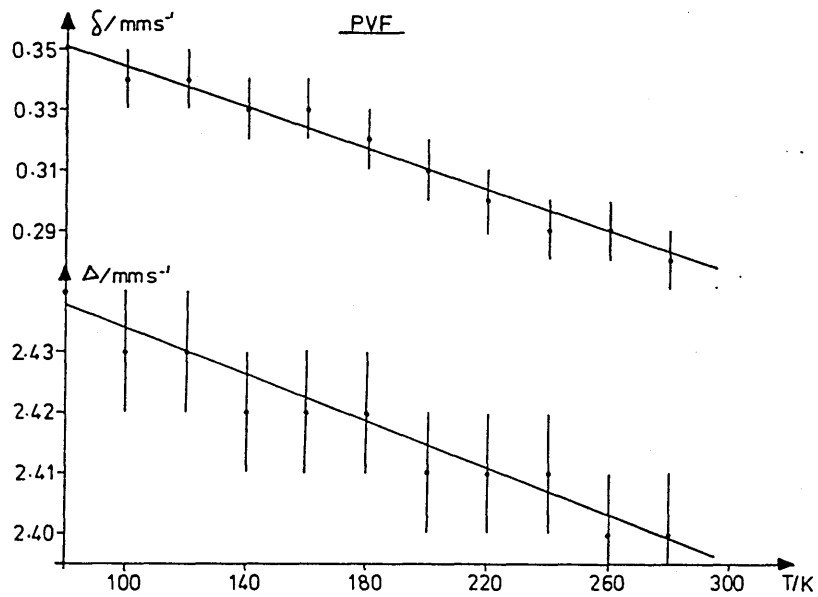
Fig. 3. Variation of the isomer shift (δ), measured relative to Fe in Pd at room temperature, and the quadrupole splitting parameter (Δ) for polyvinylferrocene.
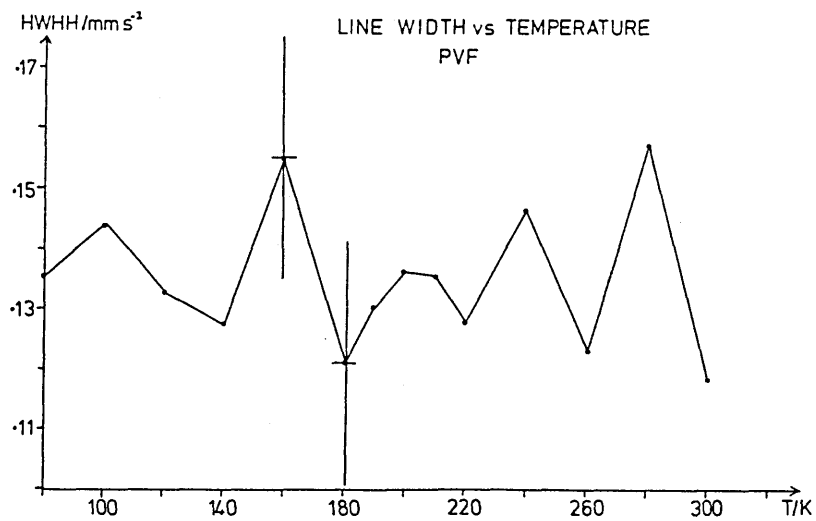

Fig. 4. Variation of the half-width at half-height of the Mössbauer aborption line with temperature for polyvinylferrocene.

To estimate $\langle x^2 \rangle$ for an amorphous material, it is assumed that on average each macro-molecule will have energy $(\overline{E}_\omega/N)$ associated with this mode. If the ith macromolecule is considered to be a classical harmonic oscillator, then its mean square displacement in one direction is

$$\langle x_i^2 \rangle = \tfrac{1}{3}\left(\frac{\overline{E}_\omega/N}{M\omega^2}\right).$$

Thus the three degenerate modes at frequency ω will each give a contribution to the mean square displacement of

$$\langle x_i^2 \rangle_\omega = \frac{\hbar}{6MN\omega} \coth\left(\frac{\hbar\omega}{2kT}\right). \tag{5}$$

This is the standard result for an Einstein oscillator of frequency ω, and arises essentially because of the assumption that the energy is shared equally between the N macro-molecules. This is a reasonable assumption since the Mössbauer technique effectively measures a site averaged mean square displacement.

The total mean square displacement is found by integrating over the Debye distribution function $g(\omega)$. Hence

$$\langle x^2 \rangle = \frac{\hbar}{6MN} \int_0^\infty \frac{g(\omega)}{\omega} \coth\left(\frac{\hbar\omega}{2kT}\right) d\omega.$$

The Debye–Waller factor is thus

$$2W = \frac{E_0^2}{6Mc^2\hbar N} \int_0^\infty \frac{g(\omega)}{\omega} \coth\left(\frac{\hbar\omega}{2kT}\right) d\omega,$$

where E_0 is the energy of the incident γ photon. This is the standard result from the Debye model [8] and in the high temperature limit $(T \geqslant \tfrac{1}{2}\Theta_D)$

$$2W \simeq \frac{3E_0^2 T}{Mc^2 k\Theta_D^2},$$

where Θ_D is the characteristic Debye temperature for the lattice. Thus the Debye model predicts that $\ln f$ will depend linearly upon the temperature.

The departure from linearity observed in our experimental results was considered as arising from either the excitation of intramolecular modes as proposed by Litterst et al. [9], or from anharmonic effects in the intermolecular potential.

4.2. INTRAMOLECULAR MODES

As the temperature of the solid rises, intramolecular modes will become excited, and it was considered possible that such modes with a characteristic temperature of approximately 180 K were responsible for the change in gradient. The intramolecular modes are treated as Einstein oscillators since they are equivalent to the optic modes in a crystalline material. In principle, there will be $3(n - 1)$ modes, where n is the number of atoms in each macromolecule. However, many of the modes will only be excited at high temperature (above the glass transition temperature), and consequently the number of modes is taken to be n_R, the number of repeating units in the macromolecule. This is equivalent to ignoring vibrations which occur within the repeating unit, and only considering vibration of the ferrocene sidegroup.

In the absence of a detailed model of the molecular structure, and force constants, it is not possible to determine the motion of each repeating unit for the intramolecular modes. As before, it is assumed that the energy for each mode is shared between the repeating units. The $3(n_R - 1)$ intramolecular modes are all assumed to have the same angular frequency ω_E, and the mean square displacement of a repeating unit associated with one such mode will be

$$\langle x^2 \rangle_{\omega_E} = \frac{\hbar}{6 m_R n_R \omega_E} \coth\left(\frac{\hbar\omega_E}{2kT}\right),$$

where m_R is the mass of the repeating unit. Noting that $m_R n_R = M$, then the intramolecular and intermolecular modes may be combined to give

$$\langle x^2 \rangle_{\text{tot}} = \frac{\hbar}{6MN} \int_0^\infty \frac{g(\omega)}{\omega} \coth\left(\frac{\hbar\omega}{2kT}\right) d\omega + \frac{3(n_R - 1)\hbar}{6M\omega_E} \coth\left(\frac{\hbar\omega_E}{2kT}\right). \quad (6)$$

This expression was found to give an adequate fit to the experimental data, with a suitable choice of Einstein frequency (see fig. 5). However, the parameter premultiplying the second term was found to be unacceptably high.

The failure of the intramolecular model may be seen by the following simplified argument. In the temperature region above Θ_D, but below the Einstein temperature $\Theta_E = \hbar\omega_E/k$, the Debye–Waller factor derived from eq. (6) may be written

$$\ln A = 7.33 - 0.0082\,T - 6.26\coth\left(\frac{387}{T}\right)$$

PVF

0   40   80   120   160   200   240   280   320   T/K
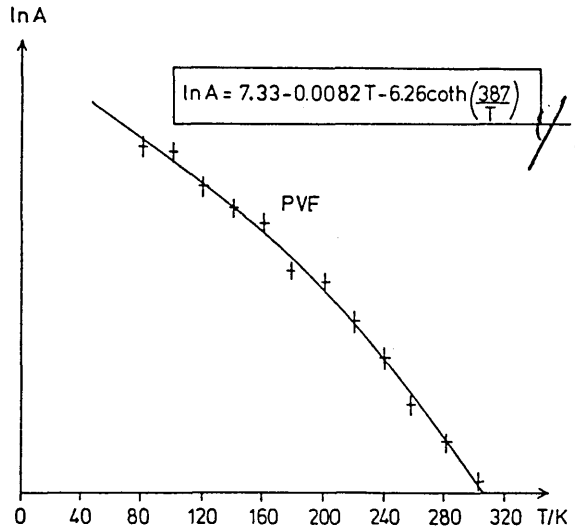
Fig. 5. Fit to experimental data of polyvinylferrocene using a combination of intramolecular and intermolecular modes.

$$2W \simeq \frac{3E_0^2}{Mc^2 k}\left[\frac{T}{\Theta_D^2} + \frac{(n_R - 1)}{6\Theta_E}\right] \quad \text{for } \Theta_D < T < \Theta_E .$$

For temperatures above the Einstein temperature

$$2W \simeq \frac{3E_0^2}{Mc^2 k}\left[\frac{T}{\Theta_D^2} + \frac{(n_R - 1)T}{3\Theta_E^2}\right] \quad \text{for } \Theta_E < T .$$

Thus the maximum fractional change in the slope Δm of the $\ln f$ against T graph will be

$$\Delta m = \frac{(n_R - 1)\Theta_D^2}{3\Theta_E^2} . \tag{7}$$

The fractional change in slope in the temperature range 80 to 300 K was typically 0.5. The data appeared to show a transition at approximately 180 K, which could be identified with the temperature at which the function coth $[\hbar\omega_E/2kT]$ showed the greatest change in slope. This occurs when

$$\frac{\hbar\omega_E}{2kT_0} \simeq 2.2, \quad \text{i.e.} \quad \Theta_E \simeq 4.4\, T_0 = 790\,\text{K}.$$

The Debye temperature is typically 50 K, and this results in a required value of $n_R > 375$. Clearly this is in disagreement with the experimental value of n_R of approximately 10 [see molecular weight determinations, sect. (2.3)]. The model was modified to allow for a range of values of ω_E, but this still failed to give a significant value for n_R. Hence, it was concluded that consideration of intramolecular modes could not account for the large change in slope observed experimentally.

4.3. ANHARMONIC POTENTIAL

Boyle et al. [12] observed a non-linear temperature dependence for the recoilless fraction of metallic tin in the temperature range Θ_D to $4\Theta_D$, where Θ_D for tin is 142 K. They demonstrated that this non-linearity arises because of the anharmonic nature of the potential in which each tin atom is situated. Zener and Bilinsky [13] considered the effect of thermal expansion and showed that

$$2W \simeq \frac{3E_0^2 T}{Mc^2 k \Theta_D^2} \left[1 + \frac{2V\beta}{3RK} (T - \tfrac{3}{8}\Theta_D) \right], \tag{8}$$

where R is the gas constant, K is the isothermal compressibility, β is the high temperature volume expansion coefficient, and V is the molar volume.

The experimental results were fitted to the equation

$$\ln A = B - CT - DT^2 \tag{9}$$

using a least squares method. The parameters C, D and Θ_D are given in table 3 for each sample, and three of the corresponding fits to the experimental data are shown in fig. 6. It can be seen that eq. (9) gives a consistent fit to the experimental data, and that the parameters appear to be independent of the internal bonding within the macromolecule. The parameter $2V\beta^2/3RK$ of eq. (8) can be estimated from assumed values of $\beta = 2 \times 10^{-4}\,K^{-1}$ and $K = 3 \times 10^{-10}\,Pa^{-1}$, obtained by comparison with data available for polystyrene and PVC. Taking a typical molecular weight of 1000 and a density of 2×10^3 kg m^{-3} gives a molar volume $V = 5 \times 10^{-4}$ m^3 mol^{-1}. Hence,

$$\frac{2V\beta^2}{3RK} = 5 \times 10^{-3} K^{-1}.$$

Table 3

Parameters derived from fitting $\ln A = B - CT - DT^2$ to experimental data in the range 80–300 K

|	C $(\text{K} \times 10^{-3})$	ΔC $(\text{K} \times 10^{-3})$	D $(\text{K}^2 \times 10^{-5})$	ΔD $(\text{K}^2 \times 10^{-5})$	Θ_D (K)	$\Delta \Theta_D$ (K)
PVF (anionic)	3.5	1.4	2.6	0.4	43·	9
PVF (radical) 1	2.6	1.4	2.4	0.4	49	14
PVF (radical) 2	2.7	0.4	2.4	0.1	48	4
PDVF (cyclic)	3.1	1.0	2.6	0.3	46	8
PDVF (linear)	2.5	0.8	1.8	0.2	50	9
ferrocene	7.3	1.6	0.3	0.4	76	9
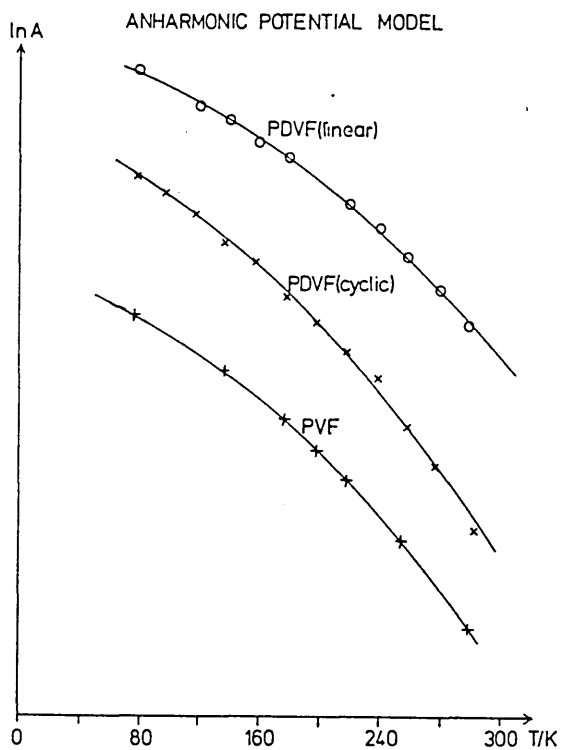
Fig. 6. Fits to the experimental data of polyvinylferrocene (anionic), polydivinylferrocene (cyclic), and cationic polydivinylferrocene (linear) for an anharmonic potential. Relative position of curves on the vertical scale is arbitrary.

This is a factor of approximately 2 less than the experimentally observed parameter. A similar discrepancy was observed for tin by Boyle et al. [12], and was explained by an extension of the arguments of Zener and Bilinsky [13].

Thus this evidence suggests that the non-linear temperature dependence of $\ln f$ arises from the anharmonic potential in which each macromolecule is situated. This is further supported by the observation that the non-linearity does not depend upon the different structure of the repeating unit of the polymers studied.

5.   Discussion

The non-linear temperature dependence of $\ln A$ over the range 80−300 K was observed to be similar for all the amorphous polymers studied. This suggested that the deviation from linearity did not depend strongly upon the molecular structure of the polymer as it had been clearly shown that PVF, PDVF (cyclic) and PDVF (linear) have significantly different structures. In particular, the nature of the ferrocene side-group is modified from a simple ferrocene unit having a single bond to the backbone (I) for PVF, to a bridged ferrocene having two bonds in the backbone (II) for PDVF (cyclic) and to a more complex polyaddition structure (IV) for PDVF (linear). If the dominant mechanism responsible for the deviation from linearity is associated with motion of the sidegroup, then it would be expected that the behaviour should be significantly different for these three polymers.

The development of the Debye model for amorphous materials, which initially ignored any intramolecular vibrations, yielded a similar result to the Debye−Waller factor for crystalline solids. When this was extended to include intramolecular modes, treated as Einstein oscillators, it was possible to fit the experimental data, but this approach did not yield physically realistic fitting parameters. However, a good fit to the experimental data was achieved when an anharmonic potential was assumed for each macromolecule. This gave good agreement between the observed fitting parameters and those predicted by the model. It is also interesting to note that when one set of experiments were carried out with longer run times (table 3 : PVF (radical) 2), the improved quality of experimental data was reflected in the reduced errors associated with the fitting parameters. The experimental data for crystalline ferrocene was also fitted in the same way, and yielded an anharmonic term which was smaller than the fitting error, and a Debye temperature which can be compared with the second-moment values of Hill and Debrunner [14].

Litterst et al. [9] have also observed an anomalous behaviour of the temperature dependence of the recoilless fraction of polyvinylferrocene. They were able to explain their observations on the basis of an anharmonic hindered motion of the ferrocene sidegroups as a whole, which are pictured as moving between conformational states. It is apparent that, if this mechanism was dominant in our polymers, then it should be expected that the behaviour of the three types of polymer would be different.

6. Conclusions

We have observed a similar non-linear dependence of $\ln A$ with temperature for a number of amorphous polymers containing ferrocene units in different structural arrangements. It was not possible to account for the observed behaviour on the basis of a modified Debye model for amorphous materials when intramolecular vibrations were included. However, a good fit to the experimental data could be obtained, with physically significant fittings parameters, if it was assumed that each macromolecule vibrated within an anharmonic potential.

References

[1]   M.H. George and G.F. Hayes, J. Polymer Sci. 14(1976)475.

[2]   T. Kunitake, T. Nakashima and C. Aso, J. Polymer Sci. Part A–1, 8(1970)2853.

[3]   S.L. Sosin, L.V. Jashi, B.A. Antipova and V.V. Koshak, Vysokomol. Soedin, Ser. B 12 (1970)699.

[4]   A.G. Nagy, I. Dezsi and M. Hillman, J. Org. Met. Chem. 117(1976)55.

[5]   M. Hillman and A.G. Nagy, J. Org. Met. Chem. 184(1980)433.

[6]   G.C. Corfield, J.S. Brooks and S. Plimley, ACS Symposium Series 195(1982)123.

[7]   G.C. Corfield, J.S. Brooks and S. Plimley, Polymer Preprints ACS Div. Polymer Chem. 23 (1982)270.

[8]   A.J.F. Boyle and H.E. Hall, Rep. Prog. Phys. 25(1962)441.

[9]   F.J. Litterst, A. Leif, D. Nuyken and H. Alcala, Hyp. Int. 12(1982)317.

[10]   A. Trautwein, R. Reschke, I. Dezsi and F.E. Harris, J. de Phys. 12(1976) C6–463.

[11]   J.M. Williams and J.S. Brooks, Nucl. Instr. Meth. 128(1975)363.

[12]   A.J.F. Boyle, D. St. P. Burbury, C. Edwards and H.E. Hall, Proc. Phys. Soc. 77(1960)129.

[13]   C. Zener and Bilinsky, Phys. Rev. 50(1936)101.

[14]   C.R. Hill and P.G. Debrunner, J. de Phys. 37(1976) C6–41.